# Industrial applications of functional nanocelluloses

Charlène Reverdy

▶ **To cite this version:**

Charlène Reverdy. Industrial applications of functional nanocelluloses. Chemical and Process Engineering. Université Grenoble Alpes, 2017. English. NNT : 2017GREAI080 . tel-03081233

**HAL Id: tel-03081233**
**https://theses.hal.science/tel-03081233**

Submitted on 18 Dec 2020

**HAL** is a multi-disciplinary open access archive for the deposit and dissemination of scientific research documents, whether they are published or not. The documents may come from teaching and research institutions in France or abroad, or from public or private research centers.

L'archive ouverte pluridisciplinaire **HAL**, est destinée au dépôt et à la diffusion de documents scientifiques de niveau recherche, publiés ou non, émanant des établissements d'enseignement et de recherche français ou étrangers, des laboratoires publics ou privés.

Communauté
UNIVERSITÉ Grenoble Alpes

# THÈSE

Pour obtenir le grade de

## DOCTEUR DE LA COMMUNAUTE UNIVERSITE GRENOBLE ALPES

Spécialité : **Matériaux, Mécanique, Génie civil, Electrochimie**

Arrêté ministériel : 25 mai 2016

Présentée par

## « Charlène REVERDY »

Thèse dirigée par **Julien BRAS, Maître de Conférences, Grenoble INP**, et
codirigée par **Naceur Belgacem, Professeur, Grenoble INP**

préparée au sein du **Laboratoire de Génie des Procédés Papetiers**
dans **l'École Doctorale I-MEP2 – Ingénierie – Matériaux, Mécanique, Environnement, Energetique, Procédés, Production**

# Industrial applications of functional nanocellulose

Thèse soutenue publiquement le **«16 Novembre 2017»**, devant le jury composé de :

**Pr, Didier, LEONARD**
Professeur à l'Université Lyon1, Président
**Dr, Gilles, SEBE**
Maître de Conférences à l'Université de Bordeaux, Rapporteur
**Pr, Monika, ÖSTERBERG**
Professeur à Aalto University, Rapporteur
**Dr, Elisa, ZENO**
Ingénieure au Centre Technique du papier, Examinateur
**Dr, Julien, BRAS**
Maître de Conférences à Grenoble INP, Directeur de thèse
**Pr, Naceur, Belgacem**
Professeur à Grenoble INP, rôle, Co-Directeur de thèse
**Mr, Guillaume, MOREAU**
Ingénieur R&D aux Papeteries du Léman, Membre invité

*This PhD project has been funded by Association Nationale Recherche Technologie (ANRT) under the CIFRE convention N° 2014/0443 and by Papeteries du Léman.*

# Acknowledgements

I address my first acknowledgments to my jury members: Pr. Didier Léonard, Pr. Monika Österberg, Dr. Gilles Sèbe and Dr. Elisa Zeno. It was a real pleasure to have you all in my defense, for your very interesting questions and for your time. A special thank will go to the two reviewers of my manuscript Dr. Gilles Sèbe and Pr. Monika Österberg who took time to read the manuscript and give a detailed feedback. I also gratefully thank Pr. Didier Léonard for accepting to be the chair of the defense and to held the role very nicely.

Les seconds iront bien évidemment à mes directeurs de thèse, Julien Bras, Naceur Belgacem et Jocelyne Dumas. Je vous remercie tous pour votre implication dans le projet et pour votre grande aide. C'est grâce à vous que j'ai beaucoup appris et évolué durant ces trois années.

Merci Julien pour toutes ces propositions de collaborations et projets, qui, bien qu'elles me faisaient souvent râler (:D), m'ont permis de m'amuser et m'épanouir mais aussi de voyager pour une thèse riche de nouvelles connaissances. Merci Naceur pour tes lumières, tes discussions politiques et puis aussi pour ces encouragements positifs qui font du bien.

Je n'oublie pas non plus Guillaume Moreau, qui a été toujours présent pendant le projet et qui a toujours été là pour répondre à toutes mes questions et me tenir informée des projets et des avancées de l'entreprise. Je remercie aussi toute l'équipe de PDL qui m'a appris pleins de choses lors de mes déplacements. Je remercie Raphaël pour son aide en PFE et en thèse.

Evidemment, merci à tous ceux du LGP2, qui ont été là durant cette thèse. Merci aux deux directeurs connus pendant cette période Evelyne Mauret et Didier Chaussy pour leur implication dans la vie du laboratoire. Merci au service technique pour avoir toujours été d'une grande aide, pour votre gentillesse, votre sourire et votre humour. Merci au service informatique pour l'aide apportée. Merci à ceux qui sont là aussi pour nous aider dans les équipes, Cécile parce que tu fais beaucoup de choses pour nous et parce que c'est marrant de t'entendre nous engueuler, Bertine parce tu m'a appris pleins de trucs au MEB et parce que t'es qu'une vieille bique avec qui on se marre bien et Stéphane parce qu'on te trouve jamais mais quand même quand on te trouve ça nous aide et parce que t'es toujours là pour nous (les femmes) rappeler qu'après trente ans rien ne sera plus pareil, de manière si sympa.

Merci à mes stagiaires, Damien, Héloïse, Abdellah et Pierre pour leur aide et pour m'avoir appris ce que c'était quand on était de l'autre côté. Merci à Karim aussi que je sais pas où mettre, parce que ca faisait du bien de pouvoir s'engueuler avec quelqu'un pour de faux, s'insulter et se faire des gestes obscènes, ca fait redescendre la pression.

Et puis il y a eu tous mes co-bureaux qui ont su brillamment me supporter, merci, Khartik, Megan qui nous a appris tous les mots de la langue anglaise qui ne sont pas très corrects et vice versa et qui nous as donné un update constant de la politique des Etats-Unis ("Arghh, we are fucked!!!"), Erwan que j'ai plus supporté qu'il ne m'a supportée (:D) parce que t'es un grand bavard et que je suis une grande associable et puis parce que tu me fais rire avec tes tableaux comparatifs et tes questionnements, Hippolyte surnommé "Hippo" que je connaissais mais que j'ai redécouverts sous un nouvel angle, parce t'as été là pour nous soutenir et nous encourager et parce que t'étais moins méchant avec moi que Vivien quand on partait en footing ou en rando et puis Mathieu même si c'était bref, je te souhaite une thèse fantastique dont je suis grave jalouse!

Après mes co-bureaux il y a mes conscrits de thèse qui m'ont aussi supportée souvent, merci, Erwan (mais j'ai déjà presque tout dis plus haut mais j'ai oublié de te dire merci pour tes conseils en whisky!), Vincent pour avoir eu le courage de venir nous dire bonjour tous les matins, pour avoir été mon co-représentant des doctorants, pour avoir magnifiquement organisé la pétanque et bien sur pour ton gâteau au chocolat et piment qui restera dans les annales (mais pas pour les bonnes raisons :D) et Vivien pour tes supers idées pour emmerder le monde, comme pourrir les bureaux, pour m'avoir garder en forme en me forçant à aller faire la montée de la bastille, du roller, de la rando etc. Merci pour toutes ces soirées bouffes ensemble évidemment, qui ont fait qu'on était plus que des conscrits de thèse je crois.

Et puis il y a tous les autres doctorants et postdoc qui sont passés par là et qui sont parfois devenus des amis, avec qui ont boit le café et avec qui on partage tous nos déboires. Merci, B&F pour toutes ces conversations développement durable, ces randos et ces bouffes, Fanny H. pour toute ton aide et ta gentillesse, pour faire semblant de râler aussi, Flavien pour tes arrivées dans notre bureau pour parler de ta life parce que t'en avais besoin ou pour nous poser des questions scientifiques auxquelles on ne savait pas répondre, Johanna parce que ca faisait du bien de faire la mauvaise langue avec toi et puis tous les autres et j'en oublierai sûrement, Seema,Florian, Jordan, Jennifer, Sébastien, Claire, Ara, Wilson, Fleur, Valentin, Lucas, Manon, Marcos, Franciele, Ying, Laetitia, Marie-Allix, Camille, Hugo,… Je souhaite à

tous ceux qui n’ont pas fini de profiter des ces moments, et puis surtout bon courage surtout!

Et puis il y a tous mes amis, ceux avec qui on s’est serré les coudes en prépa, Marion et Gwen surtout, cette thèse est une belle revanche sur ces moments difficiles. Les amis de Papèt’ évidemment et tous les autres.
Je remercie enfin ma famille, qui m’a laissé faire mes choix et m’a permis de les réaliser. Et je remercie Luc, pour m’avoir épaulée, soutenue et supportée sur la plus grande partie de ce projet.

Bref, merci à tous :)

# Table of content

General Introduction ..... 17

1. Chapter 1. Literature review ..... 29

Introduction ..... **29**

1. Toward nanocellulose industrialization ..... **31**

2. Anti-adherent and barrier coatings ..... **63**

3. (Nano)Cellulose functionalization for anti-adherence and barrier ..... **77**

Conclusion and challenges ..... **91**

**2. Chapter 2. Cellulose nanofibrils chemical and physical modification ..... 113**

Introduction ..... **113**

1. Cellulose nanofibrils aqueous modification with different organotrialkoxysilanes: influence of amine presence on surface mechanisms and properties ..... **115**

2.1. Cross-condensation of amino-propyl trimethoxy silane and propyl trimethoxy silane at low concentration for narrow dispersed nano- and micro-metric silsesquioxane particles synthesis ..... **133**

2.2. Simple method to obtain hydrophobic and antimicrobial cellulose nanopaper using silsesquioxane particles sol gel formation in aqueous conditions ..... **149**

3. Micro/nano roughness patterning of cellulose nanofibers thinfilm toward superhydrophobicity ..... **171**

3.4. Conclusion ..... **185**

**3. Chapter 3. From nanopaper to paper functionalization ..... 191**

Introduction ..... **191**

1. Paper functionalization with organotrialkoxysilane and organotrialkoxysilanes modified cellulose nanofibers coating suspension ..... **193**

2. One step coating for obtaining superhydrophobic surface using cellulose nanofibrils ..... **207**

3. From CNF-silsesquioxane paper coating to their use as binder in superhydrophobic suspension for a coating pilot trial ..... **225**

Conclusion ..... **241**

**General conclusions and perspectives ..... 245**

**Résumé français ..... 253**

**Appendix n°1.....261**

**Appendix n°2.....275**

# Scientific contributions (2014-2017)

## Publications in scientific journal

1. Bardet R., **Reverdy C.**, Belgacem N., Leirset I., Syverud K., Bardet M., Bras J.. «Substitution of nanoclay in high gas barrier films of cellulose nanofibrils with cellulose nanocrystals and thermal treatment», *Cellulose*. 2015, 22(2), 1227-1241.
2. **Reverdy C.**, Belgacem N., Moghaddam M.S., Sundin M., Swerin A., Bras J.. «One step coating for obtaining superhydrophobic surface using cellulose nanofibrils», *Colloids and Surface Part A* (2017).
3. **Reverdy C.**, Abdesselam K.A., Belgacem N., Brochier-Salon M.-C. , Gablin C., Leonard D., Bras J.. «Cellulose nanofibrils aqueous modification with different organotrialkoxysilanes: influence of amine presence on surface mechanisms and properties», to be submitted to *Cellulose* (2017).
4. **Reverdy C.**, Belgacem N., Bras J.. « Cross-condensation of amino-propyl trimethoxy silane and propyl trimethoxy silane at low concentration for narrow dispersed nano- and micro-metric silsesquioxane particles synthesis», submitted to *Journal of Colloid and Interface Science* (2017).
5. **Reverdy C.**, Willeman H., Belgacem N., Bras J.. « Simple method to obtain hydrophobic and antimicrobial cellulose nanopaper using silsesquioxane particles sol gel formation in aqueous conditions», submitted to *Applied Materials and Interfaces* (2017).

## Oral presentation

1. **Reverdy C.**, Bardet R., Belgacem N., Leirset I., Syverud K., Bardet M., Bras J..«Barrier Film Based on Cellulose Nanofibers and Tempo-Oxidized Cellulose Nanocrystals» in TAPPI Nano – International conference on nanotechnology for Renewable Materials, 2015.
2. **Reverdy C.**, Belgacem N., Brochier-Salon M.-C. , Bras J.. «Cellulose nanofibrils aqueous modification with different alkoxysilanes: influence of amino presence on surface mechanisms and properties» in TAPPI Nano – International conference on nanotechnology for Renewable Materials, 2016.
3. **Reverdy C.**, Moghaddam M.S., Sundin M., Swerin A., Bras J.. «Manufacturing and measurement of superhydrophobicity for paperbased active packaging» in COST Action

FP1405 Active and intelligent fibre-based packaging – innovation and market introduction meeting, 2016.

## Poster presentation

1. **Reverdy C.**, Raynaud S., Guérin D., Dufresne A., Belgacem N., Bras J.. « TEMPO modified cellulose nanocrystals as a biobased cross-linker for Poly vinyl alcohol films to enhance oxygen barrier properties at high humidity » in EPNOE – International Polysaccharide Conference, 2015.
2. **Reverdy C.**, Terrage D., Beury N., Moreau C., Villares A., Cathala B., Bras J.. « Xyloglucan and cellulose nanofibrils assembly for barrier material » in ACS National Meeting, 2016.
3. **Reverdy C.**, Moghaddam M.S., Sundin M., Swerin A., Bras J.. «Superhydrophobic surfaces manufacturing with nanocelluloses» in N.I.C.E. International Conference on. Bioinspired and Biobased Chemistry & Materials, 2016.
4. **Reverdy C.**, Saini S., Belgacem N., Bras J.. «Antibacterial materials development with contact active and micro-nano structured surfaces» in TAPPI Nano – International conference on nanotechnology for Renewable Materials, 2017.
5. **Reverdy C.**, Gablin C., Leonard D., Bras J., Belgacem N..« Multitechnique Study of Aminopropyltrimethoxysilane Polysiloxane Network Orientation on Cellulose Nanofibrils Surface» in SIMS XXI International Conference on Secondary Ion Mass Spectroscopy, 2017.

# Abbreviations

## Chemicals and materials

| | |
|---|---|
| AKD | Alkyl Keten Dimer |
| APMS | 3-aminoproyltrimethoxysilane |
| CNC | Cellulose Nanocrystal |
| CNF | Cellullose Nanofibril |
| PDMS | Polydimethylsiloxane |
| PEI | Polyethyleneimine |
| SQP | Silsesquioxane particles |
| TEMPO | (2,2,6,6-Tetramethylpiperidin-1-yl)oxyl |
| TFPS | (3,3,3-trifluoropropyl)trimethoxysilane |
| TMPS | Methyltrimethoxy propyl silane |

## Methods

| | |
|---|---|
| AFM | Atomic Force Microscopy |
| BET | Brunauer Emmett Teller |
| DLS | Dynamic Light Scattering |
| FEG-SEM | Funnel Electron Gun Scanning Ellectron Microscopy |
| FTIR | Fourrier Transform Infra-Red Spectroscopy |
| OP | Oxygen Permeability |
| OTR | Oxygen Transmission Rate |
| QCM-D | Quartz Crystal Microblance with Dissipation monitoring |
| SEM | Scanning Electron Microscopy |
| SEM-EDX | Scanning Electron Microscopy Energy Dispersive X-ray analysis |
| TGA | ThermoGravimetric Anlaysis |
| ToF-SIMS | Time of Flight-Secondary Ion Mass Spectrometry |
| WCA | Water Contact Angle |
| WSA | Water Shedding Angle |
| WVP | Water Vapor Permeability |
| WVTR | Water Vapor Transmission Rate |

# General Introduction

# General Introduction

Paper and board production represents 400 million ton per year all around the world (CEPI, 2016). In this overall production, different types of paper and board market can be separated, including specialty papers, which represents 6.5% of the world mass production (AWA, 2015). Specialty papers are defined by their specific performance characteristics regarding physical, optical, electrical or chemical properties but also special compliance such as security implement or particular size. The main market segment by volume, in the global specialty paper sector, is packaging (42%), followed by building and construction (15%) and food service (10%). As niche markets, electrical and medical paper represents 2% of the production.

Even if such market is small as compared to commodity papers (like printing paper, newspaper or cardboard), the growth of interest from European paper industry in this sector is rising. The main reason is the high added value of the end use material and consequently stable and higher selling price. Indeed, in a declining competitiveness of the relatively old European industry facing brand new Asian technology, commodity/low price paper production is becoming uneconomical. Furthermore society is changing toward numeric solutions in spite of classic newspaper or books and is now expecting more functionalization, more biobased solution and more recycled fiber based materials. Developing a larger portfolio including niche market products, by using the flexibility of the production process of existing machines, is the pathway employed by several companies, and especially small ones.

The specialty paper market is often concerned by consumer's trends but also governmental pushes. This leads to the need to be at the technical forefront and able to react quickly in developing new solutions. As presented in Figure 1, current impacts of the society are mainly concentrated on environmental concerns, health safety, security, life style and global digitalization. It impacts many segments of specialty paper market, and mainly packaging, food service and security.

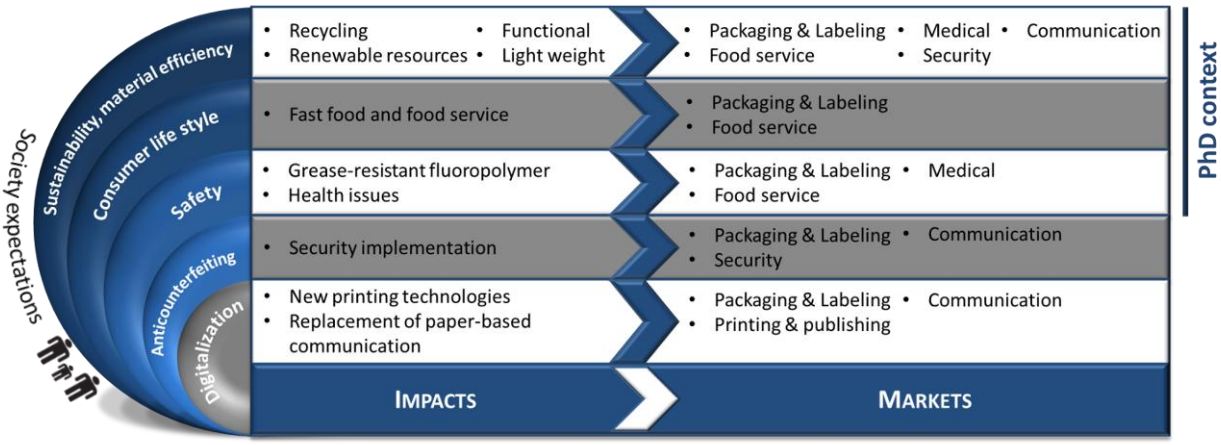


**Figure 1. Impacts of consumer or political demands on specialty paper markets. (Adapted from (AWA, 2015))**

A recent example of governmental push is the UE (and more precisely the European Food Safetey authority) concern perfluorocarbons as a serious environmental threat (Benford et al., 2008). The use of perfluoropolymer in paper industry is wide and mostly in food packaging segment. Indeed, the high grease repellency brought by such chemical is the best suitable for food wrapping paper, food transport bags or pet food applications. However, the restriction in 2008 of PFOS (perfluorooctane sulphonate) for environmental and health problems and the recent restriction of PFOA (perfluorooctanoic acid) lead to the research of alternative solutions that possibly challenge perfluoropolymer properties (European Commission, 2017).

Another example is the increase in medical safety concern in material conceived for medical environment but also in food packaging. Indeed, there is a need to stem the high rate of nosocomial diseases, which are spreading by material (and paper could be one of them) exchange between infected and non-infected people. The concern of European health commission on the release of antibacterial agent from packaging is also another reason, for which developing new antibacterial contact active material is being a major challenge.

Following the trend of green materials and company marketing strategy around it, research on biobased solution has been increased as well to find alternative to petrol and its shortage.

In this context, there is a need for specialty paper industry to develop high performance greener solutions to answer all these challenges.

Among biobased solution to study, such as starch, poly lactic acid (PLA), proteins etc., nanocellulose raised major attention in papermaking industry since last decade. Nanocellulose is a bio-based nanomaterial which can be extracted from wood pulp but also

annual plant. Two different types of nanocellulose can be defined: Cellulose nanocrystals (CNC) and Cellulose nanofibrils (CNF). CNC are rigid rod-like shape crystals and often compared as “rice” morphology, with few nanometers in diameter and hundreds in length. CNF are flexible filament of few tens of nanometers diameter but several micrometers long, often depicted as spaghetti-like material. In aqueous suspension, it depicts a gel-like behavior at very low solids content (less than 2 wt%) and possess shear-thinning effect. Both are exhibiting high mechanical properties, high aspect ratio and high chemical reactivity due

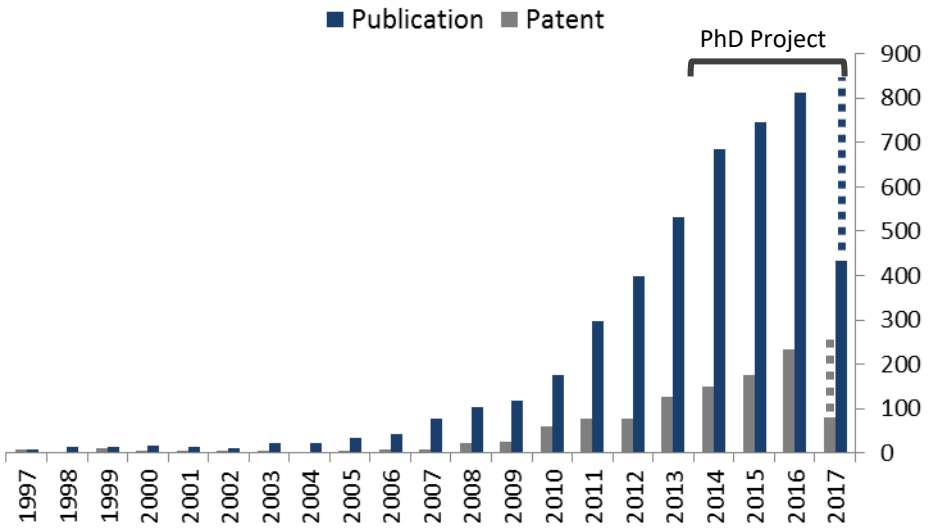


**Figure 2. Evaluation of the number of publications and patents over the past two decades regarding nanocellulose. Prediction of year 2017 are based on the first 4 months. Descriptors: "Cellulose nanofibril", "Cellulose microfibril", "Cellulose nanofiber", "CNF and cellulose", "MFC and cellulose", "NFC and cellulose", CNC and cellulose, “NCC and cellulose”, “Cellulose nanocrystal”, “cellulose nanowhisker”, “cellulose nanorod” (SciFinder, 1st May 2017)**

to their high hydroxyl group content. Interest in nanocellulose research and applications has grown in both academic and industry as shown by the exponential release of patents and publications over the last two decades (Figure 2). What is interesting to notice is that about half of scientific papers (about 3000 onto 6000) and two thirds of patents (about 800 onto 1300) have been published during the time frame of this PhD project. This figure proves by itself the high interest and novelty of topic dealing with such nanocellulose materials.

Nanocellulose is a great opportunity for papermakers who already deeply know the raw material and have, in the case of CNF, close technology to produce it. Industrial availability of both products is being to be solved with the very recent development all around the world of production sites (pilot and industrial) and also of the design of CNF production satellites that can be implemented to existing papermaking process (Hietala and Oksman, 2014), (Chauve and Bras, 2014).

Their properties have been tested with success in some specialty papers. For example, CNC films bi-refringence ability was exploited as anti-counterfeiting material in paper (Bardet et al., 2014). Also, bonding ability of CNFs were used as strengthening agent to decrease the weight of paper through constant mechanical properties (Boufi et al., 2016) and as closing structure to improve barrier properties (Aulin et al., 2010). CNF was studied as a web for better dispersion of inorganic particles in coatings and CNC as barrier and surface improvement coating layer (Bardet, 2014), (Bardet and Bras, 2014).

The potentiality of nanocellulose in creating a barrier to grease, water and in being antiadherent or antimicrobial surface has never been tested simultaneously on paper up to our knowledge. For such high performance nanocellulose based materials, the need for their surface chemical functionalization seems obvious.

The use of chemical modifiers in papermaking industry is only relying on aqueous system: either water soluble polymer or water-based emulsion. Indeed, the adaptation of the process to welcome solvent based solution in terms of security is not preferable. Thus, the scope is considerably restricted. Organotrialkoxysilanes in such problematics are very useful. Indeed, it is chemically tunable by modification of the alkyl chain length or groups and in some cases, soluble in water with no or few addition of acids or alcohol. Their structure can be very versatile as they can self-condensate to form silsesquioxane network layer or particles. Their structure is similar to silicon and could be useful for hydrophobic, non-adherent and non-wetting type of modifications.

The main purpose of this industrial PhD project (Oct. 2014- Nov. 2017) was to develop applications of functional cellulose nanofibrils in specialty paper. It is a collaboration between Bolloré Thin Paper – a papermaking company producing thin paper − and the LGP2 (UMR CNRS 5518) – a research laboratory expert in papermaking and nanocellulose – with the support of the French National Research Agency (ANRT) (CIFRE n° 2014/0443).

The company was wheeling to develop new antimicrobial paper or enhance existing silicon baking paper product property to confer greaseproof and/or non-wetting character. In this context, the PhD focuses on modifying with organotrialkoxysilanes cellulose nanofibrils and applying it as a functionalized coating material. A comprehensive approach was also needed on organotrialkoxysilanes interaction in water and with nanocellulose. Chemical, physical

and physico-chemical modification pathways were also employed to evaluate nanocellulose potentiality for this purpose (Figure 3).

The manuscript is organized in three chapters. In Chapter I, a state of the art is setting the project scientific context. Nanocellulose are defined and their potentiality as well as their industrial potentiality is overviewed. Existing solutions to provide non-adherent and greaseproof paper coating are depicted and a definition of superhydrophobic and superoleophobic surfaces is given. Lastly, existing modification or use of nanocellulose to obtain such non-adherent and grease repellent surfaces is also summarized.

In **Chapter II**, the use of the chemical reactivity of nanocellulose with organotrialkoxysilanes is assessed in order to be used as functional material. Different approaches (including chemical, physical and physico-chemical) for functionalization of cellulose nanofibers films have been done. Chapter II.1 evaluates the effect of alkyl chains end groups of organo silanes on their reactivity toward cellulose nanofibrils bonding and end material properties. Then, Chapter II.2 aims at identifying the best roughness parameters to provide superhydrophobic nanocellulose surfaces. Finally, Chapter II.3 is studying particles made out of organotrialkoxysilanes in water and their potential in modifying cellulose nanofibers to give hydrophobic and antimicrobial characters.

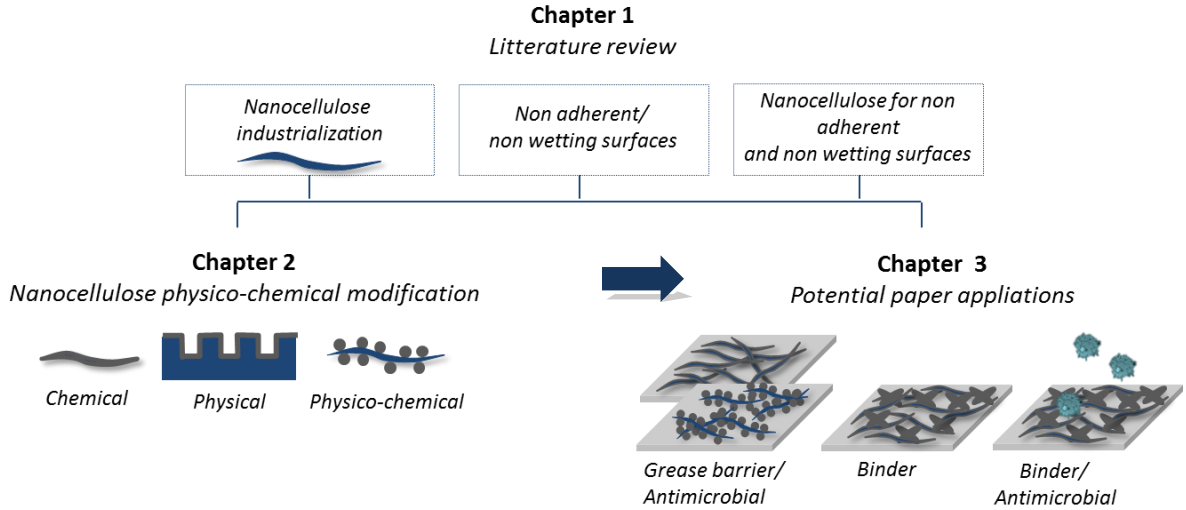


**Figure 3. Schematic representation of PhD thesis manuscript content.**

In **Chapter III**, the use of the functional nanocellulose based suspension in coating of paper is carried out. Chapter III.1.1 is assessing the potential of organoalkoxysilanes based coating on thin paper for grease barrier and antibacterial purpose. Both chemical and physico-chemical modification effects were tried. Chapter III.1.2 is using modified CNF as a replacement of

petrol based latex binder in superhydrophobic coating suspension. Finally, Chapter III.2. is assessing superhydrophobic paperboard coating as potential antibacterial adhesion reducing strategy.

The manuscript is partly based on scientific publication but also written in the form of chapters structured as a scientific publication.

This PhD thesis is providing understandings on the functionalization of CNF through chemical and physico-chemical modification as well as on chemical interaction with organotrialkoxysilanes. It also provides several possible innovative applications in specialty papers

## References


Aulin, C., Gällstedt, M., Lindström, T., 2010. Oxygen and oil barrier properties of microfibrillated cellulose films and coatings. Cellulose 17, 559–574. doi:10.1007/s10570-009-9393-y

AWA, 2015. Specialty paper and the future - A european specialty paper & paperboard market overview in global context. CEPI European Paper Week, Brussels, Belgium.

Bardet, R., 2014. Nanocellulose as potential materials for specialty papers,Ph.D manuscript, Université Grenoble Alpes.

Bardet, R., Bras, J., 2014. Cellulose Nanofibers and Their Use in Paper Industry, in: Handbook of Green Materials., World Scientific, pp. 207–232.

Bardet, R., Bras, J., Belgacem, N., Agut, P., Dumas, J., 2014. Method for Marking Paper. WO2014118466 (A1).

Benford, D., Boer, de J., Carere, A., Domenico, di A., Johansson, N., Schrenk, D., Schoeters, G., Voogt, P., Dellatte, E., others, 2008. Opinion of the scientific panel on contaminants in the food chain on perfluorooctane sulfonate (PFOS), perfluorooctanoic acid (PFOA) and their salts. EFSA J. 1–131.

Boufi, S., González, I., Delgado-Aguilar, M., Tarrès, Q., Pèlach, M.À., Mutjé, P., 2016. Nanofibrillated cellulose as an additive in papermaking process: A review. Carbohydr. Polym. 154, 151–166. doi:10.1016/j.carbpol.2016.07.117

CEPI, 2016. Key Statistics 2016 European pulp & paper industry. http://www.cepi.org/system/files/public/documents/publications/statistics/2017/KeyStatistics2016_Final.pdf

Chauve, G., Bras, J., 2014. Industrial Point of View of Nanocellulose Materials and Their Possible Applications, in: Handbook of Green Materials. World Scientific, pp. 233–252.

European Comission, n.d. COMMISSION REGULATION (EU)2017/1000 of 13 June 2017 amending Annex XVII to regulation (EC) No 1907/2006 of the European Parliament and of the Council concerning the registration, Evaluation, Authorisation and Restriction of Chemicals (REACH) as regards perfluorooctanoic acid (PFOA), its salts and PFOA-related substances.

Hietala, M., Oksman, K., 2014. technologies for separation of cellulose nanofibers, in: Handbook of Green Materials. World Scientific, pp. 53–71.

# Chapter 1
# Literature review

# Table of content

**Introduction** ..... **29**

**1. Toward nanocellulose industrialization** ..... **31**

1.1. Cellulose definition ..... 31

1.2. Nanocellulose definition and use ..... 32

1.2.1. Nanocellulose production ..... 33

1.2.3. Industrial and potential use of nanocellulose ..... 40

1.3. Nanocellulose in papermaking industry ..... 48

1.3.1. Bulk improvement of paper ..... 48

1.3.2. Surface coating of paper ..... 51

**2. Anti-adherent and barrier coatings** ..... **63**

2.1. Anti-adherent solution in paper industry ..... 63

2.1.1. Silicone coatings ..... 63

2.2. Grease barrier coatings ..... 66

2.3. Non-wetting surface ..... 68

2.3.1. Definition and measurement methods ..... 68

Surface design ..... 71

**3. (Nano)Cellulose functionalization for anti-adherence and barrier** ..... **77**

3.1. (Nano)Cellulose functionalization ..... 77

3.2. Organosilane based functionalization ..... 79

3.2.a. Hydrolysis and condensation of organoalkoxysilane ..... 79

3.2.b. Designing of material through condensation of mono or di-organoalkoxysilane solution ..... 79

3.2.c. Reaction with cellulose ..... 83

3.3. Superhydrophobic cellulosic materials ..... 86

**Conclusion and challenges...** ..... **91**

# Chapter 1. Literature review

## Introduction

The following chapter aims at introducing the basic knowledge of this PhD project which has been done within an industrial context.

*In grey and italic are comments in relation with this PhD project.*

The first part is giving an overview of existing bio-sourced raw materials used in papermaking industry and more precisely a closer focus is given on nanocellulose. As nanocellulose is the heart of this project, the material is defined, existing production methods are given and also it is assessed as industrial potential for papermaking process or paper products.

Among specialty papers, packaging and release paper are an important sector and current challenges in the industry are also reviewed in the second part. In this context, non-wetting surfaces such as superhydrophobic materials are getting more and more attention in material science and scientific knowledge under such development is then provided.

Finally, modification of nanocellulose in order to implement new non-adherent properties to this natural material and which could be helpful for a new product design is reviewed. Organosilane modification, which is of a great interest for papermaker because of aqueous reaction, is particularly described. It is assessed as chemical modifier but also physical modifier creating roughness. Existing non-wetting surfaces based on (nano)cellulose is provided to be compared to the project results.

# 1. Toward nanocellulose industrialization

## 1.1. Cellulose

The chemical identification of cellulose in plants should be attributed to Anselme Payen in 1837. From this point, almost two hundred years of researches have been done on this polymer. It was found not only in all vegetal species but also in fungi, algae, bacteria, or animals (O'sullivan, 1997).Thus, it is the most abundant polymer in the world with around 50 to 200 Gt produced annually mainly by vegetal photosynthesis but only few amount is extracted for applications (less than 5%) (Klemm et al., 2005). Cellulose within its different physical forms (fibers, regenerated cellulose or derivatives) have applications range from paper, textile, reinforcement for composites, bioplastic film, thickener or rheology modifier (Wambua et al., 2003).

Cellulose $(C_6H_{12}O_6)_n$ is a polysaccharide constituted of a linear arrangement of n anhydroglucose units (AGU) together linked through C1 and C4 $\beta_{1,4}$ glycosidic linkage (Figure 1-1). The two AGU repeating units are also called cellobiose. Polymerization degree on cellulose (n) is varying upon the natural source and can range from 500 to 10 000 for chemical wood pulp or pure cotton for example (Hon, 1994). On one side of the polymer chain is found a reducing end group which is a C1-OH in equilibrium with the aldehyde structure and on the other side a non-reducing C4-OH end group. Cellulose is composed of a high content of hydroxyl groups; 3 per AGU. These -OH groups are responsible for inter and intra molecular hydrogen bonding giving rise to a hierarchical structure.

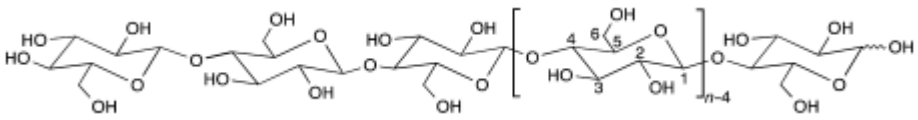

**Figure 1-1.Structure of cellulose polymer made with n anhydroglucose units (where n is the degree of polymerization (DP))**

The macromolecular structure of cellulose is hierarchically organized and presents a semi-crystalline form with amorphous region (low order) and highly crystalline form (high order). The cellulose crystal is the result of fully packed chains ordered in a regular manner and stabilized by the above mentioned hydrogen bond network. Four major polymorphs of cellulose crystals are existing, namely cellulose I, II, III and IV, among which, cellulose I is the most abundant one in nature (O'sullivan, 1997).

Cellulose I was discovered to be a combination of two polymorphs with triclinic ($I_\alpha$) and monoclinic ($I_\beta$) system for the unit cell (Atalla and VanderHart, 1984). Cellulose II is made by mercerization or dissolution/regeneration of cellulose I which is an irreversible process converting parallel chains of the cellulose I into anti-parallel chains. Cellulose II is used in the production of cellophane or viscose fiber in textile production for example. Cellulose $III_I$ can be reversibly achieved via treatment of cellulose I with an amine and $III_{II}$ via the treatment of cellulose II with the same. Cellulose $IV_I$ and $IV_{II}$ is obtained upon treating respectively cellulose $III_I$ and $III_{II}$ at 206°C in glycerol.

*In this PhD, we will focus on native cellulose at nanoscale, also called nanocellulose.*

## 1.2. Nanocellulose definition and use

As shown in Figure 1-2, crystalline part of native cellulose macromolecular structure is forming cellulose nanocrystals (CNC) while alternative part of amorphous and crystalline is forming fibers at the nanoscale called cellulose nanofibrils (CNF). CNC and CNF are called nanocellulose and CNCs are the smallest building block that can be found in cellulose. CNF with other biopolymers such as lignin and hemicellulose are arranged to create upper structured micro fibers arranged in layers, themselves creating a bigger fiber usually call lignocellulosic or cellulosic fibers with a diameter ranging from 15 to 30 µm (Figure 1-2). This hierarchical structure in plants is the key point of mechanical strength of biomass.

Cellulosic fibers as well as nanocellulose can be extracted from biomass and separated from other components constituting it.

Cellulose can be extracted from different biomass sources such as wood, annual plant, crops residues or marine biomass through mechanical and chemical treatments well-known as pulping (Huang et al., 2008). Lignocellulosic fibers pulp which is the first hierarchical material extracted is composed of lignin (20-40%), hemicellulose (15-40%), cellulose (40-60%) and a small part of extractives.

Further bleaching of the pulp permits the extraction of lignin and hemicellulose. Cellulosic fibers produced are then used as feedstock for paper, textile, cellulose derivatives or nanocellulose production.

*The last one has been recently discovered and will be one of the main materials in this PhD.*

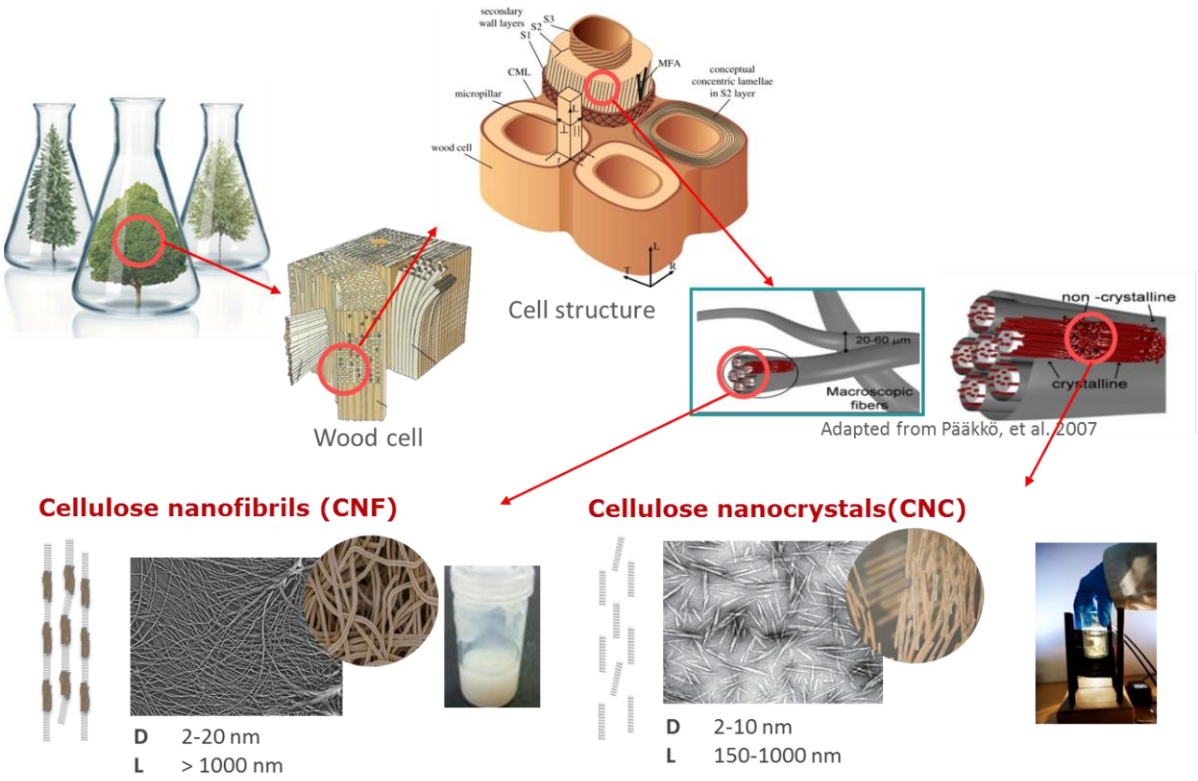


**Figure 1-2. From the biomass to the nanocellulose schematic representation.**

### 1.2.1. Nanocellulose production

Nanocellulose has been discovered in mid and late 20th century, for CNC and CNF respectively. Since the two last decades, the number of scientific publications in journals is rocketing as highlighted by Figure 1-3. Both CNC and CNF get this enthusiasm, which tends to reach a plateau last years. Subjects related to the isolation of nanocellulose, their characterization and their use.

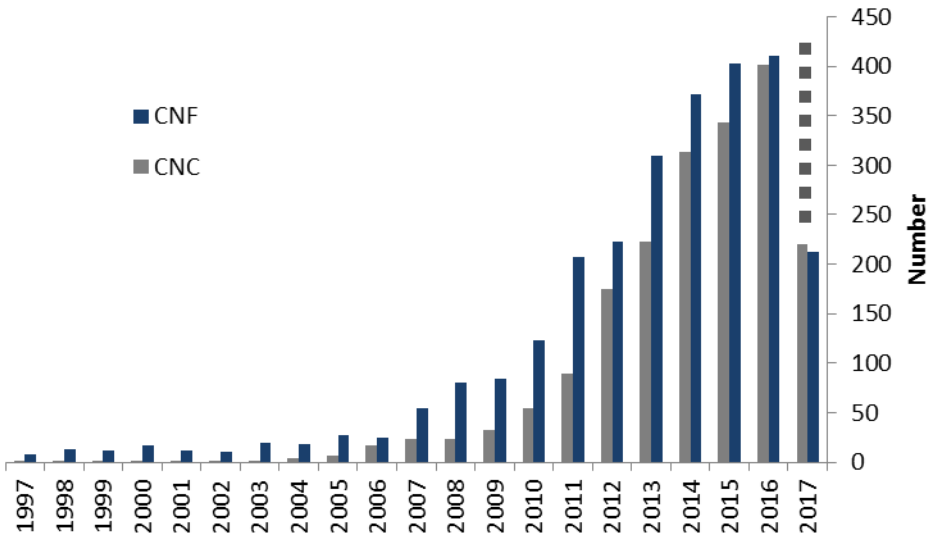


**Figure 1-3. Number of publications on cellulose nanocrystals and cellulose nanofibrils over past two decades. Research based on SciFinder and extracted with different acronyms for each nanocellulose category. (Descriptors: "Cellulose nanofibril", "Cellulose microfibril", "Cellulose nanofiber", "CNF and cellulose", "MFC and cellulose", "NFC and cellulose".) (1st May 2017).**

## Cellulose nanofibrils

Cellulose nanofibrils (CNFs) also call microfibrillated cellulose have structural dimensions of 2-60nm in diameter and several micrometers in length. As shown in Figure 1-4, the obtained suspension can depict high dispersity in size with the co-existence of fibre fragments, fines and nanofibrils at the same time. Production of CNFs has been done unintentionally for century with the refining of pulp to produce paper. But the production as a major component of a suspension is rather new.

The ones to obtain CNF were Turbak et al. (1982) and Herrick et al. (1983) by a strong mechanical treatment on a 2-3% pulp consistency with a high pressure homogenizer (80°C, 8 000psi). The resulting gel-like cellulosic material was depicting thixotropic properties and it was translucent.

After this first development, many other methods and processes were proposed in order to extract nanofibrils. The main goal has been the decreasing of energy costs and the enhancement of quality.

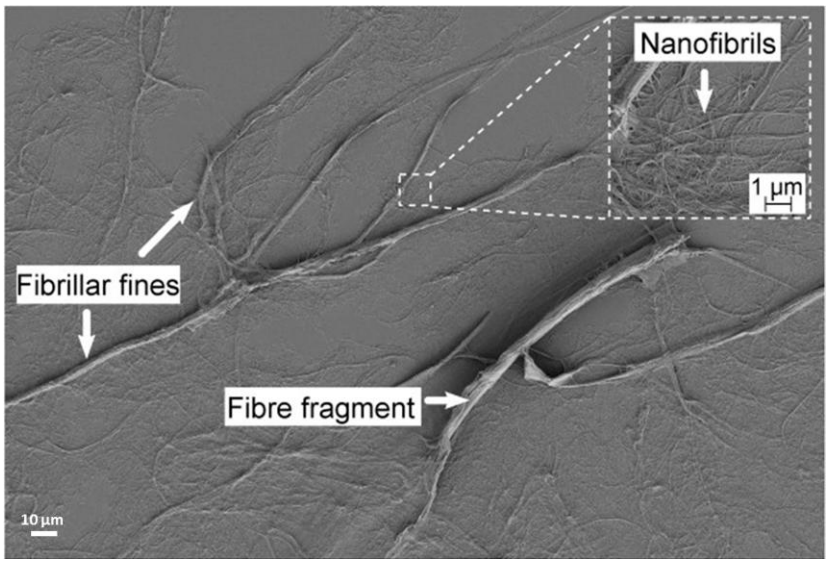


**Figure 1-4. SEM image of CNF obtained by mechanical homogeneization showing the dispersity in size of micro and nano fibrillar cellulose. (Chinga-Carrasco, 2011)**

*Biomass sources*

As cellulose, CNFs can be obtained by a variety of cellulose sources such as wood pulp (Syverud et al., 2011), annual plants (Alila et al., 2013), crops residues (García et al., 2016), (Santucci et al., 2016), algae (Hua et al., 2014), marine animals (Sacui et al., 2014) or bacteria (Gatenholm and Klemm, 2010).

However, the use of wood pulp is certainly the most common as it is already available in huge quantity due to paper production. Bleached kraft pulp but also sulfite pulp can be used and it was determined that the highest hemicellulose content the better the fibrillation was (Desmaisons et al., 2017).

Except from this, low effects of cellulose source on CNF quality and properties as material are observed (Vartiainen et al., 2015). Differences are mostly remaining on mechanical treatment and pretreatment.

*Mechanical treatment*

Mechanical treatment is used to physically disintegrate the cell wall along the longitudinal axis by applying shear forces.

Mechanical treatments existing for defribrillation until nanoscale material are based on high pressure homogenization (Pääkkö et al., 2007), microfluidization (Henriksson et al., 2008) and refining or grinding (Yuji Matsuda et al., 2001).

The GL&V Company is proposing also an industrial in-line production of CNF by a refining process. This process can produce CNF at an energy cost of 2 000€/t and at rates of 1 to 20 t/day depending on refiner configurations. Figure 1-5 is summarizing these industrial or pilot techniques.

Less conventional or emerging solutions are cryocrushing (Chakraborty et al., 2005), aqueous counter collision (Kose et al., 2011), high intensity ultrasonication (Cheng et al., 2009), steam explosion (Cherian et al., 2010), blending (Uetani and Yano, 2011), ball milling (Zhang et al., 2015b). Recently, twin screw extrusion was used to produce CNF and this technique already industrially available has a great potential (Ho et al., 2015), (Rol et al., 2017).

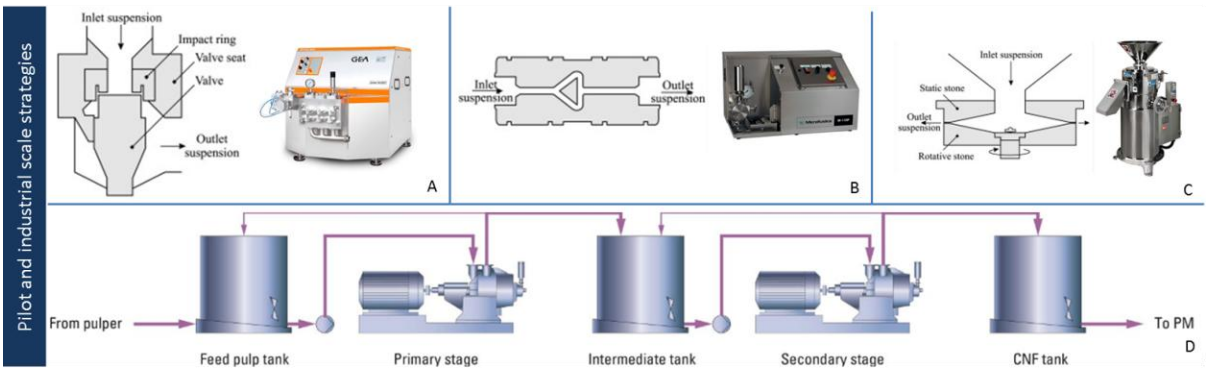


**Figure 1-5. Pilot and industrial conventional existing technology for producing cellulose nanofibrils. (A) High pressure homogenizer, (B) Microfluidization homogenizer, (C) Ultra-fine grinder, (D) Refiner**

But the energy consumption of such mechanical treatment was proved to be highly elevated (around 100 kWh/kg for unmodified cellulose preparations) which was a technological limitation has slowed down the industrial development of CNF production for decades. The research in pretreatment of the raw material before mechanical disintegration permitted to decrease this energy to as little as 1–2 kWh/kg (Tejado et al., 2012) at the end of 2000's.

***Pretreatment***

Several pretreatments were proposed in order to facilitate the extraction of nanofibrils from cellulosic fibers.

First, some mechanical pretreatments are found in the literature such as disk refining (Pääkkö et al., 2007), PFI (Henriksson et al., 2007) or valley beater. It permits a better yield and quality of end nanofiber after conventional treatment. But this kind of pretreatment does not show a big cost interest.

Mostly, pretreatments are today enzymatic or chemical.

The enzymatic pathway can involve different cellulases enzymes (endoglucanases, exoglucanases and cellobiases) which attack differently the amorphous cellulose structure but always giving a prehydrolysis which has a positive effect on further fibrillation. The use of a mono-component endoglucanase enzyme instead of a tri-component was shown to produce better fibrillation (Nechyporchuk et al., 2015). It is also reported that cellulose is not efficient under the presence of lignin which, then, has to be removed beforehand (Nechyporchuk et al., 2016). As evidence, such pre-treatment is decreasing DP but also increasing crystallinity index.

The main advantage behind the enzymatic treatment for industrial production is the low cost and environmental impact of enzyme action in addition to the fibrillation helps. Moreover, this procedure is completely adapted to papermaking industry which is already using such a strategy for refining pulp.

The last strategy is the chemical pre-treatment. The main strategy is the modification prior to mechanical disintegration. The mechanism involved is the creation of anionic or cationic surface charges on nanofibrils which will thus create repulsive forces in between and facilitate their deconstruction from the matrix. Figure 1-6 is summarizing the main existing chemical pre-treatment found in the literature.

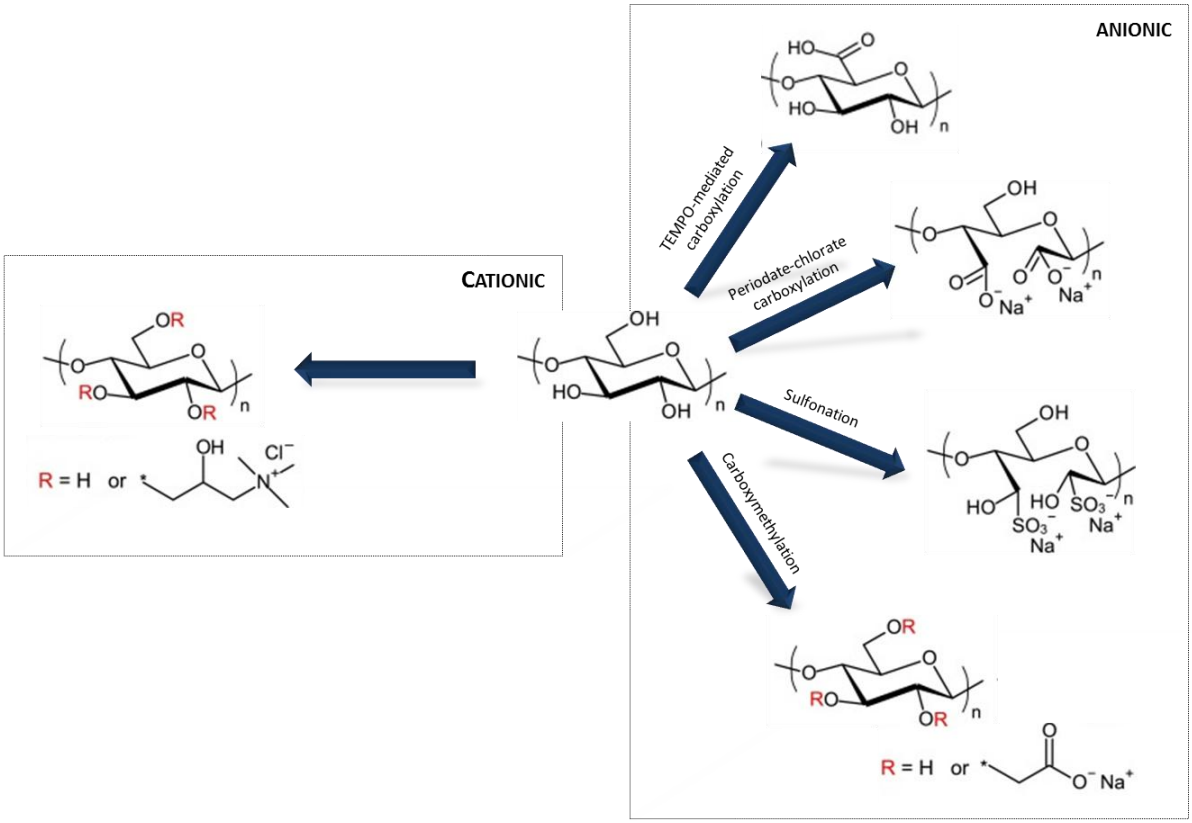


**Figure 1-6. Existing chemical pre-treatments leading to cationic or anionic cellulose species and helping in mechanical defibrillation of CNFs.**

Recently, ionic liquids (ILs) and deep eutectic solvents (DES) were proved to help also in the process of obtaining CNFs as pre-treatment (Li et al., 2012), (Sirviö et al., 2015) . ILs and DESs are able to dissolve cellulose through high interaction with the hydrogen bond network. DESs have a high potential as a solvent-based method for fibrillation as it can be biobased, with low toxicity and can be recovered. Only drawback is the temperature used during the reaction which was 100°C for 2h. No modification of the cellulose chains are made through these new pathways.

## Cellulose nanocrystals

Cellulose nanocrystals were first extracted successfully by Rånby in 1951 by submitting to cellulose fibers a controlled sulfuric-acid hydrolysis (Rånby, 1951).

Same diversity of cellulose resources can be used for producing cellulose nanocrystals. But in the case of cellulose nanocrystals, the source is affecting greatly CNCs properties and especially in terms of size (Habibi et al., 2010), as highlighted by Figure 1-7.

Acid hydrolysis is one of the two ways to permit the dissolution of amorphous region of the cellulose. The hydronium ion ($H^+$) will easily penetrate the amorphous region due to its low level of order, and promote the cleavage of the glycosidic bond leading to its dissolution in

oligomers and sugar unit, before attacking crystalline region. A non-controlled treatment could lead to complete dissolution of cellulose or to residual amorphous part. It is evident that a hydrolysis mechanism is cutting down the cellulose DP. Thus, a level-off degree of polymerization (LODP) is often used as the DP value where a stationary phase is obtained in this drop for a period of time, meaning that no more amorphous part is still present and crystalline part will start to be attacked (George and Sabapathi, 2015).

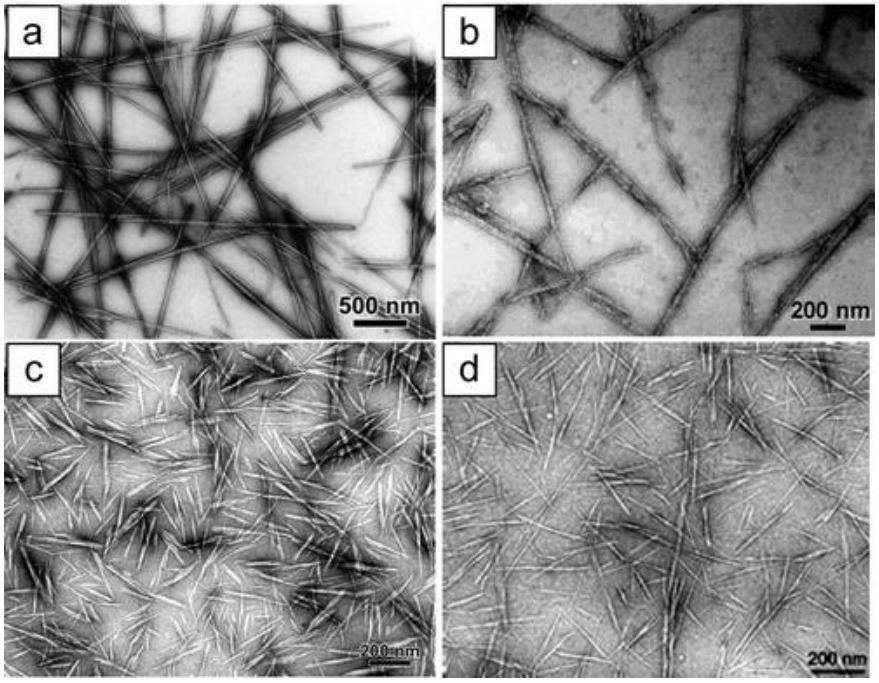


**Figure 1-7. TEM images of dried dispersion of cellulose nanocrystals derived from (a) tunicate, (b) bacterial, (c) Ramie, (d) sisal. (Habibi et al., 2010)**

The monitoring of such selective reaction is made by controlling acid concentration, temperature and time. Resulting crystallinity of cellulose nanocrystals is the same than the one of the fibers used as raw material.

Two main different acids are used: sulfuric acid ($H_2SO_4$) and hydrochloric acid (HCl). HCl pathway leads to nanowhiskers with low surface charge when $H_2SO_4$ hydrolysis give stable colloidal suspension thanks to the change of some hydroxyl groups in sulfate groups by esterification (Beck-Candanedo et al., 2005). These induced negative surface charges are avoiding the aggregation of CNC and it is why $H_2SO_4$ is much more used in literature.

Other acids were successfully tried for the same purpose such as phosphoric acid, hydrobromic acid, nitric acid or a mixture composed of hydrochloric and organic acids (Habibi et al., 2010).

Oxidation is a second method of used hydrolysis for obtaining CNCs even if it is much less common. A strong TEMPO mediated oxidation could lead to CNCs with carboxyl group surface as pre-treated CNFs (Montanari et al., 2005). As well, ammonium persulfate oxidation leads to the same COO- surface group (Castro-Guerrero and Gray, 2014). Lastly, enzymatic treatment and ILs have been used for synthetizing CNCs (B. Filson et al., 2009), (Man et al., 2011).

After any acidic treatment, a purification step involving dialysis, centrifugation or ultrafiltration is provided. Then, ultra-sonication of CNCs is usually following the synthesis of CNC in order to obtain homogeneous colloidal suspension dispersion.

*In this PhD, we will not work with CNC but focus on CNF as dispersing and coating binder for industrial applications. It was then important to update its industrial potential.*

### 1.2.3. Industrial and potential use of nanocellulose

#### Industrialization and market applications

Nanocellulose (CNF and CNC) was subjected to an enthusiasm in research but also in industry during the last decade (Figure 1-8). Until 2009, technological obstacles limited the explosion of industrialization of nanocellulose which was only restricted to few pilot scale productions or small commercial productions. Mainly, the lack of an added value and/or cutting edge application for these materials, the high production cost and competitiveness with other renewable or non-renewable materials and the precaution behind nano-toxicology were the reasons of a slow start in industry implementation. These are the reasons why almost no patents are displayed in Figure 1-8 until 2010.

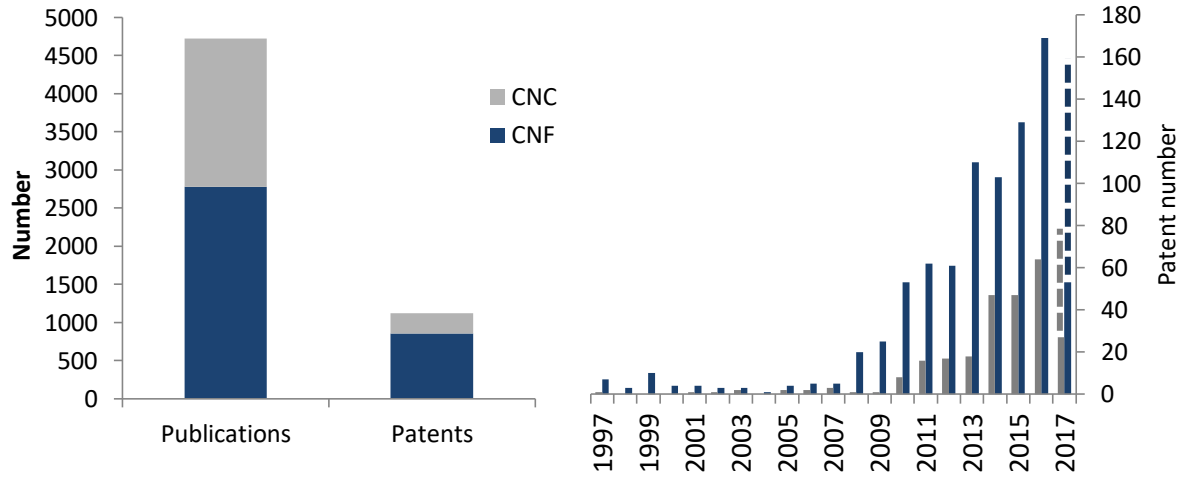


**Figure 1-8. Overall number of publications and patent from 1997 to 1st May 2017 (left side) and distribution with the two last decades for CNC and CNF patent (right). Dashed lines are predictions for the year 2017. Based on a SciFinder research. (Descriptors: "Cellulose nanofibril", "Cellulose microfibril", "Cellulose nanofiber", "CNF and cellulose", "MFC and cellulose", "NFC and cellulose", CNC and cellulose, "NCC and cellulose", "Cellulose nanocrystal", "cellulose nanowhisker", "cellulose nanorod".) (1st May 2017).**

The number of patents exploded from one per month to more than one per week within the past 5-10 years for both CNF and CNC even if it could be noticed that a higher amount was deposited for CNF (Figure 1-8). Research for applications but also low-cost methods for production were the main center of interest of these patents and publications. From this point, almost 40 companies or research laboratories started to produce nanocellulose all around the world as showed in Table 1-1. Even though no breakthrough application seems to stand out from the crowd, industrialization is moving a step forward with the development of industrial scale production plant in both CNC and CNF (Table 1-1). Producers manufacture various types of nanocellulose with different quality type and homogeneity in

size. Three producers of cellulose nanofibrils are mainly competing the market, Paperlogic in USA, Borregaard in Norway and Nippon Paper in Japan. Overall research centers or company starting to produce nanocellulose are mainly based in Europe, North America and Japan. They have targeted different end market applications within the two possibilities of main material or additive. This availability and the large input of efforts in industrial research will create a breakthrough in the technology field.

The BioBased Industry (BBI) consortium also targeted nanocellulose as the second priority in Europe, leading to an investment of 27 million euros granted partly to Borregaard to develop their MFC production. Canada has also participated in the investment of 20 million dollars for the production of cellulose nanocrystals.

**Table 1-1. Current producers for nanocellulose, with their daily production capacities and type of nanocellulose produced. * refers to research centers.**

| Company | Country | Yearly capacity | Production type |
|---|---|---|---|
| CNF/MCC/MFC plants | | | |
| Greencore composites | Canada | 40,000 t | MFC |
| FiberLean | France/switerland | 10,000 t | CNF with fillers |
| Performance Biofilament | Canada | 2,000 t | Nanofilament |
| Kruger/FPInnovation | Canada | 1,000 t | Nanofilament |
| Borregaard | Norway | 1,000 t | CNF |
| Paperlogic | USA | 730 t | CNF |
| Nippon Paper | Japan | 300 t | CNF Tempo |
| American Process Inc. | USA | 180 t | CNF |
| University of Maine * | | 110 t | CNF |
| Chuetsu Pulp & Paper | Japan | 50 t | CNF |
| DKS | | 50 t | CNF Tempo |
| Sugino Machine | | 50 t | CNF |
| Oji Holdings | | 40 t | CNF phosphorylated |
| Innventia * | Sweden | 35 t | CNF |
| CTP * | France | 35 t | CNF |
| PFI * | Norway | 35 t | CNF |
| Seiko PMC | Japan | 30 t | CNF |
| Tokushu Tokai Paper | | 30 t | CNF |
| VTT * | Finland | 15 t | CNF |
| Inofib * | France | 300 kg | CNF |
| Icar-Circo * | India | 11 t | NA |
| EMPA * | Switzerland | 5 t | CNF |
| SAPPI | Netherlands | 8 t | CNF |
| Daio Paper Corporation | Japan | NA | CNF |
| DIC corporation | | NA | CNF |
| Daicel Corporation | | NA | CNF |
| Stora Enso | Finland | NA | CNF |
| UPM | | NA | CNF |
| Bettulium | | NA | CNF Tempo |
| Norske Skog | Sweden | NA | CNF |
| Weidmann | Switzerland | NA | MFC |
| Cellucomp | UK | NA | CNF |
| BioNC | Spain | NA | CNF |
| CNC plants | | | |
| Celluforce | Canada | 365 t | Sulfated |
| American Process Inc. | USA | 200 t | NA |
| Holmen/Melodea | Sweden | 35 t | Sulfated |
| Icar-Circo* | India | 10 t | NA |
| Alberta Innovates | Canada | 7 t | Sulfated |
| Blue Goose Biorefineries | | 4 t | Sulfated |
| FPInnovations | Canada | 4 t | Sulfated |
| University of Maine * | USA | 4 t | Sulfated |
| Melodea | Israel | NA/ Pilot | Sulfated |

Mains applications of nanocellulose in the market are observed to be in large different branches from construction to packaging or automotive and cosmetics. CNC and CNF usually do not cover the same sectors. While expecting CNC in automotive polymer body reinforcement, CNF are more likely to be used in cosmetics of paper fillers. Technological readiness level is high for more than 70% of the identified application industry meaning that it is now reaching demonstration or even commercial level (Figure 1-9). Biggest sectors where the world average estimate in tons per annum of demand in nanocellulose would be the highest are packaging coating (5278 t/y), automotive body and interior (4160 t/y), replacement for plastic packaging (4153 t/y), cement (4130 t/y) and hygiene and absorbent product (3241 t/y) (Shatkin et al., 2014).

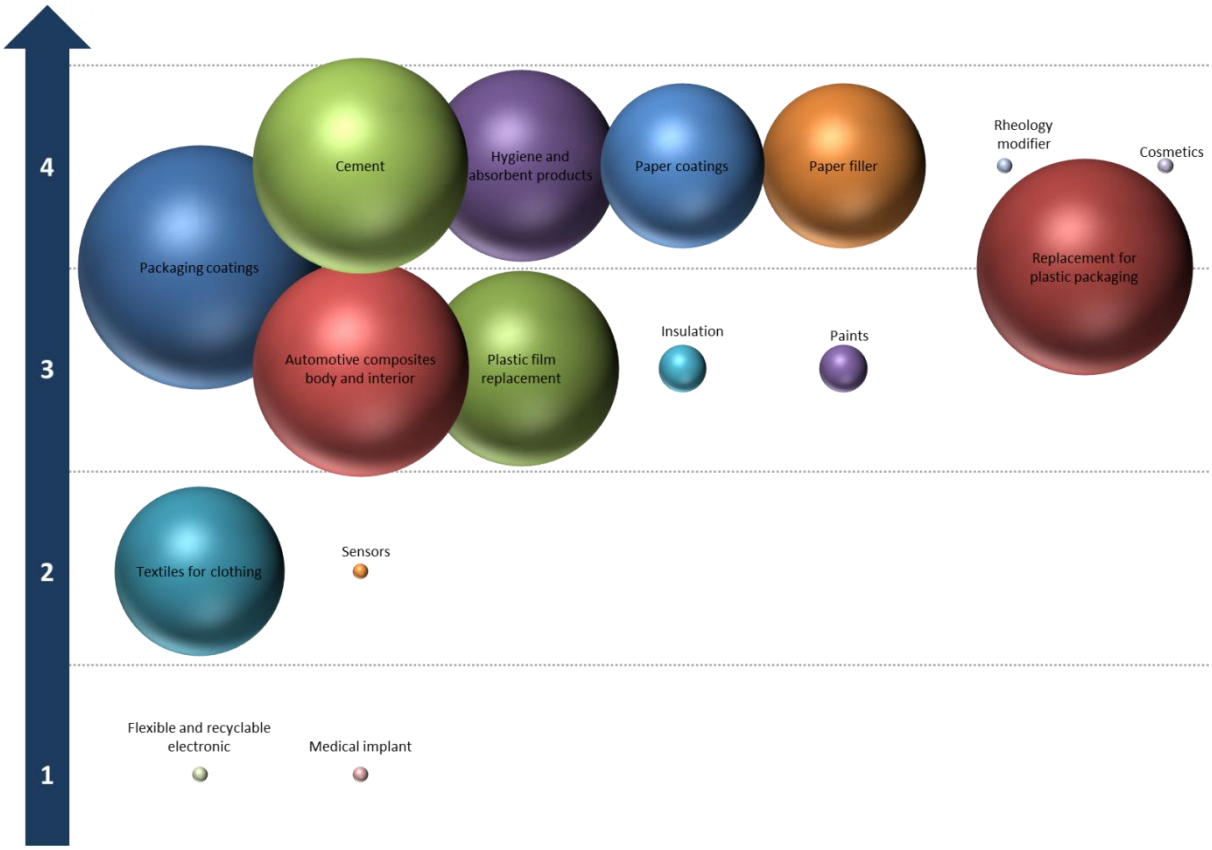


**Figure 1-9. Technological advancement (rate on 4) of each potential segment of use of nanocellulose. Horizontal axis is a random axis, size of bubbles are representing world market estimation 2014 (t/y). Small sizes are representing emerging technology and are not representative because of no available data. (Future Markets, Inc., 2016), (Shatkin et al., 2014)**

*During this PhD project, the main focus was on paper coating in specialty paper for packaging applications.*

## Nanocellulose properties and potential uses

The industrial potentialities of nanocellulose are based on their properties in aqueous suspension but also their ability to reinforce material or to have specific property as dry assembled product.

### Properties of nanocellulose in suspension

In suspension, cellulose nanofibrils and cellulose nanocrystals have the particularity to form a viscous gel at low mass concentration (2wt %). Both suspensions display a shear-thinning rheological behavior which is very interesting for coatings for example (Pääkkö et al., 2007).

**Table 1-2. Properties of CNF and CNC in suspension. Adapted from (Pääkkö et al., 2007), (Gray, 1994), (Bardet, 2014), (Puisto et al., 2012) .**

| | CNF | CNC |
|---|---|---|
| **Visual aspect** |  |  |
| **Rheological behavior** | Shear-thinning behavior<br>Depends on manufacturing process and fibrillation<br>Shear-rate hysteresis loop | Lyotropic liquid crystals with a four-region rheological behavior:<br>• Isotropic<br>• Iso and anisotropic<br>• Anisotropic<br>• gel |
| **Origin** | Gel structure with sintered flock<br>Temporary hydrogen bonding and VdW interactions | Negative surface charges and colloidal repulsions<br>Rigid rod-like particles |

Some differences are observed for CNC suspension, as highlighted by Table 1-2, due to the rod-like shape of CNC but also the charge repulsion by sulfonate content on their surface. As CNC can self-organize in a chiral nematic structure, the optical behavior is presenting an iridescence of suspension (which can be kept in the dry form of a CNC film under certain conditions (Bardet, 2014)).

In this project, as cellulose nanofibrils are the main raw material, a focus on their self-entanglement in suspension is made.

Early in their discovery, nanofibrils suspension rheology was thought to be possibly used in different applications as a rheological modifier such as in paints, cosmetics or food additives

(Albin F. Turbak, Fred W. Snyder, Karen R. Sandberg, 1982) (Herrick et al., 1983b). Since that time, several researchers proposed their use to stabilize other particles like $TiO_2$ (Bardet et al., 2013a), silver (Kaushik and Moores, 2016), carbon nanotube (Koga et al., 2013) etc. classically used in these fields. The increase in viscosity (stokes law) and the entanglement limits aggregation and sedimentations. Such suspensions have adapted rheology properties which can be finely tuned by addition of electrolyte (Naderi and Lindström, 2014) or water soluble polymers (Hoeng et al., 2017).

More details concerning paper surface coating are available latter in section I.1.3.2. Surface coating of paper.

In inkjet printing, the addition of cellulose nanofibers in the ink permits the inhibition of the coffee ring effect due to their ability to modify the rheology, disperse particles but also to retain water giving rise to more homogeneous and sharp printing images (Ooi et al., 2017). As well, in 3D printing, cellulose nanofibrils are used for their rheological properties in designing the specific ink needed. Indeed, CNFs permits the viscoelastic response of the ink needed to print long filaments and also provide mechanical properties and porosity control. As it is biocompatible, it was also used as scaffold for cell in 3D-printing tissue engineering, with a very high cell living rate in the formed hydrogel (Markstedt et al., 2015), (Sultan et al., 2017) .

Recently, this shear thinning effect of nanofibrils in suspension has retained lots of attention in oil recovery. Indeed, the trend in oil extraction today is to extract the most oil possible from a well (enhanced oil recovery), by adding liquid or gaz in the well brine aiming to help its extraction. CNF were studied as a potential material in this sector and display beneficial effects (Wei et al., 2016), (Monclin et al., 2015).

As well, the network formed by cellulose nanofibrils and their rheology was successfully assessed in regard to their ability to stabilize oil in water and water in oil emulsions for neat or hydrophobized nanofibrils of cellulose. (Andresen and Stenius, 2007a), (Lee et al., 2014), (Carrillo et al., 2015).

Such cellulose nanofibrils are thus interesting as a suspension in water as such but are also most of the time dried to obtain high performance dried material.

#### Properties of nanocellulose as a film/dry material

When dried materials are considered, main properties of cellulose nanocrystals is their outstanding mechanical properties and more particularly their Young's Modulus (between

120 and 250 GPa). This explained why most researches are focusing onto CNC nanocomposites as detailed in recent reviews (Mariano et al., 2014), (Oksman et al., 2016). They are also used in aerogel (De France et al., 2017) or in coating (Gicquel et al., 2017) but such 100% CNC materials are usually fragile compared to CNF.

Cellulose nanofibrils suspension can be dried in different ways to obtain materials. Dewatering processes are mainly casting evaporation or filtration for making CNF films also called nanopaper and freeze drying for aerogel.

**Table 1-3. General properties of CNF films in literature and comments on their explanations.**

| Properties | | | Origin |
|---|---|---|---|
| Contexture | Basis weight | 17-40 g/m² | Properties depending on homogenization, length of fibers, manufacturing method |
| | Thickness | 21-33 µm | |
| | Density | 0.8 – 1.2 | |
| | Porosity | 19-40% | |
| Optical | Transparent | | High density |
| Mechanical | Tensile strength | 100-150 MPa | High specific area, high hydrogen bonding (hydroxyl groups), CNF flexibility and ability to form an entangled network |
| | Young's Modulus | 10 -18 GPa | |
| | Elongation | 5-8% | |
| Barrier | Air permeability | 9-13 nm/Pa.s | High cristallinity and dense network with low porosity |
| | Oxygen permeability | mL/m².day | |
| | Water vapor permeability | 5-10. $10^{11}$ g/m.s.Pa | |
| | Grease barrier | | |

As a film, the dense cohesive network formed by entangled nanofibrils is giving special properties to the final material. Indeed, the as called "nanopaper" is translucent or even transparent and flexible. Compared to a paper, the nanopaper is non-redispersible in water due to the high bonding of entangled nanofibers resulting from drying.

The entangled network, closely packed, was assessed by different research groups for barrier to oxygen, water vapor or grease (Aulin et al., 2010a), (Lavoine et al., 2012a), (Österberg et al., 2013),(Bardet et al., 2015). Gas permeation is very difficult through the film

as the high crystallinity domains of CNF are blocking the gaz and pores are very small nanometer scale and tortuous. Films provide competitive values regarding oxygen and grease barrier properties. However, water vapor permeability is too high at high humidity to challenge some packaging polymers such as polyethylene terephthalate (PET) or polyethylene (PE). Multilayer strategies are usually proposed in this case with positive impact such as CNF coating on PLA (Meriçer et al., 2016).

The network formed by the CNF can be used also as a drug delivery system. Kolakovic et al., (2012) loaded several drugs in the CNF network during the film forming step with filtration. They proved that drugs, loaded at 20 to 40wt%, can be delivered slowly for several days (up to 90 days) and that interaction between drug and CNF could enhance this time. Of course, such an application would be for long time treatment diffusion and not oral immediate diffusion of a drug.

Due to the nano-size of the particles, films are presenting a very high smoothness and thermal stability and become also very interesting as a renewable materials for printing electronics substrate (Zheng et al., 2013),(Hu et al., 2013). Indeed, to ensure a good conductivity of the ink, a smooth surface is needed to give the pattern a good continuous shape that is not penetrating too much inside the substrate. This kind of research paved the way for the use of cellulose nanofibrils films as sensors, flexible electronics (Hoeng et al., 2016) etc.

Cellulose nanofibrils modification (TEMPO, silylation, phosphorylation,…) are different regarding these properties and can introduce new properties like water adsorption or fire retardancy (Ghanadpour et al., 2015). There are also lots of researches using such a functionalization to obtain antimicrobial properties (Saini et al., 2016a).

However, as CNF production has been first commercialized by paper companies, several studies are in this field, which is the focus of this PhD. Therefore an overview of accomplishments on this topic is needed.

## 1.3. Nanocellulose in papermaking industry

Papermaking industry was thought to be the most concerned by nanocellulose development. Indeed, with a century-old industry producing cellulose pulp from wood and transforming it to a material, equipments and knowledges were already in place. Cellulose nanofibrils or microfibrils were even already produced online with a harsh refining and already present in the paper. Papermakers were only lacking the extraction or homogeneity of a high quality nanofibrils suspension. Interestingly, patented innovation regarding cellulose nanofibrils are, for at least two thirds, not applied for paper (Bardet, 2014). However, lots of the cellulose nanofibrils application domains could be related to paper production. CNFs can be used as a paper furnish but also as a coating for surface improvement (Brodin et al., 2014) or also in the emulsion based coating for functionalizing paper as shown by recent review or book chapter (Oksman et al., 2014), (Boufi et al., 2016).
In the following part, by mean of simplicity, CNF could be assigned for nano or microfibrils.

### 1.3.1. Bulk improvement of paper

### Paper properties improvement

The use of nanofibers in the bulk of paper comes from the observation that fibrillation of pulp increase generally the mechanical strength. The use of cellulose nanofibrils as improvement of paper sheet resistance density and air permeability was observed due to stronger hydrogen bonds interaction in the material.

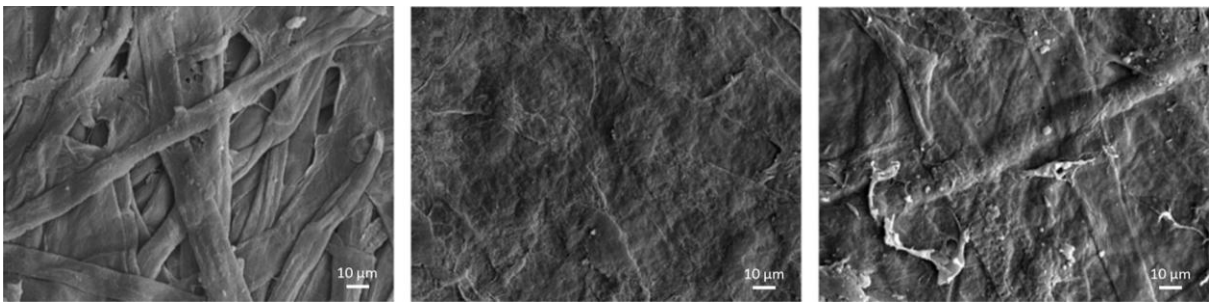


**Figure 1-10. From left to right: Bagasse fibers paper, CNF paper and paper with 30% CNF. CNF is considerably closing the paper and giving smoothness. (Hassan et al., 2011)**

First to study this effect on TMP pulp was Eriksen in 2008 who studied the impact of 4wt% of MFC addition on z-directional strength, density and air permeability. MFC were obtained by chemical pulp which seems to be an important parameter together with the chemical modification as reported by Brodin and Eriksen later (2015). Indeed, CNF obtained from

carboxylated TMP displayed lower mechanical properties but still higher than TMP CNF obtained only by homogenization (Osong et al., 2014).

The addition of higher content of CNF in paper sheet from bagasse pulp was tried up to 90% by Hassan et al. (2011). They showed that up to 30% wet tensile strength can be enhanced, after what a plateau was reached. After 30% a drop in burst and tear index was noticed. Surface of paper changed completely as showed in Figure 1-10.

The addition of 5 to 50% of hydrophobized CNF by a patented AKD based emulsion process in paper handsheet was performed by Missoum et al. (2013a). With this hydrophobization on the nanofibrillar material they could improve air permeance and mechanical strength at the same time. They get also internal sizing, meaning less water absorption of the material, giving competitive value with industrial product.

Concerning the biodegradability and compostability of such paper with 1.5% CNF, it reached obviously European standard for packaging and CNF inclusion in paper even seemed to increase degradation rate (Vikman et al., 2015).

The increasing interest for CNF addition in paper is also reflected by pilot scale trials which are more present in CNF producing company presentation.

For example, GL&V Company at the University of Maine proceeded to a trial with CNF produced with the batch refining process of their own. They studied the addition of 1 to 7% of CNF in the paper pulp in blend or machine chest. They showed an increase of 6.9% for 1% addition to 28.4% for 5% addition in internal bond but also an improvement of almost 400% of gurley porosity and a decrease in roughness of about 10% with 5% CNF (Cowles, 2016). Higher proportion up to 15% were tested at a pilot scale and reported by Paperlogic. Porosity decreased continuously with the addition of CNF while tear index seemed to gain a maximum value. They also reported a change in surface aspect (Fein, 2016).

Several examples can be listed and below are some of the opportunities and issues recently published.

## Opportunities and issues

### Polymer coating saving

As patented by UPM-Kymene and University of Maine, the addition on CNF in the bulk of paper could significantly improve release paper which is highly demanding in term of refining energy and polymer. The improvement of surface as well as barrier is lowering

refining cost and silicone lost in the paper bulk (Koskinen et al., 2017), (Bilodeau and Hamilton, 2013).

Such a strategy is very important and has been performed during this PhD with the industrial partner but is not detailed in this manuscript.

### Pigments or ash increase

The addition of more ash or pigments into the material is very interesting for papermakers as fibers cost more than ash and also because pigment is essential for brightness or opacity but deteriorate the mechanical properties of final paper.

Mörseburg and Chinga-Carrasco (2009) studied the effect of CNF addition in a multilayer thermomechanical paper sheet formation together with clays addition in the pulp. Clays usually deteriorate mechanical strength of paper as it disturbs the interfibrillar hydrogen bonding network. They showed that placing CNF in the center of the layered sheet and clays at the top with TMP pulp was beneficial for mechanical properties.

In their same pilot trial, GL&V proved that increase of ash content from 18 to 28% without deteriorating internal bond was possible with only 2.5% CNF addition in the bulk of paper(Cowles, 2016).

### *Diminution of papermaking aids quantity*

By mean of higher surface area and hydroxyl groups amount, the use of cellulose nanofibrils was thought to retain more sizing agents such as poly(amideamine (PAE) which is giving wet and dry strength. Ahola et al. (2008) studied two ways of CNF addition and PAE, as a bilayer or nanoaggregates structures. They did not observe any increase in PAE retention but a much better distribution of PAE in the matrix, leading to the multiplication of the wet tensile strength by almost five and the dry one by more than two.

### Paper recycling

As explained by Delgado-Aguilar et al. (2015) the deinking and recycling of paper such as newspapers raise the problematic of decrease of strength of recycled paper. Today, the solution to avoid this is to beat pulp to obtain more fibrillation. As consequences, dewatering process takes longer time and fibers get shortened. In their study, 1,5wt% CNF and a retention additive were proved to have a similar effect on final breaking length of deinked paper. The drainability was identified as a potential problem for runability.

### Drainability issue

But the addition of CNF, as it is with refining, increases generally water retention values of paper and thus decreases the running capacity of a papermaking machine. The dewatering time can be further deteriorated by chemical modification such as carboxymethylation, which can grow by six time in this case (Brodin and Eriksen, 2015).

In their study, Taipale et al. (2010), showed that at constant parameters, CNF increased strength at the same time of drainage but, by modifying process conditions such as polyelectrolytes, pH, salt concentration it is possible to enhance the strength without affecting drainability. Researchers from UPM-Kymene (Kajanto and Kosonen, 2012) went into a similar conclusion by proving that CNF addition by one or two percents and simultaneously addition of cationic starch do not affect dewatering process and enhance air barrier and mechanical properties which was calculated as a possible decrease of 8g/m² of grammage.

With GCC fillers also, dewatering process change was not significant with MFC addition while air permeability, mechanical strength in z-direction and light scattering were improved (Hii et al., 2012). Several other studies based on CFN-pulp and PCC composites with content of respectively (20, 10 and 70%) were done on dewatering and wet pressing effect. Results highlighted the ability of such formulations to be processed on a paper machine with an optimum solid content between 5 and 10%. Dewatering was good and permitted a wet solid cake of 33% which is quite good results for papermaking process (Rantanen et al., 2015b). Wet pressing of such material compared to raw pulp fiber was competitive (Rantanen and Maloney, 2015). Also, the same group of researchers showed that the more CNF were fibrillated the more dewatering process was long, but this could be overcome by in situ precipitation of PCC on CNF (Rantanen et al., 2015a).

In their pilot trial, Paperlogic reported a water line moving further down machine with increase CNF addition (Fein, 2016) but did not report any problem of drying and did not calculate the cost of related drying energy needs.

### 1.3.2. Surface coating of paper

Coating of paper with cellulose nanofibrils aims at functionalizing or improving paper properties and/or paper coating formulations. As a single coating material, the strategy tends to apply knowledge of CNF thin films features coated on a material. As an additive in

the coating formulation, it is more the rheological feature that is looked generally, the fibrillar interconnected network or the drying ability.

Three main challenges are held behind the use of cellulose nanofibrils. The first one is probably the high water content of the suspension. Industrially produced CNF suspension are made of 98 to 90% of water, and subsequent cost for drying get more elevated if used in a too high extent. The second is the rheological behavior of the suspension. As a very viscous

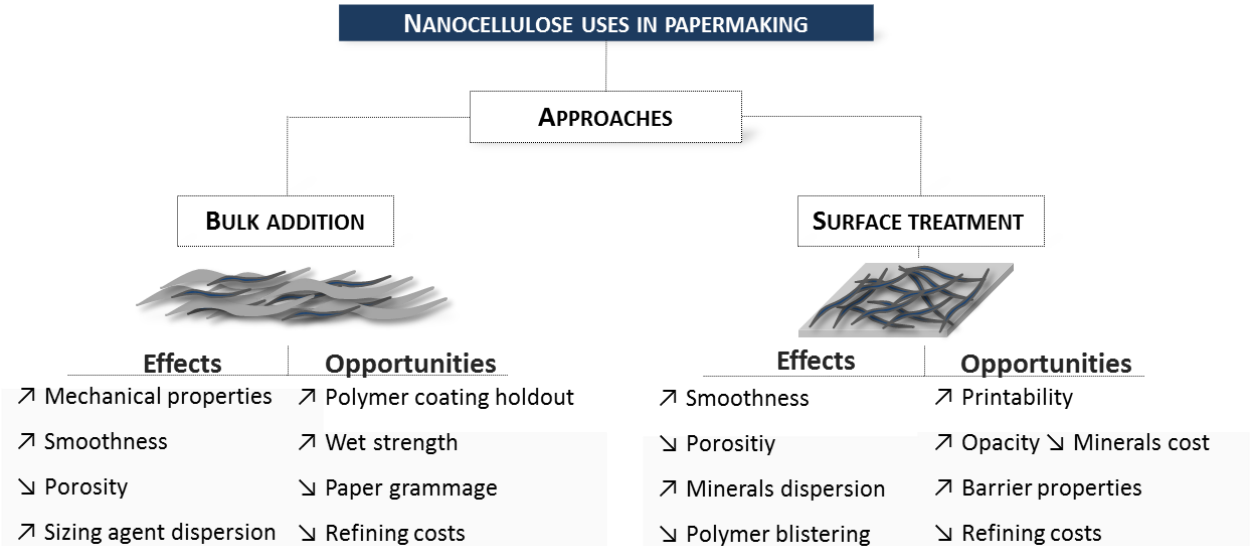


**Figure 1-11. Different uses of cellulose nanofibrils in the papermaking industry.**

material at low dry matter content, CNF show difficulties to be pumped and process with standard equipment. The third is being the coated material itself which is porous, hygroscopic and rough which makes the wanted end properties harder to obtain and completely different as a function of the paper.

Coating possibilities are wide in the industry. Mainly, in the papermaking process, are found film press, size press, spray coating, blade coating, rod coating or curtain coating. CNF coating suspension or CNF based formulation can be easily transferred to these conventional coating processes as it presents high shear and rheo-thinning effect behavior.

Coating on paper (or plastic substrate) of these CNF was performed in some studies. Various coating methods were used such as casting, filtration via sheet former, rod coating, size press, spray coating or slot die for example. Classical coating method such as rod coating do not permit high coating thickness in one passing as CNF suspension is usually containing very low amount of dry matter content (0.8 to 2wt%) (Aulin et al., 2010b). Rod coating of 2wt% CNF in one passing could reach 2g/m² of CNF layer but further increase would involve more passing above the previous one to reach 14g/m² after 10 passing, which is industrially

not viable (Lavoine et al., 2014a). Size-press coating seems to have a major drawback corresponding to the high pressure in between the two rolls, leading to the penetration of CNF inside the material and the opening of the paper structure (Lavoine et al., 2014a). The coating weight is, as consequence, very low with 3g/m² after three passes. Size press coating with different methods (flooded nip or metered), rod coating and cylinder coating were compared and a predictive model of coating weight according to nip pressure, solid content or speed was tried to be applied in some case (Finley Richmond, 2014). After parameters modification, the coating weight with flooded size press is between 1 to 5 g/m² maximum. The metered size press was able to coat higher amount comparing to the flooded one. Spray coating with a 2wt% CNF suspension can provide coating layers from 3-4g/m² up to 13-14 g/m² (Beneventi et al., 2014). Authors showed that, with this technique, after 6g/m² the layer was able to close highly porous paper. New technology for spraying CNF industrially, called HydraSizer®, showed that, the more the CNFs were coated at the beginning of the wet end of the papermaking process the more it penetrates into the material (Fein, 2016). Interestingly, slot die coating seems to be a very good opportunity as well. By controlling process parameters such as web speed, feeding pressure in the coater, web to slot distance, slot die opening thickness, it is possible to deposit a layer of CNF up to 16g/m² in one passing (Kumar et al., 2016). They also overcome water retention, responsible for paper cracks by the addition of 3 pph of CMC.

Such a coating of CNF modified or not, can be used for different end applications.

### Printability

Printing process requires usually a smooth and a relatively closed surface so that ink is not penetrating into the material and narrow shape line with high definition can be made.

This is especially true regarding printed electronics where conductive inks should be able to create a continuous line to ensure its conductive property. Studies tends to prove that cellulose nanopaper have greater smoothness and low porosity as compared to paper and can be competitive with polymers in regard to these specific properties (González et al., 2014). Depending on printed material, a sintering process of the ink could be asked and therefore, the material should handle temperature up to 250°C without deformation. Printed electronic evolution is moving toward flexible and transparent supporting material. In this way, polymers but also paper and nanopaper are advantageous. As reviewed by

Hoeng et al. (2016), CNF and CNC were studied for two major purposes: enhancing the material surface properties or create flexible and transparent devices. We will focus only on the first part. In the review, mainly CNF was studied as, according to authors, it is the main material employed for this in the literature.

Nanopaper was proved to be relevant as a material for enhancing surface properties for printing electronics (Hsieh et al., 2013), (Nogi et al., 2013). In their study, Hsieh et al. (2013) compared two conductive ink printing processes on three different substrates which where paper, nanopaper and conventional polyimide substrate. Electrical resistance of the line

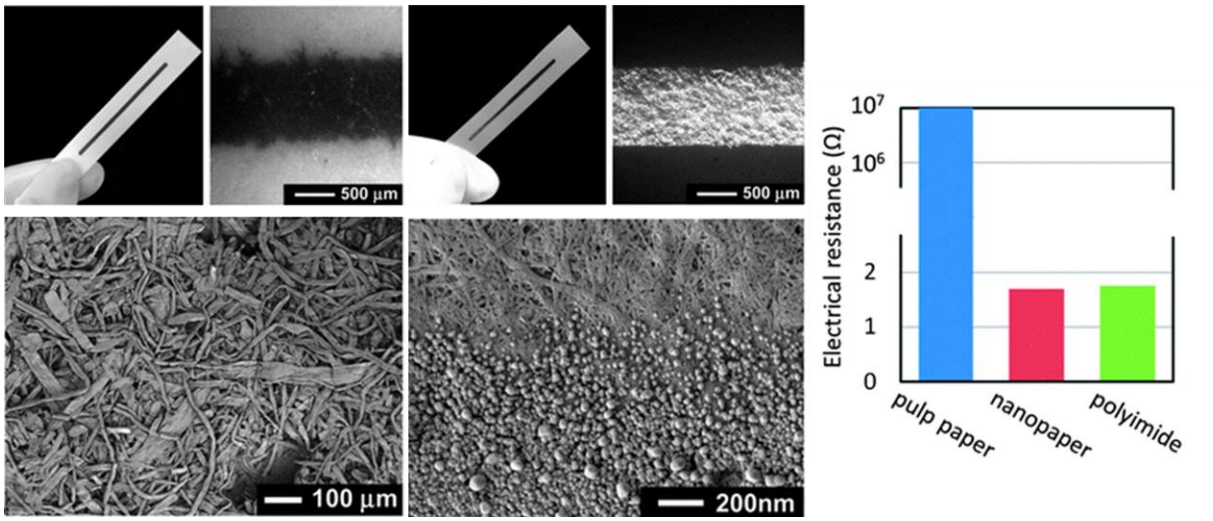


**Figure 1-12. Silver particles ink lines on a paper (left and a nanopaper (right) with different observation scale. Electrical resistance of the lines compared with polyimide film.Adapted from Hsieh et al. (2013).**

made by the first printing process was very high for paper while a 180 time lower value was reported for nanopaper. Depending on the ink chosen, the value was sometimes higher but they also to equalize the value on a polyimine smooth film. The inkjet printing was shown to be relevant, by obtaining similar conductivity for nanopaer and plastic while traditional paper was out of the goal. They even show that nanopaper was more interesting than polyimide while having a sintering process.

The effect of chemical treatment on these properties was evaluated by (Chinga-Carrasco et al., 2012). They demonstrated that better resolution is obtained with TEMPO CNF compared to CNF film as a higher smoothness is obtained due to reduced nanofibril size. But the high surface energy of the film was a disadvantage regarding ink spreading. Carboxymethylated CNF modified hexamethyldisilanaze provided as a good compromise for the printing of conductive lines.

Composites structures were also studied with CNF being as an additive for dispersing highly smooth clay that is kaolin. After a calendering process, the material was as smooth as PET and provide similar conductivity (Torvinen et al., 2012).

However, these studies are made on free standing CNF films but no publication regarding CNF coating on a paper is available at this moment. Hamada et al. (2010) presented the effect of pure CNF coating as well as CNF-clay coatings on printability with a flexographic process. It was shown that a 3g/m² layers was beneficial for printing density. They also compared CNF with other classical starch coating and did not show any significant improvement.

Recently, at the TAPPI Nano conference gathering expert and industrial companies working with nanocellulose, the FiberLean Technology Ltd presented their work on corrugated cardboard coating (Svending et al., 2017). In the context of increasing demand for printed white cardboard box for packaging and marketing purpose, the need to develop an in-line white coating before inkjet printing is valuable. The coating was done with MFC (20%) and minerals such as ground calcium carbonate (80%). The coating has a good opacity, optical brightness and porosity which increase with increasing coating grammage (from 10 to 40 g/m²). They proved an ink density after inkjet printing above conventional white test liner used for such box.

### Barrier coating

Coating of CNF onto paper was thought to improve barrier properties because of natural tight network. As nicely reviewed by (Lavoine et al., 2012b), some researcher proved the efficiency of CNF films to be barrier to oxygen and grease and were then expected to be very promising as packaging material or as a coated material in a multi-layer strategy.

CNF films were first assessed regarding oxygen permeability by Syverud and Stenius (2009) on 35g/m² nanopaper made with cellulose microfibrils extracted from bleached spruce sulfite pulp. They found a value of oxygen permeability between 0.352 and 0.505 of 17 $ml.mm.m^{-2}.day^{-1}.atm^{-1}$ at 0% relative humidity on top side and 50% on bottom. This is competitive to other synthetic polymer and even lower. No measurement was done at higher relative humidity which is important as CNF films under humid conditions tend to swell, thus, degrading barrier properties.

Liu et al. (2011) evaluated CNF extracted from bleached sulfite pulp film properties at different ranges of humidity. At 0 %RH, value was under detection limit, at 50 %RH they got 0.048 and at 95 %RH 17.8 ml.mm.m$^{-2}$.day$^{-1}$.atm$^{-1}$. Differences between the two studies are held behind the thickness difference by an order of two and also the humidity profile used. Meanwhile, reaching high oxygen permeability is also a consequence of thickness because of increasing possible pathway distance and also because most pores are localized at the surface and not interconnected with the others.

However, oxygen permeability is also a consequence of pore closing and tortuosity as shown in the same study with the implementation of montmorillonite clay. Indeed, fiber swelling at high relative humidity consequently opens pores. Montmorillonite as a platelet like material, included at 50 wt% in the film closed the structure and increased the pathway distance through the film. This technique decreased by 5 the oxygen permeability at 95 %RH while having same value at 0 and 50 %RH. Another study on this topic confirmed the positive impact of clays and compared with the addition of Tempo-CNC (TCNC) (Bardet et al., 2015). Reverdy et al. shared this result at the TAPPI Nano 2015 conference proving that the addition up to 33 % of TCNC in CNF network followed by a thermal treatment was almost competitive with cellulose nanofiber and nanoclays composite at high relative humidity regarding oxygen and water vapor permeability.

The effect of chemical modification was also compared with carboxymethylation of CNF by Aulin et al. (2010b) and a decrease by 4 to 6 fold was observed with this modification at 50%RH. TEMPO oxidation is also a very good modification as it shortens fibers and thus decreases porosity. As shown by (Shimizu et al., 2016), TEMPO oxidized CNF extracted from softwood bleached kraft pulp provide OP value in the order of 0.2 ml.mm.m$^{-2}$.day$^{-1}$.atm$^{-1}$ at 50 % relative humidity and 10 ml.mm.m$^{-2}$.day$^{-1}$.atm$^{-1}$ at 80% RH which is lower than non-modified CNF films . The counter ion of the carboxyl group was proved to have a significant impact on OP as well. Indeed, replacing $Na^{2+}$ by $Ca^{2+}$ reduce the OP from 0.2 to 0.002 ml.mm.m$^{-2}$.day$^{-1}$.atm$^{-1}$ at 50%RH and from 10 to 0.08 ml.mm.m$^{-2}$.day$^{-1}$.atm$^{-1}$.

During a collaboration in parallel with this PhD, we have also proved the interest of using xyloglucans (XG) for such an application. Results showed that an excess of XG inside CNF network followed by a thermal treatment enhanced the oxygen barrier properties of the materials while without thermal treatment it does not. As well, coated paper with these

suspensions showed that a excess of CNF compared to XG was beneficial to a grease barrier when coated with 7 g/m² (Reverdy et al., 2016).

Regarding coatings of such CNF, Syverud and Stenius (2009) coated a CNF layer from 2 to 8g/m² which was deposited by filtration using sheet formation. The air permeability was shown to be decreased by two to 100 respectively to the increased coated grammage.

Similarly, Aulin et al. (2010b) studied the effect of the coating of carboxymethylated CNF on the air permeability of a kraft and a greaseproof paper. A coating grammage between 0.25g/m² and 1.8g/m² was applied with a rod coater (Figure 1-13). The air permeability of the kraft paper was divided by almost 15000 times while for greaseproof paper, which is a relatively closed paper, by 3000.

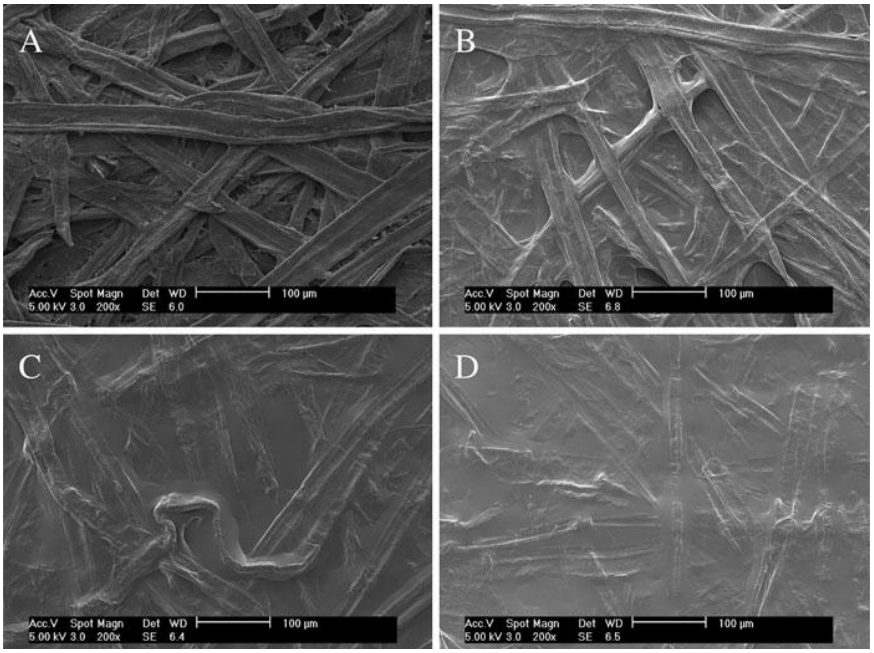


**Figure 1-13. E-SEM picture of uncoated (a) and MFC-coated unbleached papers with coat weights of ca. 0.9 (b), 1.3 (c) and 1.8 g/m2. (Aulin et al., 2010b)**

The growing interest in surface coating with CNF is observable thanks to pilot scale trials as well as to industrial developments of coating device. Recently, Kumar et al. (2016), coated a CNF suspension in a pilot scale slot die coater on a paper with a roll-to-roll process and assessed the barrier properties. They also showed that 1g/m² has already a positive impact on it. They showed that after 6g/m² coated layer grammage, the WVTR value drops of almost 85%. Authors precise that even if this value is fairly lowered, the obtained value of around 100 g/(m².day) is still very high to fit packaging requirement. Exactly the same tendency regarding air permeability is observed. Value drop from 1 µm/(Pa.s) to below

detection limit (0.05 µm/(Pa.s)) after 6g/m². The evaluation of barrier properties was also extended to oil barrier as it is a very important parameter for packaging material. They were the first to our knowledge to propose the measurement of heptane vapor transmission rate in this context. No heptane vapor was detected at a coated layer of 9 g/m² and above and even at 6g/m² the detection was close to zero. A KIT test was performed on the paper, which is a very selective test for packaging material. Base paper got a KIT test of 0 as well as coated paper with 1g/m². After what, 4g/m² obtained a KIT of 1 and this value keep increasing until reaching a value of 10 for 11g/m² coated. A 6g/m² showed a KIT of 8 which is already a fairly good value. As well, after 50h no mineral oil transmission through the material was observed for the paper coated with 9g/m² CNF layer. CNF coating is showed to improve greatly paper performance with barrier. But the high WVTR value of the hydrophilic CNF is also a problem. The need of a large coating layer is important to meet packaging goals and the cost of CNF is too high at the moment to provide competitive solution. This way, some researches focused on multi-layer material where advantages of all material are combined to create a high value end product.

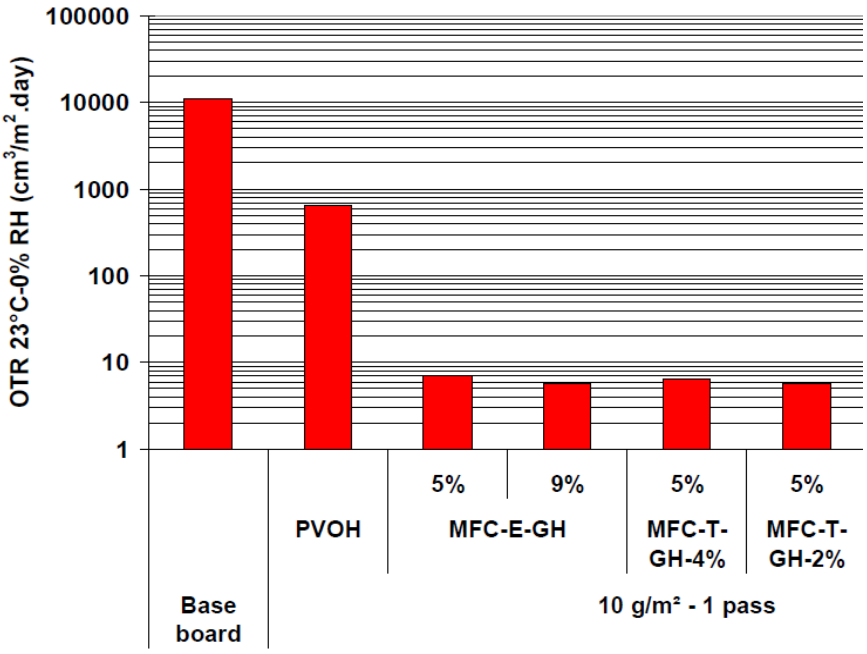


**Figure 1-14. MFC for barrier improvement in PVOH pilot scale coatings (Guezennec, 2012)**

The VTT research center in Finland presented recently their work on multi layered packaging made of PET-CNF or PET-CNF-LDPE with modified CNF. Plasma sylilated CNF as well as TEMPO CNF were tried and TEMPO CNF in between PET and LDPE showed a KIT of 12 a mineral oil barrier. However, the price of the material was doubled (Jari Vartiainen, 2014).

Similar to multilayer, Aulin and Ström (2013) deposited on a cardboard a layer of CNF followed by a layer of alkyd resin. A 3g/m² coating of CNF was enough for providing smooth enough structure so that the oil based second layer was easily applied. They determine that 14g/m² to 20g/m² of alkyd resin coating was enough to provide competitive WVTR value for packaging application. Hult et al. (2010) proposed also a strategy with a pre-coat of CNF with dynamic sheet former and second coat with shellac. While only CNF coating is having no effect on WVTR, the effect of shellac permit a tenfold increase of the barrier. But CNF have a great impact on OTR value and the additional shellac layer permits also to decrease this value by six times. However, the film formation has to be improved to reach value for packaging application.

Patent was deposited by the university of Maine for the surfacing of a paper with CNF for release paper (Bilodeau and Hamilton, 2013). Release papers, usually siliconized, are high cost product because of two factors: paper high refining demand and silicon price. CNF coating permits the reduction of roughness and the closing of pores and thus further refining of paper is not needed if a CNF coating is applied. It is also reducing the use of silicone by avoiding polymer penetration into the material.

Additionally to CNF coating in one or with a multi-layer strategy, CNF in barrier coating as additive also demonstrated interesting results. In her work, Guezennec (2012) showed that including CNF in a PVOH suspension for paperboard coating is limiting the blistering effect of PVOH layer during drying. As a consequence, 5wt% of CNF provide better water vapor barrier properties and oxygen barrier property (Figure 1-14) of a conventional coating 10g/m² coating and also enhanced the runnability.

### Other properties

Emulsion based coating are widespread in papermaking industry and particularly oil in water system. Indeed, coating process of paper generally does not permit the use of a solvent based solution. Silicon coating but also latex are probably the most used emulsion in paper solution. These products are usually stabilized with surfactant emulsifiers such as polyvinyl alcohol (PVA) or anionic species. But emulsions can also be stabilized by solid particles such as silica, clay minerals, carbon black, etc (Chevalier and Bolzinger, 2013). These emulsions are called Pickering emulsion. Recently, it was demonstrated that oil in water emulsion and water in oil emulsion could be stabilized by particles such as nanocellulose. Althougth CNC

stabilizing oil in water emulsion showed very promising results (Kalashnikova et al., 2013), (Capron et al., 2017), modified or neat microfibrillated cellulose seem to be a more challenging product raw material. Indeed, Lif et al. (2010) tried to use MFC for stabilizing diesel oil without any success. They showed that MFC were able to stabilize it only with the help of an emulsifier while both products alone failed in achieving this goal. Andresen and Stenius (2007a), showed that their previously developed hydrophobized CNF with chlorodimethyl isopropylsilane (Andresen et al., 2006) were able to stabilize water in toluene emulsion. They showed that increasing amount of CNF stabilize the emulsion against gravity induced sedimentation, probably due to the increasing viscosity in the oil phase. Higher substitution degree of CNF is also leading to bigger particles size according to the same study. Winuprasith et al. (2013) proved the effect of fibrillation degree on oil droplet size and emulsion stability, showing that the higher fibrillation was the higher stability and the smaller oil droplet. They explained this stabilization by the strong three dimensional network formed by CNF

However, none of these studies assessed the effect of nanocellulose while the emulsion is coated or a material is formed out of it.

*During this PhD project, such an emulsion strategy has been tested for silicon coating. Different CNF were evaluated as stabilizer of aqueous silicon emulsion and composites made of CNF and silicon were mechanically tested and assessed with regard to biodegradability.*

In coating formulation, CNF network can act as a binder for particles or nanoparticles stabilization and efficient dispersion. It has been noticed in several applications such as metallic or carbon particles distribution or $TiO_2$ dispersion on paper coating. $TiO_2$ is used as opacifying agent in thin paper. In the study, different strategies were employed to manufacture films, one by simple blending of MFC and $TiO_2$, the other by a premix, meaning by manufacturing MFC with $TiO_2$ and the last one by synthetizing through sol-gel reaction the $TiO_2$ inside the MFC suspension. The best opacifying properties were obtain with the premix method followed by the simple blending. The MFC were proved to disperse greatly the particles leading to higher properties than conventional $TiO_2$ coatings with the same particles quantity, permitting cost savings (Bardet et al., 2013). More recently, a study used CNF as binder for nanographite and carbon black particles for conductive paper applications (Kumar et al., 2017). They obtained lower electrical resistance of the coating than

conventional one, and they showed that even with a low solid content suspension (3%) the process is viable. A calendering process was also proved to be beneficial to the conductivity efficiency.

*In this manuscript, CNF are employed as silsesquioxane particles binder as well as precipitated calcium carbonate particles for superhydrophobic coating.*

Antimicrobial grafting but also release properties was also investigated for packaging coating with CNF.

The entangled network permits to release slowly molecules by entrapping them, limiting their diffusion speed. Caffein model molecule was mixed in CNF and coated on a

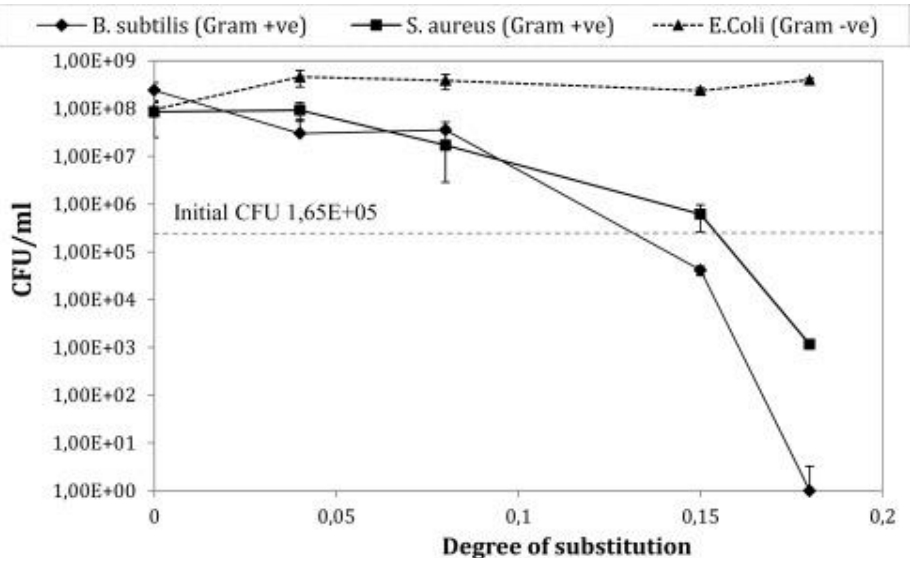


**Figure 1-15. Quantitative antimicrobial activity assessment for different degrees of substitution of CNF with 2,3-epoxypropyltrimethylammoniumchloride for Gram positive and Gram Negative bacteria. (Saini et al., 2016a)**

paper substrate and this sample was compared to a caffein soaking in the paper and a soaking followed by a pure CNF coating (Lavoine et al., 2014b). With the CNF/caffeine coated suspension, the model molecule was released in a higher amount and within longer time than reference samples.

The high grafting density makes also the CNF better for reaching antibacterial minimum inhibitory concentration upon contact. Saini et al. (2016a) showed that a modification of CNF with 2,3-epoxypropyltrimethylammoniumchloride at a DS of 0.18 was efficient without leaching of the antibacterial molecule (Figure 1-15).

*In this manuscript, antibacterial activity of modified CNF and resulting coating on paper will be measured.*

In order to evaluate the potentiality of cellulose nanofibrils in specialty paper and mainly for anti-adherent, non-wetting or antibacterial coating, an overview of existing solutions is provide.

# 2. Anti-adherent and barrier coatings

## 2.1. Anti-adherent solution in paper industry

### 2.1.1. Silicone coatings

Anti-adherent papers are not common and usually considered as specialty papers. About 22 million square meters silicone release paper was manufactured in 2015 and half this production is intended for labels. Polydimethylsiloxane (PDMS) or usually called “Silicone” is probably one of the most used polymers for anti-adherent properties after Teflon®. Its biocompatibility but also its thermal and UV stability make it a good choice for a large type of applications (aeronautics, medical implants, food contact…). Silicon industry has been adapting its product for each industry and application by modifying final mechanical properties but also by adapting pre-product form (silicone oil, silicone emulsion in solvent or in water etc.). The mechanism of reaction however is very similar.

## Mechanisms

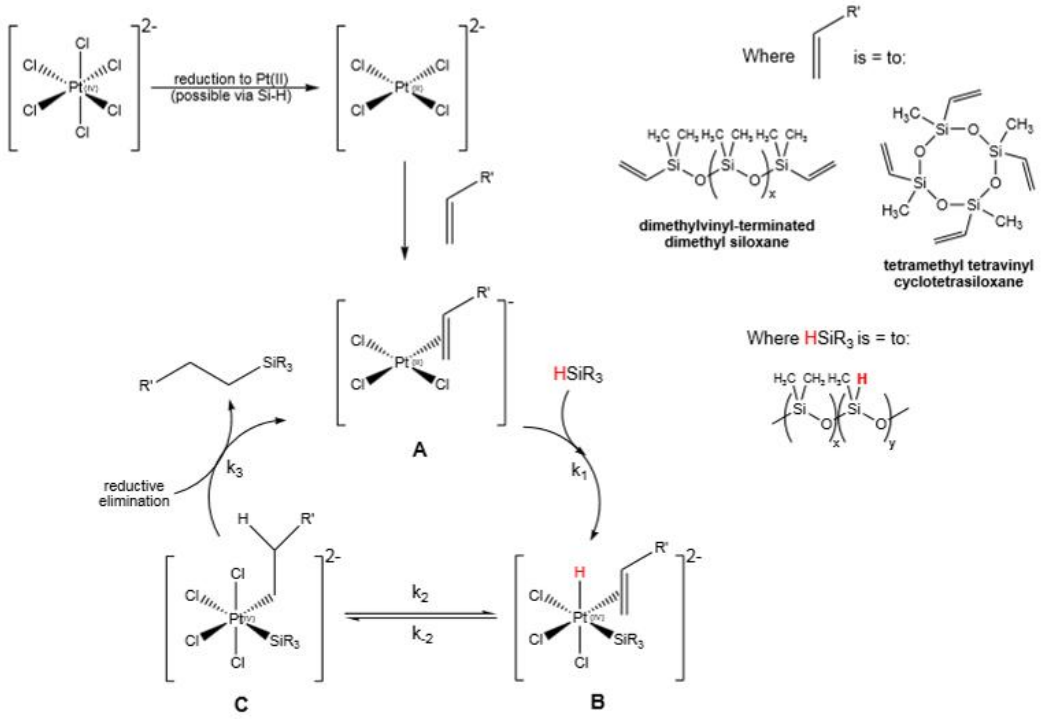


**Figure 1-16. Catalysis cycle in silicone synthesis. Reproduced from Sylgard® Cure Inhibition Characterization**

Mechanism of hydrosylilation (Figure 1-16) in PDMS is involving a catalyst which is based usually on platinium species as it gave the best reactivity but can be based on other metal catalyst such as Rutenium or Ir. Karsdedt or Speir type of catalyst are well known for silicone cross-linking.

## Industrial problem in paper industry

In the paper industry, the silicone suspension is prepared by mixing the base emulsion containing polysiloxane polymers and the catalyst emulsion containing the platinum catalyst and polysiloxane at ratio varying from 88-96/12-4. In one of the emulsion is present an inhibitor which prevents the mix to cross-link when in the chest and which will evaporate during drying. The emulsion is then usually applied with a size-press or a film press (on line

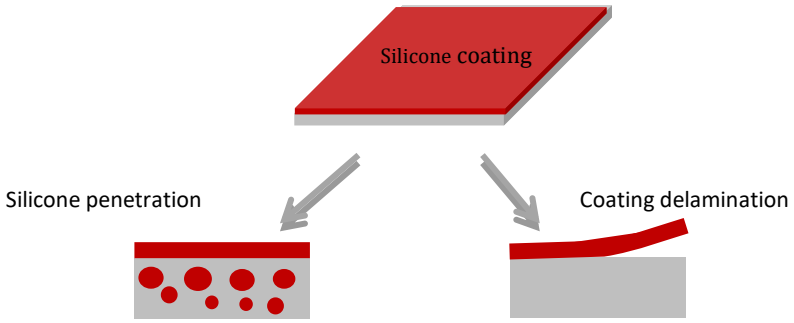


**Figure 1-17. Two mains problems faced in industry: silicon penetration and delamination.**

or off line) and cured by heating.

Main use of silicon paper is intended for back paper of adhesive label and as baking paper.

In patent literature, two main problems are tried to be overcome: silicone low adhesion on paper and silicone penetration inside paper (silicone cost is high for paper industry) (Figure 1-17).

The problem of cohesion between substrate and silicone coating is mainly resolved by the addition of an intermediate functionalized layer. UPM Kymene, for example patented a thin layer of a vinylic or silane grafted hydrosoluble polymer such as polyvinyl alcohol (PVOH) (Koskinen et al., 2013). Thus, hydroxyl groups will link to the paper substrate and the grafted site to the silicone by interacting in the cross-linking process (Fantini, 2014). As such delamination is occurring mainly in labels dorsal, peeling forces are much higher and this was not determined as a main problem for the industrial partner.

However, the silicone penetration inside the material is a major problem for the industrial partner, who needs to decrease such a loss.

In Table 1-4 are presented patented solutions to overcome the penetration by either modifying coating suspension rheology, paper surface or the end product. Modifying coating rheology was patented by the Glatfelter company (Reed, 1993). The idea was to use long aliphatic chain polymer such as polyethylene oxide with molecular weight of at least 100 000g/mole. They claimed for better holdout properties due to a better film formation and a lower penetration in the paper. Densification or surface closing of the paper substrate is a more recent strategy. Physical closure of paper pores is a good solution to avoid silicone penetration if no specific standard for the paper is required. Moring and Pahl (2006) proposed the calendering which is permitting no chemical addition and the densification of the paper. It has also the advantage of smoothing the surface, leading to a more efficient covering. However, this technique is energetically demanding. Applying a surface primer is also permitting smoother surface and closure of paper pores as well. Koskinen and Tani (2001) patented a formulation with CMC, latex and PVA in this purpose while Kosonen and Kajanto (2014),Bilodeau and Hamilton (2013) proposed a biobased solution with cellulose nanofibrils primer coating or insertion in the bulk paper. The last one used for limiting cost in silicon coating is using the embossing process to reduce the contact between the substrate and the adhesive product and thus less coating amount is necessary.

Among these solutions, two locks are pertinent for this PhD project, i.e. the CNF coating and the embossing. The latter is quite old and need another step in the process of paper manufacturing. We have tried to add this roughness but "inside" the paper machine, during the coating. The first solution with CNF coating is very recent (same year than this PhD beginning). It is also very interesting because of the need to have material inside the paper that is food-contact approved, such as cellulose.

**Table 1-4. Patented solutions for overcoming silicon penetration in the paper at different steps of the production.**

| Application step | Solution | Process | References |
|---|---|---|---|
| **Silicon suspension** | Viscosity increase | Thickener addition | (Reed, 1993) |
| **Base paper** | Densification/ surface treatment | Calendering | (Moring and Pahl, 2006) |
| | | Coating PVA/CMC/ latex | (Koskinen and Tani, 2001) |
| | | Coating or adding in bulk CNF | (Kosonen and Kajanto, 2014) ,(Bilodeau and Hamilton, 2013b) |
| **End product** | Contact food/paper reduction | Embossing | (Talja and Moro, 2004) |

This patent was evaluated with CNF and TEMPO CNF during this PhD and compared to other biosourced material such as starch. Results are not displayed in the manuscript.

## 2.2. Grease barrier coatings

Due to the increasing demand of food packaging industry, greaseproof paper has been developed for decades. Greaseproof papers are characterized by a non-permeation but also non-wetting of the oil. The best technical solutions today are the coating of perfluoro polymers with long alkyl chains (C8) wich gives oil-repellency trough fluor atoms. For low quality greaseproof paper, the strategy is relying on clogging pores with starch, PVOH, glassine paper, wax or polyethylene or on modifying paper structure with sulfuric acid (vegetable paper).

| Solution | Fluorinated product | Reference |
|---|---|---|

| | | |
|---|---|---|
| **C6 and addition of inorganic particles** | fluoroalkylsilane, cationic fluorinated compound , or fluorinated polyacrylate | (Johnston et al., 2014) |
| **Double layer of PVOH or starch and C7 or inf.** | Methacrylate with perfluoroalkyl from C1 à C7 | (Takemura and Kawana, 2014) |
| **Blend of starch/lecithin** | — | (Satyavolu et al., 2012) |
| **Sizing with starch** | — | (Kelárek, 2015) |
| **Binder/Filler/ Calcium carbonate and protein composition** | — | (Jr, 2014) |

But due to serious environmental threat of C8 perfluoroalkyl and the progressive banning in countries worldwide, greaseproof paper manufacturers have to find new solutions to replace it. Recent patents are now focusing on the decreasing of alkyl chain but also on the improvement of low quality greaseproof coatings as summarized in Table 1-5.

**Table 1-5. New patents on greaseproof paper coating.**

CNF are also known for their grease barrier properties close to the highly refined greaseproof paper. Lavoine et al. (2014) have proved that a layer of 7 g/m² is sufficient for limiting oil penetration.

*Up to our knowledge nobody tried to mix with other polymers or silane/silicon for improving such greaseproof paper. This approach has been tested during this PhD.*

## 2.3. Non-wetting surface

### 2.3.1. Definition and measurement methods

Surfaces are reacting differently regarding wetting of a liquid. With water, for example, on a hydrophilic surface, the liquid will tend to spread on the surface while on a hydrophobic surface it will less. To define more precisely this property, the contact angle (CA, θ) at the triple point (interface water/solid/air) is determined by the intersection between the solid/liquid interface and the tangent at the liquid/vapor interface. It is measured after the controlled deposition of a water droplet thanks to the sessile drop method. The wetting property of a flat surface is then characterized by the Young's equation (Young, 1805):

$$Cos(\theta) = \frac{\gamma_{SV} - \gamma_{SL}}{\gamma_{LV}}$$

Where $\gamma_{SV}$, $\gamma_{SL}$, $\gamma_{LV}$ are the interfacial surface tensions with the solid (S), vapor (V) and liquid (L). If the water contact angle (θ) is inferior to 90° then the surface is hydrophilic, if above 90° it is hydrophobic and above 150° superhydrophobic (Figure 1-18).

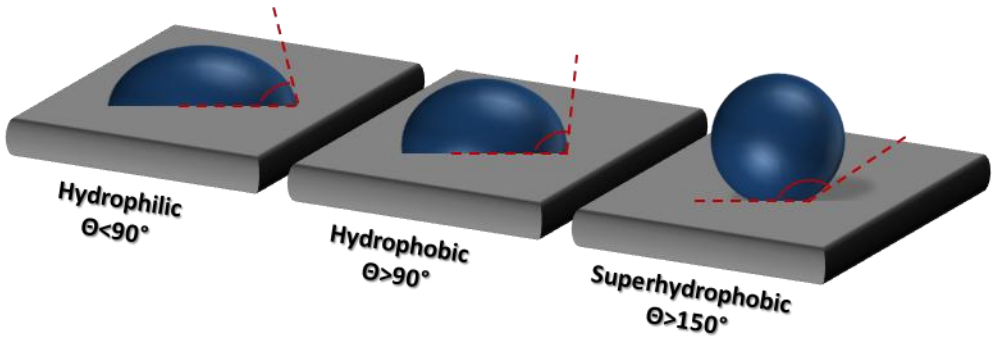


**Figure 1-18. The different states according to the static contact angle of a water droplet.**

Dynamic contact angles are usually determined to characterize more precisely a surface which will be used in a dynamic wetting process (coating, inkjet printing…). It can be measured by tilted plate method, Wilhelmy method or modified sessile drop method (Eral et al., 2013). Measured angles from these methods are advancing ($\theta_A$) and receding ($\theta_R$) angles which are the angles at the triple point on a drop in motion on the tested surface (Figure 1-19). $\theta_A$ being the front angle of the droplet and $\theta_R$ the back angle, the relation $\theta_A \geq \theta_R$ is always true. The difference between advancing and receding angle is called contact angle hysteresis (CAH) and is due the chemical homogeneity or roughness of the material. CAH is

reflecting the energy dissipated during the flow of the liquid on the surface and is also the wetting of the surface.

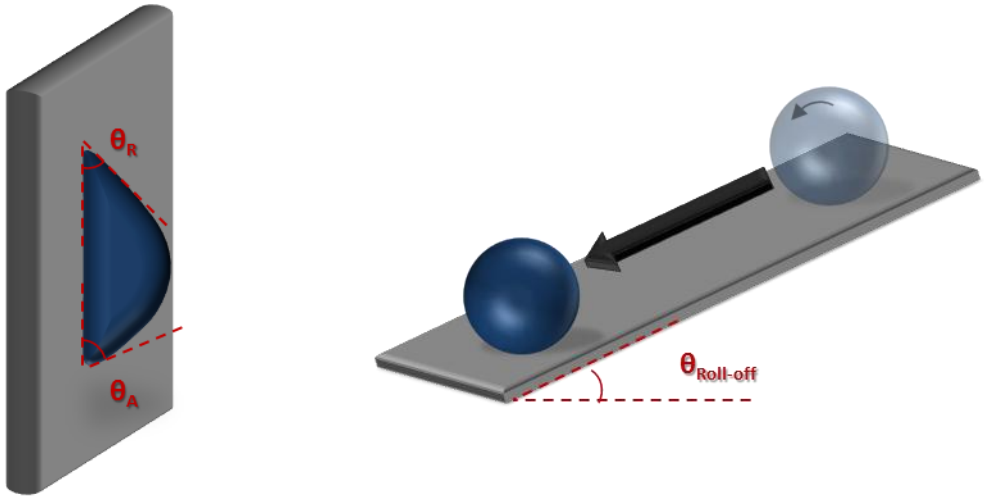


**Figure 1-19. Schematic representation of advancing and receding angle measurement with the tilted plate method (left) and roll-off measurement (right)**

Some surfaces depict a static water contact angle above 150°. These surfaces are classified as superhydrophobic (SH) or ultrahydrophobic. In this precise case, it is usually the roughness of the surface that is creating this increase. The same flat surface will obtain a typical value between 90 and 120°. Theorically this is the highest point of what can bring the chemistry to lower the surface energy (Onda et al., 1996),(Lee et al., 2007).The resulting contact angle of rough surface is thus called “apparent contact angle” (θ*).

For superhydrophobic surfaces, contact angle hysteresis calculated through dynamic contact angles measurement can vary according to adhesion of water. The droplet usually slides on the surface easily and the phenomenon is enhanced when the surface is tilted. Below a CAH of 10°, the surface is usually classified as self-cleaning surface (Bhushan and Jung, 2011) , meaning that the droplet is not only sliding but is also rolling (which enhance the ability to take dust in the movement) . This roll-off angle is determined by the angle formed by the tilted surface when a drop of the liquid is rolling off the surface (Figure 1-19). The drop is deposited on the flat surface and then tilted. Sometimes, when the adhesion forces are too strong, it cannot be measured (i.e the drop sticks to the surface) and a water shedding angle was developed (Zimmermann et al., 2009). The difference is that the drop is deposited on an already tilted surface.

These differences between CAH for superhydrophobic surfaces are the consequences of two major phenomenons that are expressed by the "famous" Wenzel or the Cassie-Baxter states. The Wenzel state is corresponding to a wetting state where the droplet is pinned at the surface and the liquid is penetrating the capillarity. Resulting high CAH is observed. Cassie-Baxter theory relies on a formation of open-air pockets (connected to the atmosphere) in the roughness valley leading to low CAH (Patankar, 2004), (Wang and Jiang, 2007).

The Wenzel model is thus relying on a homogeneous solid surface on which liquid is interacting (Figure 1-20). The following equation rules the model:

$$\cos\theta^* = r.\cos\theta$$

Where θ* is the apparent contact angle, θ the Young contact angle and r the surface roughness defined by the ratio between actual surface area over projected surface area. Thus, a hydrophilic rough surface will have apparent contact angle below Young angle while a hydrophobic rough surface will display an apparent angle higher.

When the drop is suspended over air pocket (Figure 1-20), meaning on a composite surface made of solid and air, the Cassie-Baxter state is ruled by:

$$\cos\theta^* = f_1.\cos\theta_1 + f_2.\cos\theta_2$$

Where $f_{1\ is}$ the fraction of solid in contact with liquid, $\theta_1 = \theta$ the Young angle of the solid, $f_2$ the air/liquid fraction with $f_2 = (1 - f_1)$ and $\cos\theta_2 = -1$ leading to:

$$\cos\theta^* = f_1.(\cos\theta + 1) - 1$$

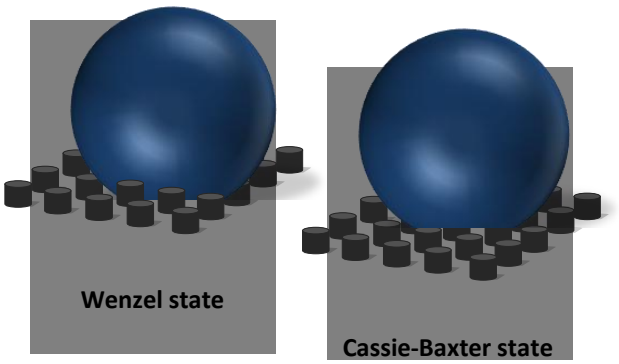


**Figure 1-20. Schematic representation of the Wenzel and Cassie Baxter state of a liquid droplet on a rough surface**

It seems that both states can coexist for one superhydrophobic surface depending on droplet internal pressure, external pressure or also if the water droplet is forming through vapor phase or not. For the same surface and the same sliding angle, it was demonstrated that in the Cassie regime, a droplet slides when 200 times smaller than in the Wenzel state (Lafuma and Quéré, 2003). The transitional state (or Cassie impregnated state) is existing

(Dupuis and Yeomans, 2005) and was defined as a third state of superhydrophobicity (Wang and Jiang, 2007). Two other states were also categorized. One is called the lotus state and is a highly stable Cassie state which is achieved by combination of micro and nano scale hierarchical roughness. It shows very low CAH and thus the "self-cleaning" effect. And the last one is called the "Gecko" state which is a modified Cassie-Baxter state where part of air pocket are sealed between the liquid and the solid (Wang and Jiang, 2007). A summary of all possibilities of state with a surface is depicted in Figure 1-21.

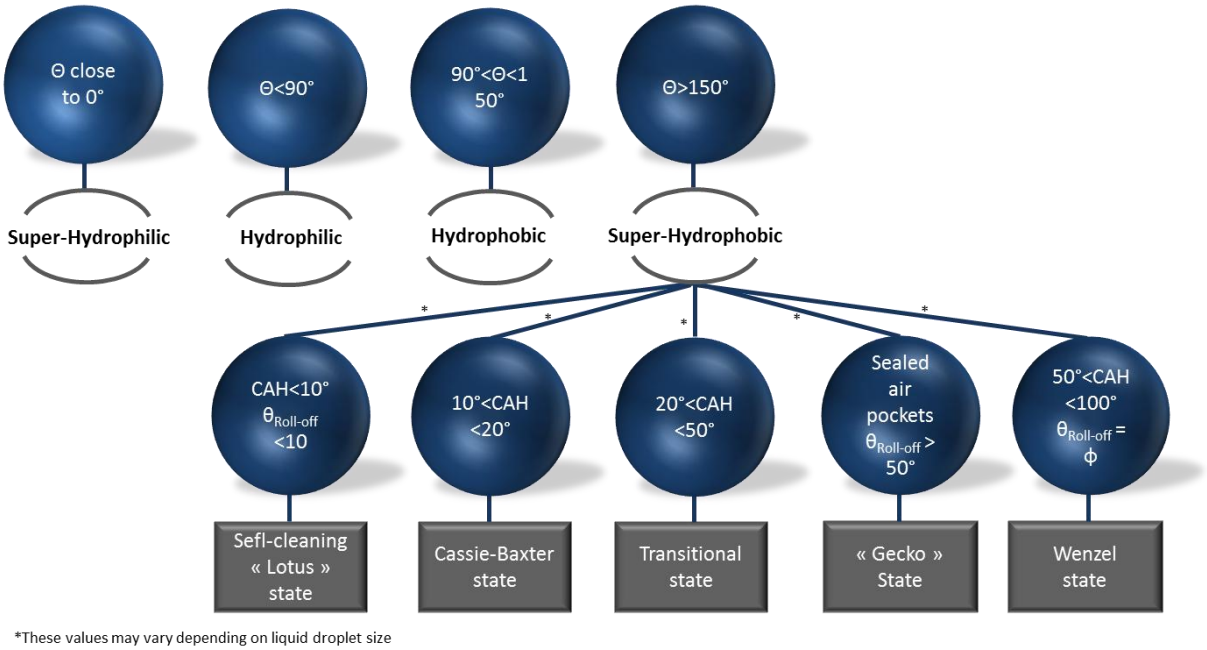


**Figure 1-21. Summary of different wetting state for superhydrophobic surfaces. (Callies et al., 2005) (He et al., 2004), (Li et al., 2011), (Hejazi and Nosonovsky, 2013)**

What is clearly demonstrated is that the surface organization will strongly influence adherence properties of paper.

### 2.3.2. Surface design

Nature is the most powerful engineer in the world that has developed during thousand-year incredibly efficient material and mechanisms for living being. Depending on environment, surfaces were designed on animals and plants in order to be self-cleaning or water repellent (superhydrophobic surface), oil or low surface tension liquid repellent (superoleophobic), both under air condition (amphiphobic) or superhydrophobic under oil and superoleophobic under water (superlyophilic). While designing such kind of surfaces, engineers get first inspired by nature and try to mimic it. Lotus (Koch et al., 2009) and rose (Bhushan and Her, 2010) inspired superhydrophobic designs while leafhoppers (Rakitov and

Gorb, 2013) or collembola (Hensel et al., 2013) superoleophobic or even amphiphobic and fish scales superlyophilic surfaces (Wang et al., 2015).

In this section will be discussed only surface design for superhydrophobic and superoleophobic surface under air as it is the main application expected in the paper industry.

Self-cleaning and superhydrophobic properties are usually hidden behind the term of "Lotus leaf effect" and "rose petal effect". The first one relate to a self-cleaning Cassie-Baxter state and the last to a high adhesive superhydrophobic Wenzel state. While observing hundreds of plants surface structure that show superhydrophobic properties, Barthlott and Neinhuis (1997) found out that all structures were similar made by a hierarchical roughness. As shown in Figure 1-22 on the lotus leaf, a micro-roughness created by papilla is present in a regular manner while at the same time, a nano-roughness made by epicuticular wax crystlals is covering it. As reported by Su et al. (2010), this dual roughness is extremely important for having a stable Cassie-Baxter state. Surface structures of plants and animals to create superhydrophobic property were reviewed by Darmanin and Guittard (2015) and it shows how different can be the organization of the structure to reach the same goal: convex papilla, hair, spheres, or scales, with singular or dual roughness.

Superoleophobicity on a material is much more difficult to obtain as the surface tension of oils such as hexadecane or octane is at least 2 times lower than water surface tension. Very few materials have intrinsic oil repellency except highly fluorinated chemicals. However, superoleophobic properties can be found on springtails skin (Hensel et al., 2013) even though nature is not able to produce fluorinated material. As for superhydrophobicity, superoleophobicity can still be achieved with oleophilic material if the roughness structure is re-entrant (overhanging or mushroom-like) (Bellanger et al., 2014) which is the case with bronchosome on sprintails skin (Figure 1-22). It was also noticed that arrangement of the bump was hexagonal or rhombic.

In conclusion, from the observations from nature, obtaining a superhydrophobic surface remains first on a regular micro-roughness with eventually nano-roughness to stabilize a self-cleaning state. The hydrophobicity of the material in contact is preferable even though it is not mandatory as it was reported by some researchers in the case of Lotus leaf where the wax water contact angle by itself is $\theta_w = 74°$ (Cheng et al., 2006). But in this last case, a

re-entrant structure on the roughness seems to be the key point of overcoming this hydrophilicity. Same re-entrant structures are highly recommended for designing superoleophobic surface as few materials have oleophobic property.

In the mimicking of nature, these structures were produced artificially and studied. Usually employed parameters to define the structure are: “d” the structure width or diameter (if round shape), “a” the clearance or p the pitch for the evaluation of distance between each structure and finally “h” the height of the relief. Parameters are schematically defined in Figure 1-23.

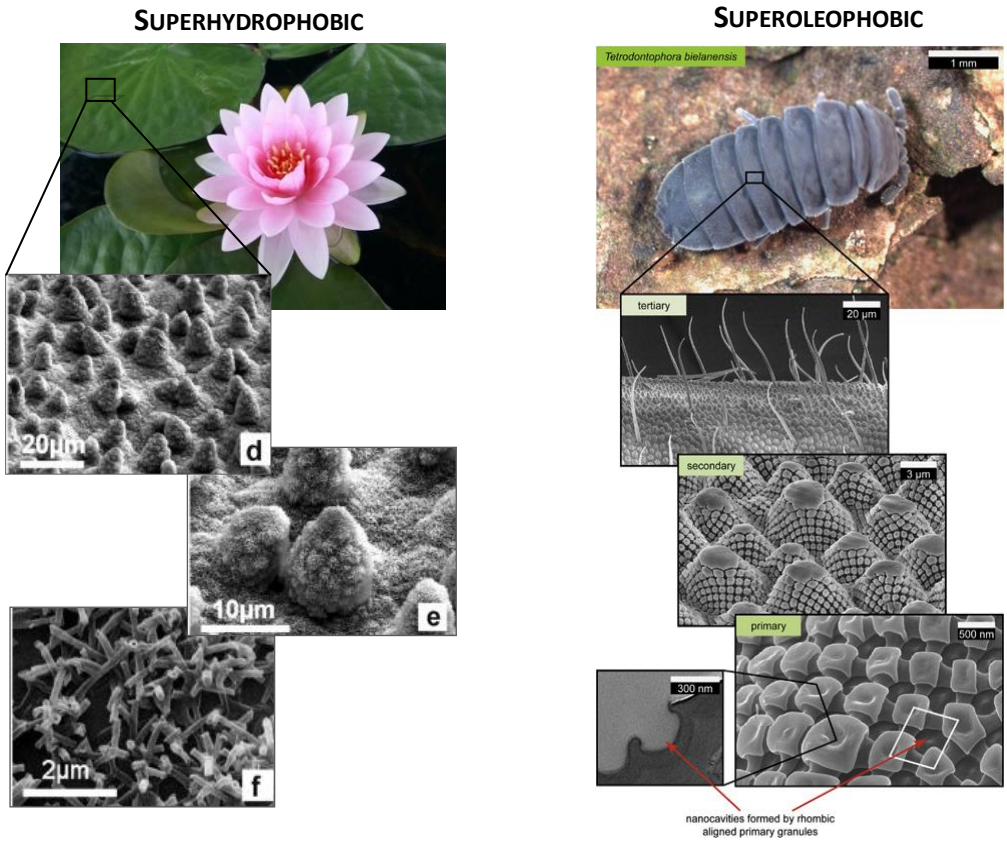


**Figure 1-22. Example of micro/nano structures existing in nature. Left side is a superhydrophobic surface from Lotus leaf (Nelumbo Nucifera) (Koch et al., 2009) and right side is a superoleophobic surface from sprintails (T. Bienalensis) skin (Hensel et al., 2013).**

To minimalize the transition between Wenzel and Cassie-Baxter, Patankar thus proposed to design at the intersection of the two equations to obtain a robust surface with a point of intersection that should be the closest from -1 to give the highest superhydrophobic property. Patankar (2003) proposed a model to design a superhydrophobic surface based on these parameters relying on following equations:

$$\cos\theta^{*,c} = B(1 + \cos\theta) - 1$$

$$\cos\theta^{*,w} = (1 + \frac{4B}{(d/h)})\cos\theta$$

Where

$$B = \frac{1}{(c/d+1)^2}$$

With θ the Young contact angle of the surface (flat).

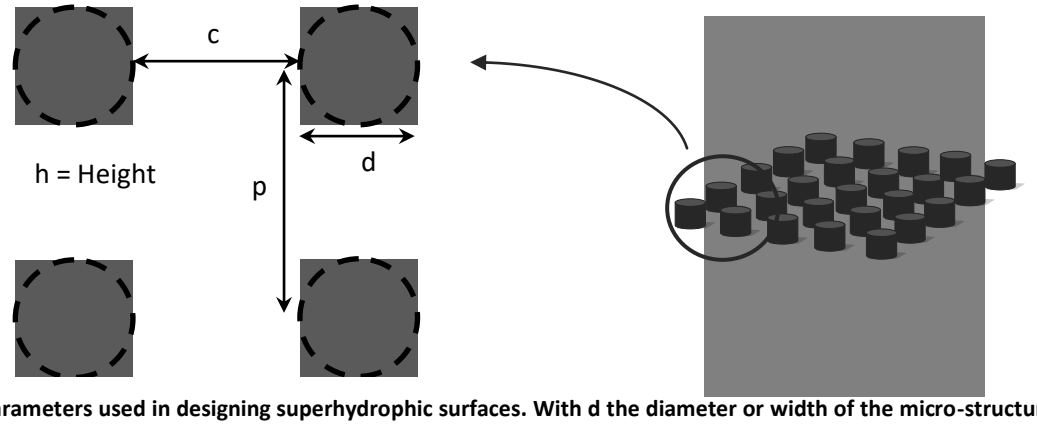


**Figure 1-23. Parameters used in designing superhydrophic surfaces. With d the diameter or width of the micro-structure, c the clearance and p the pitch in between micro structure and h the height of the micro-structure.**

This study is not taking into account nano-roughness that could be implemented on the first scale relief. Bhushan and Nosonovsky (2010), worked experimentally with different geometries and also with an addition of nanostructures and resulting values are expressed in Figure 1-24. According to their research, Cassie-Baxter state, which relies only on c/d according to Patankar equations, is stabilized by nanostructure.

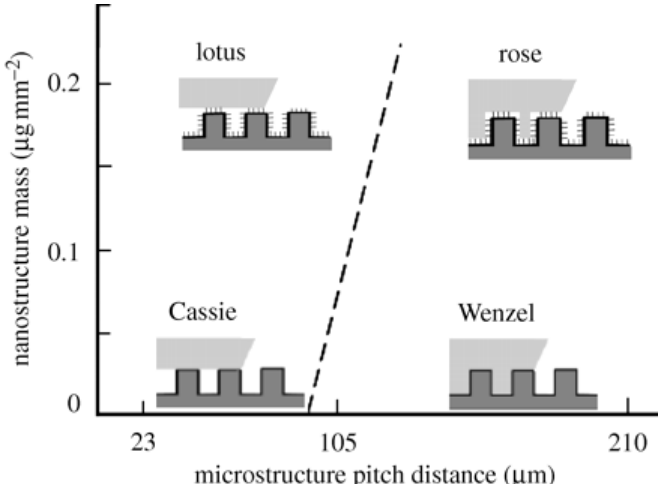


**Figure 1-24. Superhydrophobic state schematic representation depending on nanostructure density and microstructure distance. (Bhushan and Nosonovsky, 2010)**

This means that for a higher pitch distance at the limit to a Wenzel impregnating, the nanostructure permits to push the limits to a larger pitch distance before entering the transitional state. The design of superoleophobic materials is usually very close to the superhydrophobic one but further include a post treatment with fluorinated chemicals or the inclusion of fluorinated structures to obtain the desired property. Otherwise, the T-like

structure design depends on the sharpness of the cap edge (the radius), the width and the space between caps as well as the height of the overall structure.

Such roughnesses are difficult to be designed in paper industry using on-line process. This will be one of the main challenges in this PhD project.

Even if hydrophilic structures can have interesting surface properties, it is better to start from hydrophobic surface and when CNF are considered, their functionalization seems mandatory and it is detailed in the following chapter.

# 3. (Nano)Cellulose functionalization for anti-adherence and barrier

## 3.1. (Nano)Cellulose functionalization

Cellulose or nanocellulose can be functionalized mainly through the hydroxyl group present on the C6 position of the glucose unit. It can also be modified at the reducing end group comporting a hemiacetal group or on the hydroxyl groups over the cycle. As reviewed by Missoum et al. (2013) and Habibi (2014) for both cellulose nanofibrils and cellulose nanocrystals, two different strategies exist consisting in either non-covalent or covalent linkage of moieties. Figure 1-25 is giving an overview of used molecules or polymers for modifying cellulose nanofibrils before 2013.

Non-covalent CNF modifications have the advantages of being easily processable in water with, for example, surfactants. As reviewed by Tardy et al. (2017), both nonionic nanocellulose (as produced) as well as anionic nanocellulose (TEMPO CNF or carmoxymethylated CNF for example) can be functionalized by this pathway. It is well-known modification route in paper industry as well as in wood modification. On CNF, it was proved to be efficient for giving a hydrophobic character only by electrostatic interactions. Cetyltrimethylammonium bromide (CTAB), dihexadecyldimethylammonium bromide (DHDAB) and didodecyldimethylammonium bromide (DDDAB) were three surfactants employed on TEMPO-CNF in the study. The adsorption was confirmed and the hydrophobic character was able to be monitored by anionic and cationic charge balance. Not complete hydrophobic nanopaper was obtained but a significant change was observed (Xhanari et al., 2011). It is also noteworthy to mention that one of the drawbacks of such modification is the low resistance of the bounding interaction compared to covalent modification, which could be a serious problem if the surfactant is leaching in its environment.

Covalent modifications are involving either molecules grafting or polymer grafting. The last can be divided in two grafting approaches, namely “grafting onto” and “grafting from”. Such graftings are most of the time used for compatibilization with a polymer matrix. Grafting onto pathway is done by the grafting of an existing polymer with a functional end group with a functional group on the nanocellulose. Such approach is difficult because of steric hindrance resulting to poor grafting density. Polycaprolactone (PCL) was grafted onto

TEMPO oxidized CNF with this method but modifications of TEMPO-CNF (alkyl bearing) as well as PCL modification (azide) was necessary to obtain successful results (click chemistry) (Benkaddour et al., 2013).

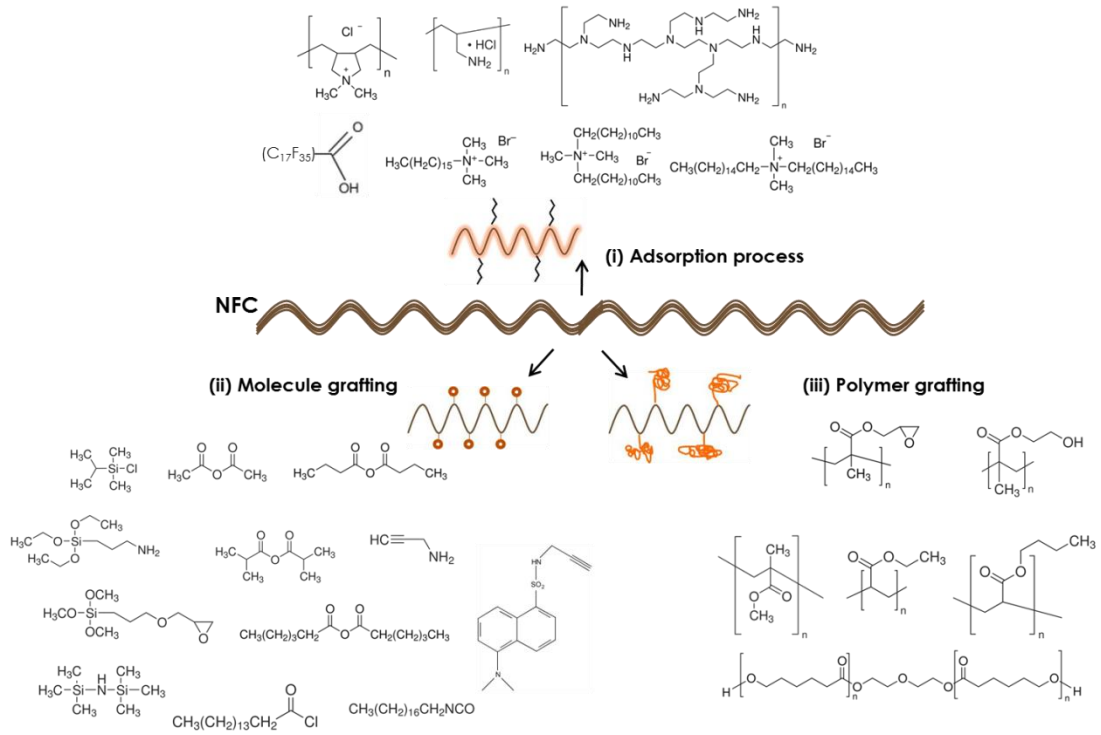


**Figure 1-25. List of used reagents to modify cellulose nanofibrils surface. (Missoum et al. 2013)**

Grafting from consists in nanocellulose coverage during mixing of the monomer solution and then thanks to an initiator, start the polymerization from these monomer. This approach was used to graft PCL in an easier manner via ring opening polymerization using stannous octoate ($Sn(Oct)_2$) (Lönnberg et al., 2011). Atom transfer radical polymerization (ATRP) or surface initiated ATRP (SI-ATRP) were recently used to graft polymer without any ring structure such as poly(*n*-butyl acrylate) and poly(2-(dimethyl amino)ethyl methacrylate) brushes (Morits et al., 2017). In this study, they showed that a careful balance of polymer brushes was needed in order to avoid CNF backbone disintegration. Finally free radical polymerization can be used on CNFs. As an example, it was used to tune their hydrophobic properties using methacrylate monomers and cerium ammonium nitrate as initiator after CNF oxidation and grafting of vinylic groups (Littunen et al., 2011).

Many covalent reactions for grafting molecules have been tried such as esterification, etherification, sylilation (Andresen et al., 2006), amidation (Saini et al., 2016b) or urethanization directly on nanocellulose.

In this PhD work, a barrier on cellulose nanofiber surface highly hydrophobic and which favor release is targeted. If the comparison is made with silicon, sylilation is seen as most relevant strategy for modifying cellulose nanofibrils so a closer focus is made on it. (Araki, 2013) (Habibi, 2014)

## 3.2. Organosilane based functionalization

### 3.2.a. Hydrolysis and condensation of organoalkoxysilane

In material science, organosilanes are key molecules in the applications of adhesion promoters, coupling agent or even as surface primers. We have seen that they have been recently used to modify, in mild reaction conditions, nanocellulose (Lu et al., 2008). The understanding of their reaction in their alcoholic or aqueous media has been investigated for decades. Two competing mechanisms rule:

**Hydrolysis** $RSi(OR')_3 + 3H_2O \rightarrow RSi(OH)_3 + 3R'OH$

**Condensation** $RSi(OH)_3 + RSi(OH)_3$ 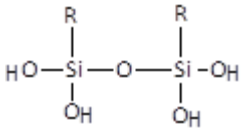 $\rightarrow$ $+ nH_2O$

Some studies attempted to understand the mechanism competition between hydrolysis (or solvolysis) and condensation of organosilane, depending on organic group, pH, concentration or alcohol part in the solvent. Reactions were followed by NMR (Brochier Salon and Belgacem, 2010), (Brochier Salon et al., 2008a), (Brochier Salon et al., 2008b) or FT-IR (Peña-Alonso et al., 2006). Main conclusions are that acidic pH and also low concentration of silane are stabilizing hydrolysis while basic pH, high concentration of silane and temperature are favoring condensation. Amino silanes are thus naturally favoring their self-condensation. It is also shown that they undergo specific condensation structuration such as a 8-membered cycle among highly crosslinked structures as well.

In this PhD work, three different organosilanes will be followed by $^{29}Si$ NMR in solution in order to determine the point of hydrolysis where the most of the hydroxyl groups are formed for each one. This measured time will further be used as a reference to put nanocellulose in contact. The aminosilane will be followed in 100% aqueous media.

### 3.2.b. Designing of materials through condensation of mono or di-organoalkoxysilane solution

Crosslinking of organoalkoxysilane ($R'_nSi(OR)_{4-n}$) is known to form either a gel, precipitated particles,oil, etc. depending on alkyl chain and and tri-alkoxy group but also catalyst proportion and concentration of chemical in their solvent (Loy et al., 2000), (Dong and Ha, 2012), (Wang et al., 2000), (Shimojima et al., 1997).

Particles are mainly used as fillers in polymer matrices and are processed through hydrolytic, non-hydrolytic sol-gel routes, mini-emulsion reaction or biomimetic approaches (Arkhireeva et al., 2005).

The hydrolytic Stöber method created in 1968 (Stöber et al., 1968) to produce controlled silica particles is the starting point of a bunch of researches. Starting from tetralkoxysilane (TEOS) in ethanolic medium, Stöber developed monodisperse micro-sized silica particles by hydrolysis and condensation catalyzed by ammonia. The reaction is ruled by a first step of hydrolysis:

$$Si(OC_2H_5)_4 + 4H_2O \rightarrow Si(OH)_4 + 4C_2H_5OH$$

And a second step of condensation catalyzed by ammonia:

$$Si(OH)_4 \rightarrow SiO2 + 2H_2O$$

After this, researchers tend to modify, surface properties, charge and pores by condensing TEOS with organoalkoxysilane.

$$Si(OC_2H_5)_4 + 4H_2O \rightarrow Si(OH)_4 + 4C_2H_5OH$$

$$Si(OH)_4 + RSi(OH)_{3\ or\ 4} \rightarrow RSiO2 + 2H_2O$$

Where R is the organic forth substituent (vinyl, alkyl…).

To further tune properties of the silica particles for example to enhance polymer/silica interface or to control porosity or polarity for drug carrier, different paths were followed. Organoalsoxysilanes were used as surface modifier for inorganic particles or as a reactive material to functionalize the inner part of ending hybrid material produced. The resulting families are summarized in Figure 1-26 (Croissant et al., 2016).

In this thesis, organosilica paticles produced are classified in the category of “high organic content non-porous silsesquioxane particles”. A closer focus is thus given to this section.

As reviewed by (Kuroda et al., 2014), synthesis of silica material with alkoxysilane and organoalkoxysilane paves the way for a wide range of possible structures.

One of the first to report particles synthesis from one trialkoxyalkylsilane in water and catalyzed with ammonia was (Choi et al., 1998). They studied the synthesis of organosilica particles derived from phenyltrimethoxysilane (PTMS), methyltrimethoxysilane (MTMS) or methyltriethoxysilane (MTES) and the influence of chemical concentration on particle size. The immiscibility of the silane was thought to be the basis principle of particles formation. They showed the increase of particle size from around 500nm to 2µm with concentrations in organoalkoxysilane ranging from 0.25mol/L to 2mol/L and with a fixed 1mol/L concentration of ammonia. The ethoxy group compared to methoxy was shown to accelerate particle growth concluding that hydrolysis was faster with the release of methanol rather than

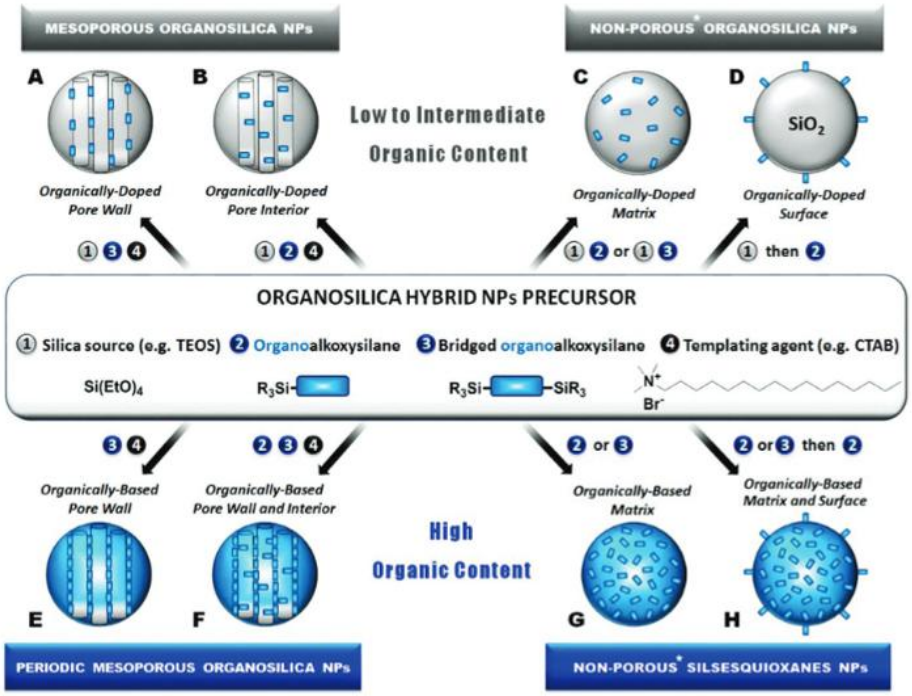


**Figure 1-26.Summary of what type of organosilica particles is obtained through different combination of chemicals. (J.Croissant et al.)**

ethanol.

In 2011, (Dirè et al., 2011) analyzed the effect of the organic group on the formation of particles. Methyltriethoxysilane (MTES), ethyltriethoxysilane (ETES), vinyltriethoxysilane (VTES), phenyltriethoxysilane (PhTES), pentyltriethoxysilane (ATES), octyltrietoxysilane (OTES) and 3-aminopropyltriethoxysilane (APTES) were studied. The sol was containing ethanol at appropriate acidic pH to dissolve silane for 4h before addition of a 2.3M ammonia solution. On the same silane, increasing HCl proportion lead to bigger and widespread in size particles, while increasing ethanol lead to an Oswald ripening effect which lead to coalescence of particles. Here again is the proof of a need of certain insolubility to obtain

narrow dispersed particles. Indeed, increasing ethanol in acidic media is favoring hydrolysis and stability over condensation as studied by (Brochier Salon et al., 2008a). Thus, enhancing nucleation (hydrolysis) is leading to smaller particles. Regarding all organoalkoxysilane, average particles size obtained varies from 60±28 nm to 466±106 nm. The observed trend was the longer organic chain the bigger the particles. Difference in thermal behavior as well as surface energy was observed.

More recently (Brozek et al., 2017) synthesized their particles with different organo tri-ethoxy and methoxy silanes in an water-ethanol solution without any help of surfactant and catalyzed by sodium hydroxide. Their study highlights relations between conditions of reaction and end material properties. More precisely, they found for different organic groups, the proper amount of ethanol and also water to hydrolyze the material efficiently and the amount of solvent to avoid aggregation. Increasing NaOH quantity yield to a diminution of particle size and oragnoalkoxysilane concentration was set to around 2wt%.

To summarize, impacting factors on shape, morphology and properties:

- $T_{OH}$ structures initially present at the time of condensing catalyst addition.
- Catalyst proportion and type ($NH_4OH$, NaOH or aminosilane)
- Organoalkoxysilane concentration
- And organic groups

The use of amino silane as a condensing material was a choice of this thesis in order to impart antimicrobial activity without leaching of the agent.

This particular way of making the particles was investigated by few researchers. First paper on a close subject to be published was probably the one of (van Blaaderen and Vrij, 1993) were they showed a cross condensation on the 3-aminopropyltriethoxysilane (APS) with TEOS. It is (Ottenbrite et al., 2000) that introduced the same phenomenon with organotrialkoxysilane and APS. Both studies showed that only a part of the aminosilane in the reaction medium was introduced in the particles (around 30% only). This result was then approved by (Heitz et al., 2006) and (Liu et al., 2005). In their dual mixture of alkoxysilane, (Dirè et al., 2011)showed that the addition of APTES to MTES rapidly increased the particles size until forming raspberry-like particles at high level.

Proposed structure of repartition of the aminosilane in the matrix was never proposed. But from all this information, it could be hypothesized that the few $T_{OH}$ and part of $T_1$ or $T_2$

structures could act as cross-condensor reservoir while $T_3$ could act as binder between formed particles.

### 3.2.c. Reaction with cellulose

*Silylation*

The first study on silylation was done by Gousse et al. in 2002 and was performed on CNCs with isopropyldimethylchlorosilane, n-butyldimethylchlorosilane, n-octyldi-methylchlorosilane and n-dodecyldimethylchloro-silane in solvents (Goussé et al., 2002). They could provide hydrophobized CNC with stable suspension properties in non-polar solvent and keep the CNCs morphology at the same time when DS was kept between 0.6 and 1.

Later, the same approach was used to silylate CNF with isopropyldimethylchlorosilane (Goussé et al., 2004) (Andresen et al., 2006). The later study showed that CNF films were turned hydrophobic and exactly from a contact angle of 28±4 to 146±8 for high DS (0.9). This almost superhydrophobic property was due, according to authors, to the increase of roughness measured on the film that residual non-fibrillated fibers were creating. Such modified CNF were tested successfully for their ability to create stable water in oil pickering emulsions (Andresen and Stenius, 2007b).

But the use of chlorosilane to modify nanocellulose in suspension required time consuming solvent exchange and also proper security around HCl vapor production during reaction. Chemical vapor deposition of chlorosilane was attempted on nanocellulose aerogel, which reduce the time of reaction (Aulin et al., 2010c) (Cervin et al., 2012). Octyltricholosilane (OTCS) and 1H,1H,2H,2H-perfluorodecyltrichlorosilane (PFOTS) were respectively employed. With OTCS, they reported a 150°±4 contact angle with water and a total absorption of non-polar liquid. With PFOTS, they recorded a 144° and 166° for hexadecane and castor oil respectively and 71° and 96° for a flat CNF film. Nothing was reported for water contact angle and no penetration test of oil through the flat film was reported. Recently, the same procedure with PFOTS was employed to modify a filter paper (Phanthong et al., 2016) which was previously coated with nanocellulose. The resulting surface showed amphiphobic properties but nothing was mentioned on grease barrier after a prolonged contact.

An easy to process modification with a cationic silane, octadecyldimethyl(3-trimethoxysilylpropyl)-ammonium chloride (ODDMAC), was employed. After the

hydrolyzation of methoxy group in a water/methanol solution, the resulting tri-silanol or dimer was kept in contact with hydroxyl groups of cellulose nanofibrils for 2h. At the end a purification step was used and CNF were casted, dried and cured at 110°C. The main objective of this was to give an antimicrobial activity, which was successful but unfortunately, nothing was reported on surface properties such as surface energy (Andresen et al., 2007).

In the continuity of soft chemistry, Panaitescu et al. (2007) directly grafted with (3-Aminopropyl)-triethoxysilane (APES) in ethanol/water previously dried nanocellulose for enhancement of compatibilization in polymer matrix within two hours of mixing and three of heating. On CNC different organoalkoxysilane (Aminopropyltriethoxysilane, n-propyltrimethoxysilane, methacryloxypropyltrimethoxysilane, and acryloxypropyltrimethoxysilane) were grafted in aqueous media only (Raquez et al., 2012). Zhang et al. proposed a silylation with methyltrimethoxy silane in water and catalyzed by vacuum evaporation to create aerogel. A polydimethylsiloxane network was achieved giving high water contact angle up to 147 and improvement in mechanical properties. Finally Wang et al. (2016) successfully investigated the possibility to spray dried the modified nanocellulose in suspension.

Regarding adhesion of such silane on the substrate, a group worked on the adhesion of silylated nanocellulose from hemp on glass or aluminum substrate and showed a positive effect of it, which was even better with gamma-aminopropyltrimethoxysilane than epoxy or methacryloxy fellows (Pacaphol and Aht-Ong, 2017).

No publication to our knowledge is providing a fast procedure for sylilation of nanocellulose in water, wich will be proposed in this work.

### Organic-inorganic composites

First to propose the reaction of silanol to create silica on nanocellulose was Dujardin et al. (2003) who tried to replicate the nematic structure with a synthesis of mesosporous silica on cellulose nanocrystals. They use the addition of tetramethoxysilane and NaOH to create a network in between CNC further calcined to remove the organic part. The idea was then extended with tetraethylorthosilicate (TEOS) and TMOS and adjusted through pH and concentration and it was able to obtain a chiral nematic order that reflects light at a different wavelength (Shopsowitz et al., 2010), (Shopsowitz et al., 2012), (Kelly et al., 2012)

and also loaded with metal nanoparticles for sensors applications (Qi et al., 2011). An acid-based TEOS modification of surface permits the creation of silica nanowires (Scheel et al., 2009). Although methods used are very close to Stöber method, no silica beads are obtained in the studies but only a silica coating network. Nothing is reported on the interaction between the silica and the CNCs.

Studies where the synthesis of spherical particles is done are less common. Particles are usually grown ex-situ or used as commercial grade and then added to cellulosic material. Such approaches were used to modify roughness/hydrophobicity on cotton fabric or nanocellulose (Zhao et al., 2010), (Le et al., 2016), or pore size of nanopaper or microfibrils coating (Garusinghe et al., 2017), (Kim et al., 2013), (Krol et al., 2015).

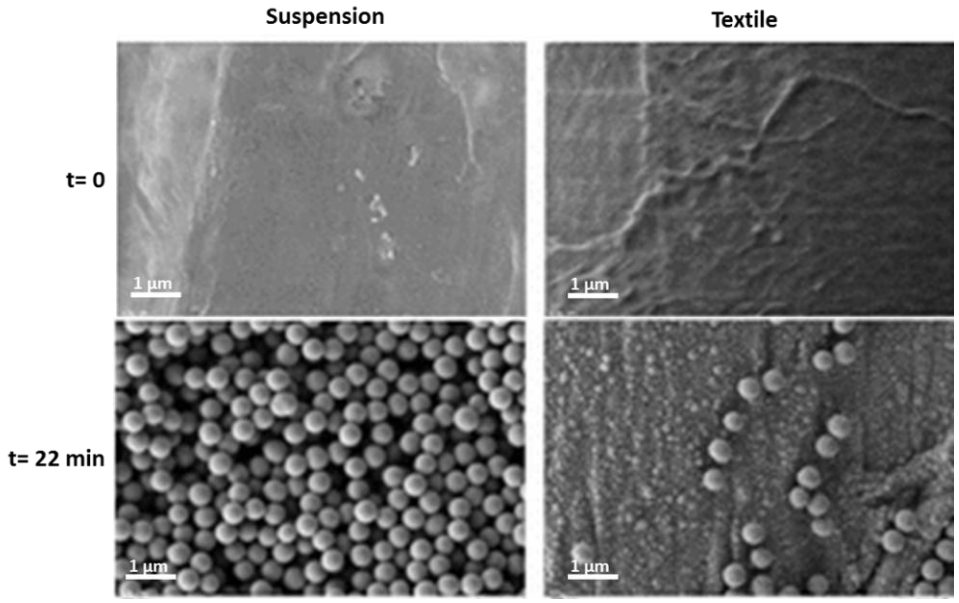


**Figure 1-27. Comparison of Stöber silica particles grown ex situ (left side) or in situ with cotton textile (right side) at 0 min ans 22 min. Adapted from (Zorko et al., 2015)**

The only paper reporting in situ growth of Stöber silica particle is presented by Zorko et al. (2015). They studied the impact of immersing a cotton fabric at different time of the Stöber reaction, showing that the presence of the fibers affect greatly the dispersity of the usual monodisperse particles (Figure 1-27). This growth was also monitored on other surface with different –OH content such as PET and it was showed that the interaction was very different leading to a thin silica film with poor adhesion.

In her master thesis, C. Maury (2014) reported also the formation of Stöber like particles inside Tempo oxidize nanofiber (TON) gel. Ammonia was changed by aminopropyltriethoxy silane (APTES) as ammonia was shown to create defects in nanofibers structure. She

investigated two routes. The first one dealt with grafting APTES on TON by peptidic link and from the ensuing mixture, the formation of silica particles with TEOS was initiated. The other approach, involved the direct formation of the particles inside the TON without any grafting.

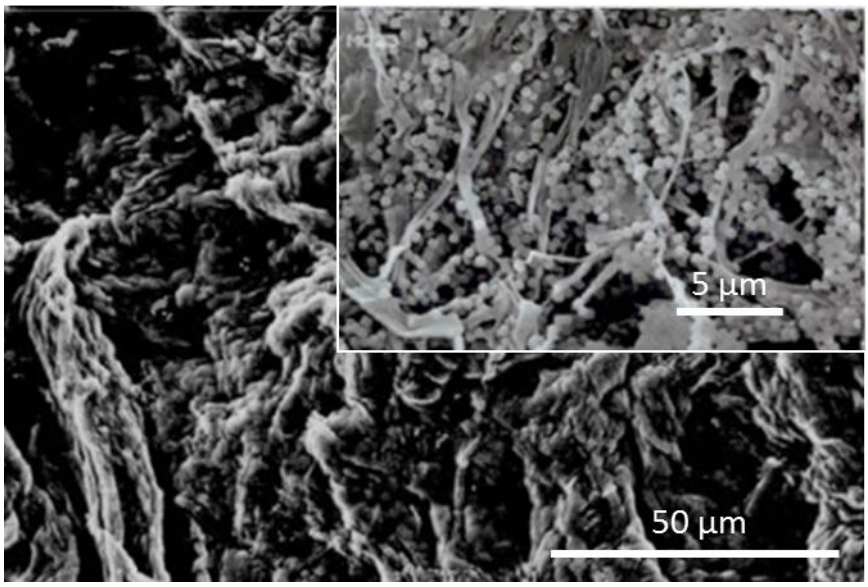


**Figure 1-28. TON gel film surface and cut in the material SEM images . TON was previously modified by APTES and subsequently subject to Söber silica particles growth. Adapted from**

The first was shown to create a continuous film on fibers with particles inside (Figure 1-28) while the other formed aggregates of particles. Introduced silica content was about 12wt% but nothing was reported on the surface energy modification. As compared to ex-situ growth of the same particles, the size was lowered from around 650nm to 500nm.

In this work, it will be proposed a formation of polysilsesquioxane particles inside cellulose nanofibrils network. Resulting hydrophobicity, durability and also antimicrobial activity will be studied.

### 3.3. Superhydrophobic cellulosic materials

Research on superhydrophobicity, which increases greatly these past ten years, is mainly based on non-renewable materials such as metal or glass for applications in boats or windows for example. Motivation on the achievement of superhydrophobicity on natural material is based on their abundancy in the world. The main problem is their high hydrophilicity regarding the high hydroxyl group content and the usual porous structures observed. It is then inherently water absorbing materials. In the transforming industry of wood or fibers, the main focus is to gain the hydrophobic property in order to control the

wettability of the material, for construction, printing, packaging and so on. To do so, internal and surface sizing is used.

The modification of renewable material into superhydrophobic like wood, paper or cotton fabrics was also studied and some really good effects were shown. In addition to the hydrophobic treatment, the roughness has to be induced if the material does not have it naturally. Ways of obtaining a 150° water contact angle are varying from bulk modification of the end material with surface modification of fibers in the case of paper or fabrics to surface modification through coating or modification of surfacing fibers (grafting) of materials. The main disadvantage to cope with is the porous material while dealing with surface modification, which becomes an asset while doing bulk modification. Indeed, the "porosity" and the natural roughness of cotton fibers for example give a micro-roughness which helps in obtaining the desired superhydrophobic state where only a nanoroughness is thus important to create with either, organic or inorganic particles or brushes/filaments. In the case of paper or nanopaper (made out with nanocellulose), this roughness is considerably lowered and it becomes more difficult to achieve this goal.

Table 1-6 is summarizing in a non-exhaustive manner, researches pathways and on the modification of natural materials for superhydrophobic properties. The use of fluorochemicals is recurring in the majority of the studies even though it was shown earlier that nature is not producing fluoro-moieties and is dealing with re-entrant structure and material with slightly higher surface energy such as wax.

While the information is given, it seems that superhydrophobicity layer on fiber material need to be in a range of 0.2 to 10 g/m² showing high difference in efficiency of treatments (Geissler et al., 2014) (Balu et al., 2008). This important criterion for industrial cost calculation is neglected in many studies.

Unfortunately, many studies focus on a different method to measure the properties of superhydrophobicity and almost no study is presenting all the measurement of static contact angle, contact angle hysteresis and roll-off or water shedding angle. Static contact angle is the main reference but it does not reflect the overall property of the superhydrophobicity state and furthermore could be insignificant for highly porous material.

Regarding the achievement of self-cleaning ability on cellulose/nanocellulose via silica based roughness and organo alkoxysilane, some studies are found in literature but are

relying on the formation of Stöber silica nanoparticles with a fluoro or silicon based post coating (Gonçalves et al.) or from modified Stöber particles with fluoro moieities (Table 1-6).

**Table 1-6. Non-exhaustive table of publications on superhydrophobic surface modification of a cellulose substrate: directly on fibers or on the already produced cellulose material.**

| Method | Applications | Fibers source | Step 1 | Step 2 | WCA | Sliding CA (°) or CAH(*) | WSA | Source |
|---|---|---|---|---|---|---|---|---|
| Fibers surface modification (Bulk) | Fabric | Cotton | PGMA brushes | Fluorocarbon derivative | 140,1-163,7 | >90 -45 | | (Li et al., 2015) |
| | | Cotton | $Si0_2$ nanoparticles LbL PAA PAH | - | 151-157 | | | (Zhao et al., 2010) |
| | | Cotton | POSS (polyhedral oligomeric silsesquioxane) | Fluorocarbon derivative | 152 | | | (Gao et al., 2010) |
| | | Cotton, wool | Silica nano-filament | - | - | - | 5-40° | (Zimmermann et al., 2008) (Artus et al., 2006) |
| | | Cotton | $Si0_2$ nanoparticles | Silane derivative | 156 | | | (Liu et al., 2014) |
| | | Cotton | $TiO_2$ nanoparticles | Fatty acid or fluorocarbon derivative | 152-164 | | | (Xue et al., 2008) |
| | Paper (polymerization) | - | Poly glycidyl methacrylate brushes | Post fluorination or fluorination during grafting | 154-170 | - | - | (Nyström et al., 2006) |
| | (Nano)Paper | - | $TiO_2$ nanoparticles | Silane derivative | | | | (Li et al., 2010) |
| | Nanocellulose aerogel | Birch kraft pulp | - | Fluorosilane derivative | 160 (w) 153(o) | - | - | (Jin et al., 2011) |
| | | Radiata pine | Polymethylsilsesquioxane | - | 150-155 | - | - | (Hayase et al., 2014) |
| Material surface modification (Surface) | Cotton fabric | Cotton | Carnauba wax Lbl | - | | | | (Lozhechnikova et al., 2017) |
| | Paper (spray) | - | Cellulose steraoyl ester | - | 150-153 | | | (Geissler et al., 2014) |
| | Paper (dip) | Filter paper | $SiO_2$ fluorinated | - | 172.4 ± 2.3 | 6.3 ± 0.3 | | (Wang et al., 2008) |
| | Paper(Lbl) | Ecalyptus kraft pulp | poly(allylamine hydrochloride)/lignosulfonate amine Lbl | - | 150.6-151.8 | | | (Peng et al., 2016) |
| | Paper (plasma vapour chemical deposition) | Filter paper | Oxygen plasma etching | Fluorocarbon | 166.7±0.9 | | | (Balu et al., 2008) |
| | | Surface | Cellulose fatty ester particles (1µm film thickness) | - | 158±1 | 5*±2 | - | (Zhang et al., 2015a) |

# Conclusion and challenges

This first Chapter is highlighting the outstanding properties of nanocellulose and in particular cellulose nanofibrils (CNF). Their use in different fields is promising and increasing research is focusing on their uses. In papermaking, application of CNF appears to have great potential in coating applications. Indeed, their rheological behavior as well as their barrier properties and their ability to disperse particles could efficiently be used.

The goal of this PhD project is to functionalize a paper surface in order to impart a non-wetting, a greaseproof, an anti-adherent or an antimicrobial property to it. The functionalization of nanocellulose to modify their hydrophilicity and to tune their properties stands out to be also a key procedure to obtain desired functionalities. In this context, organoalkoxysilanes seem to be interesting chemicals that are adaptable to a papermaking process. Their versatility obtained by changing functional groups but also by changing their physical structure (layer or particles) is very interesting for this project.

Thus, the following chapters will focus on the modification of CNF with organoalkoxysilanes and will then apply this knowledge in coating application of paper based material as presented in Figure 1-29.

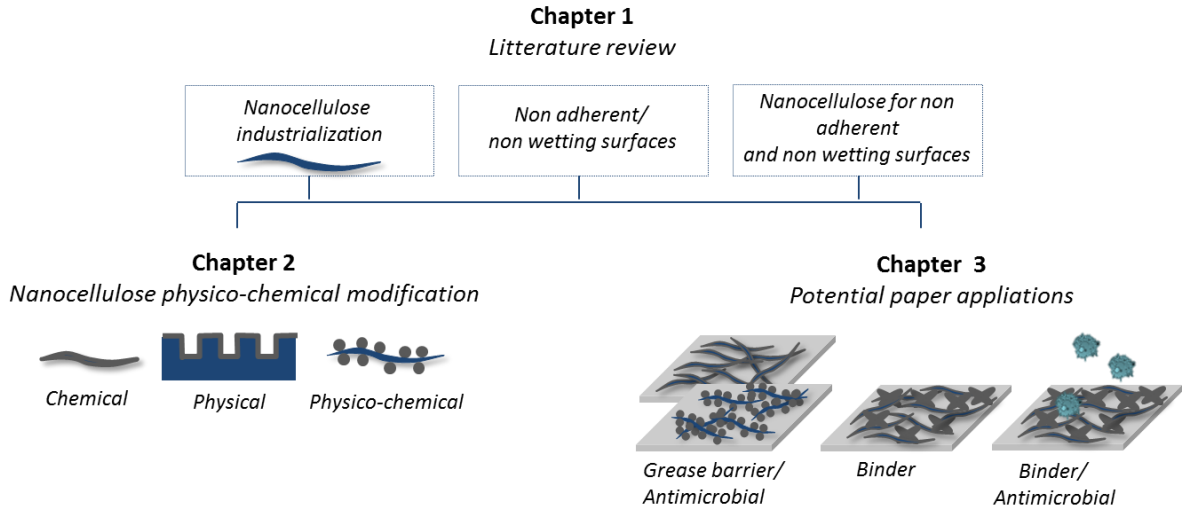


**Figure 1-29. Schematic representation of the project.**

As silane can react very differently in their medium, a first part will be dedicated to the understanding of the reaction of various organoalkoxysilanes with CNF in water and the obtention of relevant properties for the project. Also, as surface structuration is an important parameter in obtaining superhydrophobic material, the possibility of structuring

CNF by two different approaches, either by micromolding or by synthesis of particle on it, should be assessed.

In the second part of the research project, the use of modified CNF as coating material is evaluated to provide paper functions. The film forming ability and the tighten barrier network of CNF as well as their ability to disperse particles will be used in this purpose.

## References


Ahola, S., Österberg, M., Laine, J., 2008. Cellulose nanofibrils—adsorption with poly(amideamine) epichlorohydrin studied by QCM-D and application as a paper strength additive. Cellulose 15, 303–314. doi:10.1007/s10570-007-9167-3

Albin F. Turbak, Fred W. Snyder, Karen R. Sandberg, 1982. Food products containing microfibrillated cellulose. International Telephone and Telegraph Corporation, US4341807 (A)

Alila, S., Besbes, I., Vilar, M.R., Mutjé, P., Boufi, S., 2013. Non-woody plants as raw materials for production of microfibrillated cellulose (MFC): A comparative study. Ind. Crops Prod. 41, 250–259. doi:10.1016/j.indcrop.2012.04.028

Andresen, M., Johansson, L.-S., Tanem, B.S., Stenius, P., 2006. Properties and characterization of hydrophobized microfibrillated cellulose. Cellulose 13, 665–677. doi:10.1007/s10570-006-9072-1

Andresen, M., Stenius, P., 2007a. Water-in-oil Emulsions Stabilized by Hydrophobized Microfibrillated Cellulose. J. Dispers. Sci. Technol. 28, 837–844. doi:10.1080/01932690701341827

Andresen, M., Stenstad, P., Møretrø, T., Langsrud, S., Syverud, K., Johansson, L.-S., Stenius, P., 2007b. Nonleaching Antimicrobial Films Prepared from Surface-Modified Microfibrillated Cellulose. Biomacromolecules 8, 2149–2155. doi:10.1021/bm070304e

Antti Sirviö, J., Visanko, M., Liimatainen, H., 2015. Deep eutectic solvent system based on choline chloride-urea as a pre-treatment for nanofibrillation of wood cellulose. Green Chem. 17, 3401–3406. doi:10.1039/C5GC00398A

Araki, J., 2013. Electrostatic or steric? – preparations and characterizations of well-dispersed systems containing rod-like nanowhiskers of crystalline polysaccharides. Soft Matter 9, 4125–4141. doi:10.1039/C3SM27514K

Arkhireeva, A., Hay, J.N., Oware, W., 2005. A versatile route to silsesquioxane nanoparticles from organically modified silane precursors. J. Non-Cryst. Solids 351, 1688–1695. doi:10.1016/j.jnoncrysol.2005.04.063

Artus, G.R.J., Jung, S., Zimmermann, J., Gautschi, H.-P., Marquardt, K., Seeger, S., 2006. Silicone Nanofilaments and Their Application as Superhydrophobic Coatings. Adv. Mater. 18, 2758–2762. doi:10.1002/adma.200502030

Atalla, R.H., VanderHart, D.L., 1984. Native cellulose: a composite of two distinct crystalline forms. Science 223, 283–286.

Aulin, C., Gällstedt, M., Lindström, T., 2010a. Oxygen and oil barrier properties of microfibrillated cellulose films and coatings. Cellulose 17, 559–574. doi:10.1007/s10570-009-9393-y

Aulin, C., Netrval, J., Wågberg, L., Lindström, T., 2010b. Aerogels from nanofibrillated cellulose with tunable oleophobicity. Soft Matter 6, 3298. doi:10.1039/c001939a

Aulin, C., Ström, G., 2013. Multilayered Alkyd Resin/Nanocellulose Coatings for Use in Renewable Packaging Solutions with a High Level of Moisture Resistance. Ind. Eng. Chem. Res. 52, 2582–2589. doi:10.1021/ie301785a

Balu, B., Breedveld, V., Hess, D.W., 2008. Fabrication of "Roll-off" and "Sticky" Superhydrophobic Cellulose Surfaces via Plasma Processing. Langmuir 24, 4785–4790. doi:10.1021/la703766c

Bardet, R., 2014. Nanocellulose as potential materials for specialty papers. Ph.D manuscript, Université Grenoble Alpes.

Bardet, R., Belgacem, M.N., Bras, J., 2013a. Different strategies for obtaining high opacity films of MFC with TiO2 pigments. Cellulose 20, 3025–3037. doi:10.1007/s10570-013-0025-1

Bardet, R., Reverdy, C., Belgacem, N., Leirset, I., Syverud, K., Bardet, M., Bras, J., 2015. Substitution of nanoclay in high gas barrier films of cellulose nanofibrils with cellulose nanocrystals and thermal treatment. Cellulose 22, 1227–1241. doi:10.1007/s10570-015-0547-9

Barthlott, W., Neinhuis, C., 1997. Purity of the sacred lotus, or escape from contamination in biological surfaces. Planta 202, 1–8.

Beck-Candanedo, S., Roman, M., Gray, D.G., 2005. Effect of Reaction Conditions on the Properties and Behavior of Wood Cellulose Nanocrystal Suspensions. Biomacromolecules 6, 1048–1054. doi:10.1021/bm049300p

Bellanger, H., Darmanin, T., Taffin de Givenchy, E., Guittard, F., 2014. Chemical and Physical Pathways for the Preparation of Superoleophobic Surfaces and Related Wetting Theories. Chem. Rev. 114, 2694–2716. doi:10.1021/cr400169m

Beneventi, D., Chaussy, D., Curtil, D., Zolin, L., Gerbaldi, C., Penazzi, N., 2014. Highly Porous Paper Loading with Microfibrillated Cellulose by Spray Coating on Wet Substrates. Ind. Eng. Chem. Res. 53, 10982–10989. doi:10.1021/ie500955x

Benkaddour, A., Jradi, K., Robert, S., Daneault, C., 2013. Grafting of Polycaprolactone on Oxidized Nanocelluloses by Click Chemistry. Nanomaterials 3, 141–157. doi:10.3390/nano3010141

B. Filson, P., E. Dawson-Andoh, B., Schwegler-Berry, D., 2009. Enzymatic-mediated production of cellulose nanocrystals from recycled pulp. Green Chem. 11, 1808–1814. doi:10.1039/B915746H

Bhushan, B., Her, E.K., 2010. Fabrication of Superhydrophobic Surfaces with High and Low Adhesion Inspired from Rose Petal. Langmuir 26, 8207–8217. doi:10.1021/la904585j

Bhushan, B., Jung, Y.C., 2011. Natural and biomimetic artificial surfaces for superhydrophobicity, self-cleaning, low adhesion, and drag reduction. Prog. Mater. Sci. 56, 1–108. doi:10.1016/j.pmatsci.2010.04.003

Bhushan, B., Nosonovsky, M., 2010. The rose petal effect and the modes of superhydrophobicity. Philos. Trans. R. Soc. Math. Phys. Eng. Sci. 368, 4713–4728. doi:10.1098/rsta.2010.0203

Bilodeau, M. a, Hamilton, R.H., 2013. Release Paper and Method of Manufacture. CA2876083 (A1).

Bilodeau, M., Hamilton, R., 2013. Release Paper and Method of Manufacture. WO2013188739 (A1).

Boufi, S., González, I., Delgado-Aguilar, M., Tarrès, Q., Pèlach, M.À., Mutjé, P., 2016. Nanofibrillated cellulose as an additive in papermaking process: A review. Carbohydr. Polym. 154, 151–166. doi:10.1016/j.carbpol.2016.07.117

Brochier Salon, M.-C., Bardet, M., Belgacem, M.N., 2008a. Solvolysis–hydrolysis of N-bearing alkoxysilanes: Reactions studied with 29Si NMR. Silicon Chem. 3, 335–350. doi:10.1007/s11201-008-9036-4

Brochier Salon, M.-C., Bayle, P.-A., Abdelmouleh, M., Boufi, S., Belgacem, M.N., 2008b. Kinetics of hydrolysis and self condensation reactions of silanes by NMR spectroscopy. Colloids Surf. Physicochem. Eng. Asp. 312, 83–91. doi:10.1016/j.colsurfa.2007.06.028

Brochier Salon, M.-C., Belgacem, M.N., 2010. Competition between hydrolysis and condensation reactions of trialkoxysilanes, as a function of the amount of water and the nature of the organic group. Colloids Surf. Physicochem. Eng. Asp. 366, 147–154. doi:10.1016/j.colsurfa.2010.06.002

Brodin, F.W., Eriksen, Ø., 2015. Preparation of individualised lignocellulose microfibrils based on thermomechanical pulp and their effect on paper properties. Nord Pulp Pap Res J 30, 443–451.

Brodin, F.W., Gregersen, O.W., Syverud, K., 2014. Cellulose nanofibrils: Challenges and possibilities as a paper additive or coating material–A review. Nord Pulp Pap Res J 29, 156–166.

Brozek, E.M., Washton, N.M., Mueller, K.T., Zharov, I., 2017. Silsesquioxane nanoparticles with reactive internal functional groups. J. Nanoparticle Res. 19, 85. doi:10.1007/s11051-017-3771-4

Capron, I., Rojas, O.J., Bordes, R., 2017. Behavior of nanocelluloses at interfaces. Curr. Opin. Colloid Interface Sci. 29, 83–95. doi:10.1016/j.cocis.2017.04.001

Carrillo, C.A., Nypelö, T.E., Rojas, O.J., 2015. Cellulose nanofibrils for one-step stabilization of multiple emulsions (W/O/W) based on soybean oil. J. Colloid Interface Sci. 445, 166–173. doi:10.1016/j.jcis.2014.12.028

Castro-Guerrero, C.F., Gray, D.G., 2014. Chiral nematic phase formation by aqueous suspensions of cellulose nanocrystals prepared by oxidation with ammonium persulfate. Cellulose 21, 2567–2577. doi:10.1007/s10570-014-0308-1

Cervin, N.T., Aulin, C., Larsson, P.T., Wågberg, L., 2012. Ultra porous nanocellulose aerogels as separation medium for mixtures of oil/water liquids. Cellulose 19, 401–410. doi:10.1007/s10570-011-9629-5

Chakraborty, A., Sain, M., Kortschot, M., 2005. Cellulose microfibrils: A novel method of preparation using high shear refining and cryocrushing. Holzforschung 59. doi:10.1515/HF.2005.016

Cheng, Q., Wang, S., Rials, T.G., 2009. Poly(vinyl alcohol) nanocomposites reinforced with cellulose fibrils isolated by high intensity ultrasonication. Compos. Part Appl. Sci. Manuf. 40, 218–224. doi:10.1016/j.compositesa.2008.11.009

Cheng, Y.T., Rodak, D.E., Wong, C.A., Hayden, C.A., 2006. Effects of micro- and nano-structures on the self-cleaning behaviour of lotus leaves. Nanotechnology 17, 1359. doi:10.1088/0957-4484/17/5/032

Cherian, B.M., Leão, A.L., de Souza, S.F., Thomas, S., Pothan, L.A., Kottaisamy, M., 2010. Isolation of nanocellulose from pineapple leaf fibres by steam explosion. Carbohydr. Polym. 81, 720–725. doi:10.1016/j.carbpol.2010.03.046

Chevalier, Y., Bolzinger, M.-A., 2013. Emulsions stabilized with solid nanoparticles: Pickering emulsions. Colloids Surf. Physicochem. Eng. Asp., Nanoparticles@interfaces 439, 23–34. doi:10.1016/j.colsurfa.2013.02.054

Chinga-Carrasco, G., Tobjörk, D., Österbacka, R., 2012. Inkjet-printed silver nanoparticles on nano-engineered cellulose films for electrically conducting structures and organic transistors: concept and challenges. J. Nanoparticle Res. 14, 1213. doi:10.1007/s11051-012-1213-x

Choi, J.Y., Kim, C.H., Kim, D.K., 1998. Formation and Characterization of Monodisperse, Spherical Organo-Silica Powders from Organo-Alkoxysilane-Water System. J. Am. Ceram. Soc. 81, 1184–1188. doi:10.1111/j.1151-2916.1998.tb02466.x

Cowles, D., 2016. The Application of CNF to Improve Paper Properties. TAPPI Nano International conference on Nanotechnology for Renewable Materials, Grenoble, France..

De France, K.J., Hoare, T., Cranston, E.D., 2017. Review of Hydrogels and Aerogels Containing Nanocellulose. Chem. Mater. 29, 4609–4631. doi:10.1021/acs.chemmater.7b00531

Delgado-Aguilar, M., González, I., Pèlach, M.A., Fuente, E.D.L., Negro, C., Mutjé, P., 2015. Improvement of deinked old newspaper/old magazine pulp suspensions by means of nanofibrillated cellulose addition. Cellulose 22, 789–802. doi:10.1007/s10570-014-0473-2

Desmaisons, J., Boutonnet, E., Rueff, M., Dufresne, A., Bras, J., 2017. A new quality index for benchmarking of different cellulose nanofibrils. Carbohydr. Polym. 174, 318–329. doi:10.1016/j.carbpol.2017.06.032

Dirè, S., Tagliazucca, V., Callone, E., Quaranta, A., 2011. Effect of functional groups on condensation and properties of sol–gel silica nanoparticles prepared by direct synthesis from organoalkoxysilanes. Mater. Chem. Phys. 126, 909–917. doi:10.1016/j.matchemphys.2010.12.015

Dong, F., Ha, C.-S., 2012. Multifunctional materials based on polysilsesquioxanes. Macromol. Res. 20, 335–343. doi:10.1007/s13233-012-0151-x

Dujardin, E., Blaseby, M., Mann, S., 2003. Synthesis of mesoporous silica by sol–gel mineralisation of cellulose nanorod nematic suspensions. J. Mater. Chem. 13, 696–699. doi:10.1039/B212689C

Dupuis, A., Yeomans, J.M., 2005. Modeling Droplets on Superhydrophobic Surfaces: Equilibrium States and Transitions. Langmuir 21, 2624–2629. doi:10.1021/la047348i

Eral, H.B., ’t Mannetje, D.J.C.M., Oh, J.M., 2013. Contact angle hysteresis: a review of fundamentals and applications. Colloid Polym. Sci. 291, 247–260. doi:10.1007/s00396-012-2796-6

Fantini, D., 2014. Fibre-based support containing a layer of a functionalized watersoluble polymer, method of production and use thereof. Munksjö Oyj. US20140262092 A1.

Fein, K., 2016. Cellulose Nanofibrils addition to paper for improvement of barrier properties. TAPPI Nano International conference on Nanotechnology for Renewable Materials, Grenoble, France..

Finley Richmond, 2014. Cellulose Nanofibers Use in Coated Paper. Ph.D manuscript, University of Maine.

Gao, Y., He, C., Huang, Y., Qing, F.-L., 2010. Novel water and oil repellent POSS-based organic/inorganic nanomaterial: Preparation, characterization and application to cotton fabrics. Polymer 51, 5997–6004. doi:10.1016/j.polymer.2010.10.020

Garusinghe, U.M., Varanasi, S., Garnier, G., Batchelor, W., 2017. Strong cellulose nanofibre–nanosilica composites with controllable pore structure. Cellulose 1–11. doi:10.1007/s10570-017-1265-2

Gatenholm, P., Klemm, D., 2010. Bacterial Nanocellulose as a Renewable Material for Biomedical Applications. MRS Bull. 35, 208–213. doi:10.1557/mrs2010.653

G. Croissant, J., Cattoën, X., Durand, J.-O., Man, M.W.C., M. Khashab, N., 2016. Organosilica hybrid nanomaterials with a high organic content: syntheses and applications of silsesquioxanes. Nanoscale 8, 19945–19972. doi:10.1039/C6NR06862F

Geissler, A., Loyal, F., Biesalski, M., Zhang, K., 2014. Thermo-responsive superhydrophobic paper using nanostructured cellulose stearoyl ester. Cellulose 21, 357–366. doi:10.1007/s10570-013-0160-8

George, J., Sabapathi, S., 2015. Cellulose nanocrystals: synthesis, functional properties, and applications. Nanotechnol. Sci. Appl. 8, 45–54. doi:10.2147/NSA.S64386

Ghanadpour, M., Carosio, F., Larsson, P.T., Wågberg, L., 2015. Phosphorylated Cellulose Nanofibrils: A Renewable Nanomaterial for the Preparation of Intrinsically Flame-Retardant Materials. Biomacromolecules 16, 3399–3410. doi:10.1021/acs.biomac.5b01117

Gicquel, E., Martin, C., Yanez, J.G., Bras, J., 2017. Cellulose nanocrystals as new bio-based coating layer for improving fiber-based mechanical and barrier properties. J. Mater. Sci. 52, 3048–3061. doi:10.1007/s10853-016-0589-x

Gonçalves, G., Marques, P.A.A.P., Trindade, T., Neto, C.P., Gandini, A., 2008. Superhydrophobic cellulose nanocomposites. J. Colloid Interface Sci. 324, 42–46. doi:10.1016/j.jcis.2008.04.066

González, I., Alcalà, M., Chinga-Carrasco, G., Vilaseca, F., Boufi, S., Mutjé, P., 2014. From paper to nanopaper: evolution of mechanical and physical properties. Cellulose 21, 2599–2609. doi:10.1007/s10570-014-0341-0

Goussé, C., Chanzy, H., Cerrada, M.L., Fleury, E., 2004. Surface silylation of cellulose microfibrils: preparation and rheological properties. Polymer 45, 1569–1575. doi:10.1016/j.polymer.2003.12.028

Goussé, C., Chanzy, H., Excoffier, G., Soubeyrand, L., Fleury, E., 2002. Stable suspensions of partially silylated cellulose whiskers dispersed in organic solvents. Polymer 43, 2645–2651. doi:10.1016/S0032-3861(02)00051-4

Guezennec, C., 2012. Développement de nouveaux matériaux d'emballage à partir de micro- et nano-fibrilles de cellulose. Ph.D manuscript, Université Grenoble Alpes.

Habibi, Y., 2014. Key advances in the chemical modification of nanocelluloses. Chem Soc Rev 43, 1519–1542. doi:10.1039/C3CS60204D

Habibi, Y., Lucia, L.A., Rojas, O.J., 2010. Cellulose Nanocrystals: Chemistry, Self-Assembly, and Applications. Chem. Rev. 110, 3479–3500. doi:10.1021/cr900339w

Hamada, H., 2010. Nanofibrillated Cellulose with Fine Clay as a Coating Agent to Improve Print Quality., PaerCon conference, Atlanta, USA.

Hassan, E.A., Hassan, M.L., Oksman, K., 2011. Improving Bagasse Pulp Paper Sheet Properties with Microfibrillated Cellulose Isolated from Xylanase-Treated Bagasse. Wood Fiber Sci. 43, 76–82.

Hayase, G., Kanamori, K., Abe, K., Yano, H., Maeno, A., Kaji, H., Nakanishi, K., 2014. Polymethylsilsesquioxane–Cellulose Nanofiber Biocomposite Aerogels with High Thermal Insulation, Bendability, and Superhydrophobicity. ACS Appl. Mater. Interfaces 6, 9466–9471. doi:10.1021/am501822y

Heitz, C., Laurent, G., Briard, R., Barthel, E., 2006. Cross-condensation and particle growth in aqueous silane mixtures at low concentration. J. Colloid Interface Sci. 298, 192–201. doi:10.1016/j.jcis.2005.12.011

Henriksson, M., Berglund, L.A., Isaksson, P., Lindström, T., Nishino, T., 2008. Cellulose Nanopaper Structures of High Toughness. Biomacromolecules 9, 1579–1585. doi:10.1021/bm800038n

Henriksson, M., Henriksson, G., Berglund, L.A., Lindström, T., 2007. An environmentally friendly method for enzyme-assisted preparation of microfibrillated cellulose (MFC) nanofibers. Eur. Polym. J. 43, 3434–3441. doi:10.1016/j.eurpolymj.2007.05.038

Hensel, R., Helbig, R., Aland, S., Voigt, A., Neinhuis, C., Werner, C., 2013. Tunable nano-replication to explore the omniphobic characteristics of springtail skin. NPG Asia Mater. 5, e37. doi:10.1038/am.2012.66

Herrick, F.W., Casebier, R.L., Hamilton, J.K., Sandberg, K.R., 1983. Microfibrillated Cellulose: Morphology and Accessibility. J Appl Polym Sci Appl Polym Symp U. S. 37.

Hii, 2012. The effect of MFC on the pressability and paper properties of TMP and GCC based sheets. Nord. Pulp Pap. Res. J. 27, 388–396. doi:10.3183/NPPRJ-2012-27-02-p388-396

Ho, T.T.T., Abe, K., Zimmermann, T., Yano, H., 2015. Nanofibrillation of pulp fibers by twin-screw extrusion. Cellulose 22, 421–433. doi:10.1007/s10570-014-0518-6

Hoeng, F., Denneulin, A., Bras, J., 2016. Use of nanocellulose in printed electronics: a review. Nanoscale 8, 13131–13154. doi:10.1039/C6NR03054H

Hoeng, F., Denneulin, A., Reverdy-Bruas, N., Krosnicki, G., Bras, J., 2017. Rheology of cellulose nanofibrils/silver nanowires suspension for the production of transparent and conductive electrodes by screen printing. Appl. Surf. Sci. 394, 160–168. doi:10.1016/j.apsusc.2016.10.073

Hon, D.N.-S., 1994. Cellulose: a random walk along its historical path. Cellulose 1, 1–25. doi:10.1007/BF00818796

Hsieh, M.-C., Kim, C., Nogi, M., Suganuma, K., 2013. Electrically conductive lines on cellulose nanopaper for flexible electrical devices. Nanoscale 5, 9289–9295. doi:10.1039/C3NR01951A

Hu, L., Zheng, G., Yao, J., Liu, N., Weil, B., Eskilsson, M., Karabulut, E., Ruan, Z., Fan, S., T. Bloking, J., D. McGehee, M., Wågberg, L., Cui, Y., 2013. Transparent and conductive paper from nanocellulose fibers. Energy Environ. Sci. 6, 513–518. doi:10.1039/C2EE23635D

Hua, K., O. Carlsson, D., Ålander, E., Lindström, T., Strømme, M., Mihranyan, A., Ferraz, N., 2014. Translational study between structure and biological response of nanocellulose from wood and green algae. RSC Adv. 4, 2892–2903. doi:10.1039/C3RA45553J

Huang, H.-J., Ramaswamy, S., Tschirner, U.W., Ramarao, B.V., 2008. A review of separation technologies in current and future biorefineries. Sep. Purif. Technol. 62, 1–21. doi:10.1016/j.seppur.2007.12.011

Hult, E.-L., Iotti, M., Lenes, M., 2010. Efficient approach to high barrier packaging using microfibrillar cellulose and shellac. Cellulose 17, 575–586. doi:10.1007/s10570-010-9408-8

Jari Vartiainen, 2014. Improving Multilayer Packaging Performance with Nanocellulose Barrier Layer., TAPPI Nano International conference on Nanotechnology for Renewable Materials,Vancoucer, Canada.

Jin, H., Kettunen, M., Laiho, A., Pynnönen, H., Paltakari, J., Marmur, A., Ikkala, O., Ras, R.H.A., 2011. Superhydrophobic and Superoleophobic Nanocellulose Aerogel Membranes as Bioinspired Cargo Carriers on Water and Oil. Langmuir 27, 1930–1934. doi:10.1021/la103877r

Johnston, J.W., Townsend, D.F., Hagiopol, C., Talbert, L.D., Ruffner, C.G., 2014. Greaseproof paper with lower content of fluorochemicals. Georgia-Pacific Chemicals Llc. US20140102651 A1.

Jr, C.W.P., 2014. Grease, oil and wax resistant paper composition. Georgia-Pacific Chemicals Llc. US8734895 B2.

Kajanto, I., Kosonen, M., 2012. The potential use of micro-and nanofibrillated cellulose as a reinforcing element in paper. J. Sci. Technol. For. Prod. Process. 2, 42–48.

Kaushik, M., Moores, A., 2016. Review: nanocelluloses as versatile supports for metal nanoparticles and their applications in catalysis. Green Chem. 18, 622–637. doi:10.1039/C5GC02500A

Kelárek, J., 2015. Paper with Enhanced Strength and Enhanced Resistance to Fats. WO2015180699 (A1).

Kelly, J.A., Shopsowitz, K.E., Ahn, J.M., Hamad, W.Y., MacLachlan, M.J., 2012. Chiral Nematic Stained Glass: Controlling the Optical Properties of Nanocrystalline Cellulose-Templated Materials. Langmuir 28, 17256–17262. doi:10.1021/la3041902

Kim, J.-H., Kim, J.-H., Choi, E.-S., Yu, H.K., Kim, J.H., Wu, Q., Chun, S.-J., Lee, S.-Y., Lee, S.-Y., 2013. Colloidal silica nanoparticle-assisted structural control of cellulose nanofiber paper separators for lithium-ion batteries. J. Power Sources 242, 533–540. doi:10.1016/j.jpowsour.2013.05.142

Klemm, D., Heublein, B., Fink, H.-P., Bohn, A., 2005. Cellulose: Fascinating Biopolymer and Sustainable Raw Material. Angew. Chem. Int. Ed. 44, 3358–3393. doi:10.1002/anie.200460587

Koch, K., Bhushan, B., Barthlott, W., 2009. Multifunctional surface structures of plants: An inspiration for biomimetics. Prog. Mater. Sci. 54, 137–178. doi:10.1016/j.pmatsci.2008.07.003

Koga, H., Saito, T., Kitaoka, T., Nogi, M., Suganuma, K., Isogai, A., 2013. Transparent, Conductive, and Printable Composites Consisting of TEMPO-Oxidized Nanocellulose and Carbon Nanotube. Biomacromolecules 14, 1160–1165. doi:10.1021/bm400075f

Kolakovic, R., Peltonen, L., Laukkanen, A., Hirvonen, J., Laaksonen, T., 2012. Nanofibrillar cellulose films for controlled drug delivery. Eur. J. Pharm. Biopharm. 82, 308–315. doi:10.1016/j.ejpb.2012.06.011

Kose, R., Mitani, I., Kasai, W., Kondo, T., 2011. "Nanocellulose" As a Single Nanofiber Prepared from Pellicle Secreted by *Gluconacetobacter xylinus* Using Aqueous Counter Collision. Biomacromolecules 12, 716–720. doi:10.1021/bm1013469

Koskinen, K., Rissanen, M., Tani, P., Kivivasara, J., Koskinen, T., Kosonen, H., Pohjola, L., Saarinen, J., Seppälä, J., Salminen, A., 2013. A release liner composition, a base material and a method of producing a base material, and a surface treating agent for a base material and a use of a surface treating agent. UPM-Kymmene Corporation. EP2574643 A1.

Koskinen, K., Tani, P., 2001. Base paper, method to produce it and release paper. UPM-Kymmene Corporation. WO2001055507 A1.

Kosonen, M.V., Kajanto, I., 2014. Paper product and a method and a system for manufacturing furnish. UPM-Kymmene Corporation. US20140338849 A1.

Krol, L.F., Beneventi, D., Alloin, F., Chaussy, D., 2015. Microfibrillated cellulose-SiO2 composite nanopapers produced by spray deposition. J. Mater. Sci. 50, 4095–4103. doi:10.1007/s10853-015-8965-5

Kumar, V., Elfving, A., Koivula, H., Bousfield, D., Toivakka, M., 2016. Roll-to-Roll Processed Cellulose Nanofiber Coatings. Ind. Eng. Chem. Res. 55, 3603–3613. doi:10.1021/acs.iecr.6b00417

Kumar, V., Forsberg, S., Engström, A.-C., Nurmi, M., Andres, B., Christina Dahlström, Toivakka, M., 2017. Conductive nanographite–nanocellulose coatings on paper. Flex. Print. Electron. 2, 035002. doi:10.1088/2058-8585/aa728e

Kuroda, K., Shimojima, A., Kawahara, K., Wakabayashi, R., Tamura, Y., Asakura, Y., Kitahara, M., 2014. Utilization of Alkoxysilyl Groups for the Creation of Structurally Controlled Siloxane-Based Nanomaterials. Chem. Mater. 26, 211–220. doi:10.1021/cm4023387

Lafuma, A., Quéré, D., 2003. Superhydrophobic states. Nat. Mater. 2, 457–460. doi:10.1038/nmat924

Lavoine, N., Desloges, I., Dufresne, A., Bras, J., 2012a. Microfibrillated cellulose – Its barrier properties and applications in cellulosic materials: A review. Carbohydr. Polym. 90, 735–764. doi:10.1016/j.carbpol.2012.05.026

Lavoine, N., Desloges, I., Dufresne, A., Bras, J., 2012b. Microfibrillated cellulose – Its barrier properties and applications in cellulosic materials: A review. Carbohydr. Polym. 90, 735–764. doi:10.1016/j.carbpol.2012.05.026

Lavoine, N., Desloges, I., Khelifi, B., Bras, J., 2014a. Impact of different coating processes of microfibrillated cellulose on the mechanical and barrier properties of paper. J. Mater. Sci. 49, 2879–2893. doi:10.1007/s10853-013-7995-0

Lavoine, N., Desloges, I., Khelifi, B., Bras, J., 2014b. Impact of different coating processes of microfibrillated cellulose on the mechanical and barrier properties of paper. J. Mater. Sci. 49, 2879–2893. doi:10.1007/s10853-013-7995-0

Lavoine, N., Desloges, I., Sillard, C., Bras, J., 2014c. Controlled release and long-term antibacterial activity of chlorhexidine digluconate through the nanoporous network of microfibrillated cellulose. Cellulose 21, 4429–4442. doi:10.1007/s10570-014-0392-2

Le, D., Kongparakul, S., Samart, C., Phanthong, P., Karnjanakom, S., Abudula, A., Guan, G., 2016. Preparing hydrophobic nanocellulose-silica film by a facile one-pot method. Carbohydr. Polym. 153, 266–274. doi:10.1016/j.carbpol.2016.07.112

Lee, K.-Y., Blaker, J.J., Murakami, R., Heng, J.Y.Y., Bismarck, A., 2014. Phase Behavior of Medium and High Internal Phase Water-in-Oil Emulsions Stabilized Solely by Hydrophobized Bacterial Cellulose Nanofibrils. Langmuir 30, 452–460. doi:10.1021/la4032514

Lee, Y., Park, S.-H., Kim, K.-B., Lee, J.-K., 2007. Fabrication of Hierarchical Structures on a Polymer Surface to Mimic Natural Superhydrophobic Surfaces. Adv. Mater. 19, 2330–2335. doi:10.1002/adma.200700820

Li, J., Wei, X., Wang, Q., Chen, J., Chang, G., Kong, L., Su, J., Liu, Y., 2012. Homogeneous isolation of nanocellulose from sugarcane bagasse by high pressure homogenization. Carbohydr. Polym. 90, 1609–1613. doi:10.1016/j.carbpol.2012.07.038

Li, S., Wei, Y., Huang, J., 2010. Facile Fabrication of Superhydrophobic Cellulose Materials by a Nanocoating Approach. Chem. Lett. 39, 20–21. doi:10.1246/cl.2010.20

Li, S.H., Huang, J.Y., Ge, M.Z., Li, S.W., Xing, T.L., Chen, G.Q., Liu, Y.Q., Zhang, K.Q., Al-Deyab, S.S., Lai, Y.K., 2015. Controlled grafting superhydrophobic cellulose surface with environmentally-friendly short fluoroalkyl chains by ATRP. Mater. Des. 85, 815–822. doi:10.1016/j.matdes.2015.07.083

Lif, A., Stenstad, P., Syverud, K., Nydén, M., Holmberg, K., 2010. Fischer–Tropsch diesel emulsions stabilised by microfibrillated cellulose and nonionic surfactants. J. Colloid Interface Sci. 352, 585–592. doi:10.1016/j.jcis.2010.08.052

Littunen, K., Hippi, U., Johansson, L.-S., Österberg, M., Tammelin, T., Laine, J., Seppälä, J., 2011. Free radical graft copolymerization of nanofibrillated cellulose with acrylic monomers. Carbohydr. Polym. 84, 1039–1047. doi:10.1016/j.carbpol.2010.12.064

Liu, A., Walther, A., Ikkala, O., Belova, L., Berglund, L.A., 2011. Clay Nanopaper with Tough Cellulose Nanofiber Matrix for Fire Retardancy and Gas Barrier Functions. Biomacromolecules 12, 633–641. doi:10.1021/bm101296z

Liu, F., Ma, M., Zang, D., Gao, Z., Wang, C., 2014. Fabrication of superhydrophobic/superoleophilic cotton for application in the field of water/oil separation. Carbohydr. Polym. 103, 480–487. doi:10.1016/j.carbpol.2013.12.022

Liu, S., Lang, X., Ye, H., Zhang, S., Zhao, J., 2005. Preparation and characterization of copolymerized aminopropyl/phenylsilsesquioxane microparticles. Eur. Polym. J. 41, 996–1001. doi:10.1016/j.eurpolymj.2004.11.027

Lönnberg, H., Larsson, K., Lindström, T., Hult, A., Malmström, E., 2011. Synthesis of Polycaprolactone-Grafted Microfibrillated Cellulose for Use in Novel Bionanocomposites–Influence of the Graft Length on the Mechanical Properties. ACS Appl. Mater. Interfaces 3, 1426–1433. doi:10.1021/am2001828

Loy, D.A., Baugher, B.M., Baugher, C.R., Schneider, D.A., Rahimian, K., 2000. Substituent Effects on the Sol−Gel Chemistry of Organotrialkoxysilanes. Chem. Mater. 12, 3624–3632. doi:10.1021/cm000451i

Lozhechnikova, A., Bellanger, H., Michen, B., Burgert, I., Österberg, M., 2017. Surfactant-free carnauba wax dispersion and its use for layer-by-layer assembled protective surface coatings on wood. Appl. Surf. Sci. 396, 1273–1281. doi:10.1016/j.apsusc.2016.11.132

Lu, J., Askeland, P., Drzal, L.T., 2008. Surface modification of microfibrillated cellulose for epoxy composite applications. Polymer 49, 1285–1296. doi:10.1016/j.polymer.2008.01.028

Man, Z., Muhammad, N., Sarwono, A., Bustam, M.A., Kumar, M.V., Rafiq, S., 2011. Preparation of Cellulose Nanocrystals Using an Ionic Liquid. J. Polym. Environ. 19, 726–731. doi:10.1007/s10924-011-0323-3

Mariano, M., El Kissi, N., Dufresne, A., 2014. Cellulose nanocrystals and related nanocomposites: Review of some properties and challenges. J. Polym. Sci. Part B Polym. Phys. 52, 791–806. doi:10.1002/polb.23490

Markstedt, K., Mantas, A., Tournier, I., Martínez Ávila, H., Hägg, D., Gatenholm, P., 2015. 3D Bioprinting Human Chondrocytes with Nanocellulose–Alginate Bioink for Cartilage Tissue Engineering Applications. Biomacromolecules 16, 1489–1496. doi:10.1021/acs.biomac.5b00188

Maury, C., 2014. Elaboration et caractérisation de matériaux hybrides à base de nanocelluloses et de nanoparticules inorganiques. Maîtrise, Université Québec Montréal.

Meriçer, Ç., Minelli, M., Angelis, M.G.D., Giacinti Baschetti, M., Stancampiano, A., Laurita, R., Gherardi, M., Colombo, V., Trifol, J., Szabo, P., Lindström, T., 2016. Atmospheric plasma assisted PLA/microfibrillated cellulose (MFC) multilayer biocomposite for sustainable barrier application. Ind. Crops Prod., Nanocellulose: production, functionalisation and applications 93, 235–243. doi:10.1016/j.indcrop.2016.03.020

Missoum, K., Belgacem, M.N., Bras, J., 2013a. Nanofibrillated Cellulose Surface Modification: A Review. Materials 6, 1745–1766. doi:10.3390/ma6051745

Missoum, K., Martoïa, F., Belgacem, M.N., Bras, J., 2013b. Effect of chemically modified nanofibrillated cellulose addition on the properties of fiber-based materials. Ind. Crops Prod. 48, 98–105. doi:10.1016/j.indcrop.2013.04.013

Monclin, J.-P., Nelson, K., Retsina, T., 2015. Drilling Fluid Additives and Fracturing Fluid Additives Containing Cellulose Nanofibers and/or Nanocrystals. API IP HOLDINGS LLC. WO2015196042 (A1).

Montanari, S., Roumani, M., Heux, L., Vignon, M.R., 2005. Topochemistry of Carboxylated Cellulose Nanocrystals Resulting from TEMPO-Mediated Oxidation. Macromolecules 38, 1665–1671. doi:10.1021/ma048396c

Moring, R., Pahl, T., 2006. Method for manufacturing release paper. Lohjan Paperi Oy. WO2001029317(A1).

Morits, M., McKee, J.R., Majoinen, J., Malho, J.-M., Houbenov, N., Seitsonen, J., Laine, J., Gröschel, A.H., Ikkala, O., 2017. Polymer Brushes on Cellulose Nanofibers: Modification, SI-ATRP, and Unexpected Degradation Processes. ACS Sustain. Chem. Eng. 5, 7642–7650. doi:10.1021/acssuschemeng.7b00972

Mörseburg, K., Chinga-Carrasco, G., 2009. Assessing the combined benefits of clay and nanofibrillated cellulose in layered TMP-based sheets. Cellulose 16, 795–806. doi:10.1007/s10570-009-9290-4

Naderi, A., Lindström, T., 2014. Carboxymethylated nanofibrillated cellulose: effect of monovalent electrolytes on the rheological properties. Cellulose 21, 3507–3514. doi:10.1007/s10570-014-0394-0

Nechyporchuk, O., Belgacem, M.N., Bras, J., 2016. Production of cellulose nanofibrils: A review of recent advances. Ind. Crops Prod., Nanocellulose: production, functionalisation and applications 93, 2–25. doi:10.1016/j.indcrop.2016.02.016

Nechyporchuk, O., Pignon, F., Belgacem, M.N., 2015. Morphological properties of nanofibrillated cellulose produced using wet grinding as an ultimate fibrillation process. J. Mater. Sci. 50, 531–541. doi:10.1007/s10853-014-8609-1

Nogi, M., Komoda, N., Otsuka, K., Suganuma, K., 2013. Foldable nanopaper antennas for origami electronics. Nanoscale 5, 4395–4399. doi:10.1039/C3NR00231D

Nyström, D., Lindqvist, J., Östmark, E., Hult, A., Malmström, E., 2006. Superhydrophobic bio-fibre surfaces via tailored grafting architecture. Chem. Commun. 0, 3594–3596. doi:10.1039/B607411A

Oksman, K., Aitomäki, Y., Mathew, A.P., Siqueira, G., Zhou, Q., Butylina, S., Tanpichai, S., Zhou, X., Hooshmand, S., 2016. Review of the recent developments in cellulose nanocomposite processing. Compos. Part Appl. Sci. Manuf., Special Issue on Biocomposites 83, 2–18. doi:10.1016/j.compositesa.2015.10.041

Oksman, K., Mathew, A.P., Bismarck, A., Rojas, O., Sain, M., 2014. Handbook of Green Materials: Processing Technologies, Properties and Applications(In 4 Volumes). WORLD SCIENTIFIC. doi:10.1142/8975

Onda, T., Shibuichi, S., Satoh, N., Tsujii, K., 1996. Super-water-repellent fractal surfaces. Langmuir 12, 2125–2127.

Ooi, Y., Hanasaki, I., Mizumura, D., Matsuda, Y., 2017. Suppressing the coffee-ring effect of colloidal droplets by dispersed cellulose nanofibers. Sci. Technol. Adv. Mater. 18, 316–324. doi:10.1080/14686996.2017.1314776

Osong, S.H., Norgren, S., Engstrand, P., 2014. Paper strength improvement by inclusion of nano-ligno-cellulose to Chemi-thermomechanical pulp. Nord. Pulp Pap. Res. J. 29, 309–316.

Österberg, M., Vartiainen, J., Lucenius, J., Hippi, U., Seppälä, J., Serimaa, R., Laine, J., 2013. A Fast Method to Produce Strong NFC Films as a Platform for Barrier and Functional Materials. ACS Appl. Mater. Interfaces 5, 4640–4647. doi:10.1021/am401046x

O'sullivan, A.C., 1997. Cellulose: the structure slowly unravels. Cellulose 4, 173–207. doi:10.1023/A:1018431705579

Ottenbrite, R.M., Wall, J.S., Siddiqui, J.A., 2000. Self-Catalyzed Synthesis of Organo-Silica Nanoparticles. J. Am. Ceram. Soc. 83, 3214–3215.

Pääkkö, M., Ankerfors, M., Kosonen, H., Nykänen, A., Ahola, S., Österberg, M., Ruokolainen, J., Laine, J., Larsson, P.T., Ikkala, O., Lindström, T., 2007. Enzymatic Hydrolysis Combined with Mechanical Shearing and High-Pressure Homogenization for Nanoscale Cellulose Fibrils and Strong Gels. Biomacromolecules 8, 1934–1941. doi:10.1021/bm061215p

Pacaphol, K., Aht-Ong, D., 2017. The influences of silanes on interfacial adhesion and surface properties of nanocellulose film coating on glass and aluminum substrates. Surf. Coat. Technol. doi:10.1016/j.surfcoat.2017.01.111

Panaitescu, D.M., Donescu, D., Bercu, C., Vuluga, D.M., Iorga, M., Ghiurea, M., 2007. Polymer composites with cellulose microfibrils. Polym. Eng. Sci. 47, 1228–1234. doi:10.1002/pen.20803

Patankar., 2004. Transition between Superhydrophobic States on Rough Surfaces. Langmuir 20, 7097–7102. doi:10.1021/la049329e

Patankar., 2003. On the Modeling of Hydrophobic Contact Angles on Rough Surfaces. Langmuir 19, 1249–1253. doi:10.1021/la026612+

Peña-Alonso, R., Rubio, F., Rubio, J., Oteo, J.L., 2006. Study of the hydrolysis and condensation of γ-Aminopropyltriethoxysilane by FT-IR spectroscopy. J. Mater. Sci. 42, 595–603. doi:10.1007/s10853-006-1138-9

Peng, L., Meng, Y., Li, H., 2016. Facile fabrication of superhydrophobic paper with improved physical strength by a novel layer-by-layer assembly of polyelectrolytes and lignosulfonates-amine. Cellulose 23, 2073–2085. doi:10.1007/s10570-016-0910-5

Qi, H., Shopsowitz, K.E., Hamad, W.Y., MacLachlan, M.J., 2011. Chiral Nematic Assemblies of Silver Nanoparticles in Mesoporous Silica Thin Films. J. Am. Chem. Soc. 133, 3728–3731. doi:10.1021/ja110369d

Rakitov, R., Gorb, S.N., 2013. Brochosomal coats turn leafhopper (Insecta, Hemiptera, Cicadellidae) integument to superhydrophobic state. Proc. R. Soc. Lond. B Biol. Sci. 280, 20122391. doi:10.1098/rspb.2012.2391

Rånby, B.G., 1951. Fibrous macromolecular systems. Cellulose and muscle. The colloidal properties of cellulose micelles. Discuss. Faraday Soc. 11, 158–164. doi:10.1039/DF9511100158

Rantanen, J., Dimic-Misic, K., Kuusisto, J., Maloney, T.C., 2015. The effect of micro and nanofibrillated cellulose water uptake on high filler content composite paper properties and furnish dewatering. Cellulose 22, 4003–4015. doi:10.1007/s10570-015-0777-x

Rantanen, J., Maloney, T.C., 2015. Consolidation and dewatering of a microfibrillated cellulose fiber composite paper in wet pressing. Eur. Polym. J. 68, 585–591. doi:10.1016/j.eurpolymj.2015.03.045

Rantanen, J.J., Dimic-Misic, K., Pirttiniemi, J., Kuosmanen, P., Maloney, T.C., 2015. Forming and Dewatering of a Microfibrillated Cellulose Composite Paper. BioResources 10, 3492–3506. doi:10.15376/biores.10.2.3492-3506

Raquez, J.-M., Murena, Y., Goffin, A.-L., Habibi, Y., Ruelle, B., DeBuyl, F., Dubois, P., 2012. Surface-modification of cellulose nanowhiskers and their use as nanoreinforcers into polylactide: A sustainably-integrated approach. Compos. Sci. Technol. 72, 544–549. doi:10.1016/j.compscitech.2011.11.017

Reed, W.M., 1993. Silicone release coated substrate. P. H. Glatfelter Company. US5229212 (A).

Reverdy, C., 2016. Xyloglucan and cellulose nanofibrils assembly for barrier material. Poster presentation, ACS National Meeting, San Diego.

Rol, F., Karakashov, B., Nechyporchuk, O., Terrien, M., Meyer, V., Dufresne, A., Belgacem, M.N., Bras, J., 2017. Pilot-Scale Twin Screw Extrusion and Chemical Pretreatment as an Energy-Efficient Method for the Production of Nanofibrillated Cellulose at High Solid Content. ACS Sustain. Chem. Eng. doi:10.1021/acssuschemeng.7b00630

Sacui, I.A., Nieuwendaal, R.C., Burnett, D.J., Stranick, S.J., Jorfi, M., Weder, C., Foster, E.J., Olsson, R.T., Gilman, J.W., 2014. Comparison of the Properties of Cellulose Nanocrystals and Cellulose Nanofibrils Isolated from Bacteria, Tunicate, and Wood Processed Using Acid, Enzymatic, Mechanical, and Oxidative Methods. ACS Appl. Mater. Interfaces 6, 6127–6138. doi:10.1021/am500359f

Saini, S., Sillard, C., Belgacem, M.N., Bras, J., 2016a. Nisin anchored cellulose nanofibers for long term antimicrobial active food packaging. RSC Adv. 6, 12422–12430. doi:10.1039/C5RA22748H

Saini, S., Yücel Falco, Ç., Belgacem, M.N., Bras, J., 2016b. Surface cationized cellulose nanofibrils for the production of contact active antimicrobial surfaces. Carbohydr. Polym. 135, 239–247. doi:10.1016/j.carbpol.2015.09.002

Santucci, B.S., Bras, J., Belgacem, M.N., Curvelo, A.A. da S., Pimenta, M.T.B., 2016. Evaluation of the effects of chemical composition and refining treatments on the properties of nanofibrillated cellulose films from sugarcane bagasse. Ind. Crops Prod. 91, 238–248. doi:10.1016/j.indcrop.2016.07.017

Satyavolu, J.V., Hwang, K.-O., Anderson, K.R., Steinke, J.D., 2012. Lecithin-containing starch compositions, preparation thereof and paper products having oil and grease resistance, and/or release properties. Cargill, Incorported. US8192845 B2.

Scheel, H., Zollfrank, C., Greil, P., 2009. Luminescent silica nanotubes and nanowires: Preparation from cellulose whisker templates and investigation of irradiation-induced luminescence. J. Mater. Res. 24, 1709–1715. doi:10.1557/jmr.2009.0224

Shatkin, J.A., Wegner, T.H., Bilek, E.T., Cowie, J., 2014. Market projections of cellulose nanomaterial-enabled products-Part 1: Applications., TAPPI Journal, 13, 5.

Shimizu, M., Saito, T., Isogai, A., 2016. Water-resistant and high oxygen-barrier nanocellulose films with interfibrillar cross-linkages formed through multivalent metal ions. J. Membr. Sci. 500, 1–7. doi:10.1016/j.memsci.2015.11.002

Shimojima, A., Sugahara, Y., Kuroda, K., 1997. Inorganic–Organic Layered Materials Derived via the Hydrolysis and Polycondensation of Trialkoxy(alkyl)silanes. Bull. Chem. Soc. Jpn. 70, 2847–2853. doi:10.1246/bcsj.70.2847

Shopsowitz, K.E., Hamad, W.Y., MacLachlan, M.J., 2012. Flexible and Iridescent Chiral Nematic Mesoporous Organosilica Films. J. Am. Chem. Soc. 134, 867–870. doi:10.1021/ja210355v

Shopsowitz, K.E., Qi, H., Hamad, W.Y., MacLachlan, M.J., 2010. Free-standing mesoporous silica films with tunable chiral nematic structures. Nature 468, 422–425. doi:10.1038/nature09540

Stöber, W., Fink, A., Bohn, E., 1968. Controlled growth of monodisperse silica spheres in the micron size range. J. Colloid Interface Sci. 26, 62–69. doi:10.1016/0021-9797(68)90272-5

Su, Y., Ji, B., Zhang, K., Gao, H., Huang, Y., Hwang, K., 2010. Nano to Micro Structural Hierarchy Is Crucial for Stable Superhydrophobic and Water-Repellent Surfaces. Langmuir 26, 4984–4989. doi:10.1021/la9036452

Sultan, S., Siqueira, G., Zimmermann, T., Mathew, A.P., 2017. 3D printing of nano-cellulosic biomaterials for medical applications. Curr. Opin. Biomed. Eng., Additive Manufacturing 2, 29–34. doi:10.1016/j.cobme.2017.06.002

Svending, P., Kritzinger, J., Selida, T., FiberLean Technologies Ltd., 2017. Microfibrillated Cellulose Outside of the Box.

Syverud, K., Chinga-Carrasco, G., Toledo, J., Toledo, P.G., 2011. A comparative study of Eucalyptus and Pinus radiata pulp fibres as raw materials for production of cellulose nanofibrils. Carbohydr. Polym. 84, 1033–1038. doi:10.1016/j.carbpol.2010.12.066

Syverud, K., Stenius, P., 2009. Strength and barrier properties of MFC films. Cellulose 16, 75. doi:10.1007/s10570-008-9244-2

Taipale, T., Österberg, M., Nykänen, A., Ruokolainen, J., Laine, J., 2010. Effect of microfibrillated cellulose and fines on the drainage of kraft pulp suspension and paper strength. Cellulose 17, 1005–1020. doi:10.1007/s10570-010-9431-9

Takemura, M., Kawana, J., 2014. Water-resistant oil-resistant paper and method for producing same. Asahi Glass Company, Limited,WO2014098240 A1.

Talja, M., Moro, R., 2004. Baking paper. US20040115401 A1.

Tardy, B.L., Yokota, S., Ago, M., Xiang, W., Kondo, T., Bordes, R., Rojas, O.J., 2017. Nanocellulose–surfactant interactions. Curr. Opin. Colloid Interface Sci. 29, 57–67. doi:10.1016/j.cocis.2017.02.004

Tejado, A., Alam, M.N., Antal, M., Yang, H., Ven, T.G.M. van de, 2012. Energy requirements for the disintegration of cellulose fibers into cellulose nanofibers. Cellulose 19, 831–842. doi:10.1007/s10570-012-9694-4

Torvinen, K., Sievänen, J., Hjelt, T., Hellén, E., 2012. Smooth and flexible filler-nanocellulose composite structure for printed electronics applications. Cellulose 19, 821–829. doi:10.1007/s10570-012-9677-5

Uetani, K., Yano, H., 2011. Nanofibrillation of Wood Pulp Using a High-Speed Blender. Biomacromolecules 12, 348–353. doi:10.1021/bm101103p

van Blaaderen, A., Vrij, A., 1993. Synthesis and Characterization of Monodisperse Colloidal Organo-silica Spheres. J. Colloid Interface Sci. 156, 1–18. doi:10.1006/jcis.1993.1073

Vartiainen, J., Lahtinen, P., Kaljunen, T., Kunnari, V., Peresin, M.S., Tammelin, T., 2015. Comparison of properties between cellulose nanofibrils made from banana, sugar beet, hemp, softwood and hardwood pulps. O Pap. 76.

Vikman, M., Vartiainen, J., Tsitko, I., Korhonen, P., 2015. Biodegradability and Compostability of Nanofibrillar Cellulose-Based Products. J. Polym. Environ. 23, 206–215. doi:10.1007/s10924-014-0694-3

Wambua, P., Ivens, J., Verpoest, I., 2003. Natural fibres: can they replace glass in fibre reinforced plastics? Compos. Sci. Technol., Eco-Composites 63, 1259–1264. doi:10.1016/S0266-3538(03)00096-4

Wang, B., Liang, W., Guo, Z., Liu, W., 2015. Biomimetic super-lyophobic and super-lyophilic materials applied for oil/water separation: a new strategy beyond nature. Chem Soc Rev 44, 336–361. doi:10.1039/C4CS00220B

Wang, H., Fang, J., Cheng, T., Ding, J., Qu, L., Dai, L., Wang, X., Lin, T., 2008. One-step coating of fluoro -containing silica nanoparticles for universal generation of surface superhydrophobicity. Chem. Commun. 0, 877–879. doi:10.1039/B714352D

Wang, L., Sanders, J.E., Gardner, D.G., Han, Y., 2016. In-situ modification of cellulose nanofibrils by organosilanes during spray drying. Ind. Crops Prod., Nanocellulose: production, functionalisation and applications 93, 129–135. doi:10.1016/j.indcrop.2016.02.004

Wang, R., Baran, G., Wunder, S.L., 2000. Packing and Thermal Stability of Polyoctadecylsiloxane Compared with Octadecylsilane Monolayers. Langmuir 16, 6298–6305. doi:10.1021/la000206d

Wang, S., Jiang, L., 2007. Definition of Superhydrophobic States. Adv. Mater. 19, 3423–3424. doi:10.1002/adma.200700934

Wei, B., Li, Q., Jin, F., Li, H., Wang, C., 2016. The Potential of a Novel Nanofluid in Enhancing Oil Recovery. Energy Fuels 30, 2882–2891. doi:10.1021/acs.energyfuels.6b00244

Winuprasith, T., Suphantharika, M., 2013. Microfibrillated cellulose from mangosteen (Garcinia mangostana L.) rind: Preparation, characterization, and evaluation as an emulsion stabilizer. Food Hydrocoll. 32, 383–394. doi:10.1016/j.foodhyd.2013.01.023

Xhanari, K., Syverud, K., Chinga-Carrasco, G., Paso, K., Stenius, P., 2011. Reduction of water wettability of nanofibrillated cellulose by adsorption of cationic surfactants. Cellulose 18, 257–270. doi:10.1007/s10570-010-9482-y

Xue, C.-H., Jia, S.-T., Chen, H.-Z., Wang, M., 2008. Superhydrophobic cotton fabrics prepared by sol–gel coating of TiO 2 and surface hydrophobization. Sci. Technol. Adv. Mater. 9, 035001. doi:10.1088/1468-6996/9/3/035001

Young, T., 1805. An essay on the cohesion of fluids. Philos. Trans. R. Soc. Lond. 95, 65–87.

Yuji Matsuda, Mariko, H., Ueno Katsuhiko, 2001. Super microfibrillated cellulose, process for producing the same, and coated paper and tinted paper using the same.

Zhang, K., Geissler, A., Chen, X., Rosenfeldt, S., Yang, Y., Förster, S., Müller-Plathe, F., 2015. Polymeric Flower-Like Microparticles from Self-Assembled Cellulose Stearoyl Esters. ACS Macro Lett. 4, 214–219. doi:10.1021/mz500788e

Zhang, L., Tsuzuki, T., Wang, X., 2015. Preparation of cellulose nanofiber from softwood pulp by ball milling. Cellulose 22, 1729–1741. doi:10.1007/s10570-015-0582-6

Zhang, Z., Tingaut, P., Rentsch, D., Zimmermann, T., Sèbe, G., 2015. Controlled Silylation of Nanofibrillated Cellulose in Water: Reinforcement of a Model Polydimethylsiloxane Network. ChemSusChem 8, 2681–2690. doi:10.1002/cssc.201500525

Zhao, Y., Tang, Y., Wang, X., Lin, T., 2010. Superhydrophobic cotton fabric fabricated by electrostatic assembly of silica nanoparticles and its remarkable buoyancy. Appl. Surf. Sci. 256, 6736–6742. doi:10.1016/j.apsusc.2010.04.082

Zheng, G., Cui, Y., Karabulut, E., Wågberg, L., Zhu, H., Hu, L., 2013. Nanostructured paper for flexible energy and electronic devices. MRS Bull. 38, 320–325. doi:10.1557/mrs.2013.59

Zimmermann, J., Reifler, F.A., Fortunato, G., Gerhardt, L.-C., Seeger, S., 2008. A Simple, One-Step Approach to Durable and Robust Superhydrophobic Textiles. Adv. Funct. Mater. 18, 3662–3669. doi:10.1002/adfm.200800755

Zimmermann, J., Seeger, S., Reifler, F.A., 2009. Water Shedding Angle: A New Technique to Evaluate the Water-Repellent Properties of Superhydrophobic Surfaces. Text. Res. J. 79, 1565–1570. doi:10.1177/0040517509105074

Zorko, M., Vasiljević, J., Tomšič, B., Simončič, B., Gaberšček, M., Jerman, I., 2015. Cotton fiber hot spot in situ growth of Stöber particles. Cellulose 22, 3597–3607. doi:10.1007/s10570-015-0762-4

# Chapter 2
# Cellulose nanofibrils chemical and physical modification

# Table of content

**1. Cellulose nanofibrils aqueous modification with different organotrialkoxysilanes: influence of amine presence on surface mechanisms and properties .....115**

Abstract ..... 115

1.1. Introduction ..... 115

1.2. Experimental section ..... 118

1.2.1. Materials ..... 118

1.2.2. Methods ..... 118

1.3. Results and discussion ..... 121

1.3.1. Hydrolysation-condensation kinetics of silane ..... 121

1.3.2. Adsorption analysis ..... 122

1.3.3. Film characterization ..... 124

1.4. Conclusion and perspectives ..... 129

References ..... 130

**2.1. Cross-condensation of amino-propyl trimethoxy silane and propyl trimethoxy silane at low concentration for narrow dispersed nano- and micro-metric silsesquioxane particles synthesis .....133**

Abstract ..... 133

2.1.1. Introduction ..... 133

2.1.2.Materials and methods ..... 136

2.1.2.a. Materials ..... 136

2.1.2.b. Methods ..... 136

2.1.3. Results and discussion ..... 139

2.1.3.1. Effect of initial TMPS mass concentration ..... 139

2.1.3.2. Effect of molar ratio between APMS and TMPS ..... 139

2.1.3.3. Reaction kinetics and effect of parameters ..... 140

2.1.3.4. Particle physical and chemical properties ..... 142

2.1.4. Conclusion and perspectives ..... 146

References ..... 147

**2.2. Simple method to obtain hydrophobic and antimicrobial cellulose nanopaper using silsesquioxane particles sol gel formation in aqueous conditions .....149**

Abstract ..... 149
2.2.1. Introduction ..... 149
2.2.2. Experimental section ..... 153
2.2.2.a. Materials ..... 153
2.2.2.b. Methods ..... 153
2.2.3. Results and discussion ..... 156
2.2.3.1. CNF characterization ..... 156
2.2.3.2. Organotrialkoxysilane hydrolysis ..... 156
2.2.3.3. Films hydrophobicity ..... 157
2.2.3.4. Film structural properties ..... 161
2.2.3.5. Thermal stability ..... 163
2.2.3.6. Antibacterial assessment ..... 163
2.2.4. Conclusion and perspectives ..... 166
References ..... 167
**3. Micro/nano roughness patterning of cellulose nanofibers thinfilm toward superhydrophobicity ..... 171**
3.1. Introduction ..... 171
3.2. Materials and methods ..... 173
3.2.1. Materials ..... 173
3.2.2. Methods ..... 173
3.3. Results and discussion ..... 177
3.3.1. Surface morphology characterization ..... 177
3.3.2. Influence of the CNF coating onto the pattern ..... 178
3.3.3. Water contact angle ..... 179
3.4. Conclusion and perspectives ..... 181
References ..... 182
**Conclusion ..... 185**

# Chapter 2. Cellulose nanofibrils chemical and physical modification

## Introduction

As stated in **Chapter 1**, cellulose nanofibrils depict very interesting barrier properties because of the dense entangled network they formed. However the high hydroxyl groups content make it sensitive towadr water and humidity, degrading the above mentioned properties. This could be used as an asset to functionalize nanofiber through grafting or adsorption of molecule on their surface. It is particurlarly interesting to work with organotrialkoxysilanes for their modification as it permits the tunability of their properties in mild reaction conditions. It was also showed that, in the case of superhydrophobic surface development, thechemistry but also the roughness properties were also key.

The purpose of this **Chapter 2** is to provide (i) comprehension of CNF/organoalkoxysilanes interactions for better modification control, (ii) silsesquioxane particles growth on CNF to provide antibacterial and hydrophobic properties and (ii) to try to understand physical structuration possible on CNF film toward superhydrophobic property.

In **Chapter 2.1**, three different organoalkoxysilanes are studied for CNF functionalization in order to improve its barrier and hydrophobic properties.

In **Chapter 2.2**, the formation in water of silsesquioxane particles by reaction of two organotrialkoxysilanes is studied to understand mechanisms and influencing parameters in final properties. These particles will then be directly synthesized inside the nanocellulose network in aqueous medium to provide enhanced hydrophobic properties.

Lastly, in **Chapter 2.3**, potentiality of the micro-patterning of modified cellulose nanofibrils is assessed.

The entire **Chapter 2** aims at understanding key parameters in CNF functionalization in order to use it after in paper surface functionalization with it.

# 1. Cellulose nanofibrils aqueous modification with different organotrialkoxysilanes: influence of amine presence on surface mechanisms and properties

*This section is adapted from Reverdy C., Abdesselam K.A., Belgacem N., Brochier-Salon M.-C., Gablin C., Leonard D., Bras J.., Cellulose nanofibrils aqueous modification with different organotrialkoxysilanes: influence of amine presence on surface mechanisms and properties, submitted to Cellulose, (2017).*


## Abstract

The modification of CNF in aqueous or ethanolic media with organotrialkoxy silane was investigated in this work. The presence of the amine strongly affects silane hydrolysis and silanol condensation as compared with methoxy and trifluoro end-group. The amine is catalyzing the condensation procedure and, interestingly, has the advantage to give a higher hydrophobicity to the material. Regarding oxygen permeability, the presence of a hydrophilic group permits to obtain good results at high relative humidity. However, water vapor permeability is not improved. Cellulose nanofibrils modification with aminopropytrimethoxysilane paved the way for an easy aqueous nanofibrils properties tuning.


## 1.1. Introduction

Cellulose nanofibrils (CNF) have been a center of interest due to their outstanding properties such as mechanical strength or low oxygen permeability as a film and therefore could be valuable for coatings and useful for packaging application (Aulin et al., 2010), (Li et al., 2015). The nano entangled network formed by the nanofibrils can also be used as a web for dispersion of particles or even for release system of volatile molecule. As a biosourced, biodegradable and lightweight materials CNF can become a key for many applications.

Even though wood can stand up for long years in humid condition, cellulose and fibrils thereof only have the function of giving strength when other components will provide hydrophobic and antibacterial properties. With their high hydroxyl group concentration, films absorbed water and let water vapor to cross it and will also be a primary choice material for moldiness. A hydrophobic treatment is essential for its use in packaging field or

any field requiring water resistance. Many researches were carried out to impart hydrophobic properties to nanocellulose. The drawback of this high hydroxyl content becomes an asset due to the diversity in possible chemical reaction possible. From adsorption of molecule to grafting of polymer or molecule, hydrophobicity can be tuned (Missoum et al., 2013), (Habibi, 2014).

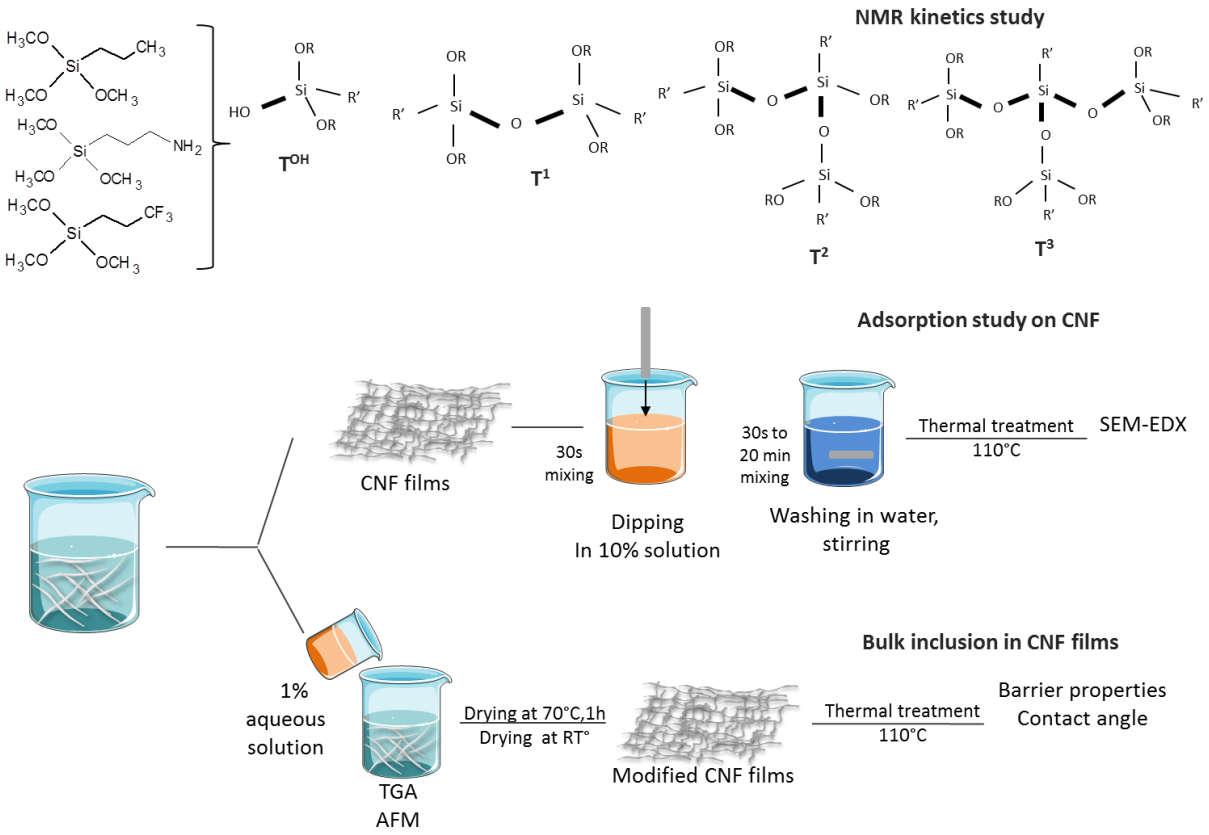


**Figure 2-1. Graphical abstract of the study**

Uppon these modifications, sylilation of cellulose or nanocellulose have been studied (Goussé et al., 2004),(Andresen et al., 2006),(Taipina et al., 2013), imparting good hydrophobicity for application in polymer matrices. Usually involving time-consuming solvent exchange procedure, research is evolving toward water born hydrophobic treatment. Organosilanes appear as more up-scalable chemicals in this type of modification. Cellulose or nanocellulose modification with organosilane was studied earlier (Paquet, 2012), (Ly et al., 2010) to impart hydrophobicity but also tunable functionnalities. Alkoxysilanes were already used for foam or aerogel applications (Zhang et al., 2015) (Zhang, 2013) as well as antimicrobial grafting (Saini et al., 2016). Gardner et al. reported also an in-situ modification with organosilane during spray drying (Wang et al., 2016). Few water born treatments are available for now to our knowledge and it is remaining a big challenge.

Missoum et al. recently developed an AKD nanoemulsion process (Missoum et al., 2016) and American Process Inc. a lignin coated CNF (Nelson and Retsina, 2015). Such hydrophobisation of cellulose nanofibrils relies mainly on an adsorption of a hydrophobic chemical on the nanocellulose surface and is active after drying.

Alkoxysilanes are well known and already industrially used for hydrophobisation and compatibilisation of mineral particles in composites (Ahti, Koski, 2002). It possesses a high reactivity in water but the elevation of temperature for the evaporation of water is essential to their linkage to hydroxyl groups. Alkoxysilanes have the properties to disperse in water and alcoholic medium. Their hydrolysis and condensation can be monitored by changing the pH, concentration or functional group (Brochier Salon and Belgacem, 2011), (Peña-Alonso et al., 2006). For example, alkosilanes with mehoxy groups were proved to react faster in their solvent than ethoxy groups probably because of steric hindrance (Kang et al., 1990).

The project here after atteTMPS to explain better how three different trimethoxysilanes with three different ending group react in their solvent and also how they are reacting with CNF. Kinetics of solvosis and condensation are assessed beforehand to choose the best condition. Analysis to explain how it is reacting with CNF is discussed in this section. Effect of silane on the barrier properties and the surface properties is also provided (Figure 2-1).

## 1.2. Experimental section

### 1.2.1. Materials

Cellulose nanofibrils are made from birch bleached kraft pulp and extracted with a mechanical and enzymatic pretreatment followed by five passings through an homogenizer. It has a dry matter content of 2,0 wt%. (3-Aminopropyl)trimethoxy silane (APMS) (Sigma Aldrich, France), propyltrimethoxy silane (TMPS) (Sigma Aldrich, France) and (3,3,3-trifluoropropyl) trimethoxy silane (TFPS) (Gelest, France) were the three models alkoxysilanes used for the study. Ethanol (98%, Roth) and acetic acid (96%, Sigma Aldrich) were used for hydrolysis medium of alkoxysilanes. All experiments were carried out with distilled water.

### 1.2.2. Methods

*Hydrolysis-condensation kinetics of silane*

Hydrolysis and condensation reaction of silane were followed by $^{29}$Si-NMR. Silanes were hydrolyzed in their deuterated solvent at a 10wt% to have and a significant signal to trace during the first eventful minutes. Data were recorded for at least 24h up to 48h depending on reactivity. Analyses were performed at Institute for nanosciences and cryogenics (INAC) at Alternative Energies and Atomic Energy Commission (CEA), Grenoble, France. Spectra were recorded on a Bruker AVANCE400 spectrometer with a BB/1H/D Z-GRD 10mm probe with a resonance at 79.4914 MHz for $^{29}$Si et 400.1316 MHz for $^{1}$H. Records were done in indicating deuterated solvent at 298K with an acquisition time of 2.3s, relaxation delay of 20s and impulsion at 45° and a spectral width of 7150 Hz, with a proton decoupling large band only during acquisition time. 32k data points are used for an acquisition on a 90 ppm window for $^{29}$Si. Before Fourier transform, zero-filling at 64K and 1 Hz exponential apodization were applied. Chemical shifting are giving compared to TMS (tetramethylsilane, $\delta$ = 0 ppm).

*CNF-alkoxysilane modification and film preparation*

Model alkoxysilanes were hydrolyzed before addition to CNF. Hydrolysation conditions are summarized in Table 2-1. Hydrolysis conditions were defined from the NMR cinetic study of each silane. PH adjustements were done by adding acetic acid accordingly. After the desired contact time with hydrolysis solvent, silanes were added directly in the CNF suspension and stirred for 1h. After this, the suspension was diluted to 0.8 wt%, homogenized with a

homogenizer (UltraTurrax T8®, IKA, France) at 12000 rpm for 30 s, let in a 240 W ultrasound bath for 3 min (Sonorex RK 52H, Bandelin, Germany) in order to remove air bubbles and casted into Teflon molds in order to obtain 40 g/m² films. A thermal treatment at 70°C followed the casting for 50 min in order to favor self-condensation of silanes was applied. Then molds were let to dry at room temperature in a fume hood for 2 to 3 days. Dried films were conditioned in a room at 23°C, 50 %RH.

**Table 2-1. Alkoxysilane hydrolysation conditions**

| Alkoxysilane | Concentration (wt%) | Water/ethanol (w/w%) | pH adjustment | Contact time (min) |
|---|---|---|---|---|
| TMPS | 1 | 100/0 | 2.3 | 1 |
| APMS | 1 | 100/0 | None | 1 |
| TFPS | 1 | 20/80 | 4 | 120 |

### Adsorption analysis

Adsorption measurements were performed with Quartz crystal microbalance with dissipation monitoring (QCM-D) (Q-Sense® E1, Biolin Scientific, Sweden). All measurements were performed under constant flow rate (17 µL/min) and temperature (23°C). Only the seventh overtone is used in the data evaluation. Absorption curves were acquired using gold-coated quartz crystals (QSX301, Biolin Scientific, Sweden). Prior to the analyses, the gold surfaces were cleaned by immersion in a "piranha" solution (30% of $H_2O_2/NH_3$, 1:3 by weight) for 15 minutes, then rinsed with Milli-Q water and finally subjected to UV/ozone treatment (ProCleaner™, Bioforce, USA) for 20 minutes. After each addition of chemicals, mili-Q water was passed through the chamber until a stable plateau was achieved. First, a 100 µM cationic polyethylenimine solution (PEI, Sigma Aldrich) was adsorbed onto the cleaned gold surfaces to facilitate CNF adsorption as well as their irreversible bonding with the crystal sensor. A 0.2 wt% CNF suspension was passed through the system until stabilization of the curves. Silanes were hydrolyzed according to Table 2-1 and and injected in the system.

Scanning electron microscopy with an energy-dispersive X-ray spectroscopy module (SEM-EDS) (LEO Stéréoscan 440, detector Si(Li) EDAX-10 mm²) was performed with a tension of 15 KeV on cross-section of CNF-silanes films to observe the behavior of silanes with CNF. Films were dipped in a 10 wt% of silane solution for 30 s, which was previously hydrolyzed according to Table 2-1. Silane concentration was chosen to be able to record a significant

signal on SEM. Films were then thoroughly rinsed with DI water for 30 s and 20 min to see the leaching effect of the proper adhesion and correlate these results to QCM-D. A thermal treatment at 110°C was done after rinsing to avoid any additional penetration effects.

Time-of-Flight Secondary Ion Mass Spectrometry (ToF-SIMS) was used to evaluate the APMS orientation on the CNF films surface. Measurements were carried out on a TRIFT III ToF-SIMS instrument from Physical Electronics operated with a pulsed 22 keV $Au^+$ ion gun (ion current of 2 nA) rastered over a 300 µm × 300 µm area. An electron gun was operated in pulsed mode at low electron energy for charge compensation. The ion dose was kept below the static conditions limit. Data were analyzed using the WinCadence software. Mass calibration was performed on hydrocarbon secondary ions. Samples were dipped in a 10% APMS solution during 30 s and washed for 20 min in an agitated water bath. Further drying was done under vaccum at 110°C except for PET samples. For some samples, no washing was done in order to observe the difference in organization of a multilayer structure and a few or single layers orientation. Three samples were analyzed in order to help interpreting results: a forced orientation, on Aluminum wich should be close to CNF in terms of hydrogen bonding possibilities (Al_APMS); a non-differenciated orientation, on polyethylene terephthalate (PET_APMS) whose surface is not giving possibility for OH bonds and finally with a CNF film (CNF-APMS).

*Film characterization*

Static contact angle measurements were obtained with the sessile drop method and were recorded and analyzed with contact angle meter (OCA20, DataPhysics Instruments GmbH) withSCA20 software. A 5 µL distilled water droplet was used for the analysis and the experiment was done at room temperature. All results are an average of at least five measurements.

Oxygen Permeability (OP) was evaluated at 23°C and 80 %HR by using a coulometric analyzer (Systech Illinois 8001, Systech Illinois USA) according to the ASTM F1927 standard. Specific exchange surface was 3.5 $cm^2$, and the testing gas was pure oxygen. Values were recorded when a plateau was reached. Each experiment was carried out in duplicates.

Water vapor permeability (WVP) was monitored at 23°C and 50 %RH according to the TAPPI standard T 464 om-12. Specific exchange surface was 3.5 $cm^2$. $CaCl_2$ salt was used as the dessicant material. Measurements were done in duplicates.

## 1.3. Results and discussion

### 1.3.1. Hydrolysation-condensation kinetics of silane

Each silane kinetics was recorded for at least 24h. Only TFPS was recorded for 10 hours and then only at 24h because of a probe problem, but results can be easily interpreted from it. As represented in Figure 2-2 the three model silanes reacted very differently.

The model propyl chain silane, TMPS, is evolving quite slowly in the medium as shown by Figure 2-2. All alkyls groups are fully hydrolyzed during the first second but decrease at the same rate T1 are formed in the medium. T2 are in a small amount after 2h30 and never gets higher than 20% while T3 is not formed. The hydrophobicity of the alkyl chains is related to this slow condensation reaction.

As a comparison, the propyl chain completed with a higher hydrophobic group such as fluor atoms is leading to a longer hydrolyzation step which is already helped by the ethanol and acetic acid condition of reaction. TOH structures are at their maximum at around 70% after 1h30 to 2h and then drop until 14h to reach a stable plateau higher than 30% (Figure 2-2 (A)). This latency which is not observed with the two others might be explained by a solvolysis with ethanol at the same time and not represented here. Condensation is also very limited (Figure 2-2 (B,C,D)) as only T1 molecules appeared in the media after full hydrolyzation (after 2h) to reach a point of 50% after 24h, which is evolving also after. T3 structures don't occur during the measurements and T2 are formed after at least 6h and increase during time. TFPS probably stabilized only after days.

With its highly hydrophilic amine function, APMS at pH of 9,5 reacts rapidly and stabilizes during the two first hours. Hundred percent of the initial structure decompose in T3OH, T1, T2 and T3 during the first 10 minutes. Confirming previous results on reactivity of alkoxysilanes (Brochier Salon and Belgacem, 2010), acidic condition (pH=4), has a more important stabilization effect on hydrolysis and prevent condensation. Natural basic pH favors condensation in the case of APMS. Compared to reaction of APMS in acetone-water mixture, reaction in pure water is quicker (Kang et al., 1990) and do not involve side reactions with amino group (Mazzei et al., 2014). This is why APMS was chosen to react with CNF in pure water condition.

From these results were chosen the hydrolyzation time and condition of silane before introducing it to CNF suspension as summarized in Figure 2-2.

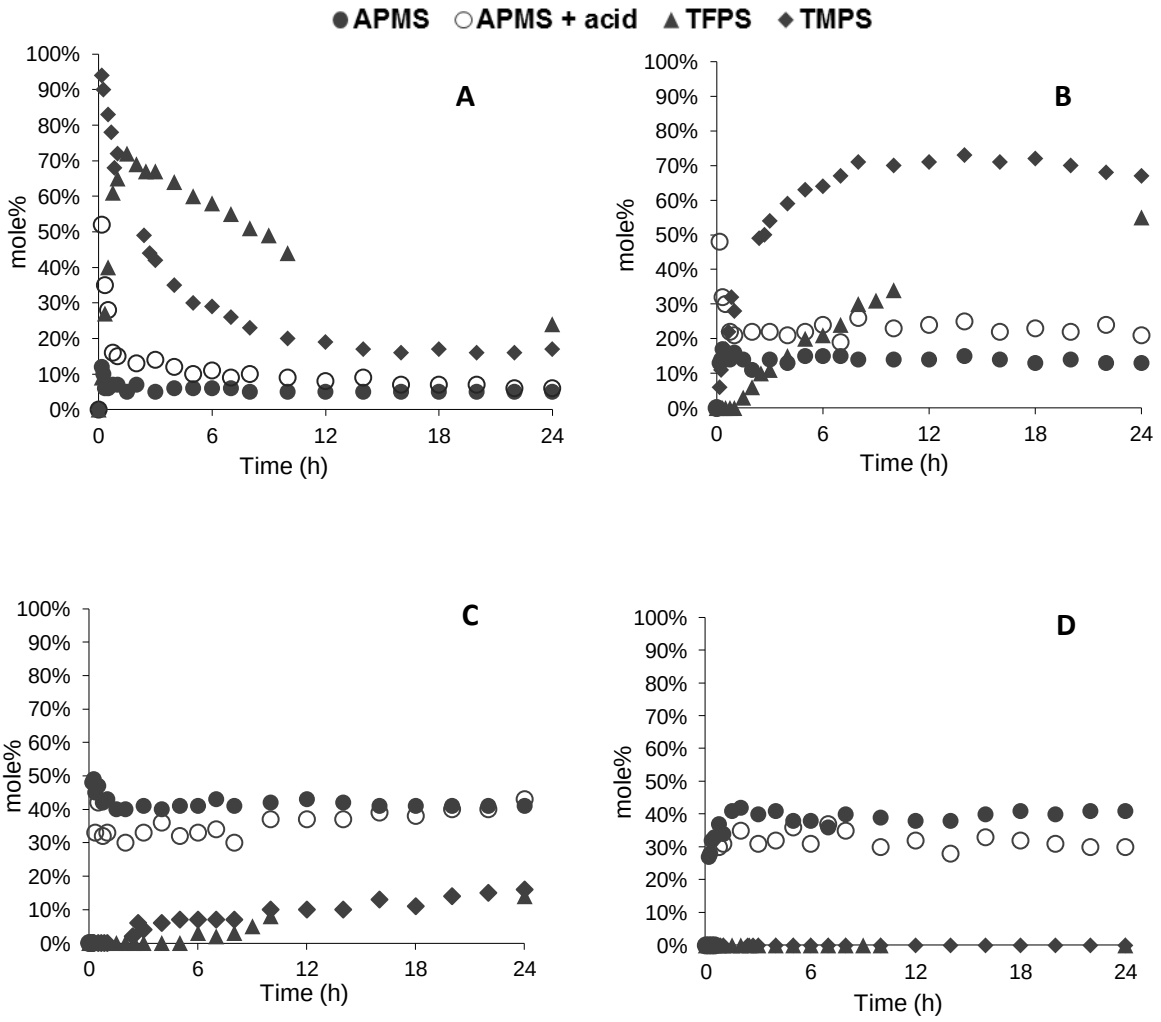


**Figure 2-2. Evolution during time followed by $^{29}$Si NMR of the three model silanes APMS, APMS in acidic condition, TFPS and TMPS. Calculated in mole% according to known total introduced quantity. (A) represents T3OH moeities, (B) T1, (C) T2, (D)T3.**

### 1.3.2. Adsorption analysis

In order to explain better the interaction between each silane and cellulose and how it is reacting depending on their functionality, adsorption analyses were carried out thanks to QCM-D and SEM-EDS.

As exposed in Figure 2-3 (A,B,C), QCM-D results show that all silanes adsorb on CNF. TMPS (A) interaction with CNF is slower compared to APMS and TFPS (C, B) as highlighted by the time needed to stabilize the signal after introduction of the chemical. Slopes observed for TFPS curves are explained by the low density of ethanol compared to water which create a signal noise when changing of solvent (Hänninen et al., 2015). It can be also noticed that desorption curves end above beginning level of the curve, and this could be explained by

swelling of CNF due to acetic acid. A clear difference is observed with the desorption of TMPS and TFPS from the CNF, while a high amount of APMS seems to stay on CNF surface. It could result from a strong adsorption happening through amine-hydroxyl interaction but also because of rapid condensation of the amino silane showed previously, leading to steric hindrance and

difficulties to wash off the condensate properly.

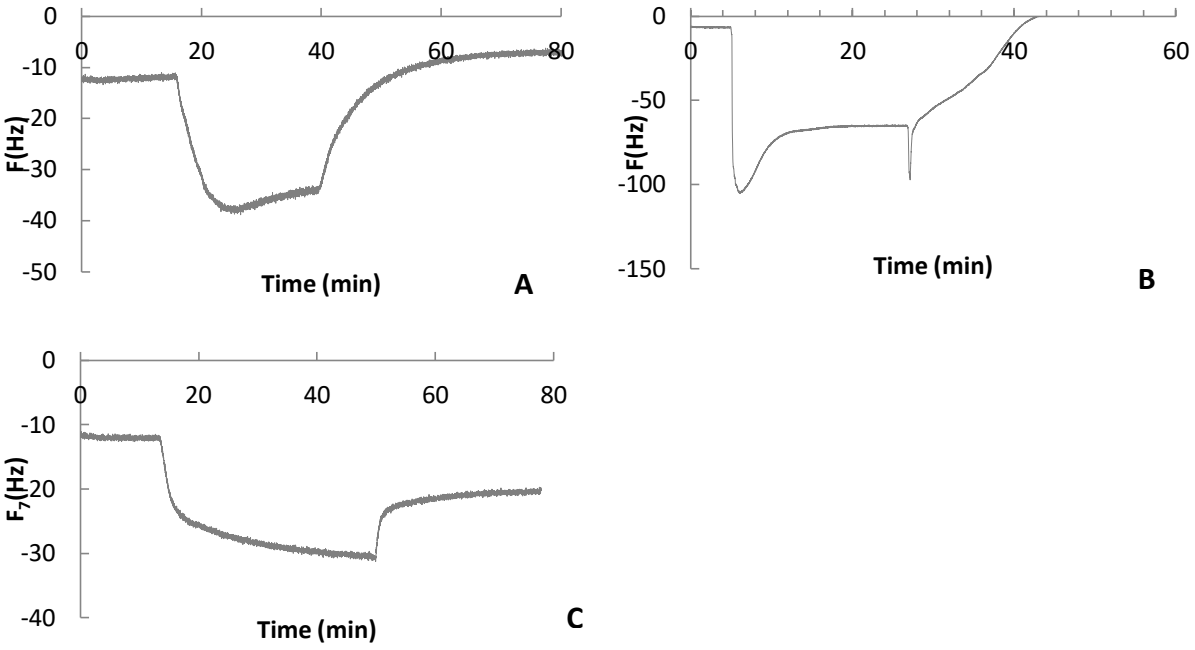


**Figure 2-3. QCM-D results of adsorption of each silane in its own reaction condition with CNF. (A) TMPS, (B) TFPS, (C) APMS.**

SEM-EDS analysis permitted to analyze adsorption of silane at different times and location and avoid effect of acetic acid and ethanol observed in QCM-D. CNF films were dipped 30s in the silane solution and washed with water 30s and 20min to be able to correlate with previous curves obtained. Cross section of the films is thick enough to be sure not to analyze the surface when pointing in the middle. As shown in Figure 2-4, TMPS and APMS penetrate inside the film within 30s while TFPS does not. It can be explained by a higher affinity with hydroxyl groups due to lower hydrophobicity of the alkyl chain. If compared to QCM-D results, these analyses confirmed the adsorption. Same experimentation was done after rinsing in DI water for 20min, and here again, APMS was detectable while TMPS and TFPS not, confirming the total desorption of these two last observed previously in QCM-D study.

The two analyzes are pointing the same phenomenon. Quick cross-linking of APMS that is revealed by NMR and strong amine-hydroxyl interaction are the reasons of high adhesion on cellulose nanofibrils.

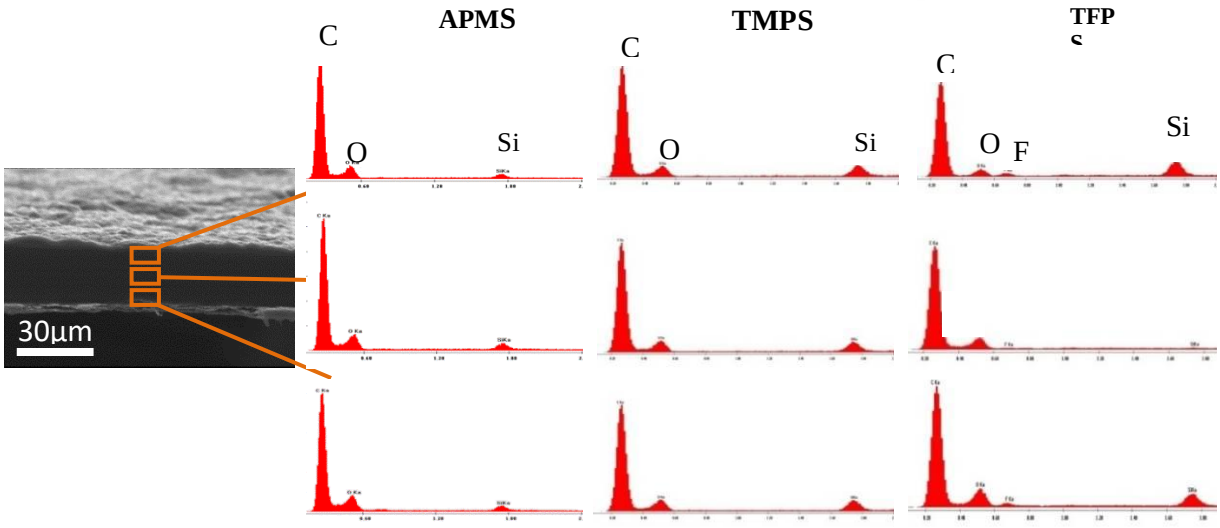


**Figure 2-4. SEM-EDS detection results of different atoms (C, O, Si and F) from cross section of CNF films after 30sd rinsing with DI water.**

### 1.3.3. Film characterization

Films tested in this section were made by mixing a 1% alkoxysilane solution in a CNF suspension for 1h at a weight ratio of 10%, casting and drying at 70°C to favor condensation. A thermal treatment at 110°C was then applied.

**Table 2-2. Water contact angle average of silane-modified CNF films**

| Type | $\Theta_w$ (°) | Std Dev |
|---|---|---|
| CNF | 38 | 8 |
| CNF_APMS | 81 | 4 |
| CNF_TMPS | 68 | 2 |
| CNF_TFPS | 59 | 1 |

Contact angle measurements were done (Table 2-2) on both side of films and averaged. Interestingly, APMS display the best water contact angle and give hydrophobicity to the hydrophilic CNF even with the presence of the amino group which should impart also hydrophilicity. The results are higher than those obtained in previous study, where a contact angle of around 58° was obtained for a simple surface grafting of aminopropyltriethoxysilane, with low content (Peresin et al., 2017). Previous study involving the ethoxyaminosilane for the modification of paper in an ethanol-water medium reported

the same phenomena, giving a contact angle around 115° (Koga et al., 2011). The difference could be due to amount of silane on the fibers but also to the averaging of upper and bottom face that are not equal due to film structure. TFPS is impacting only slightly nanofibers and these results are not concordant with a previous study on cellulose fibers (Ly et al., 2010). Zhang et al. found a 105° contact angle with water measured from sylilated sponge with trimethoxymethylsilane with same quantities even though it has to be kept in mind that freeze drying is used as a drying step.

Figure 2-5 atteTMPS to model how silane molecules are organized on CNF surface. We think that, due to the high hydrophobicity of CNF APMS films, the amine group is probably not on the extreme surface but interacts strongly with CNFs hydroxyl groups. With the high crosslinking potential given by the amine, it is also a filmogenous polymer. Fluor atoms of TFPS atoms can probably form a kind of micelle to protect themselves from water. Then, most of surface energy would be an interaction with Si-O-Si and propyl chain and could explain the similarity with TMPS results.

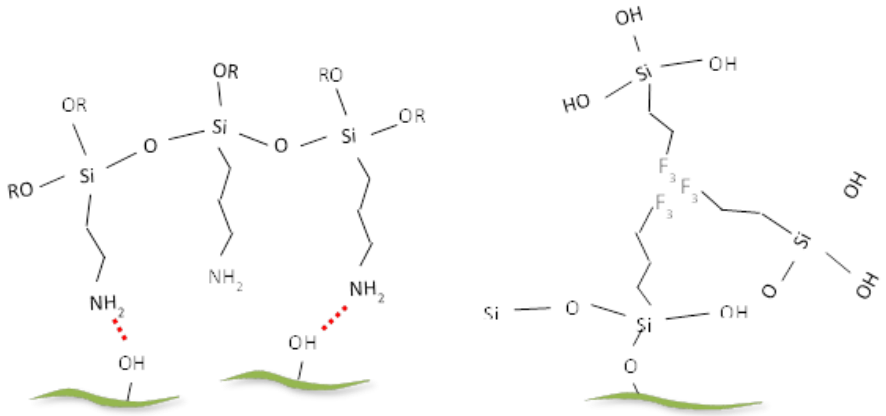


**Figure 2-5. Proposed mechanism for the arrangement of silane molecules on CNF**

ToF-SIMS analyses were done at the surface of CNF functionalized with APMS and washed but also on Aluminum and PET to compare the surface chemistry effect on the orientation of the molecule. ToF-SIMS permits the analyses of the extreme surface of a material and is expected to quantify the number of amine at the extreme surface compared with a silsesquioxane layer.

A limited extent in the surface modification of CNF with APMS was observed after washing because of the low relative intensity for $CH_2NH_2^+$. Also $CN^-$ was detected in negative mode instead of $C_2H_2^-$ which was detected for the reference CNF. These two signals are difficult to separate due their very close mass.

Reference samples (Al, PET) indicate strong modification with grafting. With Aluminium, a limited decrease in intensity of characteristic signature after washing which is very different from CNF. This was not expected as the Aluminum surface oxide was though to react the

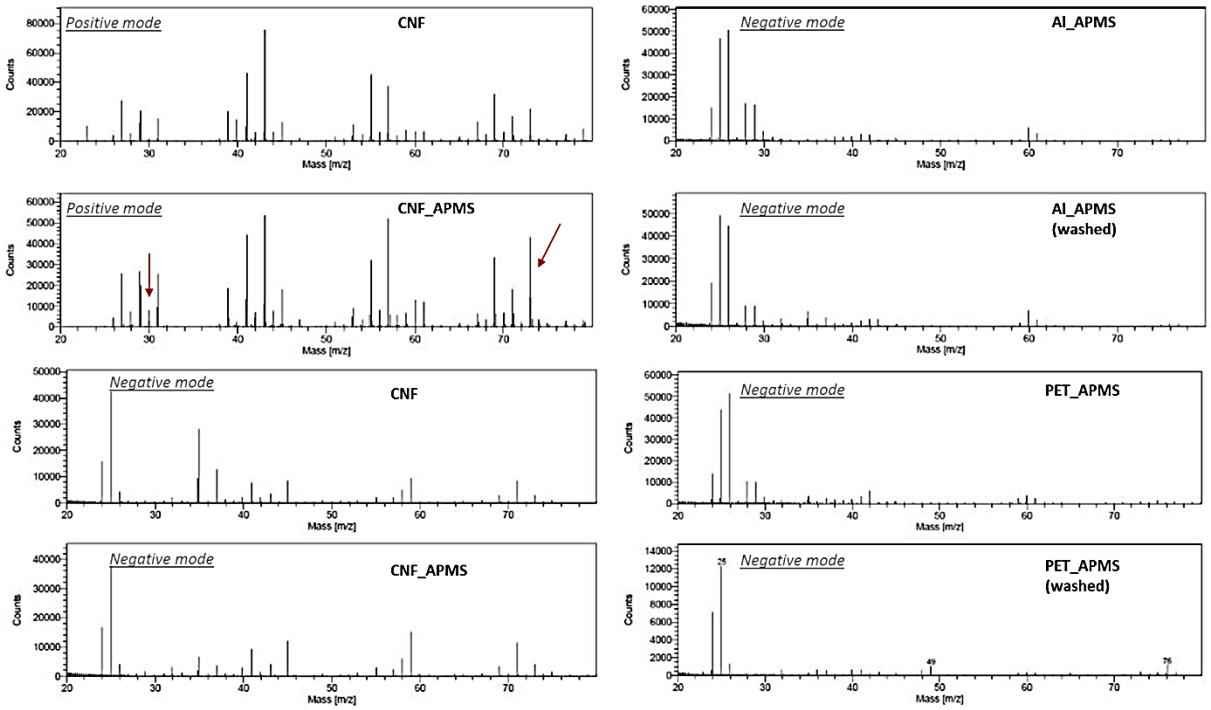


**Figure 2-6. Positive mode ToF-SIMS spectra of CNF and CNF-APMS & negative mode ToF-SIMS spectra of CNF and CNF-APMS in the 20 < m/z < 80 range, Negative mode ToF-SIMS spectra of Al-APMS, Al-APMS (washed), PET-APMS, PET-APMS (washed) in the 20 < m/z < 80 range**

same way than CNF. No grafting is observed with PET as shown by the apparition of PET characteristic peaks such as m/z=76 after washing. Indeed, APMS is not able to form any linkage with PET due to its absence of hydroxyl or hydrogen groups.

To start quantifying, the 26 ($CN^-$) / 28 ($Si^-$) ratio values were calculated and it exhibit trends that can be interpreted in terms of difference in orientation. CNF-APMS being characterized by relatively lower amine content (low relative intensity m/z=26 for that sample may also be partly related to $C_2H_2^-$ which was not separated from $CN^-$). Compared to PET or washed aluminum, their is a trend in the decreasing of the amine content at the surface with CNF which could explain the difference in water contact angle. Such results should be further investigated by the analysis of a CNF-APMS samples not washed and compared to these results.

**Table 2-3. 26 (CN-) / 28 (Si-) ratio values for each samples.**

| Samples | 26 ($CN^-$) / 28 ($Si^-$) ratio |
|---|---|
| CNF_APMS | 3.9 ± 0.8 |
| Al_APMS | 3.9 ± 0.7 |
| Al_APMS (washed) | 4.9 ± 1.1 |
| PET_APMS | 4.9 ± 1.0 |

Barrier properties were examined and especially regarding oxygen permeability at high humidity level (80 %RH). In Figure 2-7, results before and after thermal treatment at 110°C are displayed. Thermal treatment is here to favor linkage of silane with CNF through their hydroxyl groups but also to allow condensing the possible residual silanol. Compared to CNF, addition of APMS is beneficial to oxygen barrier even before thermal treatment and with a drop of around 30%. This key result shows again that fast condensation of APMS does not need any heat to create the polysiloxane hydrophobic network. Surprisingly, addition of TMPS or TFPS in CNF suspension degrades barrier properties. It can be explained either by reaction of acetic acid or by the hydrophobicity of the molecules or both. Indeed, as explained by (Peresin et al., 2017), the hydrophobicity of the material for high oxygen barrier is not only the principal parameter. In their study they showed that the presence of an amine when using sylilation is beneficial to oxygen barrier at high humidity level. They explained that the amine is interacting with water and thus permit to hinder CNF-water

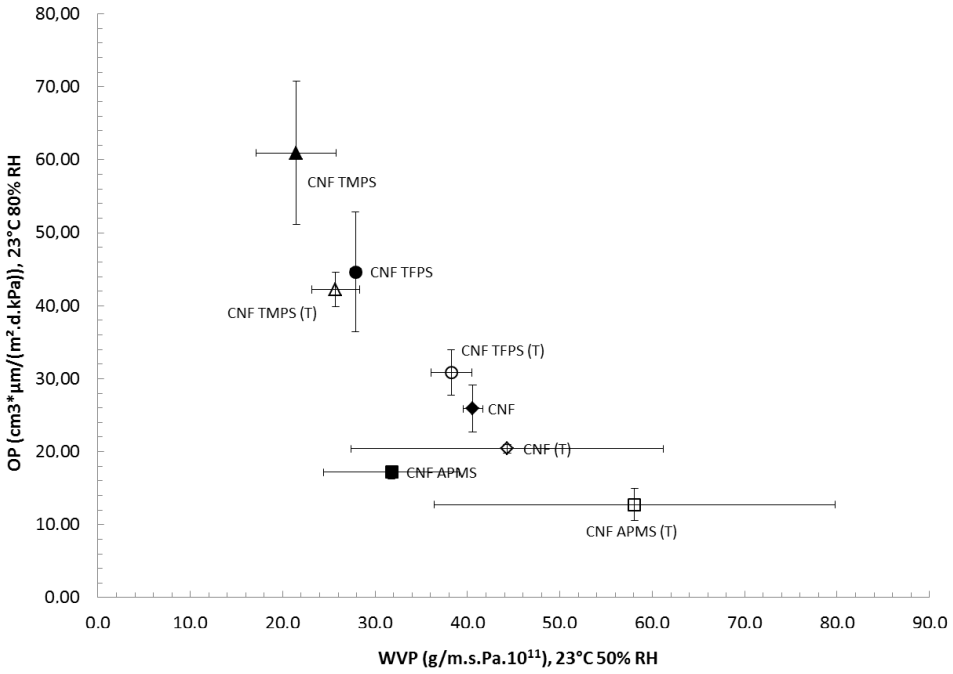


**Figure 2-7. Oxygen permeability at 23°C and 80% RH and water vapor permeability at 23°C and 50%RH of films.**

interactions. Our results are confirming this study. A control with CNF and acetic acid will be tried. In all cases, thermal treatment is beneficial but this could be explained by hornification of films as already investigated (Sharma et al., 2014). As expected, water vapor permeability (Figure 2-7) shows results at the opposite of OP tendency. APMS degrades WVP values when TMPS and TFPS enhance it. This is not surprising, as water vapor and oxygen flow inside a material is not reactive trough the same interaction with the material.

## 1.4. Conclusion and perspectives

In this section, cellulose nanofibers and silanes interations were studied with three different model silanes with different properties and solubility in water.

The best conditions for their hydrolysis and contact time with CNF were defined thanks to NMR kinetic study. NMR shows that APMS was able to condense very quickly and this is impacting later properties of CNF silane films. TMPS and TFPS are reacting with cellulose easily like APMS do. But APMS attached strongly to CNF when TFPS and TMPS only adsorb at the surface and are easily removed by washing with water.

Bulk inclusion still affects CNF properties in each case. It was proved that in these conditions, APMS favor oxygen permability. TFPS and TMPS are damaging CNF OP and increasing WVP. Water contact angle of modified film gave interesting results leading to propose a model organization of each silane. APMS is supposed to interact with cellulose with the amine function while TFPS and TMPS with the hydroxyls groups. It could explain higher contact angle and film forming property.

TOF-SIMS analysis performed on films permitted to start understanding the mechanism but should be further exploited with other samples to confirm the obtained results. Nevertheless, the ability of APMS to condense is also a primary cause of these results. Thus, a novel reaction mechanism has to be employed in order to condense faster TMPS and TFPS in the medium and probably give higher hydrophobic results and approach silicone surfaces. This can be achieved by monitoring the pH. Also, CNF-APMS could be exploited as an antimicrobial reagent thanks to amine group.

## References


Ahti, Koski, 2002. Process for hydrophobicizing particles, and their use as fillers in polymer masterbatches. Bayer Inc.. WO1998053004A1

Andresen, M., Johansson, L.-S., Tanem, B.S., Stenius, P., 2006. Properties and characterization of hydrophobized microfibrillated cellulose. Cellulose 13, 665–677. doi:10.1007/s10570-006-9072-1

Aulin, C., Gällstedt, M., Lindström, T., 2010. Oxygen and oil barrier properties of microfibrillated cellulose films and coatings. Cellulose 17, 559–574. doi:10.1007/s10570-009-9393-y

Brochier Salon, M.-C., Belgacem, M.N., 2011. Hydrolysis-Condensation Kinetics of Different Silane Coupling Agents. Phosphorus Sulfur Silicon Relat. Elem. 186, 240–254. doi:10.1080/10426507.2010.494644

Brochier Salon, M.-C., Belgacem, M.N., 2010. Competition between hydrolysis and condensation reactions of trialkoxysilanes, as a function of the amount of water and the nature of the organic group. Colloids Surf. Physicochem. Eng. Asp. 366, 147–154. doi:10.1016/j.colsurfa.2010.06.002

Goussé, C., Chanzy, H., Cerrada, M.L., Fleury, E., 2004. Surface silylation of cellulose microfibrils: preparation and rheological properties. Polymer 45, 1569–1575. doi:10.1016/j.polymer.2003.12.028

Habibi, Y., 2014. Key advances in the chemical modification of nanocelluloses. Chem. Soc. Rev. 43, 1519. doi:10.1039/c3cs60204d

Hänninen, T., Orelma, H., Laine, J., 2015. TEMPO oxidized cellulose thin films analysed by QCM-D and AFM. Cellulose 22, 165–171. doi:10.1007/s10570-014-0530-x

Kang, H.-J., Meesiri, W., Blum, F.D., 1990. Nuclear magnetic resonance studies of the hydrolysis and molecular motion of aminopropylsilane. Mater. Sci. Eng. A, Structural Materials: Properties, Microstructure and Processing 126, 265–270. doi:10.1016/0921-5093(90)90132-M

Li, F., Mascheroni, E., Piergiovanni, L., 2015. The Potential of NanoCellulose in the Packaging Field: A Review. Packag. Technol. Sci. 28, 475–508. doi:10.1002/pts.2121

Ly, B., Belgacem, M.N., Bras, J., Brochier Salon, M.C., 2010. Grafting of cellulose by fluorine-bearing silane coupling agents. Mater. Sci. Eng. C 30, 343–347. doi:10.1016/j.msec.2009.11.009

Mazzei, P., Fusco, L., Piccolo, A., 2014. Acetone-induced polymerisation of 3-aminopropyltrimethoxysilane (APTMS) as revealed by NMR spectroscopy. Magn. Reson. Chem. 52, 383–388. doi:10.1002/mrc.4076

Missoum, K., Julien, B., Naceur, B., 2016. Method for forming a hydrophobic layer. Institut Polytechnique De Grenoble. WO2015011364 (A2)

Nelson, K., Retsina, T., 2015. Processes for producing nanocellulose-lignin composite materials, and compositions obtained therefrom. Api Intellectual Property Holdings, Llc. WO2015200584 A1

Paquet, O., 2012. Cellulose surface modification with organosilanes . Ph.D manuscript. Université de Grenoble.

Peña-Alonso, R., Rubio, F., Rubio, J., Oteo, J.L., 2006. Study of the hydrolysis and condensation of γ-Aminopropyltriethoxysilane by FT-IR spectroscopy. J. Mater. Sci. 42, 595–603. doi:10.1007/s10853-006-1138-9

Peresin, M.S., Kammiovirta, K., Heikkinen, H., Johansson, L.-S., Vartiainen, J., Setälä, H., Österberg, M., Tammelin, T., 2017. Understanding the mechanisms of oxygen diffusion through surface functionalized nanocellulose films. Carbohydr. Polym. 174, 309–317. doi:10.1016/j.carbpol.2017.06.066

Saini, S., Belgacem, M.N., Salon, M.-C.B., Bras, J., 2016. Non leaching biomimetic antimicrobial surfaces via surface functionalisation of cellulose nanofibers with aminosilane. Cellulose 23, 795–810. doi:10.1007/s10570-015-0854-1

Sharma, S., Zhang, X., Nair, S.S., Ragauskas, A., Zhu, J., Deng, Y., 2014. Thermally enhanced high performance cellulose nano fibril barrier membranes. RSC Adv 4, 45136–45142. doi:10.1039/C4RA07469F

Taipina, M. de O., Ferrarezi, M.M.F., Yoshida, I.V.P., Gonçalves, M. do C., 2013. Surface modification of cotton nanocrystals with a silane agent. Cellulose 20, 217–226. doi:10.1007/s10570-012-9820-3

Wang, L., Sanders, J.E., Gardner, D.G., Han, Y., 2016. In-situ modification of cellulose nanofibrils by organosilanes during spray drying. Ind. Crops Prod., Nanocellulose: production, functionalisation and applications 93, 129–135. doi:10.1016/j.indcrop.2016.02.004

Zhang, Z., 2013. Modification chimique de la cellulose nanofibrillée par les alcoxysilanes: application à l'élaboration de composites et mousses. Ph.D manuscript. Université Sciences et Technologies-Bordeaux I.

Zhang, Z., Tingaut, P., Rentsch, D., Zimmermann, T., Sèbe, G., 2015. Controlled Silylation of Nanofibrillated Cellulose in Water: Reinforcement of a Model Polydimethylsiloxane Network. ChemSusChem 8, 2681–2690. doi:10.1002/cssc.201500525

# 2.1. Cross-condensation of amino-propyl trimethoxy silane and propyl trimethoxy silane at low concentration for narrow dispersed nano- and micro-metric silsesquioxane particles synthesis

*This section is adapted from "Reverdy C., Belgacem N., Bras J.., Cross-condensation of amino-propyl trimethoxy silane and propyl trimethoxy silane at low concentration for narrow dispersed nano- and micro-metric silsesquioxane particles synthesis, submitted to Journal of Colloid and Interface Science (2017).*


## Abstract

Cross-condensation of two organotrialkoxysilanes was studied and the obtained silsesquioxane particles were characterized. Propyltrimethoxysilane was used as the precursor organosilane whereas aminopropyltrimethoxy organosilane was used as a catalyst. Particles where synthesized as a function of the organotrialkoxysilane initial concentration but also the molar ratio between them. Reaction kinetics was followed by Dynamic Light Scattering, while the average particle diameter was measured with Scanning Electron Microscopy. BET measurements gave the specific surface area of the particles. Finally, the roughness was measured with Atomic Force Microscopy. This easy, fast and totally aqueous-based synthesis route provides narrow sized particle distribution which could be used as a functional material for surface structuration.


## 2.1.1. Introduction

Hybrid organic-inorganic particles have a great interest in material science as they combine both families' properties. Such types of product are widely developed through modification of silica particles with organic moieties *via* linkage with the functional –OH groups (silanols) sitted at their surface. Tuning particles properties is then easy, by modifying organic group at their surface.

The most versatile and available particles are probably silica $SiO_2$. A well-known and deeply understood way to synthesized narrow dispersed silica spheres is the Stöber's method (Stöber et al., 1968) which involves tetraethoxysilane (TEOS) in water/alcoholic/ammonia medium. The reaction is ruled by a first step of hydrolysis:

$$Si(OC_2H_5)_4 + 4H_2O \rightarrow Si(OH)_4 + 4C_2H_5OH$$

Followed by a second step of condensation catalyzed by ammonia:

$$Si(OH)_4 \rightarrow SiO_2 + 2H_2O$$

A bunch of other possible catalysts are known to act as well, such as mineral acid, acetic acid or titanium alkoxides (Brinker, 1988). The advantage of $SiO_2$ is the reactivity with organoalkoxysilane, forming organically-doped $SiO_2$ surface with low to intermediate organic content (Croissant et al., 2016). The Stöber's reaction can also be modified by a combination of TEOS and an organoalkoxysilane in solution forming organosilica particles with organically-doped matrix. Some groups proceeded this reaction with two organoalkoxysilane and generally one aminoalkoxysilane leading to silsesquioxane particles, usually called silsesquioxane and sometimes ormosils, with general formula is $RSiO_{3/2}$ (Dirè et al., 2011), (Heitz et al., 2006),(Ottenbrite et al., 2000). The used reaction medium is water or a mix of water with alcohol. A surfactant is also added to control the growth of particles and porosity. Nanosized particles were investigated mainly in biotechnology applications, for examples, as potential drug carrier or bioimaging particles. It was also assessed as reinforcing coating layer for glass substrate (Croissant et al., 2016), (Heitz et al., 2006).

In order to provide to a surface a specific functionnality or to create roughness, such particles could be valuable. Indeed, the chemistry can be easily tuned as well as particles size. Generally, creating roughness on a material surface in order to lower its surface energy artificially can be managed by different ways. Top-down approaches can be achieved by templating, photolithography or ion etching for example of low energy polymer or a random surface, which is secondly coated (Li et al., 2007). These materials are highly performant, but have poor chance to be produced at large industrial scale due to excessive time of their production. Usually such kind of products is used at laboratory scale in order to understand better mechanisms and theory behind or for small device in high added-values areas like microelectronics. Larger surfaces manufacturing is expected with bottom-up approaches. Such pathways include chemical vapor deposition (CVD) (Yao et al., 2011), (Crick and Parkin, 2011), electrospinning (Nuraje et al., 2013), layer by layer assembly (Brown and Bhushan, 2015), sol-gel process (Xu et al., 2010), (Latthe et al., 2014),(Xue et al., 2008), (Wu et al., 2016) and coating of rough particles such as $SiO_2$, $TiO_2$ or precipitated calcium carbonate (Zhang et al., 2007) ,(Cao et al., 2009), (Ogihara et al., 2012), (Arbatan et al., 2011). The last

process is probably the fastest and cheapest one, but usually involves a two steps procedure, one for the particles deposition and another for coating a low surface energy polymer. With the sol-gel process, dip-coating process of the surface required a long contact time to acquire superhydrophobic character, but the easy control of the particles growth and chemistry are key advantages.

In this study is presented a reaction producing organo-modified silsesquioxane particles using 3-aminopropyltrimethoxy silane (APMS) and methyltrimethoxypropyl silane (TMPS) in pure water. Through a simple and fast method, organo-functional silsesquioxane particles (SQp) are synthesized at micro scale. The main features of the particles, as a function of the reaction parameters, are reported hereafter.

### 2.1.2.Materials and methods

### 2.1.2.a. Materials

(3-Aminopropyl)trimethoxy silane (APMS) (Sigma Aldrich, France), propyltrimethoxy silane (TMPS) (Sigma Aldrich, France) are the two trialkoxysilanes use in this study. All experiments are conducted in distilled water.

### 2.1.2.b. Methods

*Silsesquioxane preparation and purification*

Silsesquioxane particles were synthesized by adding propyltrimethoxy silane (TMPS) to water at a chosen mass concentration and stirred for 10 min to allow good dispersion of the hydrophobic silane and induce hydrolysis process. (3-Aminopropyl)trimethoxy silane (APMS) is then drop wisely added at a chosen molar ratio with respect to TMPS. The suspension is mixed under strong stirring for at least 2h. Suspensions are kept at least one week before analysis to ensure that the reaction is completed and the particles have reached their final size.

SQp are defined by the initial precursor mass concentration in water initially ("x%") and the molar ratio between APMS and precursor ("xM").

When purified, the suspension was dried at 105°C, ground with mortar and soxhlet extracted with a 80/20 water/ethanol solution for 8 hours in order to remove the remaining unreacted silane.

*SEM and FEG-SEM imaging and particles measurements*

Samples were made by dropping suspension on a carbon tape and allowed to dry at room temperature. Surface was scratched partially before being metalized with a gold-palladium plasma coating. Scanning electron microscopy (SEM) was used to analyze the particle size (Quanta 200©, FEI, Japan). At least ten pictures at same magnification were recorded and the most representative one is presented here.

SEM images were used to measure the particle size, in order to be able to measure individual particles and avoid aggregation artefacts. Image-J software was used to measure diameters. Values presented are an average of 300 particles (except for low quantity particles blend) made on at least 8 different images.

FEG-SEM imaging (Zeiss® Ultra-55, USA) was performed to visually evaluate particles nano-roughness. Samples were coated with a 3 nm gold/palladium before being imaged.

*Dynamic light scattering*

In order to evaluate kinetics of particle formation and aggregation, dynamic light scattering was performed with a Nano-ZS zetasizer (Malvern Instrument). The scattered intensity was measured at a 173° angle and a temperature of 23°C. Suspensions were prepared as following: TMPS was added in water and mixed for 10 min. APMS was then added to the mixture and after 2 second mixing, an aliquot was introduced in the cuvette. Data are an average of six measurements done within one minute and the procedure was repeated 100 times (1h40).

*BET measurements*

Nitrogen adsorption were done with Nova 1200$^{e}$ apparatus and BET model was applied on obtained nitrogen adsorption isotherm in order to calculate specific surface area values of purified and non-purified silsesquioxane particles. A 50 mg sample was introduced in a 9 mm diameter bulb and let for degassing at 105 °C for 15 hours. Nitrogen adsorption is measured through pressure measurement on a sample cooled down at -196 °C.

*Density measurements*

Non purified particle density was measured with the help of a 24,879 mL pycnometer. The solvent was ethanol. Three measurements were done with at least 0.8 g of particles and averaged.

*FT-IR*

Fourrier transform infrared spectra of purified, non-purified after TGA Silsesquioxane particles were obtained with a Perkin Elmer, Parangon 1000 FTIR spectrometer equipped with spectrum software. KBr pellets were performed by mixing and grinding a 99:1 mg ratio of KBr:Silsesquioxane and pressed for 60s under a 10 t/m² pressure. Analyses were done with a 4 $cm^{-1}$ resolution in a wavelength ranging from 400 $cm^{-1}$ to 4000 $cm^{-1}$ with 32 scans. Curves were normalized at the Si-O-Si characteristic band at 1120 $cm^{-1}$.

*Elemental analysis*

The silicon, carbon, oxygen and nitrogen contents (%) were determined by inductively coupled plasma atomic emission spectroscopy (iCAP 6300 ICP Spectrometer, Thermo Scientific, USA) at the ISA laboratory (CNRS, France) on purified and non-purified powder.

*Thermogravimetric analysis*

Thermal degradation of silsesquioxane was performed by TGA (thermogravimetric analyzer-STA 6000®, Perkin Elmer Instruments, England). The weight loss curve was obtained with a

16 mg sample at a heating rate of 10 °C/min for a temperature range between 30 and 700°C and 50°C/min between 700 and 900°C. Measurement was performed under atmospheric air.

*AFM roughness analysis*

Roughness of particle surfaces was measured using an Atomic Force Microscope (AFM; Nanoscope III®, Veeco, Canada). Dried and non-purified particles were glued on adhesive tape and placed at the surface of a metal plate. Each sample was characterized with a silicon cantilever (OTESPA®,Bruker, USA) in tapping mode at five different locations. Resulting images were subjected to 1$^{st}$-order polynomial flattening to reduce the effects of bowing and tilt. Roughness was then measured on height images, by using Nanoscope Analysis software, on an adapted surface depending on particles size.

### 2.1.3. Results and discussion

#### 2.1.3.1. Effect of initial TMPS mass concentration

Particle growth was studied with different TMPS mass concentrations in water to evaluate the effect of this parameter on the formation process. For this purpose, SEM images of dried powders were recorded and particle diameters were deduced from them.

Dispersed SQp were obtained (Figure 2-9) at 0.1, 0.5, and 1% concentration. Interestingly, particles made at 0.5 % are the smallest and give a narrow dispersion as proved by the overlapping of average diameter ($d_{avg}$) and median diameter ($d_{50}$) (Figure 2-8). At 0.5 and 5%, SQp size distribution tends to follow a normal distribution. At 0.1 and 1 % two size domains were obtained and located from both side of 1 µm. At 5 and 10%, few particles can be found and aggregates are made, forming silsesquioxane dense planar network. TMPS concentration in water is then determined for the obtained geometry. As a comparison, Ottenbrite et al. (2000) used 0.8 % mass concentration of precursor and a molar ratio between catalyst and precursor equal to 3 to obtain similar silsesquioxane particles.

#### 2.1.3.2. Effect of molar ratio between APMS and TMPS

While keeping a constant precursor mass concentration at 0.5wt% in water, the quantity of APMS influences greatly the particle size (Figure 2-8). Ten times less APMS than TMPS as a

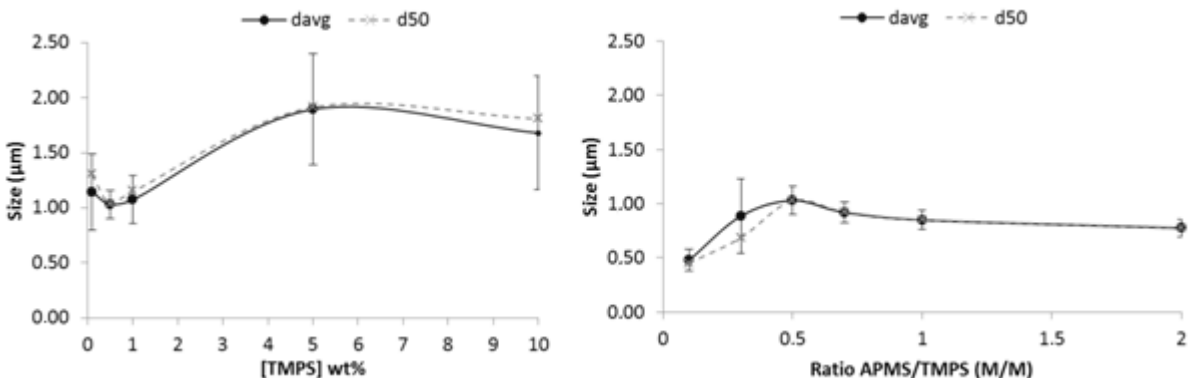


**Figure 2-8. Average diameter (davg) and median diameter (d50) of particles according to precursor initial mass concentration in water at constant silanes molar ratio (left) or according silanes molar ratio at fix initial concentration in water (0.5wt%).**

molar ratio gave particles two times smaller than those prepared at a molar ratio of 0.5 with a narrow polydispersity, although the pH was the same in both case, i.e., 9.9. Between 0.1 and 0.5 molar ratio between APMS and TMPS, a two size domain is observed. Well distributed particle sizes are then obtained with an excess of APMS with a slight reduction of

the average diameter. However while introducing increasing amount of APMS, aggregates were observed more often. This result shows the role of APMS in favoring the aggregation process. The FEG-SEM picture (Figure 2-9, down right) of 0.5%; 0.5M enlighten this aggregation process, showing small particles with diameters ranging from 50 to 200 nm on top of spheres surfaces. This phenomenon was also reported by Heitz et al. (2006) by dynamic light scaterring monitoring of particles growth process. While mixing an epoxysilane with an aminosilane in dilute suspension (1-3%), they had observed the formation of particles around 2 to 5 nm, which suddenly aggregates in larger particles in the order of the micron.

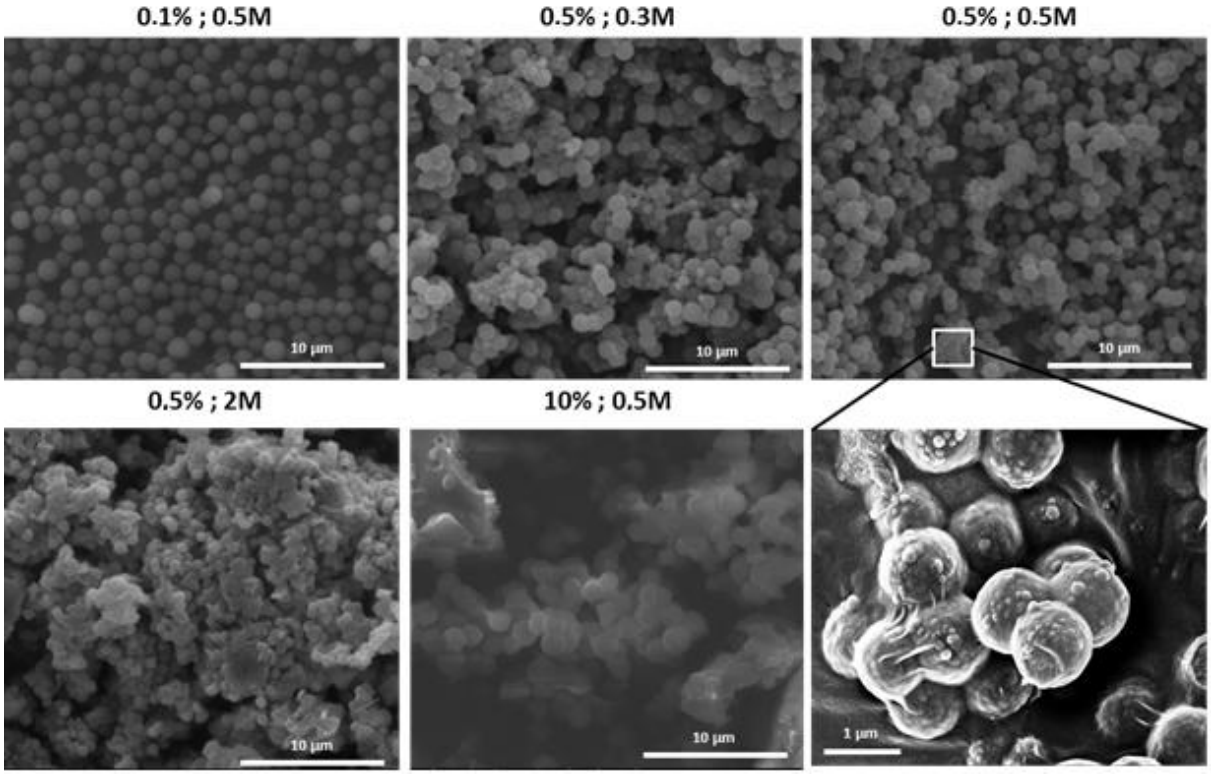


**Figure 2-9. SEM and FEG-SEM images of aged and dried silsesquioxane with different production parameters**

### 2.1.3.3. Reaction kinetics and effect of parameters

Dynamic light scattering was used to follow particles growth kinetics in water. As observed in Figure 2-10, formulation at 0.5 molar ratio (0.5M) bewteen APMS and TMPS and initial TMPS concentration at 0.5% in water, particles get their stable form around 20 min which was the time observed to obtain a turbid suspension. It is worthnoting that a decrease in the APMS content (lower values of the discussed before ratio) increased by a factor of 2 the stabilisation time. This confirms that APMS plays the role of reaction auto-catalyst. As compared to Heitz et al. (2006) study, this auto-catalytic effect was also observed. The

difference in their study is that the epoxysilane seemed to already form particles in its own in water during less than two hours, as observed through the increase in suspension turbidity. The data of TMPS at 0.5% in water is not presented here, as poor reliability on the data was obtained due to low scattering effect. The data did not show any growth but a rather stable suspension depicting the presence of particles having around 1 µm diameter, which could be micelles or pollutant.

The modification in the concentration change the particles final size, which is in agreement with SEM measurements. But final size measured by DLS are different for two suspensions. Indeed, 0.5%0.1M gave higher average diameter in the order of two and 0.1%0.5M depicts smaller diameter by an order of five. DLS measurements are probably more reliable because of *in situ* measurement and no possible effect on manual samples picking.

In all cases, narrow dispersed particles are observed, which corroborated with the values given by the visual observation.

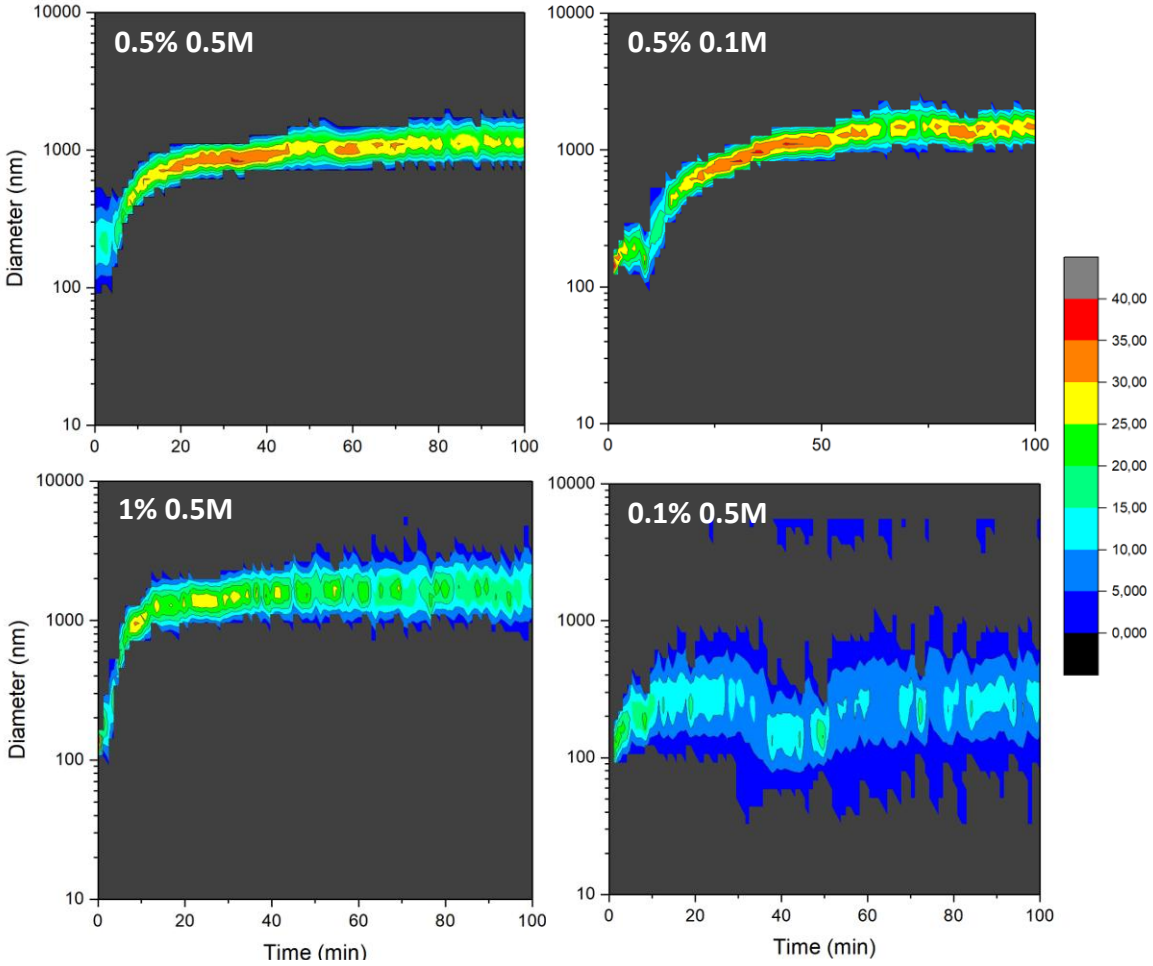


**Figure 2-10. Dynamic light scattering results for various precursor initial concentrations and molar ratios. Graphs are representing for each minute the particle distribution in size.**

### 2.1.3.4. Particle physical and chemical properties

In order to check if an APMS layer was surrounding particles which would decrease the specific surface area of the powder, BET specific surface area was measured for 0.5M purified and non-purified samples. A value of 2.9 $m^2/g$ for 0.5M purified and non purified silsequioxane particles was found. This is relatively low compared to other studies (Arkhireeva and N. Hay, 2003). Particles can thus be considered as a dense cohesive material. However, this value should be considered as an approximation due to the low amount used for the analysis, which is out of the recommendation range. Calculated density from BET SSA and average measured diameter, thus assuming that particles are completely closed, give a SSA of 1.93 $g/cm^3$ which is a little bit lower than silica (2.33$g/cm^3$), but higher than what can be done with cross condensation of TEOS with aminopropylsilane, around 1.7 -1.8 $g/cm^3$ (Van Blaaderen and Vrij, 1992). The effect of propyl chain of both TMPS and APMS on the density is thought to be more pronounced than a reaction with TEOS which has shorter chain length. A bias in the consideration that particles is completely non porous could be the reason of the result. The measurement with pycnometer gave a clear cut result of a true density of 1.18 ± 0.04 $g/cm^3$. It much more coherent and viable than the approximation obtained with BET measurement.

Thermal degradation in air of the manufactured silsesquioxane was performed for the sample made at a concentration and molar ratio of 0.5% : 0.5M type of particles. The onset degradation starts at 280°C leading to a weight loss at 900°C of 43%. This weight loss is mostly attributed to the organic part of the silsesquioxane wich slowly degrades leading to a structure close to silica cores. Whith this ratio, calculated mass loss of total organic part should provide 53% mass of $SiO_{3/2}$, which is close to that deduced from TGA curve (Figure 2-11), i.e., 57%. This effect has been already reported for structures close to this one, namely: substituted polyhedral oligomeric silsesquioxane (Fina et al., 2006), (Zeng et al., 2005), but also with silsesquioxane (Jung et al., 2012).

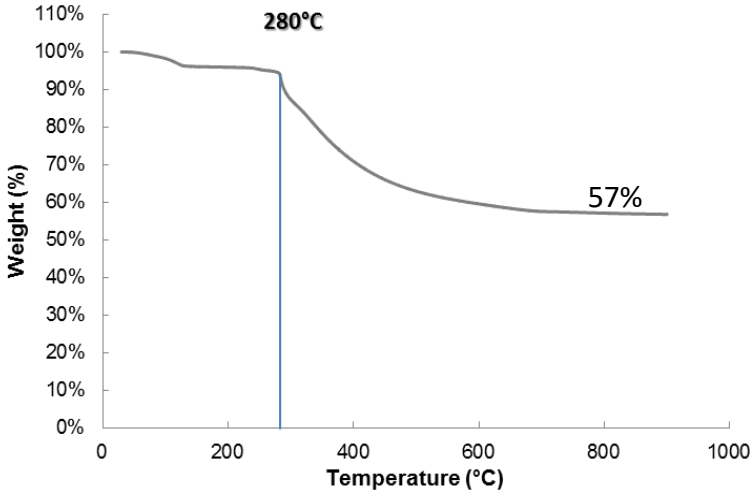


**Figure 2-11. TGA graph of 0.5% : 0.5M non-purified silsesquioxane particles.**

Fourier transform infrared spectrometry (FT-IR) was used to analyze the effect of purification and thermal treatment on these particles chemistry. Spectra bands between 2870 and 2960 $cm^{-1}$ on purified (Figure 2-12 A) and non-purified (Figure 2-12 B) SQp are typically assigned to C-H of propyl chains of APMS and TMPS. Small bumps at nearly 3380 $cm^{-1}$ is higher in intensity before purification (Figure 2-12 A) and after (Figure 2-12 B). This could be assigned to N-H stretching band or to residual Si-OH site of organoalkoxysilane which underwent hydrolysis but not condensation and/or unbound to the material. The same conclusion can be done with the 1580 $cm^{-1}$ absorption band representing N-H bending which is drastically decreased after purification. Slight decrease of $CH_3$ bending band absorption at 1375 $cm^{-1}$ could indicate that not only APMS but also few amounts of unreacted TMPS are extracted. After TGA (C), the ash present at the end of the measurement is characteristic from $SiO_{3/2}$ species with Si-O stretching bending and rocking peaks, respectively at 1120, 810 and 480 $cm^{-1}$.

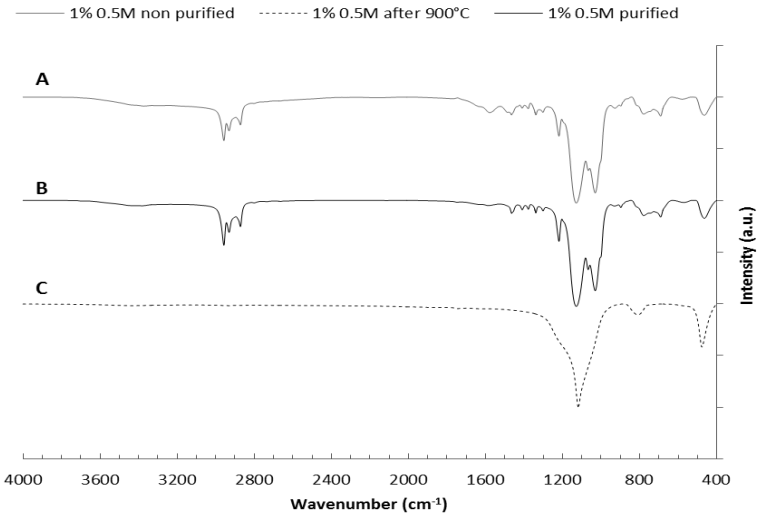


**Figure 2-12. FT-IR spectras of silsequioxane 1% 0.5M non-purified (A), purified (B) and non-purified after TGA analysis (C).**

Elemental analysis given in Table 2-4 is a significant loss of organic part after purification. Indeed, for non-purified silsesquioxanes, molar ratio between APMS and TMPS, calculated with carbon, silicon and nitrogen is 0.48 and 0.53, respectively. This result is consistent with the molar selected ratio APMS/TMPS = 0.5. These molar ratios are evolving to 0.16 and 0.17 while analyzing purified silsesquioxanes giving a loss of about 70% of the APMS molecules after purification which is qualitatively confirmed by the loss observed with FTIR spectra. This result is consistent with different studies on similar structures with two organoalkoxysilanes or with tetraethoxysilane and an aminopropylsilane, (Liu et al., 2005), (Ottenbrite et al., 2000) and (Van Blaaderen and Vrij, 1992) showing that even with a high starting content of APMS maximum 30 to 40 mol% of the initial quantity is included in the compound. This result is however surprising, as APMS is known to rapidly condense in water and form $T_3$ polysiloxane structures (Reverdy et al., 2016), (Brochier Salon and Belgacem, 2010). It will be then expected that, even if APMS is not covalently linked to silsesquioxane particles, the size of the branched structures after condensation reactions are limiting their removal during washing. This is a sign that APMS self-condensates poorly during the reaction, leading to small organizations that could be $T_3$ but certainly not tri-dimentionally crosslinked.

**Table 2-4. Elemental analysis of non-purified and purified 1% 0,5M silsesquioxanes**

| | Si (%) | C (%) | N (%) | H(%) |
|---|---|---|---|---|
| 1% 0.5M non purified | 25.13 | 34.65 | 4.33 | 7.13 |
| 1% 0.5M purified | 25.59 | 35.99 | 1.89 | 7.30 |

Such particles could be used as roughening agent in material, in order to enhance its robustness against water. Indeed, dual micro- and nano-roughness (fractal structures) are known to be the key in superhydrophobic manufacturing surfaces (Onda et al., 1996). Roughness of the surface of particles was measured with AFM in order to evaluate the potential of the particles. Average ($R_a$) and root mean square roughness ($R_q$) are presented in Table 2-5. For a 1% initial TMPS concentration, and different molar ratio between APMS and TMPS, the roughness is in the order of 15 nm and no significant change can be deduced since high standard deviations are calculated. However it is one order less than lotus leaf natural or reproduced nanostructure (Koch et al., 2009), which possibly too low to obtain a good repellency.

**Table 2-5. AFM roughness measurement of particles surface.**

| % | M | $R_q$ (nm) | $R_a$ (nm) |
|---|---|---|---|
| 1.0 | | 16.6 ± 5.7 | 13.6 ± 4.4 |
| 0.5 | 0.5 | 20.0 ± 9.8 | 16.0 ± 8.1 |
| 0.1 | | 11.3 ± 7.5 | 9.0 ± 5.9 |

### 2.1.4. Conclusion and perspectives

Organo-modified silsesquioxane spheres were produced in water through a simple and fast method. The synthesis is done in water and only methanol is released from organotrimethoxysilane hydrolysis and without any surfactants. Particles size is around 1 µm diameter and could be adjusted by varying precursor initial concentration (TMPS) but also the catalysis amount (APMS). Formation by an aggregation of smaller particles of around 100 nm and a cross-condensation between precursor and catalysis were also shown. However, the potential of variation of final particle size is narrow and a surfactant or rheological modifier could be considered to extend the possibilities in water. Inorganic cores are formed during particles nucleation leading to a thermally stable inorganic part and non-thermally stable organic part above 280°C. Surface roughness was evaluated in order to assess the potential applications in superhydrophobic surfaces but the nano-roughness is very small and might not affect water adhesion. However, the overall size of the particles is interesting as texturizing agent for surfaces.

In this study, cross condensation of APMS proved to possess a great potential as an initiator for linkage and functionalization of the particles but also for antibacterial application as no release is expected from the inorganic matrix after purification.

## References


Arbatan, T., Fang, X., Shen, W., 2011. Superhydrophobic and oleophilic calcium carbonate powder as a selective oil sorbent with potential use in oil spill clean-ups. Chem. Eng. J. 166, 787–791. doi:10.1016/j.cej.2010.11.015

Arkhireeva, A., N. Hay, J., 2003. Synthesis of sub-200 nm silsesquioxane particles using a modified Stöber sol–gel route. J. Mater. Chem. 13, 3122–3127. doi:10.1039/B306994J

Brinker, C.J., 1988. Hydrolysis and condensation of silicates: effects on structure. J. Non-Cryst. Solids 100, 31–50.

Brochier Salon, M.-C., Belgacem, M.N., 2010. Competition between hydrolysis and condensation reactions of trialkoxysilanes, as a function of the amount of water and the nature of the organic group. Colloids Surf. Physicochem. Eng. Asp. 366, 147–154. doi:10.1016/j.colsurfa.2010.06.002

Brown, P.S., Bhushan, B., 2015. Mechanically durable, superoleophobic coatings prepared by layer-by-layer technique for anti-smudge and oil-water separation. Sci. Rep. 5, 8701. doi:10.1038/srep08701

Cao, L., Jones, A.K., Sikka, V.K., Wu, J., Gao, D., 2009. Anti-Icing Superhydrophobic Coatings. Langmuir 25, 12444–12448. doi:10.1021/la902882b

Dirè, S., Tagliazucca, V., Callone, E., Quaranta, A., 2011. Effect of functional groups on condensation and properties of sol–gel silica nanoparticles prepared by direct synthesis from organoalkoxysilanes. Mater. Chem. Phys. 126, 909–917. doi:10.1016/j.matchemphys.2010.12.015

Fina, A., Tabuani, D., Carniato, F., Frache, A., Boccaleri, E., Camino, G., 2006. Polyhedral oligomeric silsesquioxanes (POSS) thermal degradation. Thermochim. Acta 440, 36–42. doi:10.1016/j.tca.2005.10.006

G. Croissant, J., Cattoën, X., Durand, J.-O., Man, M.W.C., M. Khashab, N., 2016. Organosilica hybrid nanomaterials with a high organic content: syntheses and applications of silsesquioxanes. Nanoscale 8, 19945–19972. doi:10.1039/C6NR06862F

Heitz, C., Laurent, G., Briard, R., Barthel, E., 2006. Cross-condensation and particle growth in aqueous silane mixtures at low concentration. J. Colloid Interface Sci. 298, 192–201. doi:10.1016/j.jcis.2005.12.011

Jung, C.Y., Kim, J.S., Kim, H.Y., Ha, J.M., Kim, Y.H., Koo, S.M., 2012. One-pot synthesis and surface modifications of organically modified silica (ORMOSIL) particles having multiple functional groups. J. Colloid Interface Sci. 367, 67–73. doi:10.1016/j.jcis.2011.09.016

Koch, K., Bhushan, B., Chae Jung, Y., Barthlott, W., 2009. Fabrication of artificial Lotus leaves and significance of hierarchical structure for superhydrophobicity and low adhesion. Soft Matter 5, 1386–1393. doi:10.1039/B818940D

Li, X.-M., Reinhoudt, D., Crego-Calama, M., 2007. What do we need for a superhydrophobic surface? A review on the recent progress in the preparation of superhydrophobic surfaces. Chem. Soc. Rev. 36, 1350–1368. doi:10.1039/B602486F

Liu, S., Lang, X., Ye, H., Zhang, S., Zhao, J., 2005. Preparation and characterization of copolymerized aminopropyl/phenylsilsesquioxane microparticles. Eur. Polym. J. 41, 996–1001. doi:10.1016/j.eurpolymj.2004.11.027

Ogihara, H., Xie, J., Okagaki, J., Saji, T., 2012. Simple Method for Preparing Superhydrophobic Paper: Spray-Deposited Hydrophobic Silica Nanoparticle Coatings Exhibit High Water-Repellency and Transparency. Langmuir 28, 4605–4608. doi:10.1021/la204492q

Onda, T., Shibuichi, S., Satoh, N., Tsujii, K., 1996. Super-water-repellent fractal surfaces. Langmuir 12, 2125–2127.

Ottenbrite, R.M., Wall, J.S., Siddiqui, J.A., 2000. Self-Catalyzed Synthesis of Organo-Silica Nanoparticles. J. Am. Ceram. Soc. 83, 3214–3215.

Crick R. , C., P. Parkin, I., 2011. CVD of copper and copper oxide thin films via the in situ reduction of copper(ii) nitrate—a route to conformal superhydrophobic coatings. J. Mater. Chem. 21, 14712–14716. doi:10.1039/C1JM11955A

Reverdy C., 2016. Cellulose nanofibrils aqueous modification with different alkoxysilanes: influence of amino presence on surface mechanisms and properties. TAPPI Nano Conference on Nanotechnology for Renewable Material, Grenoble, France.

Latthe S. , S., Terashima, C., Nakata, K., Sakai, M., Fujishima, A., 2014. Development of sol–gel processed semi-transparent and self-cleaning superhydrophobic coatings. J. Mater. Chem. A 2, 5548–5553. doi:10.1039/C3TA15017H

Stöber, W., Fink, A., Bohn, E., 1968. Controlled growth of monodisperse silica spheres in the micron size range. J. Colloid Interface Sci. 26, 62–69. doi:10.1016/0021-9797(68)90272-5

Van Blaaderen, A., Vrij, A., 1992. Synthesis and characterization of colloidal dispersions of fluorescent, monodisperse silica spheres. Langmuir 8, 2921–2921.

Xu, Q.F., Wang, J.N., Sanderson, K.D., 2010. Organic−Inorganic Composite Nanocoatings with Superhydrophobicity, Good Transparency, and Thermal Stability. ACS Nano 4, 2201–2209. doi:10.1021/nn901581j

Xue, C.-H., Jia, S.-T., Chen, H.-Z., Wang, M., 2008. Superhydrophobic cotton fabrics prepared by sol–gel coating of TiO2 and surface hydrophobization. Sci. Technol. Adv. Mater. 9, 035001. doi:10.1088/1468-6996/9/3/035001

Yao, L., Zheng, M., He, S., Ma, L., Li, M., Shen, W., 2011. Preparation and properties of ZnS superhydrophobic surface with hierarchical structure. Appl. Surf. Sci. 257, 2955–2959. doi:10.1016/j.apsusc.2010.10.098

Zhang, X., Jin, M., Liu, Z., Tryk, D.A., Nishimoto, S., Murakami, T., Fujishima, A., 2007. Superhydrophobic TiO2 Surfaces: Preparation, Photocatalytic Wettability Conversion, and Superhydrophobic−Superhydrophilic Patterning. J. Phys. Chem. C 111, 14521–14529. doi:10.1021/jp0744432

# 2.2. Simple method to obtain hydrophobic and antimicrobial cellulose nanopaper using silsesquioxane particles sol gel formation in aqueous conditions

*Reverdy C., Willeman H., Belgacem N., Bras J.. « Simple method to obtain hydrophobic and antimicrobial cellulose nanopaper using silsesquioxane particles sol gel formation in aqueous conditions», submitted to Applied Materials and Interfaces (2017).*


## Abstract

Cellulose nanofibrils (CNFs) films can be hydrophobized by several ways involving the use of organic solvents. Only few researches propose a water based modification. In this study, a fast hydrophobization is proposed with a low amount of added product. With the addition of two silanes, one precursor and one condenser which is aminated, the reaction media is only based on water. The method is involving the formation of a silsesquioxane film and particles formation inside the nanofibers web upon drying. Excellent results are obtained regarding hydrophobicity with a water contact angle of 111° on the top side, which is almost 5 times higher than a water contact angle with pure CNF, with only 1 wt% of silane addition in CNF films. The presence of the amine was also exploited as a possible antibacterial material for contact active surfaces.


### 2.2.1. Introduction

Among biobased materials, cellulose nanofibrils have been considered as very promising since last decades for wide applications such as paper (Brodin et al., 2014)(Bardet, 2014), composite strengthener (Lee et al., 2014), barrier material (Lavoine et al., 2012), medical (Jorfi and Foster, 2015), electronic (Hoeng et al., 2016) or water absorbent (Jiang and Hsieh, 2014). Mainly, high specific area with high hydroxyl group content on the surface gives the ability to form a strong and dense network but also to be highly hydrophilic, which can be a limitation for further applications. To obtain hydrophobic property strong enough to resist solvent, chemical modifications are mostly based on time-consuming solvent exchange

making the process barely conceivable for industry (Missoum et al., 2013), (Habibi, 2014). When aqueous solutions are considered, some researchers used nano-emulsion (Missoum et al., 2016), others proposed peptidic linkage on previously oxidized materials (Lasseuguette, 2008), others used silanes by adsorption/dehydratation monitoring (Reverdy et al., 2016) or even focused on polyelectrolyte or molecule adsorption (Xhanari et al., 2011). For example, adsorption of cationic molecules on previously carboxylated cellulose nanofibrils has been investigated to give hydrophobic properties to final CNF films in an easier manner (Syverud et al., 2011). However, only resistance to water rinsing was proved and not to solvent contact or efficiency during time even though good results are observed.

Organosilane and their chemistry are also one solution upon other to create a polysiloxane layer (also called silicone) on surface of nanocellulose. The use of toxic solvent is usually employed as controlled reaction with chlorosilane or even alkoxysilane need a complete anhydrous reaction medium leading to long solvent exchange procedure (Andresen et al., 2006), (Johansson et al., 2011). But soft chemistry, meaning organoalkoxysilane water based reaction, seems not to be a great interest, probably because of the low control quality or impact on properties or even the need to induce the covalent bonding at high temperature or in non upscalable conditions (Zhang et al., 2015), (Reverdy et al., 2016). Organosilane chemistry is already used in the functionalization of silica particles and glass fibers. Starting from the beginning, Stöber et al. (1968) obtained silica particles through the well-known Stöber reaction which gives narrow-sized nano to micrometric particles. This reaction was mainly observed and explained with the original tetraethoxysilane (TEOS) molecules condensed with ammonia. Such particles have the general formula of $SiO_2$. This sol-gel process was modified within the time by using organosilane and tetraalkoxysilane as condensing materials and similar cross condensation was observed (Croissant et al., 2016). Organoalkoxysilanes, under certain conditions, are able to form a polysiloxane sphere network as well. The use of such structures, which are easy to chemically tune by changing the organic chain or by using bridge organosilane, has been investigated in biosensor applications, drug delivery system in body or optoelectronics (Croissant et al., 2016). Fewer publications are available on cross condensation and growth of particles when two organotrialkoxysilanes are mixed together (Ottenbrite et al., 2000), (Heitz et al., 2006). The

term silsesquioxane is then determining the synthesized material from these precursors, leading to the empirical $RSiO_{3/2}$ formula (Baney et al., 1995).

To the best of our knowledge, only very few studies are getting interest on such material to form hybrid cellulose-silsesquioxane material, although relatively quick, simple and aqueous reactions are involved. The main studies approaching these materials have been done with cotton fibers or natural fiber fabrics. Indeed, roughness induced by covering the macro fiber gives, after low surface tension polymer coating, some superhydrophobic fibers with high resistance to washing (Liu et al., 2014),(Zhao et al., 2010), (Gao et al., 2010). In situ growth of such particles into nanocellulose network has barely been studied. Growth of TEOS based particles crosslinked with an aminetrialkoxysilane into TEMPO oxidized nanocellulose was recently observed (Maury, 2014) as well as the mixing of nanocellulose in already formed organically doped $SiO_2$ particles (Le et al., 2016). In this case, the effect of the nanofibers web or rheology was not mentioned on particles growth. Indeed, -OH group could affect their formation as well as viscosity can decrease the coalescence of particles. The effect of -OH group presence was only noticed very recently by Zorko et al. (2015). They studied the impact of immersing a cotton fabric at different times of the Stöber's reaction, showing the presence of the fibers affects greatly the dispersity of the usual monodisperse particles. This growth was also monitored on other surfaces with no –OH content such as PET and it showed that the interaction was very different leading to a thin silica film with poor adhesion.

Still, no research on a native nanocellulose and organotrialkoxysilane mixture condensation was studied to our knowledge. In situ growth of such hydrophobic and functionalized silsesquioxane particles could lead to hydrophobic and versatile nanocellulose networks.

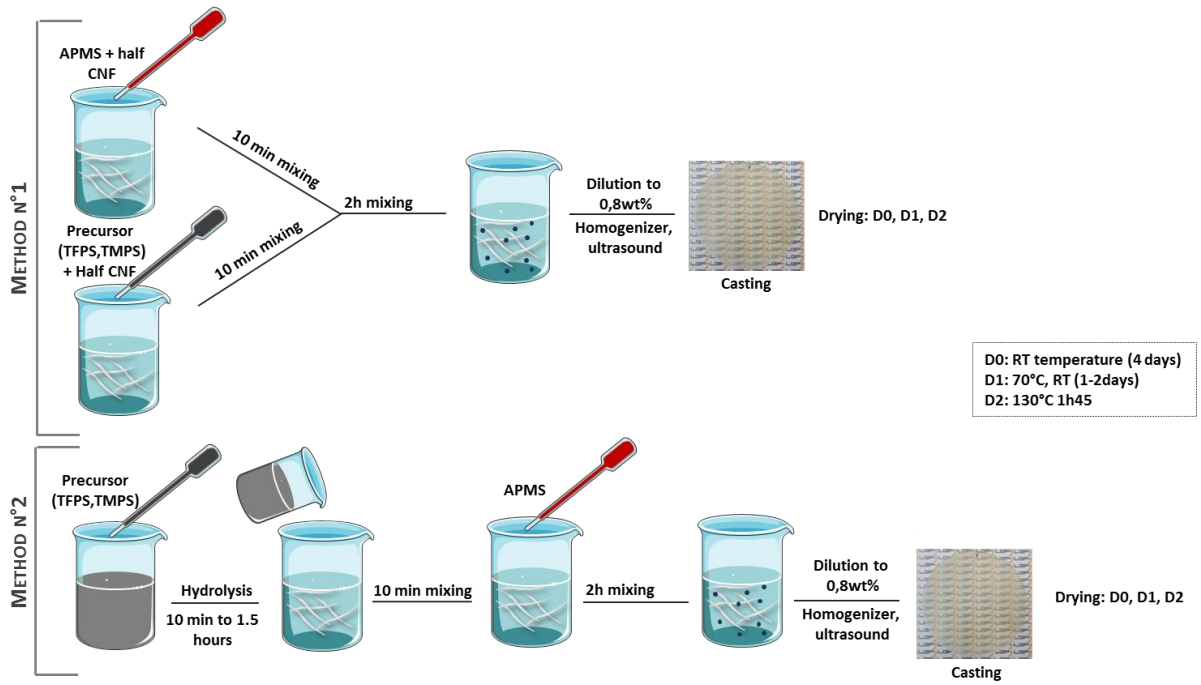


**Figure 2-13. Scheme of samples manufacturing before characterization. Two methods were used involving two different ways for managing organotrialkoxysilane hydrolysis.**

Hereafter is studied the mechanisms of *in situ* growth of silsesquioxane particles made through the cross condensation of 3-aminopropyltrimethoxy silane (APMS) with methyltrimethoxypropyl silane (TMPS) or (3,3,3-trifluoropropyl) trimethoxy silane (TFPS) (Figure 2-13). This will be compared to *ex-situ* silsesquioxane production and mixing strategy. Also, two different methods of introduction will be compared. Manufacturing method, concentration of organosilane in the media, effect of drying and organic chain are discussed. Final nanocellulose films properties are characterized regarding structure, hydrophobicity and antibacterial activity.

### 2.2.2. Experimental section

#### 2.2.2.a. Materials

Cellulose nanofibrils used in this study is an homogeneous grade made from birch bleached kraft pulp and extracted with a mechanical and enzymatic pretreatment followed by five passes through a homogenizer (GEA, Italy). It has a dry matter content of 2.0wt%. (3-Aminopropyl)trimethoxy silane (APMS) (Sigma Aldrich, France), propyltrimethoxy silane (TMPS) (Sigma Aldrich, France) and (3,3,3-trifluoropropyl) trimethoxy silane (TFPS) (Gelest, France) were the three alkoxysilanes used in this study. Ethanol (98%, Roth) and acetic acid (96%, Sigma Aldrich) were used for hydrolysis medium of alkoxysilanes. All experiments were carried out with distilled water.

#### 2.2.2.b. Methods

*CNF-silsesquioxane modification*

Two different ways for organotrialkoxysilane introduction were studied (Figure 2-13): method 1 and method 2. For method 1, the addition is made by introducing in half the suspension the precursor (TMPS or TFPS) and in the other half APMS. Each part is stirred for 10 min separately and then both fractions are mixed together. The resulting suspension is mixed with magnetic stirring for at least 2 hours at room temperature. Method 2 consists in hydrolyzing precursor by adjusting water/ethanol ratio and pH with acetic acid according to Table 2-5. Hydrolyzed organotrialkoxysilane is added to CNF suspension and mixed for 10 min. APMS is then introduced drop by drop while mixing and the suspension is allowed to react for at least 2 hours.

*CNF-silsesquioxane film preparation*

Previously prepared suspensions are then diluted to 0.8 wt% dry matter content in order to obtain smooth and flat films after being casted to obtain 40 g/m² films. Films are allowed to dry at room temperature in a fume hood for 3-4 days (D0), at 70°C for 50 min and room temperature for 2 days (D1) or at 130°C for 1h45 (D3). If not specified, drying is done at D0 conditions by default. Films are then conditioned at 23°C and 50% RH during at least 24 hours before testing.

For some experiments, a purification step was needed to assess anchoring of the modification. To do so a soxhlet extraction was carried out with a 20/80 ethanol/water solvent for 8h. Films were then let dry at room temperature.

**Table 2-5. Alkoxysilane hydrolysis condition**

| Precursor alkoxysilane | Concentration (wt%) | Water/ethanol (w/w%) | pH adjustment | Hydrolysis time (min) |
|---|---|---|---|---|
| TMPS | 1 | 100/0 | 2.3 | 1 |
| TFPS | 1 | 20/80 | 4 | 120 |

### *Cellulose nanofibrils characterization*

Cellulose nanofibrils (CNF) were observed trough optical microscopy at 50x magnifications (Axio Imager A2) and imaged with a camera assembled on it (AxioCam MRm, Carl Zeiss). Atomic force microscopy (AFM) was also used to get more accurate images (Nanoscope III®, Veeco). Samples were prepared the day before observation by diluting the suspension and dispersing it with a high-shear homogenizer (Ultraturrax ®, IKA). A drop of the suspension was deposited on mica substrates and consequently dried overnight at room temperature. A silicon cantilever (OTESPA®, Bruker, USA) was used in tapping mode at different locations. Resulting images were subjected to a 1$^{st}$-order polynomial flattening to reduce bowing and tilt effects.

Film nomenclature is “method number”_”CNF” “APMS” “precursor name” “molar ratio between APMS and TMPS”M “weight ratio between total silane content and CNF” w.

### *Characterization of films*

Static contact angles were measured with a contact angle meter (DataPhysics Instrument, DataPhysics OCA 20) at room temperature. A 5 µL distilled water drop was deposited on the surface and images were recorded for one minute and a half to monitor contact angle and drop volume evolution. Averages of at least 5 measurements were calculated for each surface to give representative results.

The thermal degradation of the samples was monitored using TGA (thermogravimetric analyzer, STA 6000®, PerkinElmer Instruments, England). The mass loss was measured starting with a 20 to 30 mg initial sample upon a heating rate of 10°C/min in the temperature range of 30–900°C under an oxidizing atmosphere (air).

Scanning electron microscopy equipped with a field emission gun (FEG-SEM) was used to observe and image the film surface morphology (Zeiss® Ultra-55, USA). Samples were coated with a 3 nm gold before being imaged at an accelerated tension of 3.0 kV and a working distance of 10 mm. For imaging the silsesquioxane network without the CNF, a thermal

treatment under air at 700°C for 1h of modified CNF films was performed. Remaining material was gently deposited on a SEM conducting stub for analysis.

Roughness parameters of samples were determined by using an optical profilometer (InfiniteFocus, Alicona) at a 50 magnification corresponding to an 11 mm working distance and a 0.10 mm² analyzed surface. Average surface roughness (Sa) was determined by picking randomly at least three different locations on the sample.

### *Antibacterial assessment*

Antibacterial activity but also possible leaching of APMS was evaluated through different procedures. First, based on standard AFNOR EN1104, pieces of modified films to be tested were placed on a B.Subtilis inoculated agar (top surface in contact). These petri plates were incubated for 3 days at 37°C and leaching ability was evaluated by the absence or presence of an inhibition zone. Experiments were repeated three times.

In a second step, a quantitative test was carried out with *S.Aureus*. A fixed amount of the film was placed in 20mL 1/500 nutrient broth and shake 24h at 37°C. Samples were then filtered and bacteria were added to 15ml of the filtrate to obtain $10^3$ CFU/mL. The solution was incubated 24h with shaking. Numbers of colony forming units (CFU) were determined by plating the incubated bacteria. Experiments were reproduced twice. The evaluation of the leaching activity was checked upon the calculation of growth value compared to inoculum concentration.

Assessment of antibacterial activity against S.Aureus was performed according to AATCC Test Method 100-1998. Sample surfaces were inoculated with 200 µL of a $10^5$ CFU/mL inoculum and incubated 24h at 37°C. Bacteria were then extracted by using 50 mL of the neutralizing solution (L-lecithin 3 g/L, sodium thiosulphate 5 g/L, L-Histidine 1 g/L, Tween 80 30 g/L, Buffer solution ($KH_2PO_4$ 0.68 g/L) 10 mL/L, (pH at 7.2 ± 0.2)). Resulting solutions were plated in order to determine the CFU number. All experiments were at least duplicated.

### 2.2.3. Results and discussion

#### 2.2.3.1. CNF characterization

Since early 2010's, it is well known that several quality grades of CNFs are available and published using various descriptions (CNF, microfibrillated cellulose (MFC), nanofibrils of cellulose or even cellulose filament). It is then very important to well characterize each grade before any use. In our case, as shown in Figure 2-15, our grade is very homogeneous, with nanofibers having a diameter around 20 ± 6 nm and a length of several micrometers.

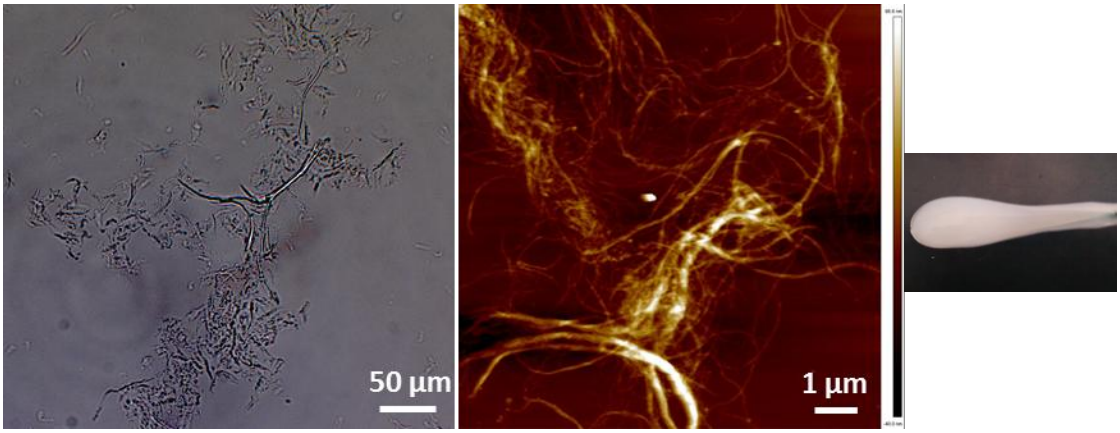


**Figure 2-14. Cellulose nanofibrils observation with optical microscope (left) and AFM (middle) and visual aspect (right).**

#### 2.2.3.2. Organotrialkoxysilane hydrolysis

Two different methods of manufacturing films were used by changing organotrialkoxysilane hydrolysis-condensation conditions. It is well known that each organosilane has a different time of hydrolysis depending on the organic chain and solvent conditions (Brochier Salon and Belgacem, 2010). Indeed, it was proved, that APMS, TMPS or TFPS did not react with the same kinetic rates regarding hydrolysis and condensation in their medium (Reverdy et al., 2016). APMS is immediately transformed to condense structures as well as TMPS (in acidic and ethanolic media) whereas TFPS is ongoing these reaction more slowly. APMS and TMPS are instantly hydrolyzed and start to condense during the first minute. However, TFPS reach its fully maximum hydrolyzed structure only after 1.5 hour. While hydrolysis reaction is taking part, it has to be reminded that methanol is release in the system, which is probably auto-catalyzing the hydrolysis mechanisms. This is why TMPS was let to react in its solvent for only one minute and TFPS for 2h. Alkoxysilanes were then introduced in CNF at the point where most of the trisilanol groups are formed. Results are

expected to show the difference when precursors are in their hydrolyzed structure at CNF contact (method 2) or are expected to form micelle in water (method 1).

#### 2.2.3.3. Films hydrophobicity

##### Modification homogeneity

Water contact angle (WCA) measurements were done on each modified film on bottom and top side to check the uniformity of the chemical modification. As expected, WCA of CNF reference film (Table 2-7) is very low and the film shows quick absorption of water. Top is lower than bottom which could be explained by a superior roughness of the top side compared to the bottom counterpart as measured by the optical profilometer (Table 2-6). Indeed, if correlated to the Cassie-Baxter equation, a hydrophilic surface becomes more hydrophilic when it is rougher.

Reference with only one silane added with method 1 or method 2 shows interestingly high WCA on top side but fairly poor WCA on bottom side. This could be explained by a demixing process taking place during the long period of drying.

For same very low amount of total silane in the film, when a precursor is used and condensed with APMS, WCA of both top and bottom sides are very high, as shown in Table 2-7. The difference between top and bottom can also be explained by Wenzel theory (Wenzel, 1936). Here, as the material becomes hydrophobic on each side, the more rough side is more hydrophobic regarding water contact angle. It is correlated with the optical profilometer measurements (Table 2-6), as the roughness from top to bottom side is decreasing by almost a half for CNF TMPS APMS 0.5M 0.05w.

**Table 2-6. Surface texture measurement of top and bottom side of films.**

| | $S_{a\ Top}$ (µm) | $S_{a\ Bottom}$ (µm) |
|---|---|---|
| CNF | 1.16 ± 0.09 | 0.54 ± 0.07 |
| 1_CNF APMS TMPS 0.5m 0.05M | 1.32 ± 0.06 | 0.72 ± 0.05 |

*Effect of organic chain*

Table 2-7 shows also no significant difference between the use of TFPS or TMPS. It is highlighting that the addition of APMS is playing a crucial role for the final material rather than initial stage of precursor. It also brings out the low impact of the terminal group of the propyl chain on CNF films properties. Whereas it is well known TFPS has a much lower surface energy as shown in a previous work with fibers giving very high contact angles (Ly et

al., 2010). This might be due to a stronger entanglement and lower roughness of CNF films as compared to the case of macroscopic fibers.

*Effect of the synthesis method*

**Table 2-7. Water contact angle of films and roughness depending on manufacturing method 1 or 2, precursor (P) and condensor (C) choices as well as total massic silane amount in the film (w). * soxhlet extracted for 8h with 80/20 water ethanol solution, [c] concentration of the total silane in water is constant.**

| | Method | (P) | (C) | Wt (w) | θw Top (°) ± | | θw Bottom (°) ± | |
|---|---|---|---|---|---|---|---|---|
| CNF | | – | | | 24 | 1 | 29 | 2 |
| Ref. | 1 | – | APMS | 0.05 | 102 | 1 | 53 | 3 |
| | | – | APMS* | 0.05 | 89 | 1 | 46 | 7 |
| | | TMPS | – | 0.05 | 111 | 2 | 56 | 1 |
| | | TFPS | – | 0.05 | 99 | 2 | 43 | 5 |
| | 2 | TMPS | – | 0.05 | 109 | 1 | 60 | 2 |
| | | TFPS | – | 0.05 | 98 | 3 | 41 | 3 |
| CNF-silsesquioxane (molar ratio P/C=0.5) | 1 | TMPS | APMS | 0.005 | 80 | 15 | 65 | 6 |
| | | TMPS | APMS | 0.01 | 111 | 3 | 91 | 11 |
| | | TMPS | APMS[c] | 0.05 | 111 | 3 | 90 | 1 |
| | | TMPS | APMS | 0.1 | 109 | 3 | 49 | 2 |
| | | TMPS | APMS[c] | 0.1 | 111 | 2 | 102 | 1 |
| | | TMPS | APMS[c] | 0.25 | 111 | 2 | 99 | 3 |
| | | TMPS | APMS[c,]* | 0.25 | 114 | 2 | 94 | 2 |
| | | TFPS | APMS | 0.05 | 108 | 6 | 93 | 3 |
| | 2 | TMPS | APMS | 0.05 | 109 | 1 | 93 | 3 |
| | | | APMS* | 0.05 | 111 | 1 | 103 | 3 |
| | | | APMS | 0.01 | 111 | 1 | 95 | 2 |
| | | TFPS | APMS | 0.05 | 97 | 2 | 86 | 0 |
| | | | APMS | 0.01 | 107 | 0 | 90 | 4 |

Both method 1 and method 2 results of CNF-silsesquioxane film surface WCA are superior to 105° on the top and 90° on the bottom. Further trials with method 1 where done, indeed this method is presenting shorter reaction time and it calls upon the use of an easier procedure. TMPS was added to the total suspension and then APMS was added drop by drop and the contrary was also done, in order to reach 0.5 m 0.05 w samples. Water contact angles of top side were similar with method 1 for both but, in the first case, when TMPS was added first in the total CNF suspension, bottom side depicted a contact angle of 59° ± 12. However, in the second procedure, when APMS was added first in the total amount of CNF, the WCA was 90° ± 14. High standard deviations were observed for bottom side for both procedures, which was not the case in the initial method.

These results show the importance of the pre-hydrolysis step of both silanes in water and their homogeneous mixing in the nanocellulose network. The method consisting in mixing one silane in half CNF suspension probably decreases the standard deviation because of a faster and larger contact between both silanes in the suspension. This result also shows that APMS is possibly more acting as a hydrophobizing layer than TMPS, which is consistent with our previous study (Reverdy et al., 2016).

*Effect of the precursor initial concentration in water and of the total silane amount*

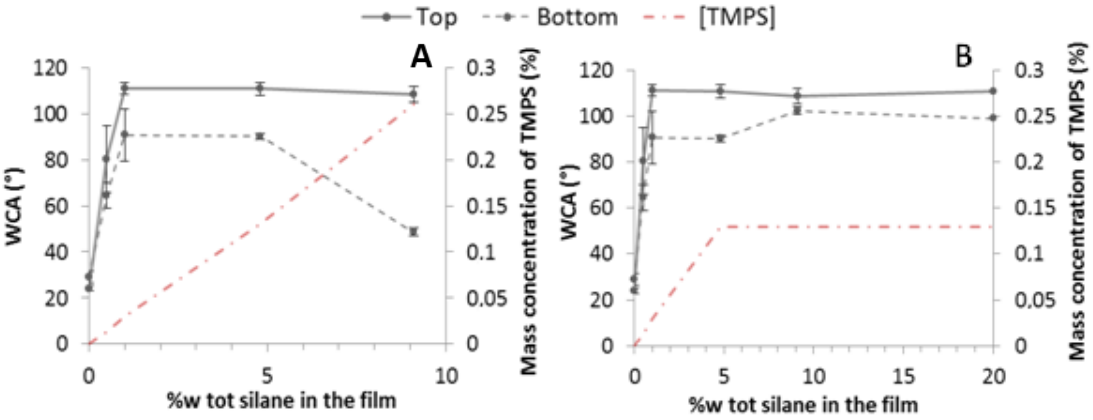


**Figure 2-15. Effect of the precursor initial concentration and the total silane amount in the film on WCA. At increasing initial concentration (A) and constant initial concentration (B).**

Different quantities of TMPS were used for the method 1. Figure 2-15 demonstrates that only 1 wt% silane in the film is enough to modify greatly surface energy of nanocellulose, after what a plateau is reached. This is less than a previous study in which they demonstrated a 110° water contact angle with 1,6 wt% of silicon atom content measured with elemental analysis (Zhang et al., 2015). And a second difference is that they performed the grafting through freeze drying of the suspension while here, only a usual and easy drying procedure is performed. Our strategy is then very promising to obtain hydrophobic nanopapers with only a very low silsesquioxane quantity in aqueous conditions. Up to our knowledge, this is the first time such an easy way is proposed. There is also a significant influence of the initial TMPS concentration in water (Figure 2-15 B) in the initial CNF suspension on homogeneity of properties (top versus bottom).

In Figure 2-15 B, after reaching the point of mass concentration of 0.13 wt%, demixion occurs leading to a lower contact angle on the bottom of the film. While conserving this concentration of 0.13 wt% (by dilution of the CNF suspension in water), a higher amount of silane can be added without creating any bottom/top difference. TMPS could be assimilated

to an amphiphilic structure when hydrolyzed as $RSi(OH)_3$ with its hydrophilic silanols and hydrophobic alkyl tail. A value between 0.13 and 0.25 as mass concentration in CNF suspension with respect to water could be assigned as a limit of solubility of organotrialkoxysilanols in CNF suspensions. After this limit, micelles could change in a biphasic system wich migrates at the top of the film, explaining the water contact angle difference between top and bottom surfaces observed in Figure 2-15 A .

*Effect of the drying conditions*

Drying conditions were evaluated in order to check if the condensation rate of silane inside the material could influence the properties of the ensuing materials (Figure 2-16). Indeed, as previously noticed, while one silane is present in the material, and dried for one hour, contact angle is much lower, possibly due to evaporation of silanol moieties (Reverdy et al., 2016). In the case of silsesquioxane, whatever the drying condition, room temperature (D0), 70°C for 1h and room temperature (D1) or 1h45 at 310°C (D3), top side contact angle is almost the same. However differences appear on the bottom side. This difference could be explained by a difference of roughness of bottom side due to the film shrinkage in both cases of faster drying.

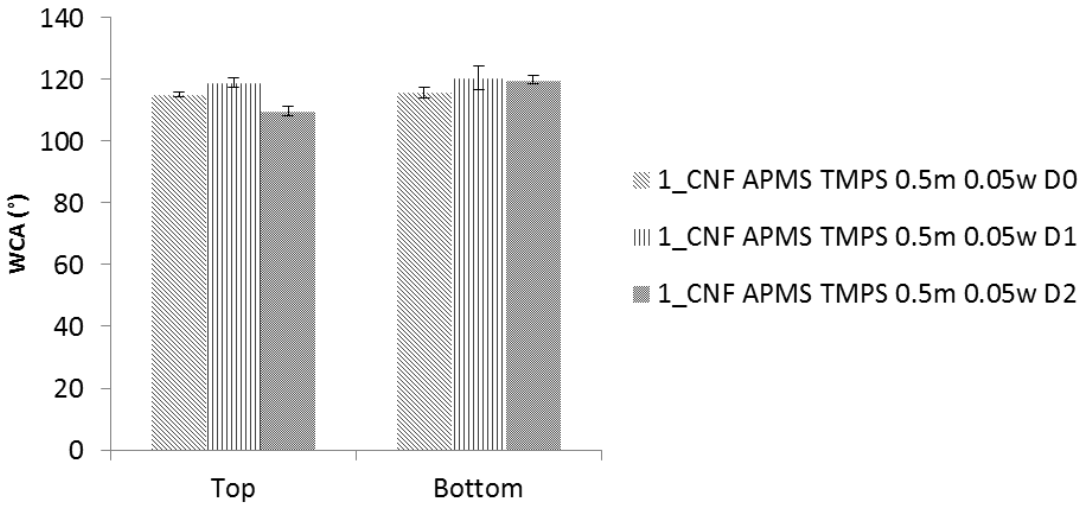


**Figure 2-16. Effect of the drying conditions on contact angle of the top and bottom surfaces of the films.**

*Modification durability*

Soxlhet extraction with a 80/20 water/ethanol mixture during 8h on CNF TMPS APMS 0,5m 0,25w did not affect the WCA (Table 2-7). The same is happening with films made with method 2 as shown by the results on 2_CNF APMS TMPS 0,5m 0,05w. At the opposite, the extraction affected the contact angle of top face of the film of the CNF-APMS reference by

decreasing it from 102° to 89°. This could be explained by an unbounded APMS present at the surface of the reference film. So silsesquioxane particles seem much more entangled or adsorbed-attached to CNF surface. This point is very positive to avoid leaching.

#### 2.2.3.4. Film structural properties

It is well known that the surface structural morphology is playing an important role over contact angle measurement. As the mixing of APMS and TMPS in water was proved to form round shape organo-modified silsesquioxane particles at low concentration, the need to analyze roughness but also arrangement of silica matrix is crucial. It is not surprising that FEG-SEM images (Figure 2-17) showed large difference between virgin and modified CNF. Highly porous surface without any modification is observed in the case of references. With only one silane (Figure 2-17 B and C) at 5 wt% regarding CNF content, the surface is changed as well. In fact, a thin layer is covering CNF surface and some small beads are observed with TMPS at the surface of some fibers. But it is much more different while both silanes are mixed together at 5wt% regarding CNF content. The layer above CNF is significantly more visible. Also, silsesquioxane pearl necklaces are observed along the surface as well as spherical particles alone (Figure 2-17 D and F) for either 5 or 25 wt% of silane amount. A breach in this layer permitted to explore the internal part of the films, where small beads of about 100nm are dispersed inside the nanocellulose network (Figure 2-17 F). After thermal treatment at 700°C for 1h, the cellulose is completely burned of as it has a degradation temperature of about 200°C to 400°C (Fisher et al., 2002). The resulting material is only the inorganic part of the silsesquioxane. As shown by images E and G (Figure 2-17), the content of silane regarding CNF is affecting the shape of the material. In the case of 5 wt% content, big beads are observed in the range of 10 µm which is much higher than what was seen in the non-treated material. A smooth layer is ungluing it and other types of structure were observed, such as needles and platelets in a fewer amount. Inside the beads or platelets, spheres of a diameter less than 100 nm are agglomerated. With a higher content (G) much more sphere of diameter around 100 nm are agglomerated and observable. Other smooth wrinkles are observed as well in other parts of the material and are not shown here.

Pearl necklaces were not proved to surround nanofibrils eventhough their curved shape is strongly reminding CNF one. One web was found to be empty which could bring the possibility that CNF can sometimes act as a template. Image analysis proved the composite structure of CNF, showing that the presence of the fibrils is probably acting as a size moderator during growth process if compared to beads size in water only.

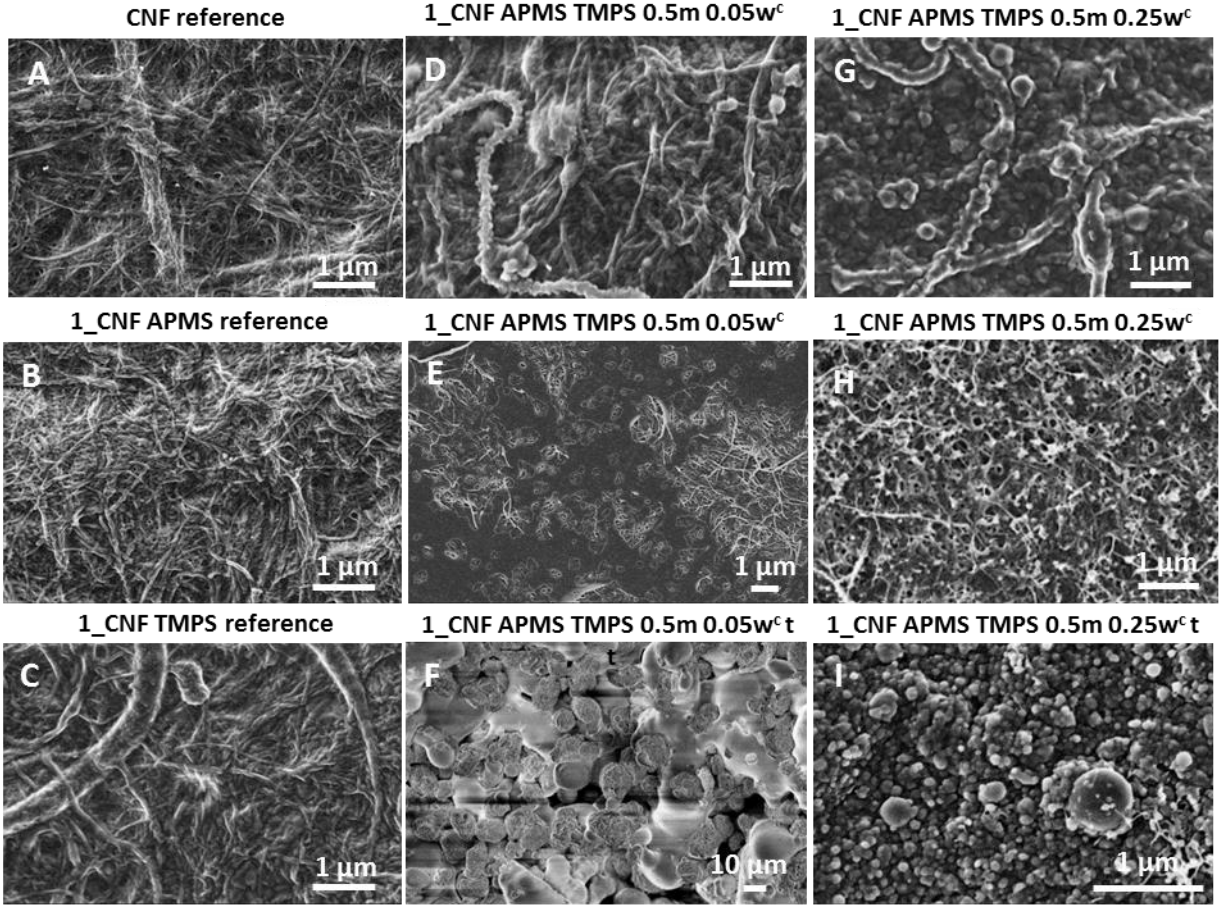


**Figure 2-17. FEG-SEM Images of top surfaces of CNF (A) and 1_CNF APMS reference (B) 1_CNF TMPS reference (C) 1_CNF APMS TMPS 0.5m 0.05w (D), bottom surface of 1_CNF APMS TMPS 0.5m 0.05w (E), 1_CNF APMS TMPS 0.5m 0.05w thermally treated (F), 1_CNF APMS TMPS 0.5m 0.25w at constant silane concentration (G) with an inside of a breach in the surface (H) and the same film thermally treated (I)." [c] "concentration of total silane in water constant. "t" thermally treated.**

It was expected that such a treatment creating micro/nano beads would increase surface roughness. As shown in Table 2-6, 5 wt% of total silane with respect to CNF slightly increases top surface roughness whereas bottom roughness is rising by almost 50%. As compared to the sylilation reported by Andresen et al. (2006), which quadrupled the roughness of their CNF because of larger fibers remaining and thus permitting to obtain water contact angles around 147°, this result is lower and explains that WCA is not going under 110°.

According to these results, a proposed mechanism is depicted in Figure 2-18, where APMS is supposed to act as a condensing material for TMPS particles giving a homogeneous repartition of inorganic part in the material.

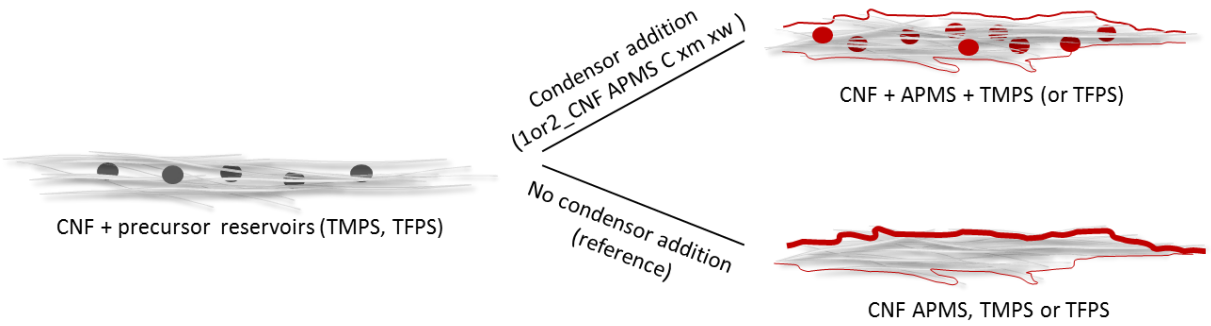


**Figure 2-18. Hypothesis of reaction mechanisms**

### 2.2.3.5. Thermal stability

Harsh condition of modification due to inclusion of basic species (APMS) could lead to a modification of the nanocellulose thermal stability. TGA was thus performed on neat and modified 0.5m 0.05w. No change in degradation temperature was observed (Table 2-8). Chars at 900°C were checked and the inclusion of a silsesquioxane network is proved to occur in the system as an increase is observed for the modified CNF.

**Table 2-8. Thermal degradation analysis of films**

| | Degradation Temperature (°C) | Chars (wt%) at 900°C |
|---|---|---|
| CNF | 199 ± 1 | 10.3 ± 3.5 |
| CNF 0.5m 0.05w | 200 ± 1 | 14.6 ± 0.2 |

### 2.2.3.6. Antibacterial assessment

In this section, only films made with a constant concentration of TMPS in the initial suspension were tested, meaning CNF with method 1, using TMPS with a total silane content of 10 to 25 wt%.

Films were evaluated for their antimicrobial activity against *B.subtilis* and *S.Aureus*. The APMS is thought to cross condensate in the matrix around cellulose nanofibers and silsesquioxane particles would be a good antimicrobial against bacteria as it contains ammonium groups well-known for this property (Saini et al., 2016). No release is expected from the matrix after purification of the material. First, non-purified films were used against *B.Subtilis* according to AFNOR NF EN 1104 to evaluate antibacterial activity and leaching

through the visualization of an inhibition zone. A large zone was observed on 1_CNF APMS TMPS 0.5m 0.10w and 1_CNF APMS TMPS 0.5m 0.25w indicating strong antimicrobial activity but also the leaching of APMS. The amount of APMS regarding CNF before purification is around 9% by weight. This observation of a zone of inhibition is in agreement with the result given by Saini et al. (2016), observing a 2mm zone around the sample containing around 10% APMS regarding CNF. A part of the APMS introduced in the reaction is thus not linked to the material. A part of APMS cross condensed with the silsesquioxane

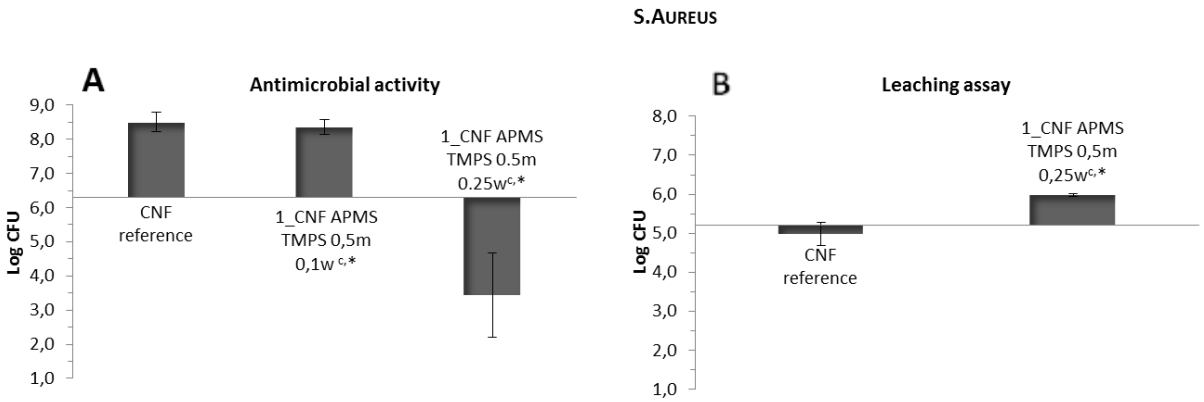


**Figure 2-19. Antibacterial assessment of purified and non-purified films against B.subtilis and S.Aureus. Leaching and activity are assessed.**

particles while probably another part only self-condensed leading to adsorbed molecules in the material.

A soxhlet extraction of unbounded APMS was carried out in a 20% aqueous solution of ethanol for 8h. A quantitative assessment based on ATCC 100-1998 method was secondly carried out against *S.Aureus* with the purified films. *S. Aureus* is a gram positive bacteria which is harder to kill than *B.Subtilis* and is relevant regarding possible applications in medical device protection for example. This test will permit to know if the APMS from the silsesquioxane network displays antibacterial activity. The amount of APMS remaining in the nanopaper was not quantified. By comparison with silsesquioxane particles purification, while synthesized in water, a loss of 60 to 70% by weight of the APMS was observed (Liu et al., 2005). With a synthesis in CNF suspension, it could be assumed that a part of APMS is also linked to CNF hydroxyl bond as shown by the water contact angle of 1_CNF APMS reference surface after soxhlet extraction.

Bacterial growth of almost 2 log was observed with the film 1_CNF APMS TMPS CNF 0.5m 0.10w and CNF reference leading to the conclusion that not enough APMS was kept inside the material. However, an average of 3 log reduction of S.Aureus strains was measured with

1_CNF APMS TMPS 0.5m 0.25w (Figure 2-19 A). This result is also consistent with the study of Saini et al. (2016) who found this order of CFU reduction for their nanopaper functionalized with APMS. Strong standard deviations in their study make the evaluation of APMS content in our samples impossible, but a range from 3 to 9wt% regarding CNF can be assumed.

A leaching test was then done on 1_CNF APMS TMPS 0.5m 0.25w to assure that no APMS molecule was released in the system. As shown in Figure 2-19 B, no bacteria killing was observed with the medium, leading to the conclusion that the nanopaper is active through contact only. Thus, an antibacterial non-leaching surface can be manufactured from a mix of CNF and silsesquioxane through a simple method if purified. This result is promising and has never been presented.

### 2.2.4. Conclusion and perspectives

Manufacturing of silsesquioxane in cellulose nanofibrils was evaluated in this study. Different conditions of addition of organotrialkoxysilane precusors and catalysts were assessed by measurement of the contact angle of the bottom and top surface of the film. High differences in the two methods were observed through non-homogeneity in both sides of the film. An optimized, fast and simple operation was proved to obtain hydrophobic nanocellulose films having an average of 100° for the water contact angle with low need of chemical. Silsesquioxanes are thought to happen in the material as well as a silsesquioxane layer in a competitive way without endangering nanocellulose integrity. The resulting mix gives a hydrophobic layer which enhanced with an elevated surface roughness.

As silsesquioxane matrix should contain amino groups due to cross-condensation between precursor and condenser, resulting films were tested and showed antibacterial activity against *S.Aureus* but also leaching of amino group. The latter is a problem regarding industrial purpose and European guidelines but can be overcome through a simple purification step with ethanol.

In this perspective, a lower APMS content might be found so that all species are included in the matrix and is still able to condense and form the silsesquioxane barrier.

## References


Andresen, M., Johansson, L.-S., Tanem, B.S., Stenius, P., 2006. Properties and characterization of hydrophobized microfibrillated cellulose. Cellulose 13, 665–677. doi:10.1007/s10570-006-9072-1

Baney, R.H., Itoh, M., Sakakibara, A., Suzuki, T., 1995. Silsesquioxanes. Chem. Rev. 95, 1409–1430.

Bardet, R., 2014. Nanocellulose as potential materials for specialty papers. Ph.D manuscript, Université Grenoble Alpes.

Brochier Salon, M.-C., Belgacem, M.N., 2010. Competition between hydrolysis and condensation reactions of trialkoxysilanes, as a function of the amount of water and the nature of the organic group. Colloids Surf. Physicochem. Eng. Asp. 366, 147–154. doi:10.1016/j.colsurfa.2010.06.002

Brodin, F.W., Gregersen, O.W., Syverud, K., 2014. Cellulose nanofibrils: Challenges and possibilities as a paper additive or coating material–A review. Nord Pulp Pap Res J 29, 156–166.

Fisher, T., Hajaligol, M., Waymack, B., Kellogg, D., 2002. Pyrolysis behavior and kinetics of biomass derived materials. J. Anal. Appl. Pyrolysis 62, 331–349. doi:10.1016/S0165-2370(01)00129-2

Gao, Y., He, C., Huang, Y., Qing, F.-L., 2010. Novel water and oil repellent POSS-based organic/inorganic nanomaterial: Preparation, characterization and application to cotton fabrics. Polymer 51, 5997–6004. doi:10.1016/j.polymer.2010.10.020

Croissant G. , J., Cattoën, X., Durand, J.-O., Man, M.W.C., M. Khashab, N., 2016. Organosilica hybrid nanomaterials with a high organic content: syntheses and applications of silsesquioxanes. Nanoscale 8, 19945–19972. doi:10.1039/C6NR06862F

Heitz, C., Laurent, G., Briard, R., Barthel, E., 2006. Cross-condensation and particle growth in aqueous silane mixtures at low concentration. J. Colloid Interface Sci. 298, 192–201. doi:10.1016/j.jcis.2005.12.011

Hoeng, F., Denneulin, A., Bras, J., 2016. Use of nanocellulose in printed electronics: a review. Nanoscale 8, 13131–13154. doi:10.1039/C6NR03054H

Jiang, F., Hsieh, Y.-L., 2014. Super water absorbing and shape memory nanocellulose aerogels from TEMPO-oxidized cellulose nanofibrils via cyclic freezing–thawing. J. Mater. Chem. A 2, 350–359. doi:10.1039/C3TA13629A

Johansson, L.-S., Tammelin, T., M. Campbell, J., Setälä, H., Österberg, M., 2011. Experimental evidence on medium driven cellulose surface adaptation demonstrated using nanofibrillated cellulose. Soft Matter 7, 10917–10924. doi:10.1039/C1SM06073B

Jorfi, M., Foster, E.J., 2015. Recent advances in nanocellulose for biomedical applications. J. Appl. Polym. Sci. 132, n/a-n/a. doi:10.1002/app.41719

Lasseuguette, E., 2008. Grafting onto microfibrils of native cellulose. Cellulose 15, 571–580. doi:10.1007/s10570-008-9200-1

Lavoine, N., Desloges, I., Dufresne, A., Bras, J., 2012. Microfibrillated cellulose – Its barrier properties and applications in cellulosic materials: A review. Carbohydr. Polym. 90, 735–764.

doi:10.1016/j.carbpol.2012.05.026

Le, D., Kongparakul, S., Samart, C., Phanthong, P., Karnjanakom, S., Abudula, A., Guan, G., 2016. Preparing hydrophobic nanocellulose-silica film by a facile one-pot method. Carbohydr. Polym. 153, 266–274. doi:10.1016/j.carbpol.2016.07.112

Lee, K.-Y., Aitomäki, Y., Berglund, L.A., Oksman, K., Bismarck, A., 2014. On the use of nanocellulose as reinforcement in polymer matrix composites. Compos. Sci. Technol. 105, 15–27. doi:10.1016/j.compscitech.2014.08.032

Liu, F., Ma, M., Zang, D., Gao, Z., Wang, C., 2014. Fabrication of superhydrophobic/superoleophilic cotton for application in the field of water/oil separation. Carbohydr. Polym. 103, 480–487. doi:10.1016/j.carbpol.2013.12.022

Liu, S., Lang, X., Ye, H., Zhang, S., Zhao, J., 2005. Preparation and characterization of copolymerized aminopropyl/phenylsilsesquioxane microparticles. Eur. Polym. J. 41, 996–1001. doi:10.1016/j.eurpolymj.2004.11.027

Ly, B., Belgacem, M.N., Bras, J., Brochier Salon, M.C., 2010. Grafting of cellulose by fluorine-bearing silane coupling agents. Mater. Sci. Eng. C 30, 343–347. doi:10.1016/j.msec.2009.11.009

Maury, C., 2014. Elaboration et caractérisation de matériaux hybrides à base de nanocelluloses et de nanoparticules inorganiques. Mémoire de Maîtrise, Université Quebec Montréal.

Missoum, K., Belgacem, M.N., Bras, J., 2013. Nanofibrillated Cellulose Surface Modification: A Review. Materials 6, 1745–1766. doi:10.3390/ma6051745

Missoum, K., Bras, J., Belgacem, N., 2016. Method for Forming a Hydrophobic Layer. Institut Polytechnique De Grenoble. US2016168696 (A1).

Ottenbrite, R.M., Wall, J.S., Siddiqui, J.A., 2000. Self-Catalyzed Synthesis of Organo-Silica Nanoparticles. J. Am. Ceram. Soc. 83, 3214–3215.

Reverdy C., 2016. Cellulose nanofibrils aqueous modification with different alkoxysilanes: influence of amino presence on surface mechanisms and properties. TAPPI Nano Conference on Nanotechnology for Renewable Material, Grenoble, France.

Saini, S., Belgacem, M.N., Salon, M.-C.B., Bras, J., 2016. Non leaching biomimetic antimicrobial surfaces via surface functionalisation of cellulose nanofibers with aminosilane. Cellulose 23, 795–810. doi:10.1007/s10570-015-0854-1

Stöber, W., Fink, A., Bohn, E., 1968. Controlled growth of monodisperse silica spheres in the micron size range. J. Colloid Interface Sci. 26, 62–69. doi:10.1016/0021-9797(68)90272-5

Syverud, K., Xhanari, K., Chinga-Carrasco, G., Yu, Y., Stenius, P., 2011. Films made of cellulose nanofibrils: surface modification by adsorption of a cationic surfactant and characterization by computer-assisted electron microscopy. J. Nanoparticle Res. 13, 773–782. doi:10.1007/s11051-010-0077-1

Wenzel, R.N., 1936. Resistance of solid surfaces to wetting by water. Ind. Eng. Chem. 28, 988–994. doi:10.1021/ie50320a024

Xhanari, K., Syverud, K., Chinga-Carrasco, G., Paso, K., Stenius, P., 2011. Reduction of water wettability of nanofibrillated cellulose by adsorption of cationic surfactants. Cellulose 18,

257–270. doi:10.1007/s10570-010-9482-y

Zhang, Z., Tingaut, P., Rentsch, D., Zimmermann, T., Sèbe, G., 2015. Controlled Silylation of Nanofibrillated Cellulose in Water: Reinforcement of a Model Polydimethylsiloxane Network. ChemSusChem 8, 2681–2690. doi:10.1002/cssc.201500525

Zhao, Y., Tang, Y., Wang, X., Lin, T., 2010. Superhydrophobic cotton fabric fabricated by electrostatic assembly of silica nanoparticles and its remarkable buoyancy. Appl. Surf. Sci. 256, 6736–6742. doi:10.1016/j.apsusc.2010.04.082

Zorko, M., Vasiljević, J., Tomšič, B., Simončič, B., Gaberšček, M., Jerman, I., 2015. Cotton fiber hot spot in situ growth of Stöber particles. Cellulose 22, 3597–3607. doi:10.1007/s10570-015-0762-4

# 3. Micro/nano roughness patterning of cellulose nanofibers thinfilm toward superhydrophobicity

## 3.1. Introduction

Superhydrophobicity is a well-known phenomenon occurring in nature to preserve plants from rain and dust and is therefore also called the self-cleaning effect. Physically it is measurable by a static water contact angle over 150° and a roll-off angle below 10° (Bhushan and Jung, 2011). Plant leaves, which are cellulose based materials, get usually their superhydrophobic state thanks to the micro and nano roughness of their surface due to papillae structure and epicuticular wax crystal (Barthlott and Neinhuis, 1997).

This ability to let a water drop rolls from a surface has been the center of interest in material research field to develop such properties. The phenomenon has also been theorized and modelled for a better comprehension. First, Wenzel theory was developed in 1936 and proposed a wetting state where water drops completely fill the roughness pattern (Wenzel, 1936). It was followed by Cassie-Baxter (Cassie and Baxter, 1944) proposing the air-pocket model, where water is suspended over the surface creating air pockets between roughness. It is now agreed that both theories could co-exist for a same material (Lafuma and Quéré, 2003).

Several studies tried to understand mechanisms of the phenomenon by creating artificially the surface with specific patterns. Various possibilities are offered such as controlled growth of particles (Zhu et al., 2005), ion etching (He et al., 2011) or soft-lithography (Liu et al., 2006) for example. Created materials were measured as such and few studies carried out a coating on the micro-patterns to provide a nano roughness or to study specific polymer.

Cellulose is the most abundant polymer in the world; it is one of the main components of wood and plants. Cellulose fibers are classically extracted from wood to produce paper or other renewable materials. These macroscopic fibers are made of micro and nano fibrils containing an amorphous and a crystalline part. Cellulose nanofibers (CNF) can be extracted by chemical pretreatment and mechanical treatments which defibrillate the core fiber. CNF have the particularity of forming a gel at very low concentration (2 wt%), that can disperse particles (Bardet et al., 2013), and form an entangled network when dried which creates a barrier material against oxygen or grease (Aulin et al., 2010), (Österberg et al., 2013).

Cellulose nanofibers are very promising in different fields such as composite reinforcement (Siró and Plackett, 2010), biomedical applications (Jorfi and Foster, 2015) or barrier materials such as food packaging. But the main drawback of CNF and cellulose in general is its high hydrophilicty which is a real challenge for several applications. Several treatments can impart hydrophobicity to cellulose nanofibers but to our knowledge, only one paper is proposing to impart a specific roughness to a CNF films in order to achieve the superhydrophobic state. Indeed, (Mäkelä et al., 2016) used very recently a roll to roll nanoimprint lithography method to impart specific pattern to a CNF or TEMPO-CNF films. They proved the possibility to mechanically modify the film structure and open their work to a possible use in superhydrophobic or antiadhesive material. Another paper, relative to a similar idea was proposed the same year by (Huang et al., 2016) with the spraying of CNF aggregates followed by phase chemical vapor deposition (CVD) with 1H, 1H, 2H, 2H-per-fuorooctyltrichlorosilane. They obtained very good results, but the CVD, often used in this purpose, is controversary due to the possible toxicity and low renewability of the chemical used or difficulty for roll-to-roll industrialization.

The idea of this study was to attempt to create on a patterned silicon substrate *via* soft lithography and coat on it some hydrophobic hydrophobic CNF in order to assess the effect of a model roughness on the contact angle of the resulting material (Figure 2-20). Micro-roughnesses were chosen according to Patankar's recommendations and different parameters were tried. CNF were casted on it to possibly create a 1-2 micrometer thick thin film with micro and nano roughness. The resulting surfaces are characterized with static contact angle 3D profilometer. Such a strategy is very difficult to obtain because of the tendency of CNF to agreggate and to shrink leading to uncontrolled thickness of the coated CNF layer onto the silicone pattern.

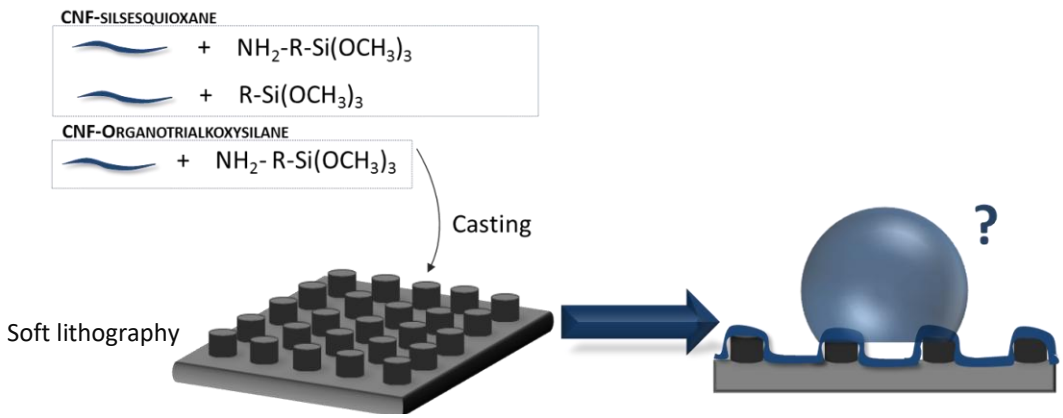


**Figure 2-20. Scheme of the project idea.**

## 3.2. Materials and methods

### 3.2.1. Materials

Cellulose nanofibrils used in the study is a made from birch bleached kraft pulp and extracted with a mechanical and enzymatic pretreatment followed by five passings through a homogenizer. It has a dry matter content of 2,0 wt%.

Two different kinds of modified CNF were tried for this study in addition to neat cellulose nanofiber.

(i) A silane modified CNF was prepared by hydrolyzing APMS for 30s in water at 10wt%. The solution was then added in CNF suspension so that APMS content was 10wt% regarding CNF. The suspension was stirred for 2h to let adsorption occur as well as self-condensation of the alkoxysilane.

(ii) Another modified CNF with silane was prepared. As compared to the first one, it permits to create in addition to the hydrophobicity, nano-spheres of silsesquioxane inside and on the surface of the material. Direct addition is made by introducing in half the suspension the precursor and in the other half APMS. Each part is mixed for 10 min and reunites. The resulting suspension is mixed for at least 2 hours.

Suspensions were kept in fridge and homogenized for 30s with an ultraturrax® before use.

Silicon Sylgard® 184 was used for pattern replicates as well as polyurethane resin (Smoothcast®).

### 3.2.2. Methods

#### Pattern design strategy

Patterns were first calculated according to Patankar's recommendations, by solving the two equations of Wenzel and Cassie Baxter theory.

The first theory is leading to the equation:

$$\cos\theta^{*,w} = r.\cos\theta$$

Where θ* is the apparent contact angle, θ the Young contact angle and r the surface roughness defined by the ratio between the actual surface area over the projected surface area.

And the second theory giving the equation:

$$\cos\theta^{*,c} = f_1.\cos\theta_1 + f_2.\cos\theta_2$$

Where $f_1$ is the fraction of solid in contact with liquid, $\theta_1 = \theta$ the Young angle of the solid, $f_2$ the air/liquid fraction with $f_2 = (1 - f_1)$ and $\cos\theta_2 = -1$ leading to:

$$\cos\theta^{*,c} = f_1 . (\cos\theta + 1) - 1$$

Both models can co-exist for the same surfaces as they are both thermodynamically stable. In order to design robust superhydrophobic pattern, meanwhile when $\theta^{*,c} = \theta^{*,w}$. (Patankar, 2003) proposed a model for designing a superhydrophobic surface based on these parameters relying on following equations:

$$\cos\theta^{*,c} = B(1 + \cos\theta) - 1$$

$$\cos\theta^{*,w} = (1 + \frac{4B}{(d/h)})\cos\theta$$

Where

$$B = \frac{1}{(c/d + 1)^2}$$

With θ the Young contact angle of the surface (flat), d the structure diameter, c the space in between two structures.

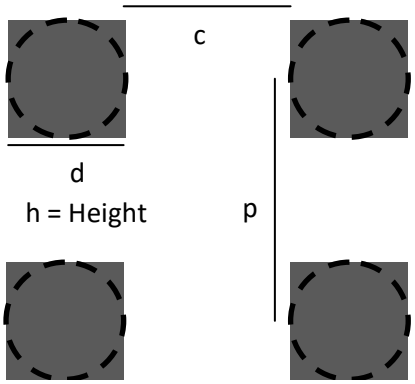


**Figure 2-21. Parameters used in designing superhydrophic surfaces. With d, the diameter or width of the micro-structure, c, the clearance and p, the pitch in between micro structures and h the height of the micro-structure.**

By solving the two equations, it is then possible to obtain an optimal pitch (p) distance to create a superhydrophobic state.

The height of the structure was fixed to 5 µm because of technical limitations in soft lithography patterning. Targeted structure diameter was 3 µm as it is close to precipitated calcium carbonate (PCC) size in papermaking industry. Indeed, because of the industrial context, the idea of studying this roughness is to eventually apply this with scalable strategy, such as coating paper with PCC followed by a spraying of CNF. A deviation of 2 µm under and above this target was chosen to observe the response of an optimal calculation with different structure parameters. As well, with the 3 µm diameter structure, a pitch deviation

from the optimal calculated was tried (± 1.5 µm) in order to overcome possible structure deviation due to CNF coating but also to test the response of such designs. Table 2-9 is summarizing the chosen parameters for the study.

**Table 2-9. Summary of pattern parameters.**

| Structure diameter | | | |
|---|---|---|---|
| 1 µm | 3 µm | 5 µm | |
| – | P6 | – | OP-1.5 |
| P3 | P4 | P5 | Optimal Pitch (OP) |
| – | P7 | – | OP+1.5 |

## Preparation of silicon micro-pillar by soft lithography

First, a SU8 micro pillar was manufactured through soft-lithography by the Upstream Technological Platform (PTA, CEA, Grenoble, France). Briefly, SU8 resin was spin coated on a silicium wafer to obtain a 5µm height layer. The wafer was then insolated with a laser (µPG 101, Heidelberg Instruments) with the pattern designed and washed to remove uncured resin.

In order to obtain a more robust pattern to make many replicates without degrading the master, it was chosen to manufacture a polyurethane replica. To do so, a silicone suspension was prepared with a 1:10 ratio of catalyst and base. The silicone suspension was degassed under vacuum during 45min and casted on the SU8 micro-pillar and again degassed for 30 min. The silicone was cured for 35min at 100°C and immediately after was detached. From this silicone replica, the polyurethane mold was done by casting the resin containing half base and half curing agent mixed together during one minute. Silicone mold is then peeled-off from the final pattern. Same procedure as the first one on SU8 is done to replicate infinitely the pattern in silicone.

## Coating of silicone molds with CNF

Previous to any coating, a corona treatment was done on the silicone material in order to increase its surface energy (Calvatron SG2—20 Kv, 20 Hz; STT supplier). Silicone patterns were placed on a conveyor, rolling at 1m/min speed. The used input intensity was 330 mA and the treatment duration was around 30 s.

Silicone molds were casted with CNF suspension. A sufficient quantity to obtain 1 g/m² of dry CNF was deposited. The coated material was let to dry at room temperature in order to avoid strong shrinkage of the film. A dry matter content of 0.4% was chosen in order to obtain an average coated thickness around 1 µm.

## Material characterization

### *Pattern observation*

Optical microscopy was used for checking the shape of the manufactured patterns. Images were recorded at 100 magnifications by using an Axio ImagerA2 optical microscope assembled with an AxioCam MRm camera (Carl Zeiss). Samples were previously sputtered with a 10nm carbon layer for the observation.

Roughness parameters of samples were determined by using an optical profilometer (InfiniteFocus, Alicona) at a 100 magnification corresponding to a 4.5 mm working distance and a 0.03 mm² analyzed surface.

Effective coating of CNF on the pattern was observed through a Quanta 200 SEM (FEI) and performed with a 2000 magnification with an accelerating voltage of 10kV. The working distance was 10.1 mm. Samples were previously coated with a 10nm carbon layer for the observation.

### *Static water contact angle measurement*

Contact angle was measured for each sample with a measuring device for contact angle measurement (OCA40, Data Physics Instruments GmbH). Water drop was dispensed with a syringe assembled with a 0.25 mm diameter needle. Static contact angle measurements were done at least three times with a 5µL water droplet. Measurements were done between 25 and 30 s contact time.

## 3.3. Results and discussion

### 3.3.1. Surface morphology characterization

Before the coating of the manufactured replicates of the SU8 patterns in silicone, the surfaces were analyzed with 3D profilometer in order to confirm the accuracy of the replicates compared to the designed material. Table 2-10 reports the pitch (p) and the diameter (d) of the theoretical design structure, which were successfully reproduced as shown by the measured values. However, a large difference in height value is observed. Indeed, for pattern n° 5 for example only an average value of 1.3 µm height is measured and for pattern 7 only 800 nm which is almost 75 to 85% less than the wanted height. Such difference explains the variation between predicted and measured water values. The manufactured samples depict higher θ values than silicone itself, but no superhydrophobic states were observed.

**Table 2-10. Pattern design parameters, real measured values and subsequent static water contact angle depending on coating.**

| | Designed structure | | | Measured Structure | | | $\theta_{w\ theo}$ (°) | | $\theta_{w\ meas}$ (°) | | | | | | | |
|---|---|---|---|---|---|---|---|---|---|---|---|---|---|---|---|---|
| Pattern n° | d (µm) | p (µm) | h (µm) | d (µm) | p (µm) | h (µm) | Wenzel | Cassie | Silicon | | CNF | | CNF 0.5m 0.25w | | CNF APMS 0.10 | |
| P0 | – | – | – | – | – | – | – | – | 110 | ± 3 | 23 | ± 6 | 61 | ± 4 | 15 | ± 9 |
| P3 | 1 | 3.3 | | – | – | – | 160 | 159 | 118 | ± 0 | 33 | ± 4 | 47 | ± 12 | 37 | ± 10 |
| P4 | 3 | 6.2 | | – | – | – | 147 | 147 | 119 | ± 2 | 22 | ± 2 | 22 | ± 5 | 49 | ± 12 |
| P5 | 5 | 8.6 | 5 | 5.0 ± 0.1 | 8.4 ± 0.2 | 1.3 ± 0.1 | 140 | 140 | 135 | ± 1 | 26 | ± 12 | 49 | ± 1 | 44 | ± 8 |
| P6 | 3 | 4.7 | | – | – | – | 180 | 136 | 121 | ± 3 | 34 | ± 3 | 89 | ± 1 | 36 | ± 9 |
| P7 | 3 | 7.7 | | 3.0 ± 0.1 | 7.5 ± 0.1 | 0.8 ± 0.1 | 131 | 154 | 122 | ± 2 | 24 | ± 4 | 46 | ± 10 | 43 | ± 5 |

This result is confirmed by the 3D profilometer that gives a visual result of pattern n°5 (Figure 2-22). It shows that some of the structures are missing, probably because of a breakage during demolding procedure. It also pictures the highly define contouring of the

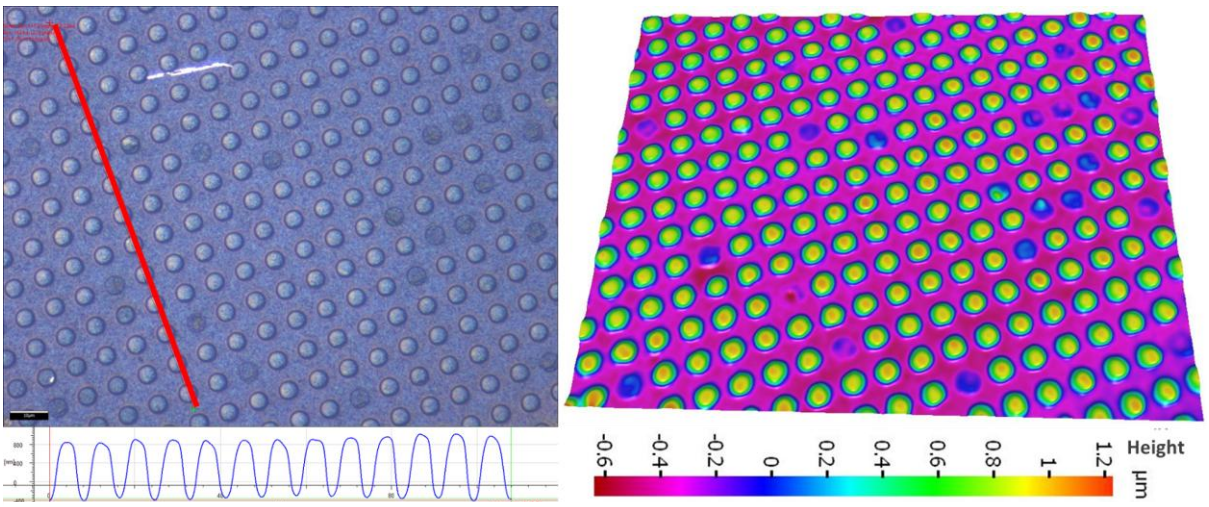


**Figure 2-22. Pattern n°5 microscopic pictures with pattern measurement (left) and 3D image (right).**

structure but also the poor height definition. The 3D image shows that the cylinders are round shaped on the top, leading to the conclusion that this failure in molding procedure is probably due to low penetration of silicone inside the holes of the structure. This difficulty to obtain perfectly designed surface with this molding/soft lithography strategy was not expected and was very disappointing. More efforts should be assessed in this step of silicon molding to understand what happens and how to overcome this issue. Despite this problem, we decided to stay on the process by coating this unadapted surface, at least to check feasibility of our strategy.

### 3.3.2. Influence of the CNF coating onto the pattern

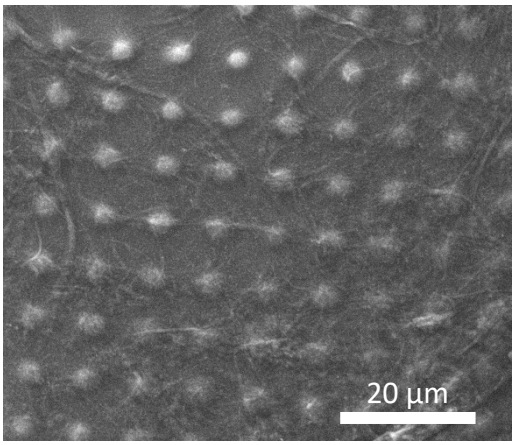


**Figure 2-23. SEM picture of the silicosn pattern n°7 coated with unmodified CNF.**

The coating with the different CNFs was performed on all surfaces even though the height was too small. As observed in Figure 2-23, showing the pattern n°7 coated with CNF observed with SEM, the pattern coating is still present but the surface is not completely homogeneously coated. Big fibers, present in the suspension, covered entirely parts of the pattern and empty areas are also visible. But there are also parts that seem to shape the pattern.

Figure 2-24 represents 3D analysis of pattern n°7 coated with CNF-silsesquioxane (CNF APMS 0.5m 0.25w). The pattern without any coating (ϕ) shows that there is no absence of cylinder observable on the structure. When coated, the pattern is not well defined but still detected as viewed with the 3D structure. Measurements were done from profile lines extracted from the 3D picture. The average peak to peak length observable was measured to be 7.3 µm which is only a 5 % deviation from the original designed structure. This confirms that CNF are able to shape the pattern without covering all the structure. However, the average height peak-to-valley is only in the order of 100 nanometers, which is much lower than measured on uncoated pattern. It means that CNF are filling the gaps in between each structure leading to a failure in obtaining a perfectly defined shape. This filling issue was expected with this solvent casting strategy and other strategies like ultrasound nanospray were tested, giving encouraging results, but no further investigations were possible due to nozzle clogging. This is a second challenge which should be overcome to obtain perfectly designed surface. Dipping and Layer by Layer systems might be a solution.

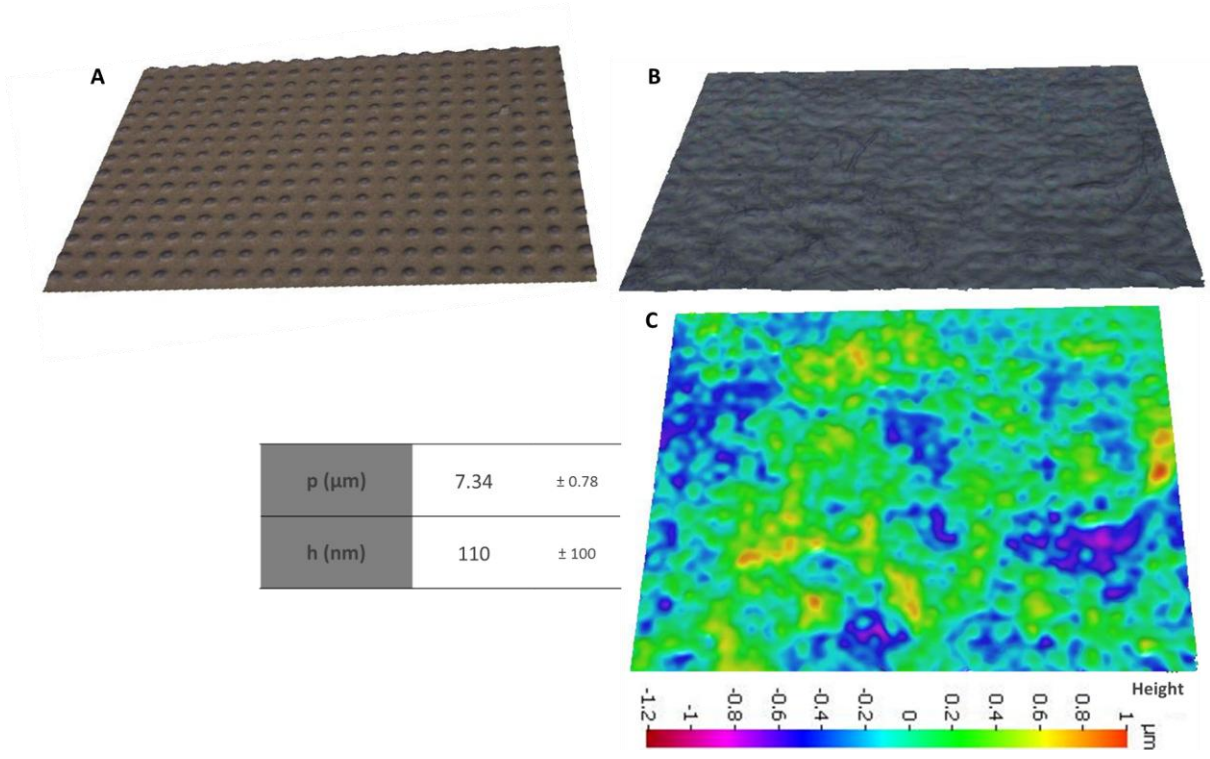


**Figure 2-24. Pattern n°5 3D image without (A) and with the coating (B) of CNF APMS 0.5m 0.25w. 3D depth color map of the coated pattern (C). Table of the measured pitch on ten measurements (p) and height in between two pics (h).**

### 3.3.3. Water contact angle

The resulting static water contact angles of coated surfaces were measured (Figure 2-25): P0 pattern (smooth silicone) shows that modification toward hydrophobicity of CNF is unsuccessful (<90°) for CNF APMS 0.1 and CNF 0.5m 0.25w $^{c*}$. It is contradicting results of the previous sub-chapter obtained with the 40 g/m² nanopaper. It could be explained by an insufficient silsesquioxane layer at the surface of the coating leading to an open question on how the silsesquioxane get arranged in the nanopaper *vs* the silicone. Thus, the different water contact angle those are all higher in the case of a roughened surface than with the smooth surface for CNF APMS 0.1, can be discussed. Indeed, a possible composite effect between CNF coating and silicone as the coating can be non uniform (see Figure 2-23) could result in such increase. Indeed, according to Wenzel theory, a roughened hydrophilic surface should be more hydrophilic which is not the case. With the CNF APMS and silsesquioxane, all samples depict inferior results except P6 pattern.

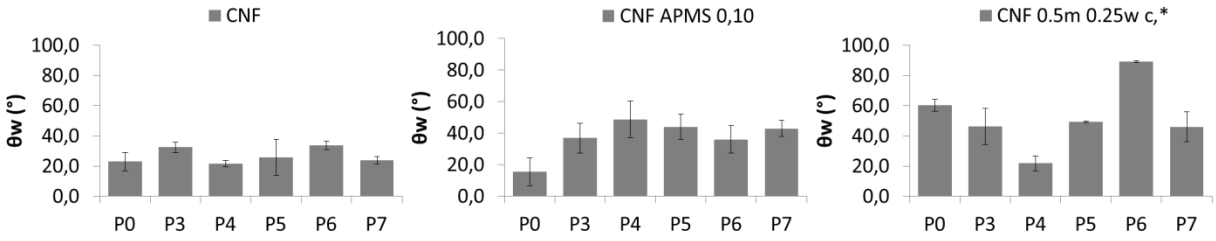


**Figure 2-25. Static water contact angle on coated designed patterns with CNF, CNF APMS 0.1 and CNF 0.5m 0.25w $^{c*}$**

More attempts to obtain designed patterned of hydrophobic CNF should be tested. Indeed, such a fundamental analysis will be beneficial for application requirements.

## 3.4. Conclusion and perspectives

The purpose of this study was to roughen cellulose nanofibrils thin films by casting on a structured surface in order to analyze the possibility to modify their wetting state by this method. The surface structuration was obtained by soft lithography. Replicates of the master structures were done with PDMS. Designed structures had diameter between 1 and 5 µm and spacing between them were defined with Patankar's recommendations. Unfortunately, replicates manufactured did not reach the designed height of 5 µm and the resulting static water contact angles did not get to the superhydrophobic state. CNF still proved to be able to shape such structure. However it seems to fill gaps more than coat the structure.

This study is a starting in the comprehension of the phenomenon. The main problem to overcome is the replicating process to reach at least a 3 to 5 µm height. Further perspectives could also to be the use of CNF with higher hydrophobicity but also the use of surface primer to enhance the adhesion of the CNF onto the structure so that a higher definition of the roughness would be reached.

## References


Aulin, C., Gällstedt, M., Lindström, T., 2010. Oxygen and oil barrier properties of microfibrillated cellulose films and coatings. Cellulose 17, 559–574. doi:10.1007/s10570-009-9393-y

Bardet, R., Belgacem, M.N., Bras, J., 2013. Different strategies for obtaining high opacity films of MFC with TiO2 pigments. Cellulose 20, 3025–3037. doi:10.1007/s10570-013-0025-1

Barthlott, W., Neinhuis, C., 1997. Purity of the sacred lotus, or escape from contamination in biological surfaces. Planta 202, 1–8.

Bhushan, B., Jung, Y.C., 2011. Natural and biomimetic artificial surfaces for superhydrophobicity, self-cleaning, low adhesion, and drag reduction. Prog. Mater. Sci. 56, 1–108. doi:10.1016/j.pmatsci.2010.04.003

Cassie, A.B.D., Baxter, S., 1944. Wettability of porous surfaces. Trans. Faraday Soc. 40, 546–551. doi:10.1039/TF9444000546

He, Y., Jiang, C., Yin, H., Chen, J., Yuan, W., 2011. Superhydrophobic silicon surfaces with micro–nano hierarchical structures via deep reactive ion etching and galvanic etching. J. Colloid Interface Sci. 364, 219–229. doi:10.1016/j.jcis.2011.07.030

Huang, J., Lyu, S., Fu, F., Chang, H., Wang, S., 2016. Preparation of superhydrophobic coating with excellent abrasion resistance and durability using nanofibrillated cellulose. RSC Adv. 6, 106194–106200. doi:10.1039/C6RA23447J

Jorfi, M., Foster, E.J., 2015. Recent advances in nanocellulose for biomedical applications. J. Appl. Polym. Sci. 132, n/a-n/a. doi:10.1002/app.41719

Lafuma, A., Quéré, D., 2003. Superhydrophobic states. Nat. Mater. 2, 457–460. doi:10.1038/nmat924

Liu, B., He, Y., Fan, Y., Wang, X., 2006. Fabricating Super-Hydrophobic Lotus-Leaf-Like Surfaces through Soft-Lithographic Imprinting. Macromol. Rapid Commun. 27, 1859–1864. doi:10.1002/marc.200600492

Mäkelä, T., Kainlauri, M., Willberg-Keyriläinen, P., Tammelin, T., Forsström, U., 2016. Fabrication of micropillars on nanocellulose films using a roll-to-roll nanoimprinting method. Microelectron. Eng. 163, 1–6. doi:10.1016/j.mee.2016.05.023

Österberg, M., Vartiainen, J., Lucenius, J., Hippi, U., Seppälä, J., Serimaa, R., Laine, J., 2013. A Fast Method to Produce Strong NFC Films as a Platform for Barrier and Functional Materials. ACS Appl. Mater. Interfaces 5, 4640–4647. doi:10.1021/am401046x

Patankar., 2003. On the Modeling of Hydrophobic Contact Angles on Rough Surfaces. Langmuir 19, 1249–1253. doi:10.1021/la026612+

Siró, I., Plackett, D., 2010. Microfibrillated cellulose and new nanocomposite materials: a review. Cellulose 17, 459–494. doi:10.1007/s10570-010-9405-y

Wenzel, R.N., 1936. Resistance of solid surfaces to wetting by water. Ind. Eng. Chem. 28, 988–994. doi:10.1021/ie50320a024

Zhu, L., Xiu, Y., Xu, J., Tamirisa, P.A., Hess, D.W., Wong, C.-P., 2005. Superhydrophobicity on Two-Tier Rough Surfaces Fabricated by Controlled Growth of Aligned Carbon Nanotube Arrays Coated with Fluorocarbon. Langmuir 21, 11208–11212. doi:10.1021/la051410+

# Conclusion

The present **Chapter 2** is providing new insight of cellulose nanofibrils modification with organoalkoxysilanes regarding modification strategy and control.

**Chapter 2.1**, is giving a comparison on the use of three different organoalkoxysilanes. The propyl chain modification was proved to change completely their hydrolysis kinetics in water but also the resulting properties of CNF nanopaper. Thus, 3-aminopropylsilane was proposed as an interesting chemical to impart good hydrophobicity but also improved oxygen barrier property.

**Chapter 2.2.1**, showed the potential of the cross-condensation of the 3-aminoproyltrimethoxysilane with either trimethoxypropylsilane of trifluoropropyl trimethoxysilane. It was demonstrated that spherical hydrophobic particles can be created with a simple and fast method in water. Initial concentration as well as molar ratio of the two silanes was proved to be the key parameters in the synthesis control.

In **Chapter 2.2.2**, the knowledge of previous study was applied to the synthesis of these silsesquioxane particles inside the CNF network. It was showed that the presence of CNF was decreasing drastically particles size. Also, very few amount of total silane is permitting very good hydrophobic properties. It is a fast and simple method that is completely applicable to an industrial context. The aminosilane, above 12 wt% in the film, was also proved to impart antimicrobial activity.

Lastly, in **Chapter 2.3**, the micro-patterning cellulose nanofibrils thin film was attempted in order to induce superhydrophobic property to the already hydrophobic CNF. Soft lithography was used to obtain the masters, but the expected properties of the designed material were not achieved. No conclusion is then possible but it was shown that CNF could shape to a certain extent a pattern.

Results obtained from this Chapter are hoped to be applied in papermaking coating. The good hydrophobic, antibacterial and barrier properties obtained with nanopapers could then possibly be reproduced at the surface of a light and flexible paper.

# Chapter 3
# From nanopaper to paper functionalization

# Table of content

**Introduction** ..... **191**

**1. Paper functionalization with organotrialkoxysilane and organotrialkoxysilanes modified cellulose nanofibers coating suspension** ..... **193**

1.1. Introduction ..... 193

1.2. Experimental section ..... 195

1.2.1. Materials ..... 195

1.2.2. Methods ..... 195

1.3. Results and discussions ..... 198

1.3.1. Coating with cellulose nanofibril-organoalkoxysilane suspension ..... 198

1.3.2. Evaluation of organotrialkoxysilanes coating with cellulose nanofibrils ..... 200

1.4. Conclusion and perspectives ..... 205

References ..... 206

**2. One step coating for obtaining superhydrophobic surface using cellulose nanofibrils** ..... **207**

Abstract ..... 207

2.1. Introduction ..... 207

2.2. Experimental section ..... 210

2.2.1. Materials ..... 210

2.2.2. Methods ..... 210

2.3. Results and discussions ..... 213

2.3.1. CNF characterization ..... 213

2.3.2. Influence of solids content and pigment ratio on coating formula ..... 213

2.3.3. Surface wetting characterization ..... 215

2.3.4. Surface organization and roughness ..... 217

2.4. Conclusions and perspectives ..... 220

Acknowledgement ..... 220

References ..... 221

**3. .....From CNF-silsesquioxane paper coating to their use as binder in superhydrophobic suspension for a coating pilot trial** ..... **225**

3.1. Introduction ..... 225
3.2. Materials and methods ..... 227
3.2.1. Materials ..... 227
3.2.2. Methods ..... 227
3.3. Results and discussions ..... 231
3.3.1. CNF-silsesquioxane coating at laboratory scale ..... 231
3.3.2. Toward CNF-silsesquioxane use as binder in superhydrophobic formulation in pilot scale ..... 234
Conclusion and perspectives ..... 238
References ..... 239

# Chapter 3. From nanopaper to paper functionalization

## Introduction

This **Chapter 3** aims at introducing results obtained from **Chapter 2** with model CNF nanopaper in papermaking coating applications. In the industrial context of this PhD, the main purpose was to develop a paper surface with antimicrobial activity, superhydrophobic character, and anti-adherence or grease barrier properties.

In **Chapter 1**, it was noticed that CNF could act as potential barrier against grease after coating onto a paper based surface. Further modification of the CNF with organoalkoxysilanes was thought to probably improve such properties. It is the main objective of **Chapter 3.1** to assess such potentiality with 3-aminopropyltrimethoxysilane. The high potential of this molecule reaction with nanocelluloses was highlighted in **Chapter 2.1**. The anti-adhesive properties are also assessed in this part as well as antibacterial activity.

The **Chapter 3.2** is evaluating the potential of hydrophobic CNF as binder for a superhydrophobic coating. As CNF by itself were not successfully textured in Chapter 2.3, the use of CNF to replace a synthetic latex binder to coat mineral hydrophobic particles with the objective to develop a more sustainable superhydrophobic paper is assessed. Formulation parameters are investigated.

Lastly, **Chapter 3.3** is evaluating CNF-silsesquioxane coating onto paper for anti-adherent and hydrophobic properties. It is also used as binder for the coating of a suspension toward paper superhydrophobic functionalization. A pilot scale investigation is also provided as potential further industrial development.

# 1. Paper functionalization with organotrialkoxysilane and organotrialkoxysilane modified cellulose nanofibers coating suspension

## 1.1. Introduction

In different industrial applications from highly sophisticated to daily used materials such as label dorsal or cooking pan, the non-adherence of a material is sought. Usually made of the functionalization of a structure through coating, the two different polymers commonly used are polytetrafluoroethylene (PTFE, Teflon©) or polydimethylsiloxane (PDMS, silicon). With a surface energy around 18-23 mJ/m², they represent the most anti-adhesive materials in the world. Their stability to moderate heat and UV made them also very interesting. However, as PTFE is hard to process and expensive, the biggest part of the non-adherent polymer market is turned toward PDMS. PDMS is also expensive mainly due to the cost of production. It is formed through the cross-linking of vinylterminated dimethysiloxane and dimethyl, methylhydrogen siloxane with a platinum-based catalyst. Even tough ppm of this catalyst is used, it makes its price relative to the metal cost. But PDMS has been developed in many fields of industry due to its liquid (oil) form. Depending on the end application, PDMS can be found as oil, or an emulsion in apolar solvent but also in water. Paper industry, which is using it for label and for food contact in baking paper, utilizes mainly water-based emulsion of silicone.

The relative high cost of silicon for paper industry (around five times higher than pulp itself) forced the industry to use the lowest amount possible, which is around 0.5 to 1.5g/m² in baking paper. As a consequence, highly refined paper is produced to obtain a smooth paper to overcome losses of silicon in roughness grooves, which is a costly procedure. Other drawback of the PDMS is its non-ability to be recycled or biodegraded due to the high cohesive network formed and the high hydrophobicity of the PDMS. This makes the industry not able to recycle the improper paper in the initial production stream at high amount, due to presence of stickies in the pulp, which endanger fiber network cohesion. In the case of baking paper, the low coated amount (less than 10wt% of the overall material) make the paper still biodegradable in the standard definition, which is not the case for high coating amount used in label dorsal for example. After cross-linking reaction, silicon becomes an

inert polymer, which cannot be functionalized further for example with antibacterial activity or greaseproof function.

For this purpose, organotrialkoxysilane could be a possible versatile solution to obtain such properties along with the low adherence. Indeed, the chemical formula of condensed organoalkoxysilane is closed to PDMS with additional alkyl chain and can be used in aqueous media (Paquet, 2012), (Zhang et al., 2015) which is very important for papermaking application. For example the grafting of paper with perfluorosilane has already been carried out but no experiments were done on on other properties than wetting (Ly et al., 2010). Organotrialkoxysilanes can self-condense at room temperature during time depending on conditions of reaction (Brochier Salon and Belgacem, 2010) which could be difficult to monitor industrially. The low viscosity of such a solution, approaching water, makes it also difficult to coat it on a paper. The use of cellulose nanofibrils is expected to act as a thickening agent (Dimic-Misic et al., 2014) but also as a reactional vector permitting, through

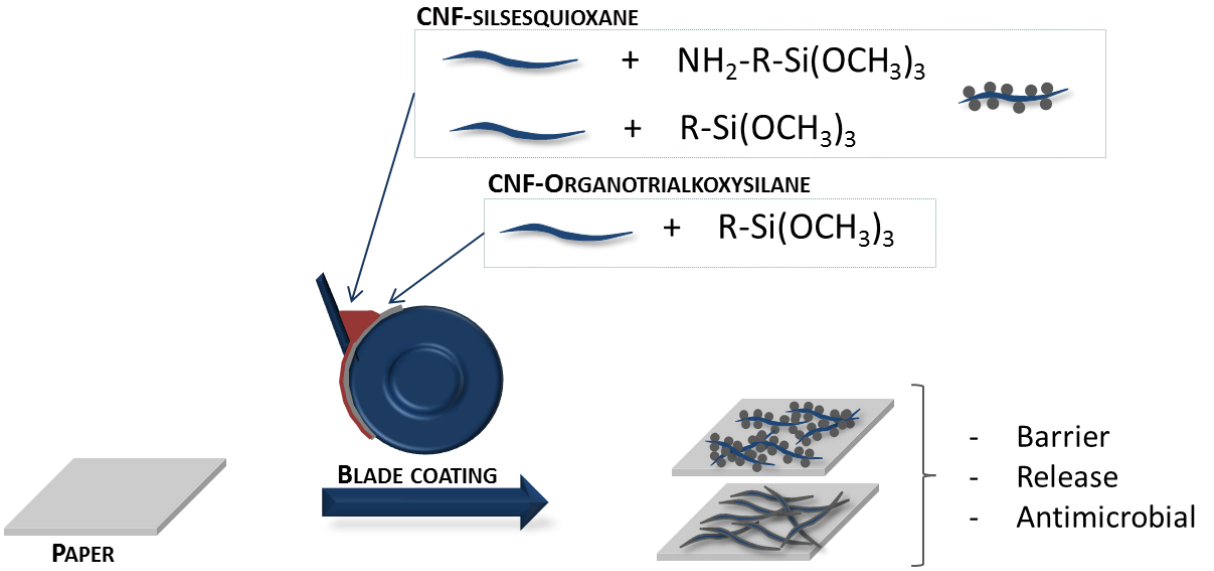


**Figure 3-1. Scheme of the overall study. Two different functionalization of CNF were coated on a paper and grease barrier, release and antimicrobial properties were assessed.**

interaction of silanol with cellulose hydroxyl groups, to stabilize a linear form of the organosilsesquioxane network rather than a complete branched structure.

In this section is proposed a study of the coating of organoalkoxysilane on paper with the help of nanocellulose. Nanocellulose is proposed as a vector of the organotrialkoxysilanes. Paper properties regarding contact angle, grease barrier, adhesion and antibacterial activity are measured.

## 1.2. Experimental section

### 1.2.1. Materials

Cellulose nanofibrils (CNF) is a "semi-commercial" grade (CTP, France) made from birch bleached kraft pulp and extracted with a mechanical and enzymatic pretreatment followed by five passings through a homogenizer (GEA, Italy). It has a dry matter content of 2,0 wt%. (3-Three organoalkoxysilanes were used for the study i.e. Aminopropyl)trimethoxy silane (APMS) (Sigma Aldrich, France), propyltrimethoxy silane (TMPS) (Sigma Aldrich, France) and (3,3,3-trifluoropropyl) trimethoxy silane (TFPS) (Gelest, France). Ethanol (98%, Roth) and acetic acid (96%, Sigma Aldrich) were used as hydrolysis medium of alkoxysilanes. Distilled water was used all along these experiments.

Paper was provided by Papeterie du Léman and it was a highly refined paper of 40 g/m². The paper produced for silicone baking paper is not coated for the purpose of the study.

### 1.2.2. Methods

*Coating suspensions* were prepared by hydrolyzing the organoalkoxysilane directly in the CNF suspension at various pH and times. APMS was coated at normal pH while TMPS and TFPS at pH 4 if not precised. Silanes were added drop by drop in the CNF suspension while mixing with magnetic stirring.

For CNF-silsequioxane suspension, half of the CNF was blended with the APMS while the other part was added to TMPS, for 10min. CNF-APMS and CNF-TMPS were then mixed together for at least 2h. The suspension was used as such.

*Coating* was achieved with a laboratory scale blade coater (Euclid Coating System, Inc) with a 2 bar pressure applied on it and a constant speed. Papers were taped to the coating cylinder before coating and were then dried directly on the cylinder with an air dryer to avoid wrinkles and further dried on a contact cylinder drier under tension at 105° for 3 min. To obtain the desired grammage, the operation was repeated three times onto each paper.

*SEM-EDX*

Scanning electron microscopy with an energy-dispersive X-ray spectroscopy module (SEM-EDX) (LEO Stéréoscan 440, detector Si(Li) EDAX-10mm²) at a 15 KeV tension was performed on cross-sections of the coated paper films to observe the coating thickness and penetration inside the material.

*Contact angle* with water were obtained with the sessile drop method and were recorded and analyzed with the contact angle meter (OCA20, DataPhysics Instruments GmbH) with SCA20 software. A 5µL distilled water droplet was used for the analysis and the experiment was performed at room temperature. All results are an average of at least three measurements.

*Grease barrier test* was done with the TAPPI T-507 method. A piece of blotting paper of 6.1*6.1 cm² was impregnated with commercial sunflower oil colored with Sudan III red dye. The blotting paper was placed onto the coated surface of the sample previously cut in 8*8 cm² square. A fresh blotting paper of 8*8 cm² was placed under the sample to replicate the penetrated oil. A weight of 365 g was deposited on it. The sandwich was then placed in an oven at 60°C for 4h. Oil spots area were measured by image analysis after image scanning, color thresholding, area selection and measurement using the ImageJ software.

Grease permeability was also assessed with ISO 16532-2 method. It consists in the deposition of a droplet from "KIT" solution N°X on the sample surface. KIT number depends on the proportion of toluene, n-heptane and ricin oil. Resulting oil solutions of variable viscosity and surface tension are obtain, giving an "aggressiveness" scale from 1 to 12, 12 being the most "aggressive" oil. After 15s the excess of oil is wiped with an absorbent paper. The penetration of the oil in the paper is assessed right away. If the oil did not penetrate the paper, which can be assessed by the transparency induced by the oil penetration in the material, the operation is repeated with an oil number superior to the previous one until there is a penetration. The last KIT number proving oil resistance is the KIT value. Average on three measurements is presented in this manuscript.

*Practical adhesion* of the coating was measured with peeling test. It was assessed with a modified FINAT FTM 1 test method at 180° at a speed of 300 mm/min with a standardized adhesive 7475 from 3M Company. Tape was placed onto the surface of the coated paper and pressed three times with a 2 kg roll. The peel off force of the adhesive from the paper was measured and the obtained values are presented as the average of 10 measurements.

An industrial method was also tried to evaluate the ability of the paper to release a pastry cooked on it (Bretzel). The frozen bretzel pastry was dipped in a solution of sodium bicarbonate and placed on the paper. It was then cooked in an oven at 215°C for 20 min. The ability to release the pastry was evaluated on a 0 to 5 arbitrary scale, where 0 is assigned to

the samples when the paper sticks to the bretzel and 5 is attributed when no force is needed to separate one from the other.

*Antibacterial activity* was assessed with *B.Subtilis* according to standard AFNOR EN 1104. A piece of the paper sample to be tested was placed on a *B.Subtilis* inoculated agar (coated surface in contact). Produced petri plates were incubated for 3 days at 37°C and leaching ability was evaluated by the absence or presence of an inhibition zone and antibacterial activity by the presence or not of bacteria under the sample. Experiments were repeated three times.

A quantitative assessment was performed according to AATCC Test Method 100-1998 with *B.Subtilis*. Samples surface were inoculated with 200µL of a $10^5$ CFU/mL inoculum and incubated 24h at 37°C. Bacterias were then extracted by using 50mL of the neutralizing solution (L-lecithin 3 g/L, sodium thiosulphate 5 g/L, L-Histidine 1 g/L,Tween 80 30 g/L, Buffer solution ($KH_2PO_4$ 0.68 g/L) 10 mL/L, (pH at 7.2 ± 0.2)). Resulting bacterial solutions were plated in order to determine the colony forming unit (CFU) number.

## 1.3. Results and discussions

**Table 3-1. Summary of the sample coated with poly-organotrialkoxysilane and CNF.**

| | Coating suspension composition | | | | Basis weight (g/m²) | | | Grease permeability | | | Peeling force (N) | Static water contact angle (°) |
|---|---|---|---|---|---|---|---|---|---|---|---|---|
| | Silane | CNF | Ratio Silane/CNF | DM (%) | Silane | CNF | Total | T 507 (cm²) | KIT (n°) | Turpentine (min) | | |
| Base paper | – | – | – | – | – | – | – | 43 ± 3 | 0 | 0.25 | 1124 ± 24 | 117 ± 2 |
| Primabake | – | – | – | – | – | – | – | 1 ± 0.4 | 0 | – | 9 ± 1 | 116 ± 2 |
| Coated base paper | × | ✓ | 0/100 | 2.0 | 0 | 2.6 | 2.6 | 31 ± 0.4 | – | – | – | 42 ± 2 |
| | APMS | × | 100/0 | 10 | 8.2 | 0 | 8.2 | 0.6 ± 0.4 | 0 | 29 | 904 ± 97 | 110 ± 2 |
| | APMS | × | 100/0 | 10 | 3.2 | 0 | 3.2 | 0.2 ± 0.2 | – | – | 1160 ± 75 | 98 ± 2 |
| | APMS | ✓ | 85/15 | 13.3 | 2.9 | 0.5 | 3.4 | 26 ± 5 | – | 0.25 | – | 110 ± 2 |
| | APMS | ✓ | 50/50 | 4.0 | 0.9 | 0.9 | 1.7 | 35 ± 0.4 | – | – | – | – |
| | APMS | ✓ | 15/85 | 2.4 | 0.2 | 1.0 | 1.2 | 35 ± 2 | – | – | – | 85 ± 4 |
| | TMPS | × | 100/0 | 10 | 3.5 | 0 | 3.5 | 33 ± 2 | – | – | – | 110 ± 2 |
| | TMPS | ✓ | 85/15 | 13.3 | 4.4 | 0.8 | 5.2 | 32 ± 2 | – | – | – | 98 ± 3 |
| | TMPS | ✓ | 85/15 | 13.3 | 3.1 | 0.5 | 3.6 | 37 ± 1 | – | – | – | 103 ± 3 |
| | TMPS | ✓ | 85/15 | 13.3 | 2.0 | 0.4 | 2.4 | 33 ± 2 | – | – | – | 98 ± 2 |
| | TMPS | ✓ | 50/50 | 4.0 | 0.5 | 0.5 | 1 | 34 ± 3 | – | – | – | – |
| | TFPS | ✓ | 15/85 | 2.4 | 0.2 | 1.4 | 1.6 | 42 ± 2 | – | – | – | 55 ± 4 |
| | TFPS | ✓ | 15/85 | 2.4 | 0.5 | 3.1 | 3.6 | – | 0 | – | – | 90 ± 5 |

### 1.3.1. Coating with cellulose nanofibril-organoalkoxysilane suspension

*Evaluation of organotrialkoxysilane coating without cellulose nanofibrils*

The ability to create a coated film on paper from pure organoalkoxysilanes (TMPS, TFPS or APMS) was first assessed by its hydrolyzis in water for 2h and then blade coating of the resulting suspension onto the paper surface. The ability of APMS to condense easily in polysiloxane, showed previously by $^{29}$Si NMR is here confirmed (Reverdy et al., 2016). Indeed, from SEM-EDX analysis (Figure 3-2), it is evidenced that APMS is a film forming silane while TMPS is not. With the amine, APMS is not reacting the same way and is not or barely penetrating the material as it was established previously with cellulose nanofiber film (Reverdy et al., 2016). A strong interaction between cellulose and the amine is potentially one of the causes of such a surface coating.

APMS could be seen as a great barrier material by itself with such a dense film on paper. To the best of our knowledge, this has never been proposed in literature. Grease permeability measured with the T-507 method, meaning with sunflower oil, 100% APMS with relative low coating grammage give excellent results, as no grease passed through it (Figure 3-4).The KIT

test on the paper was 0, meaning that even for a pure APMS coating, it is not resistant to aggressive oil.

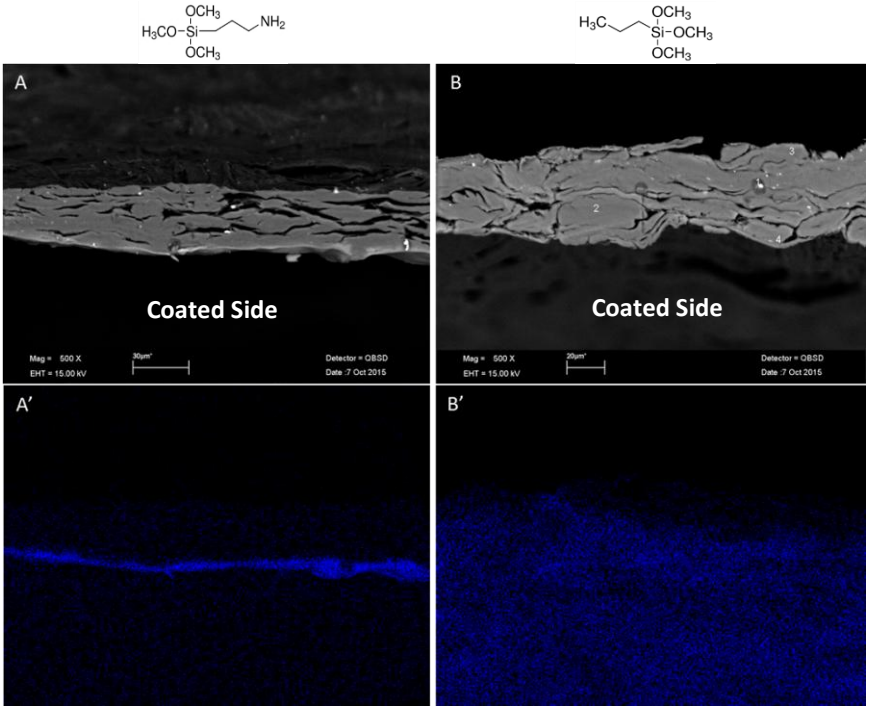


**Figure 3-2. Paper coated with 100% organotrialkoxysilane solutions hydrolyzed for 2h. SEM pictures of APMS coating (A) and SEM-EDX with Si mapping (A') and TMPS (B) and (B').**

Cellulose nanofibrils inclusion in the coating suspension is thought to provide higher resistance toward oil by closing better the system to avoid oil penetration.

The same coating, with two different grammages, was tested for peeling force and compared to an industrial silicon paper, as well as, to the original paper itself (Figure 3-3). The force to detach the standardized tape from paper is considerably higher than that for industrial baking paper made with the same raw paper. APMS coating is reducing slightly the necessary force, from 6 to 20% for 3.2 to 8.2 g/m² respectively. The difference induced by higher coating amount can be explained by a combined effect of smoothing effect of irregularities and total coverage of fibers.

The addition of CNF inside the suspension could help in the smoothing effect by helping in coating coverage but also limits silane penetration, as observed with SEM-EDX (Figure 3-2).

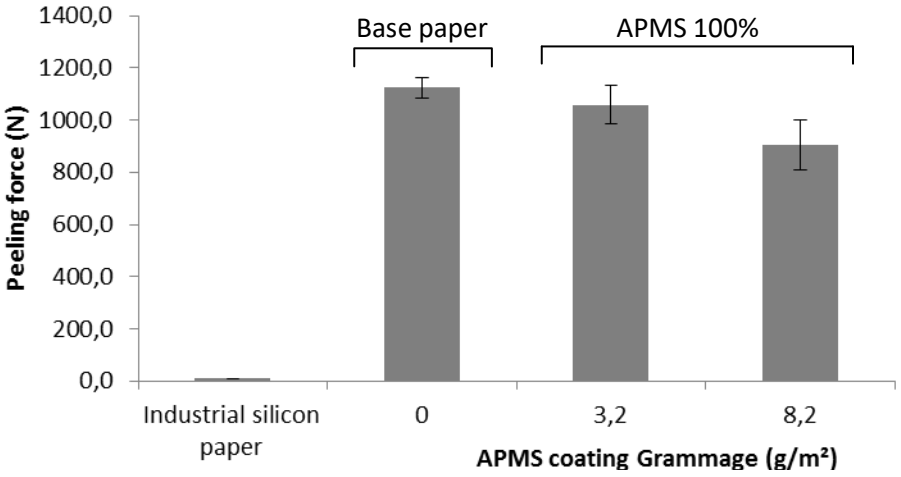


**Figure 3-3. Peeling test at 180° results on coated and uncoated paper surface.**

### 1.3.2. Evaluation of organotrialkoxysilane coatings with cellulose nanofibrils

Cellulose nanofibrils were added with various amounts inside the coating suspension in order to measure the effect of the inclusion on grease barrier. Indeed, it has been proved by (Lavoine et al., 2014) that a coating of about 6 g/m² of CNF onto paper helps decreasing grease penetration. Figure 3-4 is depicts the stained area of the blotting paper placed below the sample depending on coating grammage and APMS percentage in the suspension as dry matter. While no APMS, at 0%, the coating is only done with CNF, and when 100% the coating layer is only made of APMS. Unfortunately, due to variation in viscosity of coating formulation, it was not possible to coat similar amount (basis weight) (Table 3-1). The base paper itself is depicting a stained area value of 42.5 ± 2.6 cm² (meaning that the entire surface was covered with grease). A 2.6g/m² of unmodified CNF coating decreases the stained area by almost 30%, which is the consequence of the closing of the paper porosity. While CNF is included with APMS, a loss in barrier properties is observed when compared to a 100% APMS layer. But this might be only due to the lower basis weight coated. Indeed (Aulin et al., 2010) proves that there is a limit low value to obtain air barrier with coated paper. However, the inclusion of CNF and APMS together give comparable barrier properties toward sunflower oil than for a pure CNF coating. What could explain the difference between the addition of 15 w% of CNF and 0 wt% of CNF (i.e 100 % silane) is the creation of a web disrupting the APMS dense layer by creating a preferential pathway for the oil.

These first results prove that quantity of silane is key. The higher is the better. Meanwhile a minimum amount of coating is necessary to obtain barrier. To confirm this, different basis weight were tested with the highest amount of silane (Figure 3-4).

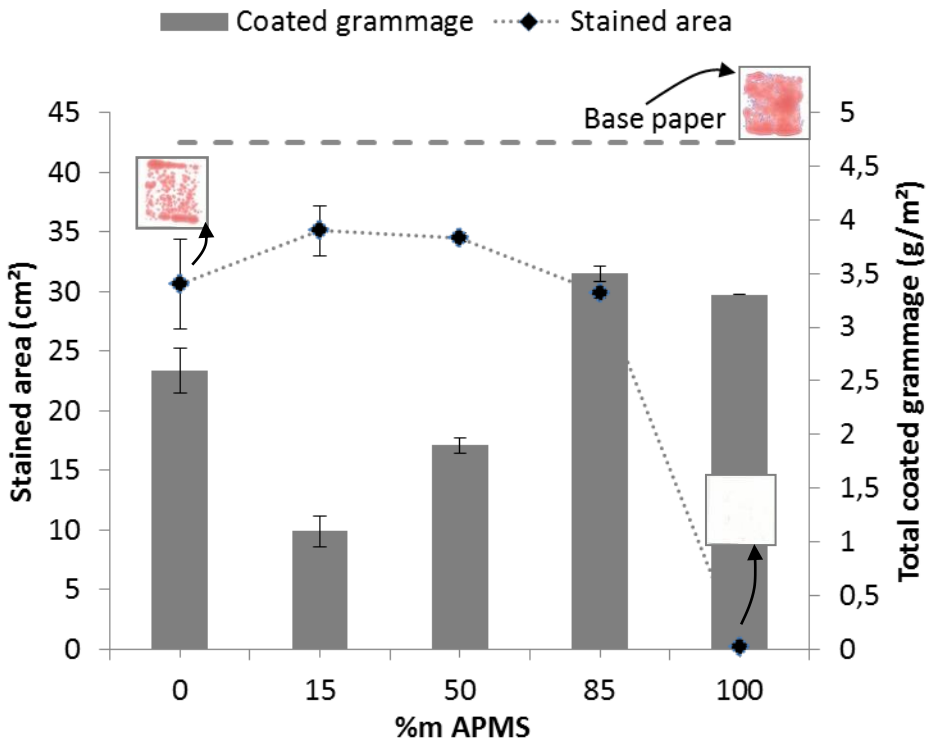


**Figure 3-4. Effect of APMS quantity on grease barrier properties**

*Effect of grammage coating and hydrolysis time at fix CNF/APMS ratio*

For low inclusion of CNF (15%) the barrier to grease was measured for different grammage of coating. While the effect of coating grammage of suspension made with TMPS is relatively low (Figure 3-5B), leading to poor grease barrier paper, even for more than 5 g/m² layer, the coating with APMS become completely barrier to grease for layer around 6 g/m² (Figure 3-5C). The film forming property of APMS is again showed, while TMPS might not react the same way. Trials with TFPS, hydrolyzed in ethanol/water medium, acetic acid and CNF depicted the same trend than TMPS, even though it has fluorine atoms, which would be expected to bring greaseproof protection. The main difference between TMPS, TFPS and APMS is clearly the film forming effect, not present in the hydrophobic organoalkoxysilane form, i.e. TMPS and TFPS.

Figure 3-5, shows results for TMPS at three different hydrolysis times 0, 6 and 12 hours. TMPS was hydrolyzed with acetic acid following previous conditions determined in water

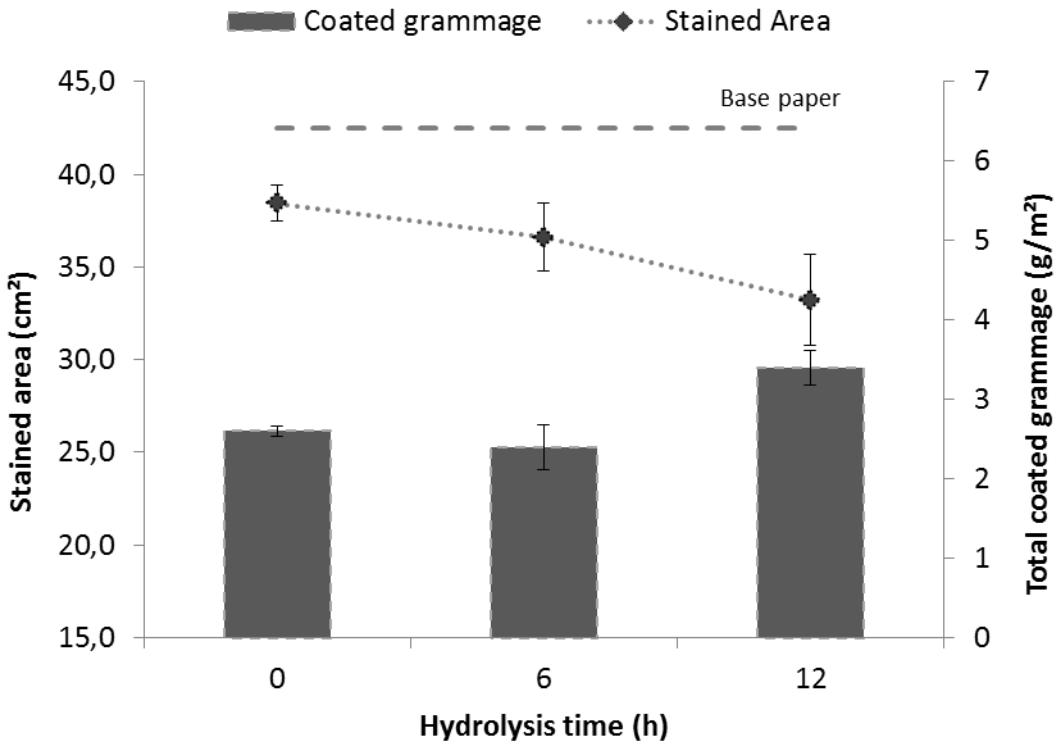


**Figure 3-5. Impact of hydrolysis time on grease barrier properties at same CNF content (15wt%) for TMPS.**

(Chapter 2). Even though TMPS in water is showing evolution during time with different percentage in T0, T1 and T3 structures, the impact on the coating properties is negligible, as observed by the stagnation in oil quantity transpiercing the material for close coating grammage (Figure 3-5). This result could be assigned to the heat treatment exerted on the coated paper. Indeed, it is proved that heat is favoring organotrisilanol condensation. As TMPS hydrolyzes completely and almost immediately in aqueous acidic medium, and start to condense, the heat treatment, which is curing the system is accelerating this state and does not depend on the initial structure composition of the suspension. The same was observed for APMS hydrolyzed with CNF for 15 min and 2 hours, as shown in (Figure 3-5C), no difference in the final properties are observed.

Similarly to peeling, an industrial test was tried on these coatings. The method consists in cooking a bretzel on the paper surface and peels it off to assess the ability to act as a baking release paper. As well, for peeling test with 100% APMS, no improvement was observed, compared to the base paper.

It was noticed that after a period of time (weeks), the paper coated with APMS started to yellow. This is probably due to the reaction of amine with carbonyl groups present on cellulose in low quantity, forming Schiff base, and reported by some studies (De la Orden and Urreaga, 2006), (Urreaga and de la Orden, 2006). This could be a drawback for the industry.

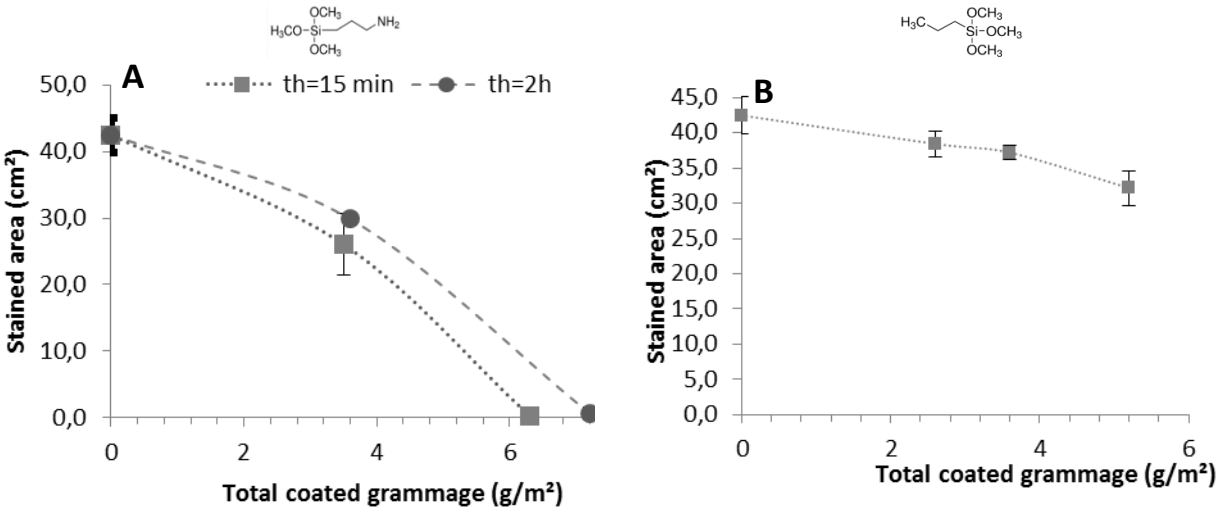


**Figure 3-6. Impact of hydrolysis and coating grammage on grease barrier properties at same CNF content (15 wt%) for APMS (A). Effetc of grammage only at same hydrolysis time (15 min) for TMPS (B).**

### Coating of APMS based suspension and effect on antimicrobial properties

Polymer constructed with primary to tertiary amine, are known to kill bacteria by interacting with the outer cell membrane, leading to increase permeability of the latter and the death of the bacteria. APMS was already proved to have a bactericidal effect even when grafted with nanocellulose (Saini et al., 2016). Papers coated with different amount of APMS/CNF up to 3.2 g/m² of the APMS/CNF at a ratio of 85%, leading to a coat of 2.7g/m² pure APMS were

| Coated APMS (g/m²) | Bactericidal (B.Subtilis) |
|---|---|
| 0 | × |
| 0.4 | × |
| 1.4 | × |
| 2.7 | ✓ |

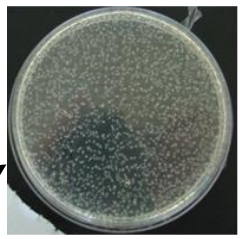

Base paper

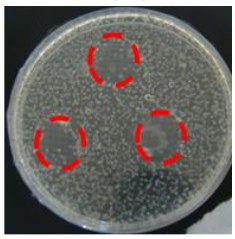

Coated paper APMS 85%; 3,2 g/m²

**Figure 3-7. Contact testing on B.Subtilis. Reference paper and coated paper are presented.**

submitted to a first qualitative antibacterial test against the gram positive *Bacillus Subtilis* bacteria. The amine presents in the APMS was revealed to be in sufficient amount at the surface, while 2.7 g/m² is coated to obtain the desired property, as shown by the three inhibition zones where no bacteria growth is observed under the sample (Figure 3-7).

A quantitative test (Figure 3-8) was also done on *B.Subtilis* on the last sample and complete killing of the bacteria on the surface was observed while a growth is observed on the traditional paper.

No leaching tests were carried out with this sample, which could be interesting. No inhibition zone was observed with the first test but the question can be argued, if APMS is or not leaching into the medium. The leaching is probable as few short oligomers might not have linked with the overall silsesquioxane layer, as it was shown with the soxhlet extraction of reference CNF APMS film in the Chapter 2.

Based on these results it is possible to obtain good grease barrier and antimicrobial paper by coating about 6 g/m² of a coating of APMS and CNF. To the best of our knowledge this is the first time CNF plays the work of rheological modifier and skeleton structures. However, release and antiadherent properties are not achieved.

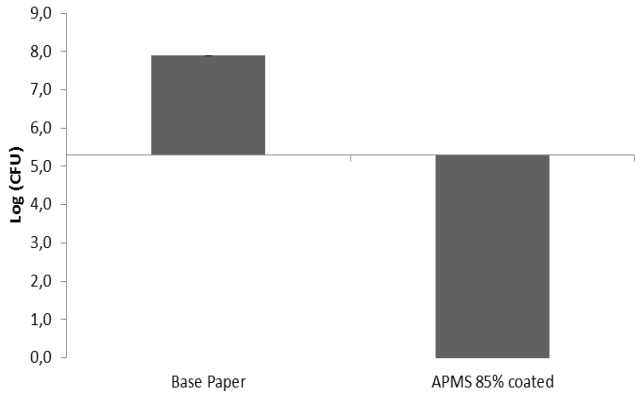


**Figure 3-8. Quantitative assessment on B.Subtilis with a coating of 3.2 g/m² and 85% of APMS**

## 1.4. Conclusion and perspectives

In this section, the ability to functionalize an industrial paper with suspension of CNF and silane or silsesquioxane was assessed. CNF were used as a bio-template for vectoring silane and polysilsesquioxane network but also, in the case of silsesquioxane particles synthesis, to constraint the particles formation to nanometric size.

The particular behavior of APMS toward cellulose was again pointed here by the formation of a silsesquioxane film on the surface of paper, even without CNF. The ability of APMS network to close the paper toward grease penetration was proved for a coating grammage around 3 g/m². However, the inclusion of CNF in the network, rather than improving this property is lowering it. Also, even though silsesquioxane network could be structurally considered as close to silicon, no important decrease in surface energy was achieved.

Same observations were done with functional coating of silsesquioxane particles in CNF network. Although hydrophobicity of the coating was reached, no further functionalization could efficiently be demonstrated. Due to low coating amount (around 2 g/m²), no antibacterial effect was measured which is different from results obtain through 40 g/m² film formation. As showed by antibacterial activity of pure APMS at 3 g/m², it indicates that high APMS amount is needed on the paper surface, which was not possibly attainable on the thin industrial paper used in this work and coating laboratory equipment limit.

## References


Aulin, C., Gällstedt, M., Lindström, T., 2010. Oxygen and oil barrier properties of microfibrillated cellulose films and coatings. Cellulose 17, 559–574. doi:10.1007/s10570-009-9393-y

Brochier Salon, M.-C., Belgacem, M.N., 2010. Competition between hydrolysis and condensation reactions of trialkoxysilanes, as a function of the amount of water and the nature of the organic group. Colloids Surf. Physicochem. Eng. Asp. 366, 147–154. doi:10.1016/j.colsurfa.2010.06.002

De la Orden, M.U., Martínez Urreaga, J., 2006. Photooxidation of cellulose treated with amino compounds. Polym. Degrad. Stab. 91, 2053–2060. doi:10.1016/j.polymdegradstab.2006.01.013

Dimic-Misic, K., Ridgway, C., Maloney, T., Paltakari, J., Gane, P., 2014. Influence on Pore Structure of Micro/Nanofibrillar Cellulose in Pigmented Coating Formulations. Transp. Porous Media 103, 155–179. doi:10.1007/s11242-014-0293-8

Lavoine, N., Desloges, I., Khelifi, B., Bras, J., 2014. Impact of different coating processes of microfibrillated cellulose on the mechanical and barrier properties of paper. J. Mater. Sci. 49, 2879–2893. doi:10.1007/s10853-013-7995-0

Ly, B., Belgacem, M.N., Bras, J., Brochier Salon, M.C., 2010. Grafting of cellulose by fluorine-bearing silane coupling agents. Mater. Sci. Eng. C 30, 343–347. doi:10.1016/j.msec.2009.11.009

Paquet, O., 2012. Cellulose surface modification with organosilanes, Ph.D manuscript, Université de Grenoble.

Reverdy Charlène, 2016. Cellulose nanofibrils aqueous modification with different alkoxysilanes: influence of amino presence on surface mechanisms and properties, TAPPI Nano international conference, Grenoble, France.

Saini, S., Belgacem, M.N., Salon, M.-C.B., Bras, J., 2016. Non leaching biomimetic antimicrobial surfaces via surface functionalisation of cellulose nanofibers with aminosilane. Cellulose 23, 795–810. doi:10.1007/s10570-015-0854-1

Urreaga, J.M., de la Orden, M.U., 2006. Chemical interactions and yellowing in chitosan-treated cellulose. Eur. Polym. J. 42, 2606–2616. doi:10.1016/j.eurpolymj.2006.05.002

Zhang, Z., Tingaut, P., Rentsch, D., Zimmermann, T., Sèbe, G., 2015. Controlled Silylation of Nanofibrillated Cellulose in Water: Reinforcement of a Model Polydimethylsiloxane Network. ChemSusChem 8, 2681–2690. doi:10.1002/cssc.201500525

# 2. One step coating for obtaining superhydrophobic surface using cellulose nanofibrils

*This section is adapted from Reverdy C., Belgacem N., Moghaddam M.S., Sundin M.., Swerin A., Bras J.. «One step coating for obtaining superhydrophobic surface using cellulose nanofibrils», submitted to Colloids and Surface Part A (2017).*


## Abstract

The development of superhydrophobic surfaces has emerged in last decades because of high potential for self-cleaning or anti-fouling objects. In this work is proposed a one-step approach using a suspension of hydrophobized precipitated calcium carbonate and biobased cellulose nanofibrils as a binder to fix and distribute the particles. The suspension is coated on a paperboard and wetting behavior of the surface is assessed. Static, advancing and receding contact angle with water as well as roll-off and water shedding angle are measured and compared to a coating made with styrene butadiene latex as binder instead of cellulose nanofibrils. Modified CNFs with alkyl ketene dimer show promising results for the fast manufacturing of superhydrophobic paperboard. Indeed, an improved static water contact angle of 150° was reached. In addition, the use of CNFs enable the improvement of coating quality avoiding the crackling effect, which makes powerful the use of nanocellulose as a renewable binder.



Keywords: superhydrophobic, cellulose nanofibrils, paperboard.


## 2.1. Introduction

Nature is inspiring scientists and engineers with ideas on how to solve technological problems. The Velcro® invention is probably the most famous one, invented by a Swiss engineer by mimicking burdock seeds “hooks-loop” attachment (Mestral, 1961). The same inspiration was taken for anti-fouling, low drag or self-cleaning surfaces which already exist on shark skins or lotus and rose leaves (Ball, 1999), (Marmur, 2004),(Feng et al., 2008). The Lotus and rose effects is now understood, owing to the hierarchically rough wax coating on their surface which give the superhydrophobic character. End use applications are for example self-cleaning windows, walls, textiles or ships (Nosonovsky and Bhushan, 2009).

Mimicking nature is not an easy task and many solutions to produce superhydrophobic surfaces are based on a two steps surface modification (Shieh et al., 2010),(Ma et al., 2005),(Li et al., 2016). First, the surface is artificially roughened and then hydrophobized with a low-surface-energy chemical. The roughening can be achieved by different methods (Xue et al., 2010), (Celia et al., 2013): nanoparticle induced structure, phase separation creating porous material, lithography, or growth of particles directly on the surface. Silanes, fluoropolymer or waxes are used to decrease the surface energy. Several publications relate to one step surface modification.

In their article Zimmermann et al. (2008) modified natural and synthetic fibers in a one-step approach by fabricating polymethylsilsesquioxane nanofilament via gas phase grafting on their surface. The physico-chemical properties of the grafted nanoscopic filaments coated on the microscopic textile fibers is preventing water-adhesion. A water based one step superhydrophobic coating was also developed by Mates et al. (2014) using nanoclay with fluoroacrylic copolymer in a spray coating method. In 2010, an economic and simple water based coating was developed by using precipitated calcium carbonate hydrophobized with fatty acids such as sodium oleate and stearate (Hu and Deng, 2010). Particles were simply sprayed on an adhesive tape. Similarly, Swerin et al. (2016) used hydrophobized calcium carbonate and developed a one-step coating with a latex binder commonly used for paperboard surfaces. Different dry solid contents were achieved, giving rise to superhydrophobic surfaces with a contact angle above 150°. However, most of the solutions have the drawback of using toxic or petrobased compounds instead of sustainable and biobased ones. In order to achieve the required roughness, recently, nanoscale wax (Lozhechnikova et al., 2017), lignin particles, and structured cellulose derivatives (Zhang et al., 2015) have been used. As binder and dispersing agent, nanocellulose is among the most promising biobased material candidate. Developed in the 1980's (Turbak et al., 1982), it is available industrially and well known in composites (Mariano et al., 2014), barrier materials (Lavoine et al., 2012), paper (Bardet, 2014), as well as in medical (Jorfi and Foster, 2015) and electronic applications (Hoeng et al., 2016).

Cellulose nanofibrils can, with their high specific area and entangled network, stabilize and disperse inorganic particles to gain for example conducting or barrier properties (Li et al., 2015), (Hamedi et al., 2014), (Sehaqui et al., 2010). Using nanofibrillated cellulose as a binder

in coating formulations to replace synthetic latex is a particular interest in industrial development. The entangled network formed by nanofibrils clearly help in dispersing minerals particles such as TiO2, reducing the required amount and thus lowering the cost of pigments used in the coating (Bras et al., 2015). As a renewable, biodegradable, light and non-toxic material, nanocellulose can decrease the carbon footprint and can be used in diverse applications such as packaging.

Arbatan et al. (2012) were the first to use cellulose nanofibrils (CNF) as a dispersant and binder for precipitated calcium carbonate (PCC) to provide superhydrophobicity onto cotton filter paper surface. The two step procedure involved the dip-coating in a CNF-PCC slurry follow by a dip-coating in an AKD solution in n-heptane. Good retention of PCC was observed and contact angles above 150° were achieved. Using nanocellulose as a binder for a one step superhydrophobic coating has so far not been tested as it needs the development of a hydrophobic nanocellulose. To develop the industrial feasibility, the hydrophobicity should preferably be made in aqueous solution in a viable process.

In this study, AKD-modified hydrophobic CNF and silane-modified CNF were used as a binder for hydrophobic calcium carbonate one step coating on a paperbased material (Figure 3-9). The obtained coated surface was characterized with wetting measurement, static and dynamic contact angles with water. Dispersion of particles was assessed by scanning eletron microscopy (SEM) and roughness by optical profilometry.

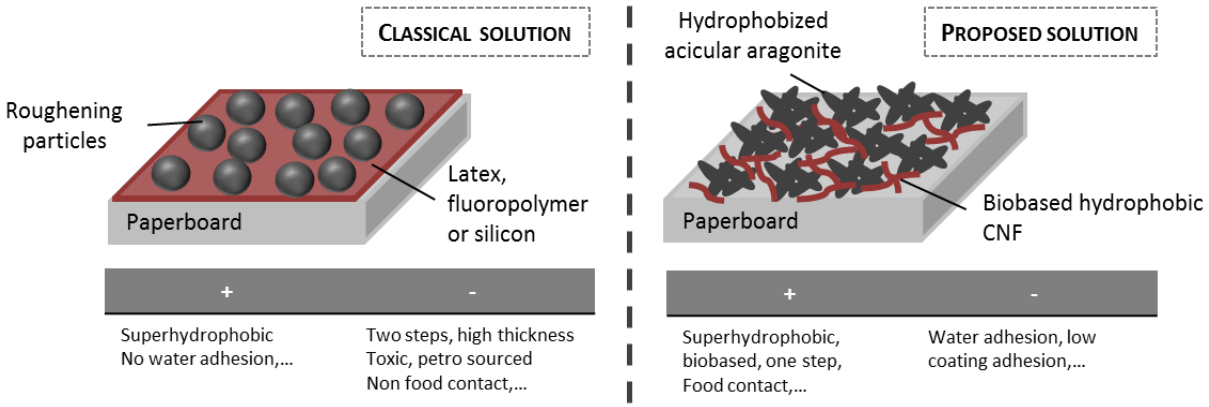


**Figure 3-9. Scheme of the project: Replacing latex by cellulose nanofibrils in a paperbased coating superhydrophobic suspension**

## 2.2. Experimental section

### 2.2.1. Materials

Acicular aragonite (Sturcal H) was provided by Minerals Technologies. Styrene butadiene latex (DL-930) was supplied from Styron, with a Tg of 5°C and a dry matter content of 50%. Sodium oleate (88-92%) was purchased from Carl Roth. Neat nanocellulose were manufactured from bleached kraft birch pulp with an enzymatic pretreatment followed by five passes through a homogenizer (Ariete NS3075, GEA Niro Soavi, Italy) and were purchased from CTP, France. AKD (Alkyl Ketene Dimer) hydrophobized reference CNF was purchased to InoFib, France. Amino propyl trimethoxy silane (APMS) 98% was purchased to Sigma Aldrich and used for modification of the nanocellulose.

The coated substrate was a paperboard of 232 g/m² (Cupforma Natura, Stora Enso) made with different layers of sulfate and CTMP pulp.

In all experiments, milliQ water was used.

### 2.2.2. Methods

*Cellulose nanofibrils modification*

APMS was first hydrolyzed for 30 s in water at 10 wt%. The solution was then added in a CNF suspension so that APMS content was 20 wt% with respect to CNF. The suspension was stirred for 2 h to let adsorption occur as well as self-condensation of the organotrialkoxysilane. Suspensions were kept in a refrigerator before use. This procedure is adapted from (Reverdy Charlène, 2016) considering hydrolysis and self-condensation analysis by $^{29}$Si NMR.

The CNF-AKD was prepared by Inofib using similar CNF and a procedure with nanoemulsion (Missoum et al., 2016).

*Coating suspensions preparation*

The coating suspensions were prepared following an adapted protocol from Swerin et al. (2016) Sodium oleate salt was first dissolved at 1 wt% in water under stirring at 45 °C during 10 min. Dry aragonite pigment were added slowly and mixed for 20 min at a solid content with respect to water of around 30 wt%. Finally, the latex binder was mixed using a PTFE blade stirrer for 5 min.

As CNF suspension have only a 2 wt% solids content and the need of a final coating suspension at high dry matter content is crucial, the preparation method was adapted in

order to moderate the dilution by addition of extra-water. For, CNF-APMS r4, CNF-APMS r10, CNF-AKD r10 and CNF AKD r20 formulations, Na-oleate was dissolved in water at 5, 2, 0.2 and 0.1 wt% respectively and CNF suspension was added prior to aragonite implementation, in order to obtain 30% solids content of aragonite with respect to water (Na-oleate dissolution water and water from CNF suspension). Suspension was stirred for 20 min and finally the remaining CNF was added and mix for 5 min.

### *Paperboard coating*

Coating was done using a rod coater (K202 control coater, RK Printcoat Instrument). A 40 µm wet film was deposited on each sample at a 4 m/min speed. Drying of material was achieved using an oven at 90°C for latex and neat CNF based coating suspension; and at 120°C for CNF-AKD and CNF-silane in order to facilitate the activation of the hydrophobizing reaction.

### *Surface characterization*

#### Coated grammage

Coated grammage on paperboard was determined after stabilizing all samples for 24 h in a conditioned room at 23 °C, 50 %RH. Briefly, 5x5 cm² samples were cut from the samples at different locations weighted. The average grammage determined on the non-coated paperboard was substracted to the value to obtain the coated layer grammage. Values were averaged with at least three measurements.

#### *Advancing and receding angles*

Wilhelmy method, performed for measuring wetting properties of porous and hygroscopic material, is ruled using the following equation:

$$F(h,t) = P\gamma cos\theta + Fw(t) - \rho Ahg$$

Where F is the detected force, P the wetted perimeter of the plate, γ the surface tension of the probe liquid, Θ the liquid-solid-air contact angle, ρ the probe liquid density, A the cross-sectional area of the plate, h the immersion depth and g the gravitational constant.

First, surface tension of distilled water was determined before each start. Samples were cut in two pieces fixed on a double sided tape on a glass plate. Edges were glued with a wood glue in order to avoid any water uptake from there. Wetting measurements were done by 10 consecutives immersing/withdrawal cycles of 15 mm of the sample in water. $\Theta_A$ and $\Theta_R$ (advancing and receding angle) were determined by linear regression of the immersion and withdrawal curves to zero depth (h=0).

*Contact, roll-off and water shedding angle*

All samples were measured with a device for contact angle measurement (OCA40, DataPhysics Instruments GmbH). Water was dispensed with a needle of 0.25 mm diameter. Static contact angle measurements were done at least five times with a 5 µL water droplet. When it was possible, roll off angle was measured by tilting the plate from 0° to 90° after dropping a 10 µL drop of water. The angle is determined as the last angle the plate was tilted before the drop rolls. Water shedding angle was determined by recording the smallest angle at which the drop is rolling when the plate is already tilted before dropping. At least five measurements were performed and average calculated.

*Water absorption*

Water absorption was assessed by a standard Cobb test measurement using smaller tested surface. Briefly, the sample is sealed by a 10 $cm^2$ cylinder and 10mL of water is added with a contact time of 60 s. Water is poured out and excess water is absorbed by a blotting paper with the help of a heavy roll. The humid sample is weighted directly after this and water absorption is reported as the mass of water absorbed per area of the sample.

*Microscopic analyses*

SEM pictures were obtained using a Quanta 200 SEM (FEI) and performed with a 400x and 2000x magnification with an accelerating voltage of 10 kV. The working distance was 10.2 mm. Pieces of paperboard were placed on a double-sided adhesive carbon tape and coated with a 10 nm carbon layer.

Atomic force microscopy (AFM), (Nanoscope III®, Bruker) was used to characterize CNF and CNF-AKD. A suspension sample was pre-diluted and dispersed with a high-shear homogenizer (Ultraturrax ®, IKA) at $10^{-4}$ wt % and a drop of the sample was deposited on mica substrates and dried overnight at room temperature. It was characterized with a silicon cantilever (OTESPA®,Bruker) in tapping mode at different locations. Resulting images were subjected to $1^{st}$-order polynomial flattening to reduce the effects of bowing and tilt. The most representative images are presented in this study for both SEM and AFM.

Pictures from optical microscopy were recorded at 50x magnifications by using an Axio ImagerA2 optical microscope assembled with an AxioCam MRm camera (Carl Zeiss).

*Optical profilometry analyses*

Roughness parameters of samples were determined by using an optical profilometer (InfiniteFocus, Alicona) at a 20x magnification corresponding to a 19 mm working distance and a 0,66 mm² analyzed surface. Lateral resolution was 1 µm and lateral was 200 nm. Chosen cut-off wavelength used to get rid of possible interferences of paperboard curling with roughness measurement data was 8 mm. Samples were carbon coated in order to enhance the contrast of the white coating. Average surface roughness ($S_a$) was determined with, at least, five different images for each sample.

## 2.3. Results and discussions

### 2.3.1. CNF characterization

As shortly described, CNF are one of the very promising biobased materials since 2010's and Europe has even decided it is the second priority of its bioeconomy. Such materials are now available industrially. However it exists in a large range of qualities depending on mechanical fibrillation or pretreatment as reviewed by (Nechyporchuk et al., 2016). It is thus important to characterize it before any use. Figure 3-10 shows that the CNF used in this study is homogeneously fibrillated with a few bigger elements, a gel-like structure at low concentration suspension and dimension of nanosized fibril of about 20 ± 6 nm diameter and 3.0 ± 1.7 micrometers length.

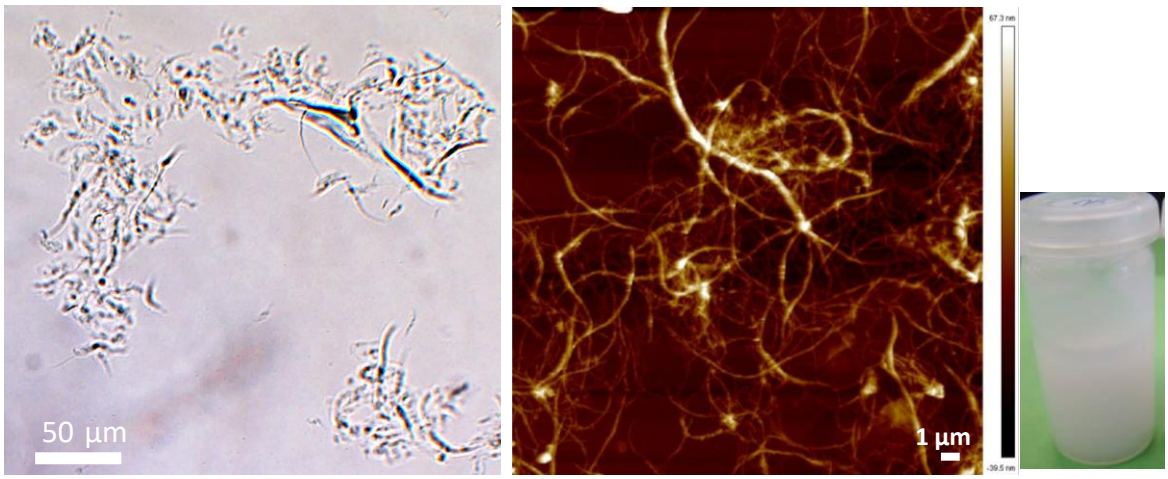


**Figure 3-10. Cellulose nanofibers in suspension observed with optical microscope (left) and AFM (right) and the gel suspension (middle).**

### 2.3.2. Influence of solids content and pigment ratio on coating formula

Robust superhydrophobic properties are often obtained when two conditions are fulfilled: surface hydrophobicity and micrometer or nanometer roughness. For this purpose, coating

formulations were adapted according to the binder. Indeed, latex reference binder is at 50% dry solids content latex while the modified CNF is around 2 w% solids content. The solids content of the CNF-based coating was increased by adding a higher proportion of PCC. The solids content was thus increased from 9 to 15 and 18% increasing the ratio of coated PCC against binder solid content from 4 to 20 wt%. In the case of hydrophobized CNF with AKD, the proportion of Na-oleate had to be decreased to the minimum required to impart hydrophobicity to PCC without endangering the hydrophobization process of CNF that is based on a heat activated nano-emulsion (Table 3-2). Such limitations lead to the formulation of five suspensions with different solids content but also different composition. As controls, one suspension at same PCC concentration in water as CNF-AKD r20 and one with 5% of latex in total were prepared. The latter is equivalent to the one previously tested by co-authors (Swerin et al., 2016).

**Table 3-2. Coating formulations used for coating of paperboard.**

| | Total solid content (%) | Composition of dry matter (wt%) | | | Suspension stability | Coating grammage (g/m²) | PCC retention |
|---|---|---|---|---|---|---|---|
| | | Pigments | Fatty acid | Binder | | | |
| Latex r4 | 33 | 78 | 2 | 20 | +++ | 19 ± 4 | +++ |
| Latex r20 | 18 | 95 | 0.3 | 5 | +++ | 9 ± 3 | + |
| CNF-APMS r4 | 9 | 78 | 2 | 20 | +++ | 4 ± 3 | +++ |
| CNF-APMS r10 | 15 | 89 | 2 | 9 | +++ | 14 ± 4 | ++ |
| CNF-AKD r10 | 15 | 91 | 0.3 | 9 | +++ | 14 ± 4 | ++ |
| CNF-AKD r20 | 18 | 95 | 0.3 | 5 | +++ | 21 ± 2 | + |
| Pigments | 17 | 99.7 | 0.3 | 0 | +++ | 16 ± 3 | - |

All suspensions were stable before processing it but a coating suspension dewatering was observed for all formulations during the process. As expected, the grammage increased with the solids content but interestingly, at same PCC to binder ratio and solids content, formulation with CNF-AKD is able to coat in one-step as twice as much as with latex (CNF AKD r20 against Latex r20). This is probably due to the rheological behavior of CNF which permits to thicken the suspension and form a gel (Dimic-Misic et al., 2013), (Nechyporchuk et al., 2016). However, without any binder there is a slight tendency to decrease the coating grammage but it is less significant. The retention (or adhesion) of PCC on the paperboard was not observed without binder, the coating easily cracks and powders when touched. At a ratio of 20 between pigments and binder, the retention on the coating was low but still improved, and no cracks were observed. The particles attachment increased with increasing

binder addition level. A higher PCC-binder ratio than 4 was not tried so this ratio could be decreased as part of future optimization. However, such ratio cannot be done with CNF yet, due to their too high water content, leading to too much dilution of the suspension and the loss of superhydrophobic coating properties.

### 2.3.3. Surface wetting characterization

Wetting measurements done with the Wilhelmy method showed during the first cycle, advancing and receding angles for each sample. The latex reference formulation gave the best values of advancing angles of 140° (Figure 3-11). CNF based coatings showed inferior advancing angle between 120 and 130° for CNF-AKD and CNF-APMS respectively. This is probably a result of CNF contact angle with water resulting in water attachment on the surface. As shown from results for hydrophobized CNF surfaces (detailed later), CNF-AKD are slightly hydrophobic and CNF-APMS slightly hydrophilic. High standard deviation could be a sign of a non-homogeneous surface coating (or even a leaching of PCC). High hysteresis in each case is signifying that a water adhesion occurs. Complete surface wetting after the first withdrawal was observed. This result shows that we have a Wenzel or intermediate wetting state. The surface superhydrophobic property is not maintained after immersion in water. Before and after each measurement, the water surface tension was determined and the significant drop was attributed to the leaching of PCC and oleate.

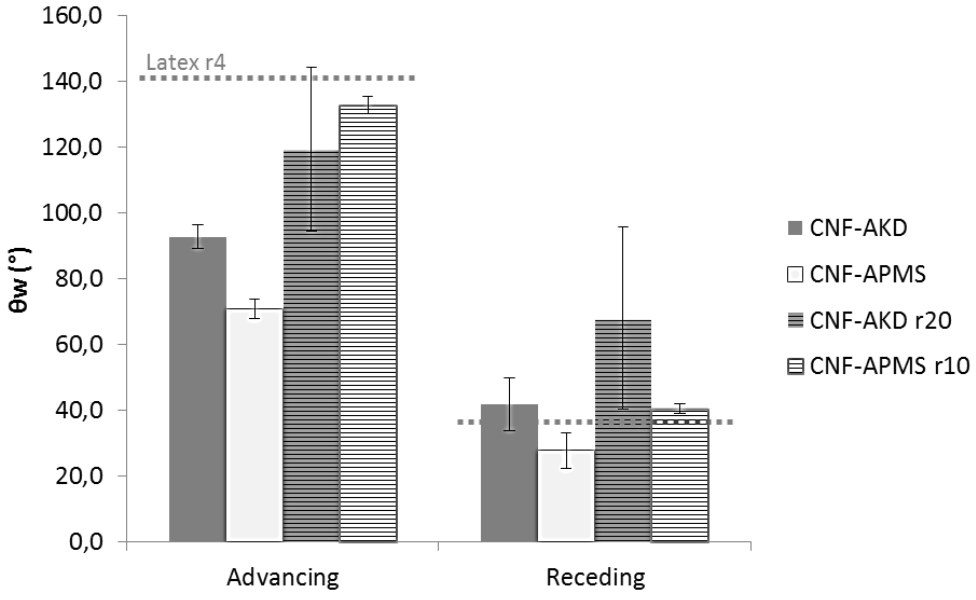


**Figure 3-11. Wilhelmy wetting measurement on coated paperboard.**

As roll-off angle was not possible to measure with other surface than Latex r4 due to water adhesion, a water shedding angle (WSA) measurement was performed (Zimmermann et al.,

2009). Water is rolling off the surface when it is tilted at 2,5° and 17° for latex r4 and CNF-AKD r20 respectively (Table 3-3). If we compare some PCC-binder ratio, CNF-AKD r20 is lower than latex r20, maybe due to a higher aggregation of PCC with latex than with CNF. The WSA values show that the CNF based coating cannot be defined as superhydrophobic because the roll-off angle needs to be below 10°. The roll-off was only measureable for the superhydrophobic latex reference, and showed a high standard deviation (Table 3-3), probably due to a low homogeneity of the coating even with latex.

**Table 3-3. Surface characterization of samples: water adhesion and absorption, surface roughness (Sa).**

| Sample | Water shedding angle (°) | Roll-off angle (°) | Cobb (g/m²) | $S_a$ |
|---|---|---|---|---|
| Paperboard | **>90** | **>90** | **20.8 ± 0.5** | **3.5 ± 0.3** |
| Latex r4 | **3** | **21 ± 12** | **9.8 ± 0.6** | **3.9 ± 0.2** |
| Latex r20 | **38** | **>90** | **–** | **–** |
| CNF-APMS r10 | **>90** | **>90** | **29.9 ± 1.1** | **–** |
| CNF-AKD r20 | **17** | **>90** | **35.4 ± 0.6** | **6.0 ± 0.5** |
| Pigments | **13** | **>90** | **–** | **–** |

The Absorption of water of the material was assessed by the Cobb test. Such superhydrophobic surface would presumably not absorb water or at least to a low amount. The Cobb test showed a more than three time higher absorption in the case of CNF-AKD as binder compared to superhydrophobic latex coated paperboard. This could be explained by a low cohesion of the coating leading to the infiltration of water through the PCC which have less oleate content on their surface than the reference ones. It is also possible that the hydrophobization of the CNF was strongly affected by the oleate and that the CNF stays hydrophilic.

Figure 3-12 shows the effect of hydrophobization of CNF with either AKD or APMS on the static contact angle. Hydrophobic character was successfully obtained on CNF coated paperboard in both cases. The use of hydrophobized PCC with oleate to roughen the surface clearly imparts superhydrophobic contact angle to it. Even though latex gives the best result with a contact angle of 157°, a good result is obtained with CNF-APMS r10 and an excellent with CNF-AKD r20. The probable contact between water and CNF is not a problem within low

period of time; with CNF-AKD r20 150° is achieved. With only pigment coating a water contact angle of 141° ± 4 was obtained and 143° ± 2 with the same latex quantity, which are values worse than CNF-AKD r20. This means that CNF is beneficial to the roughening of the surface, probably because of higher coating density or its nano roughness. However, no absorption over low period of time was observed for the two references. It is thus possible to say that the water absorption observed with CNF is probably only due to CNF and not surface structure. The lower value of CNF APMS r10 could be the result of density of PCC due to the higher CNF proportion in the coating and thus lower dry solids content. Using a two steps procedure, Arbatan et al. (2012) found a contact angle of 154.9° ± 3.3 using 5% nanocellulose binder in concord with our results. However, a tilting angle of only 5° was necessary to roll the drop. The difference is probably due to the functionalization method. Indeed, as the second step is to hydrophobize with AKD the whole surface, cellulose nanofibrils cannot anymore play a role in water adhesion. In our case, the disruption in cellulose hydrophobization process is clearly a cause of higher roll-off angle. However, if this problem can be overcome, a one-step water-based coating procedure is more ecofriendly and scalable as the post-coating of AKD using non-aqueous solvents.

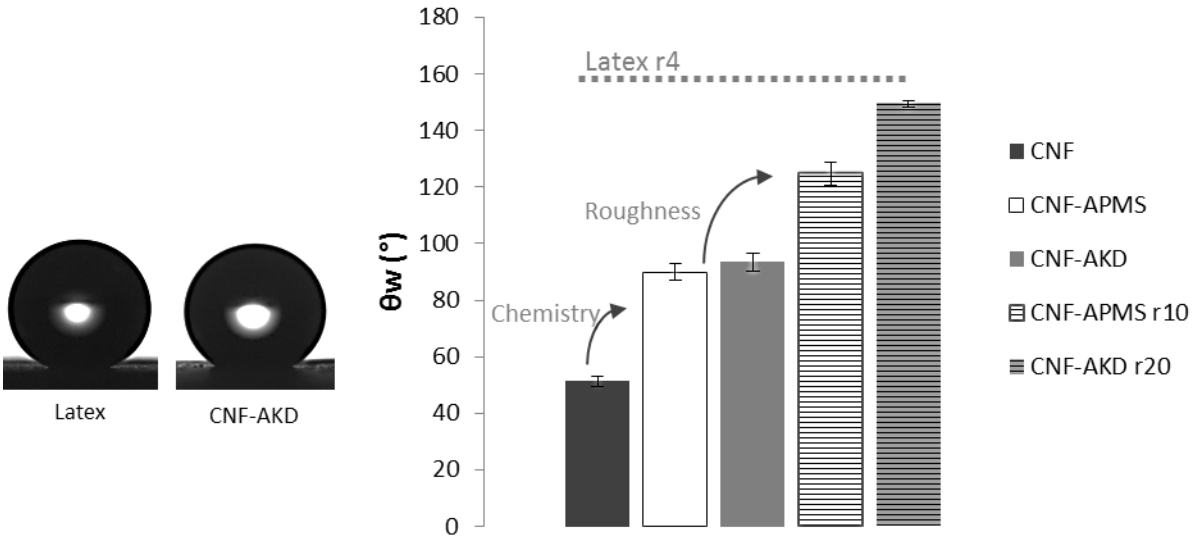


**Figure 3-12. Static water contact angle on manufactured samples**

### 2.3.4. Surface organization and roughness

In our case, the obtained superhydrophobic surface displays strong adhesion to water and is best described as intermediate or Wenzel (Wang and Jiang, 2007). The water adhesion could be attributed to a higher spacing value between PCC particles due to PCC distribution within

the CNF network giving rise to a rose petal effect rather than a lotus leaf effect (Bhushan and Nosonovsky, 2010). Indeed, the rose petal shows high water adhesion while the drop stays on its surface but is able to repeal droplets when tilted. It could also be attributed to natural water adhesion and high specific surface area of CNF which are not fully hydrophobized by AKD or APMS treatment. An optimization of this hydrophobicity should be considered as

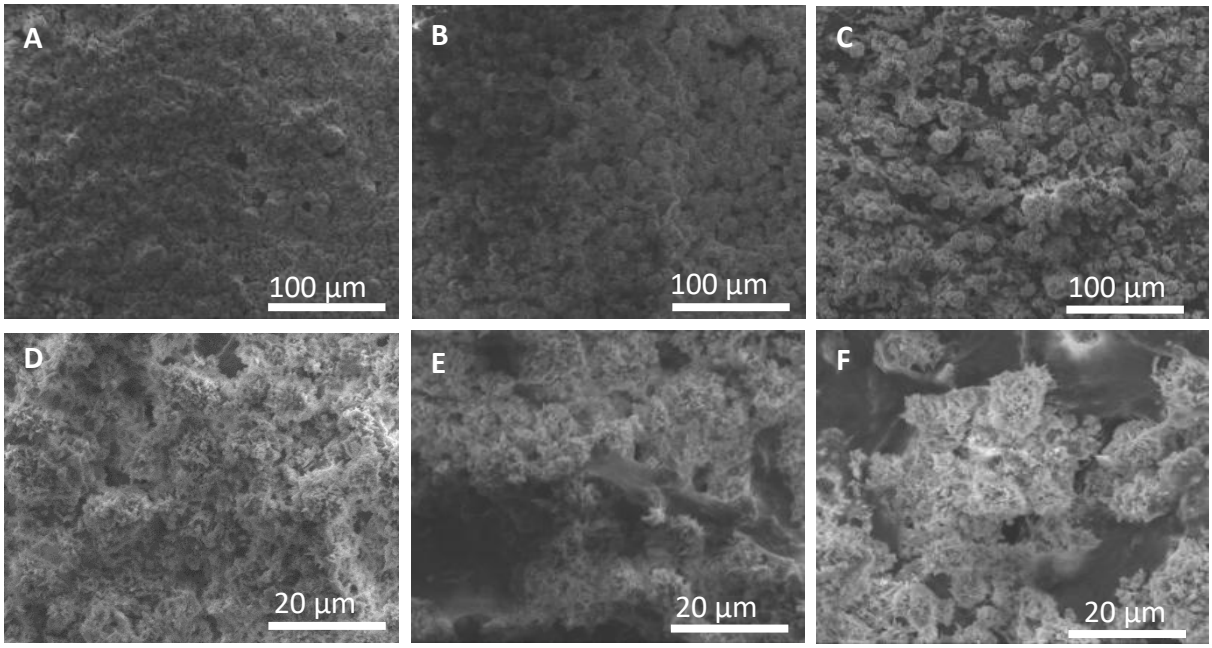


**Figure 3-13. SEM images of coated surfaces. A. Latex r4 at 400x magnification ; B. CNF-AKD r20 at 400x magnification; C. CNF-APMS r10 at 400x magnification; D. Latex r4 at2000x magnification; E. CNF-AKD r20 at 2000x magnification ; F. CNF-APMS r10 at 2000x magnification**

perspective.

For this purpose, SEM images of the surface but also 3D-profilometry reconstitution were performed to determine what could possibly be the dominant parameter. On Figure 3-13 (A, B and C) is observed the surfaces at same magnification of Latex r4, CNF-AKD r20 and CNF-APMS r10 respectively. In A and B cases, precipitated calcium carbonate particles are highly packed while it is not the case in C. A little difference is observable between A and B. At a closer at the surfaces which adhere to water, CNF can be seen in between particles but also on it.

Regarding measured roughness, $S_a$ values are much higher in the case on CNF-AKD r20 than reference superhydrophobic latex (Table 3-3). The average height is thus higher while using CNF as binder. This result could then be in favor of the hypothesis that it is CNF/ water attachment and low PCC cohesion which is the result of water adhesion. Interestingly, PCC is

giving the same value than paperboard surface which could be attributed to natural fibers roughness, although surface profile is completely different.

As compared to surface modification in the study of Arbatan et al. (2012) much more clustered PCC are observed here. This is due to the choice of acicular aragonite which is agglomerated in this case giving larger micro and a nano roughness.

## 2.4. Conclusions and perspectives

The use of nanocellulose as a binder for a superhydrophobic in a one-step coating suspension was successfully proven. The coating suspension is achieved in water by mixing hydrophobized cellulose nanofibrils (CNF) with acicular aragonite (PCC) and sodium oleate. An AKD modified cellulose nanofibrils can also be used at a range of 5 wt% in the suspension to achieved superhydrophobic behavior. A 150° static contact angle with water is obtained and a water shedding angle of 17.5° is recorded. The surface is showing strong adhesion with water and high contact angle hysteresis such as rose petal surface. A stronger hydrophobization of CNF could overcome this feature and the development of CNF with higher dry matter content would be a key point to have the possibility to increase their content in the coating and consequently pigments retention value.

Such superhydrophobic surface obtained with biobased materials is then very promising for innovative paperboard materials for applications in biobased building, lab-on-chip microfluidic devices and food packaging.

## Acknowledgement

The PhD project has been partly funded by ANRT CIFRE and Bollore Thin Paper. The collaboration with Swedish partners was possible thanks to COST action FP1405 ActInPak STSM (Short Term Scientific Mission). LGP2 is part of the LabEx Tec 21 (Investissements d'Avenir –grant agreement no.ANR-11-LABX-0030) and of the PolyNat Carnot Institut (Investissements d'Avenir – grant agreement no. ANR-16-CARN-0025-01). RISE Research Institutes of Sweden provided funding and the Nils and Dorthi Troëdsson Foundation for Scientific Research supports an adjuncht professorship at KTH for AS.

## References


Arbatan, T., Zhang, L., Fang, X.-Y., Shen, W., 2012. Cellulose nanofibers as binder for fabrication of superhydrophobic paper. Chem. Eng. J. 210, 74–79. doi:10.1016/j.cej.2012.08.074

Ball, P., 1999. Engineering Shark skin and other solutions. Nature 400, 507–509. doi:10.1038/22883

Bardet, R., 2014. Nanocellulose as potential materials for specialty papers.

Bhushan, B., Nosonovsky, M., 2010. The rose petal effect and the modes of superhydrophobicity. Philos. Trans. R. Soc. Math. Phys. Eng. Sci. 368, 4713–4728. doi:10.1098/rsta.2010.0203

Bras, J., Belgacem, N., Bardet, R., Agut, P., Dumas, J., 2015. Opacifying Layer for a Paper Medium. EP2890845 (A1) Abstract of corresponding document: WO2014033409 (A1).

Celia, E., Darmanin, T., Taffin de Givenchy, E., Amigoni, S., Guittard, F., 2013. Recent advances in designing superhydrophobic surfaces. J. Colloid Interface Sci. 402, 1–18. doi:10.1016/j.jcis.2013.03.041

Dimic-Misic, K., Gane, P.A.C., Paltakari, J., 2013. Micro- and Nanofibrillated Cellulose as a Rheology Modifier Additive in CMC-Containing Pigment-Coating Formulations. Ind. Eng. Chem. Res. 52, 16066–16083. doi:10.1021/ie4028878

Feng, L., Zhang, Y., Xi, J., Zhu, Y., Wang, N., Xia, F., Jiang, L., 2008. Petal Effect: A Superhydrophobic State with High Adhesive Force. Langmuir 24, 4114–4119. doi:10.1021/la703821h

Hamedi, M.M., Hajian, A., Fall, A.B., Håkansson, K., Salajkova, M., Lundell, F., Wågberg, L., Berglund, L.A., 2014. Highly Conducting, Strong Nanocomposites Based on Nanocellulose-Assisted Aqueous Dispersions of Single-Wall Carbon Nanotubes. ACS Nano 8, 2467–2476. doi:10.1021/nn4060368

Hoeng, F., Denneulin, A., Bras, J., 2016. Use of nanocellulose in printed electronics: a review. Nanoscale 8, 13131–13154. doi:10.1039/C6NR03054H

Hu, Z., Deng, Y., 2010. Superhydrophobic Surface Fabricated from Fatty Acid-Modified Precipitated Calcium Carbonate. Ind. Eng. Chem. Res. 49, 5625–5630. doi:10.1021/ie901944n

Jorfi, M., Foster, E.J., 2015. Recent advances in nanocellulose for biomedical applications. J. Appl. Polym. Sci. 132, n/a-n/a. doi:10.1002/app.41719

Lavoine, N., Desloges, I., Dufresne, A., Bras, J., 2012. Microfibrillated cellulose – Its barrier properties and applications in cellulosic materials: A review. Carbohydr. Polym. 90, 735–764. doi:10.1016/j.carbpol.2012.05.026

Li, J., Kang, R., Tang, X., She, H., Yang, Y., Zha, F., 2016. Superhydrophobic meshes that can repel hot water and strong corrosive liquids used for efficient gravity-driven oil/water separation. Nanoscale 8, 7638–7645. doi:10.1039/C6NR01298A

Li, Y., Zhu, H., Shen, F., Wan, J., Lacey, S., Fang, Z., Dai, H., Hu, L., 2015. Nanocellulose as green dispersant for two-dimensional energy materials. Nano Energy 13, 346–354. doi:10.1016/j.nanoen.2015.02.015

Lozhechnikova, A., Bellanger, H., Michen, B., Burgert, I., Österberg, M., 2017. Surfactant-free carnauba wax dispersion and its use for layer-by-layer assembled protective surface coatings on wood. Appl. Surf. Sci. 396, 1273–1281. doi:10.1016/j.apsusc.2016.11.132

Ma, M., Mao, Y., Gupta, M., Gleason, K.K., Rutledge, G.C., 2005. Superhydrophobic Fabrics Produced by Electrospinning and Chemical Vapor Deposition. Macromolecules 38, 9742–9748. doi:10.1021/ma0511189

Mariano, M., El Kissi, N., Dufresne, A., 2014. Cellulose nanocrystals and related nanocomposites: Review of some properties and challenges. J. Polym. Sci. Part B Polym. Phys. 52, 791–806. doi:10.1002/polb.23490

Marmur, A., 2004. The Lotus Effect: Superhydrophobicity and Metastability. Langmuir 20, 3517–3519. doi:10.1021/la036369u

Mates, J.E., Schutzius, T.M., Bayer, I.S., Qin, J., Waldroup, D.E., Megaridis, C.M., 2014. Water-Based Superhydrophobic Coatings for Nonwoven and Cellulosic Substrates. Ind. Eng. Chem. Res. 53, 222–227. doi:10.1021/ie402836x

Mestral, G.D., 1961. Separable fastening device. US3009235 (A).

Missoum, K., Bras, J., Belgacem, N., 2016. Method for Forming a Hydrophobic Layer. US2016168696 (A1).

Nechyporchuk, O., Belgacem, M.N., Bras, J., 2016. Production of cellulose nanofibrils: A review of recent advances. Ind. Crops Prod., Nanocellulose: production, functionalisation and applications 93, 2–25. doi:10.1016/j.indcrop.2016.02.016

Nosonovsky, M., Bhushan, B., 2009. Superhydrophobic surfaces and emerging applications: Non-adhesion, energy, green engineering. Curr. Opin. Colloid Interface Sci. 14, 270–280. doi:10.1016/j.cocis.2009.05.004

Reverdy Charlène, 2016. Cellulose nanofibrils aqueous modification with different alkoxysilanes: influence of amino presence on surface mechanisms and properties.

Sehaqui, H., Liu, A., Zhou, Q., Berglund, L.A., 2010. Fast Preparation Procedure for Large, Flat Cellulose and Cellulose/Inorganic Nanopaper Structures. Biomacromolecules 11, 2195–2198. doi:10.1021/bm100490s

Shieh, J., Hou, F.J., Chen, Y.C., Chen, H.M., Yang, S.P., Cheng, C.C., Chen, H.L., 2010. Robust Airlike Superhydrophobic Surfaces. Adv. Mater. 22, 597–601. doi:10.1002/adma.200901864

Swerin, A., Sundin, M., Wåhlander, M., 2016. One-pot waterborne superhydrophobic pigment coatings at high solids with improved scratch and water resistance. Colloids Surf. Physicochem. Eng. Asp. 495, 79–86. doi:10.1016/j.colsurfa.2016.01.058

Turbak, A.F., Snyder, F.W., Sandberg, K.R., 1982. Food products containing microfibrillated cellulose. US4341807 (A).

Wang, S., Jiang, L., 2007. Definition of Superhydrophobic States. Adv. Mater. 19, 3423–3424. doi:10.1002/adma.200700934

Xue, C.-H., Jia, S.-T., Zhang, J., Ma, J.-Z., 2010. Large-area fabrication of superhydrophobic surfaces for practical applications: an overview. Sci. Technol. Adv. Mater. 11, 033002. doi:10.1088/1468-6996/11/3/033002

Zhang, K., Geissler, A., Chen, X., Rosenfeldt, S., Yang, Y., Förster, S., Müller-Plathe, F., 2015. Polymeric Flower-Like Microparticles from Self-Assembled Cellulose Stearoyl Esters. ACS Macro Lett. 4, 214–219. doi:10.1021/mz500788e

Zimmermann, J., Reifler, F.A., Fortunato, G., Gerhardt, L.-C., Seeger, S., 2008. A Simple, One-Step Approach to Durable and Robust Superhydrophobic Textiles. Adv. Funct. Mater. 18, 3662–3669. doi:10.1002/adfm.200800755

Zimmermann, J., Seeger, S., Reifler, F.A., 2009. Water Shedding Angle: A New Technique to Evaluate the Water-Repellent Properties of Superhydrophobic Surfaces. Text. Res. J. 79, 1565–1570. doi:10.1177/0040517509105074

# 3. From CNF-silsesquioxane paper coating to their use as binder in superhydrophobic suspension for a coating pilot trial

## 3.1. Introduction

In the context of functionalizing paper for antiadherent, antibacterial or superhydrophobic paper, the use of CNF-silsesquixoane could be of a great interest. Today existing solutions focus on smooth layer of silicon which is expensive and detrimental regarding environmental impact of such an antiadherent, due its difficulty to be recycled or to be biodegradable. During the framework of this Ph.D, we have tried either to limit silicon content or to favor its fragmentation by using CNF with commercial silicon latex. These results are more detailed in a confidential industrial report.

Another solution is to be inspired by nature and to create, by coating a rough and hydrophobic surface onto the paper, a specifically designed surface mimicking lotus leaf (Marmur, 2004) or allium ursinum bottom surface which is a specific plant growing in our area. This strategy is well known for self cleaning plastic or glass or wood surface (Chen et al., 2012), (Lozhechnikova et al., 2017) but still very innovative in paper industry. Moreover only few researchers managed to produce superhydrophobic surface in one-step process (Wang et al., 2008) (Swerin et al., 2016) and two steps are usually necessary (Arbatan et al., 2012), (Balu et al., 2008).

Regarding our strategy, organotrialkoxysilanes were proved to form silsesquioxane beads in nanocellulose network in the previous Chapter 2.2. The reaction in water of a hydrophobic precursor, here methyltrimethoxypropyl silane and an amine catalyst, 3-aminopropyltrimethoxysilane creates particles of around 1 µm diameter. The same reaction in a CNF network showed to considerably decrease particles size and, with low silane content, to hydrophobize and give antibacterial activity to a 40 g/m² nanopaper (as shown in Chapter 2.2.1.).

A similar reaction was investigated by (Maury, 2014) in TEMPO modified nanocellulose network but using classic sol-gel precipitation using the tetraethyl orthosilicate and 3-aminopropyltriethoxysilane, as starting reagents. But, to the best of our knowledge, no

application in paper coating was investigated. It is a rather new subject that is proposed in the following study.

It is proposed here to assess the coating of such modified CNF suspension onto paper at lab scale but also roll-to-roll pilot scale. The resulting antiadherence and hydrophobic characters as well as the antibacterial activity will be measured.

## 3.2. Materials and methods

### 3.2.1. Materials

For this study, the CNF used were manufactured *via* an enzymatic pretreatment followed by a mechanical treatment through a homogenizer (Ariete NS3075, GEA Niro Soavi, Italy) and were purchased from CTP, France.

The silsesquioxane particles were synthesized by reacting 3-amino propyl trimethoxy silane (APMS) 98% and trimethoxypropylsilane (TMPS) purchased from Sigma Aldrich.

Paper used in the first section is a 40g/m² uncoated and highly refined (°SR>75) paper from Papeterie du Léman (Bolloré Thin paper, Publier, France) made with hardwood and softwood pulp and sized with AKD. This paper was used for all laboratory scale trials.

For superhdrophobic coating suspension preparation, scalenohedral precipitated calcium carbonate (PCC) (Precarb 120, Shaeffer Kalk) with a $d_{50}$ around 1.3 µm was use in this experiment and kindly provided by Papeteries du Léman. Sodium oleate (97 %, ROTH) was used to hydrophobize the PCC particles.

For pilot scale trials, a printing paper manufactured by Clairefontaine with a grammage of 80g/m² was used. The difference in the paper between lab and pilot scale study was needed because of its better resistance to coating with low dry matter content suspension. The possibility of paper breakage during coating was thus avoided.

In all experiments, distilled water was used.

### 3.2.2. Methods

*Cellulose nanofibrils modification*

The modification of CNF consists in the formation of silsesquioxane network as mentioned in Chapter II.2. Briefly TMPS is added in half the suspension of neat CNF and in the other half APMS is added. Each part is mixed for 10 min separately and then together for at least 2 hours at room temperature. Four types of CNF were prepared: (i) CNF APMS TMPS 0.5m 0.05w; i.e mix of CNF with a ratio of 0.5 M between APMS and TMPS at 5% solid content compared to CNF , and then three others with increasing concentration of silsesquioxane compared to CNF from 10%, 25 and even 50% which are respectively (ii) CNF APMS TMPS 0.5m 0.1w, (iii) CNF APMS TMPS 0.5m 0.25w and (iv) CNF APMS TMPS 0.5m 0.5w.

For the pilot trial, molar ratio between TMPS and APMS was chosen to be 0.5 and the ratio between dry total silane content and dry CNF was fixed to 0.1.

*Coating suspension preparation for the pilot trial*

The coating suspensions were prepared following an adapted protocol from (Swerin et al., 2016). Sodium oleate salt was first dissolved at 2 wt% in water under mechanical stirring at 45 °C and 300 rpm during 10 min. CNF suspension was added, in order to obtain a 30% solid content of aragonite with respect to water. Dry aragonite pigments were added slowly and mixed for 20 min. Finally, the remaining CNF suspension was mixed for 5 min.

*Paper coating*

The coating at lab scale was done using a laboratory blade coater (Euclid Coating System, USA). A pression of 1.2 bars was applied on the blade. Drying of material was achieved using an air drying system followed by a contact drying at 110°C for 5 min.

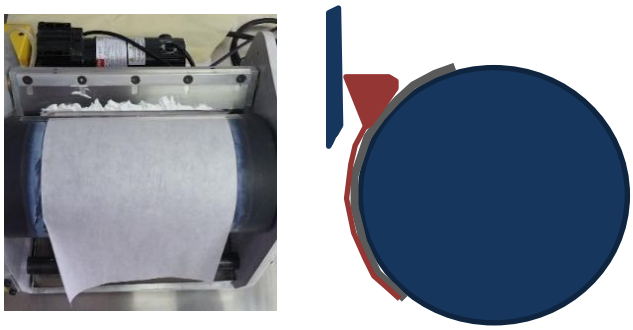

**Figure 3-14. Laboratory blade coater (left) and schematic representation (right).**

Coating at the pilot scale was done using a roll to roll coater (RK Coater, England). Trials were performed at 13.5 and 18.5 m/min on a 20 cm coating width. Pressure applied on the over roll knife system was 20 psi and drying was achieved through in-line systems of three IR drying section (3*1kW) and an air drying section at 200°C.

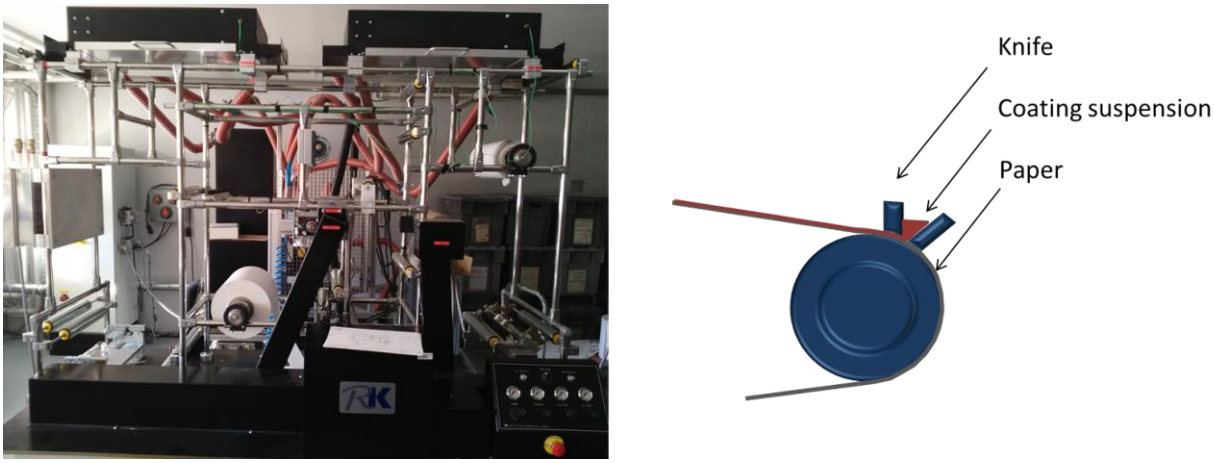


**Figure 3-15. Picture of the pilot coater used in the experiment and schematic representation on the coating module.**

### *Coating characterization*

#### Coated grammage

For the laboratory scale grammage determination, the grammage of the entire A4 sample was deduced from the coated one. Values were averaged between three samples made with the same parameters.

For the pilot trial, coated grammage on paper was determined after stabilizing all samples for 24 h in a conditioned room at 23 °C, 50 %RH. Various 10x10 cm² parts of the paper were chosen and weighted. To obtain the average coated grammage, the average grammage of non-coated paper was substracted from the obtain value. Values were averaged with at least ten measurements.

#### *Static Water Contact angle*

Static water contact angle were measured by the deposition of a 5 µL drop on the sample surface. An optical camera (OCA20, DataPhysics Instruments GmbH) was used to record images of the drop and the SCA20 software was used to determine the angle at the triple line. Average measure of at least 5 measurements is expressed.

#### *Water Roll-off angle*

Roll-off angle was measured by dropping a 10 µL water drop on the surface of the sample and tilting the sample. The angle after what drop was rolling all the way down to the sample was recorded. Average of three measurements is given here.

#### Water shedding angle

The water shedding angle was measured by dropping a 10 µL water drop from a known height and to record the lowest angle value that the drop starts to roll down to the end of the sample (2 cm). The value is an average of five measurements.

#### *Antiadherence property*

A peeling test was used to determine the practical adhesion of a standardized tape (7475, 3M Company). It was assessed with a modified FINAT FTM 1 test method at 180° at a speed of 300 mm/min. A 2 kg roll is applied three times to obtain a reproducible attachment between the sample and the tape. Average measured force in order to peel off the adhesive from the paper is presented in this work based on the average of 10 measurements.

#### *Antibacterial property*

It was carried out with *B.Subtilis* bacteria following the standard AFNOR EN 1104. Agar is inoculated with *B.Subtilis* and the piece of the paper sample to be tested was placed on it

(coated surface in contact). Produced petri plates were incubated for 3 days at 37°C and antibacterial activity was assessed by the presence or not of bacteria under the sample. Experiments were repeated three times.

## 3.3. Results and discussions

### 3.3.1. CNF-silsesquioxane coating at laboratory scale

The introduction of low content of organotrialkoxysilanes in a particular way in CNF suspension was proved to be highly beneficial for rendering cellulose nanopaper hydrophobic but also antimicrobial (Chapter 2.2). Indeed, the introduction of less than 5 wt% of a mix of TMPS and APMS is creating silsesquioxane nanoparticles inside the film and is also creating a silsesquioxane layer on its top. This layer is expected to act as a hydrophobic, barrier layer when coated on paper. The silsesquioxane layer, rendered bendable, and giving probably nano-nanoroughness to the paper, is also expected to help in the releasing properties by decreasing contact between a tape or a cake and the coated paper.

*Practical adhesion on coated layer*

The functionalization on the paper was tried for anti-adhesiveness of tape as shown in Figure 3-16. The roughness induced by silsesquioxane layer and particles as well as the chemical structure close to silicon, was thought to help in non-adhesion properties. However, only a slight tendency to decrease the peeling force was observed for 5 wt% and 25 wt% silane addition regarding CNF content. CNF layer gave a very low peeling force, which is due to the delamination of the coated layer onto the tape. This means also that silsesquioxane is probably promoting CNF layer adhesion onto the dried hydrophobic substrate when post-coated.

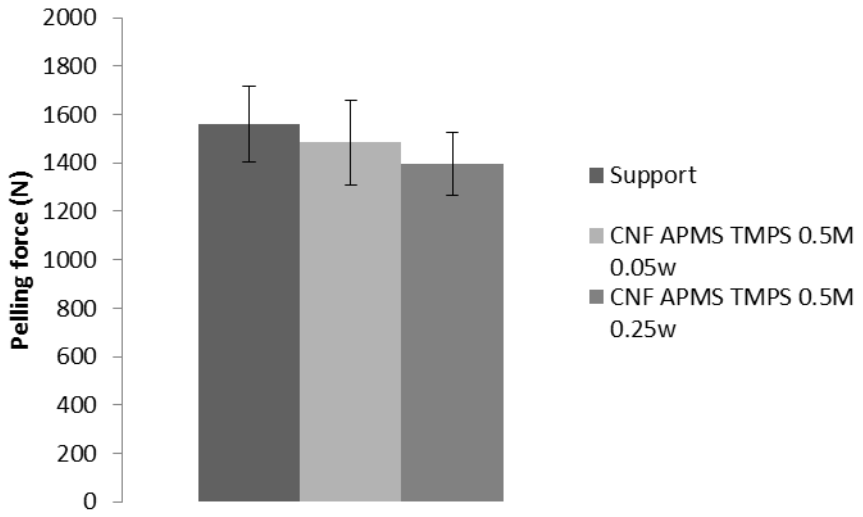


**Figure 3-16. Force to peel a tape at 180° fixed on the coated paper.**

*Antibacterial activity of the resulting coated paper*

As APMS crosslinks, the APMS leaching is then limited (or even absent), which gives contact active antimicrobial paper. As it was shown in Chapter 3.1 while APMS is coated alone or with CNF, a layer of 2.7 g/m² is necessary to obtain an antimicrobial property. It is thought that with silsesquioxane particles, the amine is pointing toward the outer surface of the particles and could lead to an enhancement of amine density and thus of antibacterial activity with low amount of APMS.

| APMS/TMPS (M/M) | Silsesquioxane /CNF (w/w) | Layer coating (g/m²) | Equivalent coated APMS (g/m²) | Bactericidal (B.Subtilis) |
|---|---|---|---|---|
| 0 (neat CNF) | | 1.9 | 0 | × |
| 0.5m | 0.05w | 1.8 | 0.03 | × |
| 0.5m | 0.1w | 1.5 | 0.05 | × |
| 0.5m | 0.25w | 2.2 | 0.2 | × |

**Figure 3-17. Bactericidal effect of coating layer of CNF-silsesquioxane blend on Bacillus Subtilis.**

Coated papers were submitted to an inhibition zone test with *Bacillus Subtilis*. As represented in Figure 3-17, coated grammage are very low for all the samples and consequently for equivalent APMS content. Through the knowledge of previous study showing the need of a continuous coating of at least 2.7g/m² of APMS to expect a killing of bacteria, it is not surprising that none of the sample showed bactericidal effect. The hypothesis that the formation of silsesquioxane particles and layer could favor a diminution in coating grammage was not possibly confirmed. To obtain 2.7 g/m² of APMS, a coating of 15g/m² would be needed with a formulation with 50wt% of silsesquioxane regarding CNF. Such coating amount was not possible to process with our laboratory scale coater.

*Water contact angle as a function of the coating formulation*

Concerning contact angle, both phenomenon of fast condensation, silsesquioxane particles and addition of propyl chains gave interesting results concerning water contact angles. Indeed, as shown in Figure 3-18, only 10 wt% of total amount of silane in CNF suspension, with a minimum coating grammage of 1.4 g/m² is enough to create a hydrophobic coating with a low amount of material. These results increase further more with the addition of silane content up to 50 wt%. The contact angle of the base paper surface is not included inside the value as it is around 115° due to internal AKD sizing.

The difference in contact angle between nanopaper manufactured in Chapter 2 and the coating here could be explained by a lower amount of silsesquioxane per square meter. Indeed, nanopapers were made to reach an approximate grammage of 40g/m², meaning almost 40 times higher than the basis weight of the coated layer. It would be very pertinent to measure the roughness but this was not possible in this study. Higher possible roughness induced by inclusion of bigger particles with the same functionality was attempted as a comparison.

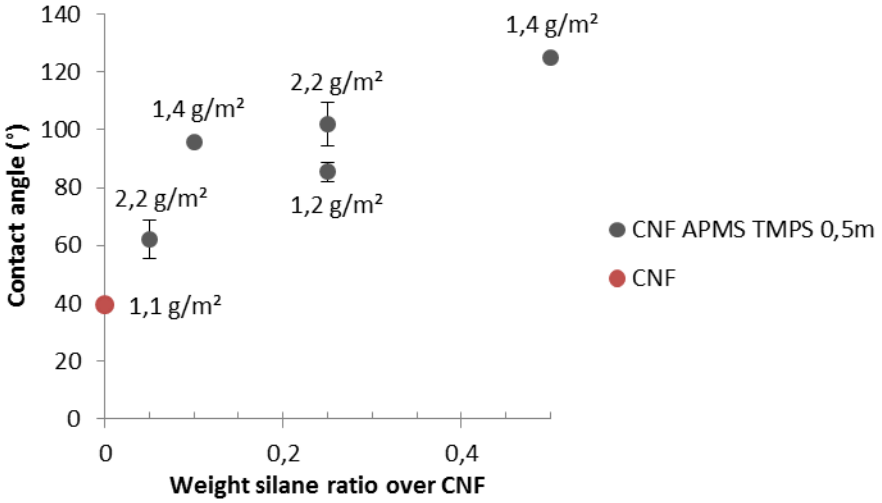


**Figure 3-18. Water contact angle of coating of CNF-silsesquioxane suspension depending on silane content ration on nanocellulose weight**

Two different coatings were done at same grammage (2.2 g/m²), with the same amount of silsesquioxane regarding CNF: 25 wt%. The first sample, 1_ CNF APMS TMPS 0.5m 0.25w was done by *in-situ* silsesquioxane synthesis; separating half the CNF suspension, hydrolyzing and mixing TMPS and APMS for 10min separately and mixing both suspensions together for more than 2 hours. The second one is made by mixing previously soxhlet purified silsesquioxane particles synthesized at 1% in TMPS initial concentration in water with a molar ratio between APMS and TMPS of 0.5. Particles were included in CNF, mixed with a high shear homogenizer and coated on paper. With this second strategy, the hydrophobic property was not successfully achieved as shown by the low water contact angle obtained in Figure 3-19. A lack in film formation of silsesquioxane layer onto CNF but also the bad dispersity of the hydrophobic particles inside CNF hydrophilic network could explain this high difference. To test at pilot scale we then decided to add PCC rough particles as successfully tested in Chapter 3.2.

The hydrophobicity obtained with CNF silsesquioxane with the in situ method could be valuable in the design of coating formulations where this property is needed. Especially, such behavior could be used to replace conventional synthetic binder and keep a one-pot functionalization.

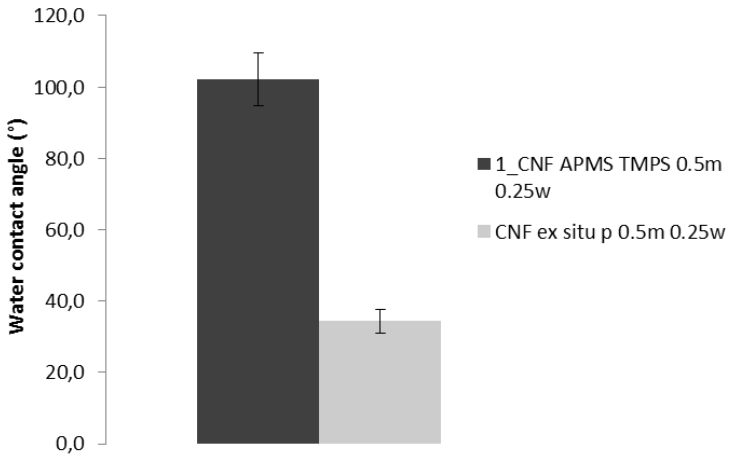


**Figure 3-19. Water contact angle between same formulations with direct formation of silsesquioxane particles in CNF medium or by inclusion of silsesquioxane particles synthesized in water and added in CNF.**

### 3.3.2. Toward CNF-silsesquioxane use as a binder in superhydrophobic formulation at pilot scale

*Evaluation at laboratory scale*

First of all, the use of CNF-silsesquioxane as a binder in specific coating formulations to obtain a superhydrophobic paper was tried at the laboratory scale. As proceeded in the previous Chapter 3.2, CNF were used as a replacement of latex styrene butadiene in the formulation. It was adapted to the thin paper of 40 g/m² instead of the paperboard and PCC were chosen according to industrial partner availability. Indeed, PCC aragonite are not anymore commercial grade and not easy to obtain. Thus scalenohedral PCC, produced directly on industrial partner production site were used. The blade coating system was also chosen because of the thin paper instead or the bar coating. Indeed, this laboratory apparatus is permitting to coat a paper more easily under tension, which avoids shrinking effect. Bar coating was suitable for paperboard as it is thick enough to stand up against shear and shrinkage due to water uptake and release.

**Table 3-4. Coating suspension formulation**

| Ratio PCC/oleate | Ratio PCC/CNF | CNF-silsesquioxane | Dry matter content (%) |
|---|---|---|---|
| 40 | 10 | CNF APMS TMPS 0.5m 0.10w | 14 |

As presented in Table 3-4, a formulation with a PCC ratio to CNF of 10 was chosen in order to compare the value with the coating made in Chapter 3.2 with CNF-APMS. The CNF silsesquioxane were made with a mix of APMS and TMPS at a molar ratio of 0.5 and a total silane amount of 10 % which is two times less than in Chapter 3.2 with only APMS.

As exposed in Table 3-5, one coating but also 5 successive coatings were evaluated for superhydrophobic properties. It consists in coating and drying the paper and start again the procedure. As one coating only gave good results but not enough to obtain the drop rolling

**Table 3-5. Static water contact angle of the coating after 1 pass and after 5.**

| Static water contact angle (°) | | Roll-off angle (°) | |
|---|---|---|---|
| 5 coatings | 1 coating | 5 coatings | 1 coating |
| 147 ± 3 | 140 ± 4 | 28 ± 2 | – |

on the surface, the coating layer was artificially enhanced by this way. It was also noticed that the highly viscous coating suspension was not homogeneously coated from the top to the bottom because of the suspension retraction onto the blade due the cylinder speed. Coated grammage by these successive coatings went from 1.9 to 7.7 g/m² and a better static contact angle, close to superhydrophobic (150°) was obtained. The drop was also rolling, and a roll-off angle of 28° ± 2 was measurable for this lab scale coating.

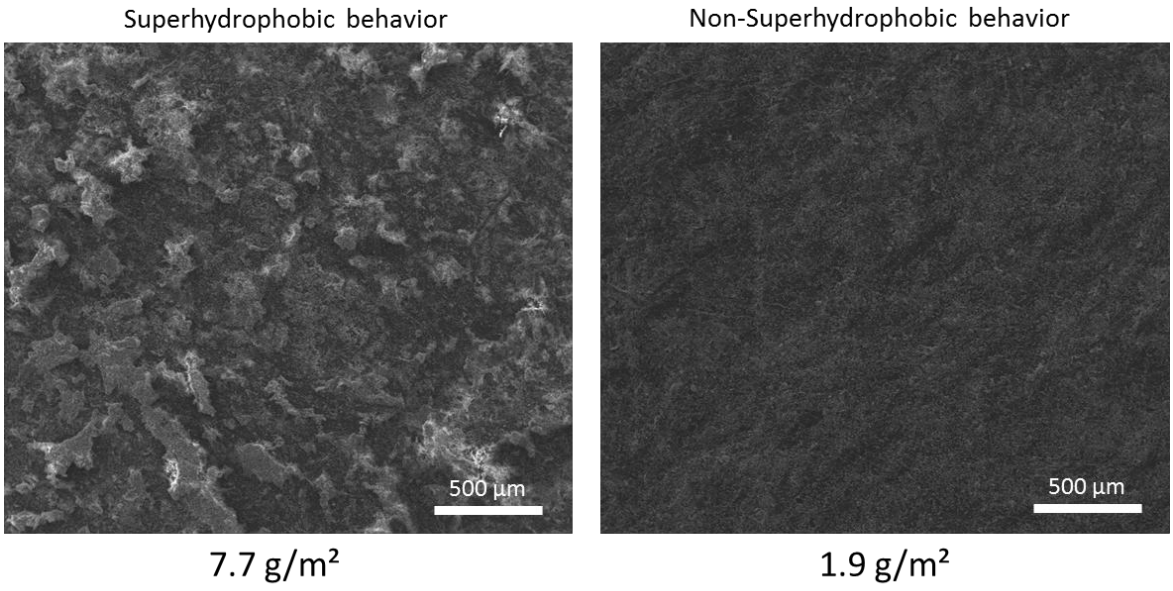


**Figure 3-20. Paper coating of PCC/CNF-silsesquioxane and oleate formulation with five passes (left) and one (right).**

Static water contact angle was almost the same than for CNF-AKD with a PCC/CNF ratio of 20 (Chapter 3.2.). A roll-off angle was measurable, which was not the case with CNF-AKD because of water adhesion to the substrate immediately after the drop deposition. It is also much better than the formulation with CNF-APMS with the same PCC/CNF ratio of 10.

SEM pictures of the surface were taken in order to understand the difference between five successive coatings and only one. As observed in Figure 3-20, one coating is relatively smooth compared to five coating. It is perhaps due to the dusting effect of the coating already observed earlier. Indeed, when coating a second layer on the top of the previous one, the suspension could have taken non-attached PCC, forming these uncontrolled roughness observed.

The behavior of the suspension at pilot scale was needed in order to see if only one pot coating could still give good results. Indeed, 5 successive coatings are not adaptable in a papermaking process.

### *Evaluation at pilot scale*

The same formulation was tried at pilot scale as the one in Table 3-4 but in larger amount i.e. 500 g. The pilot coater was equipped with a knife over roll coating system as depicted in Figure 3-15 which is a good system for highly viscous formulations such as this one. In this case gravity is helping to keep the suspension in contact with the paper. The coating was smooth and without any hole. The only remarkable defect was the presence of some craters probably due to the foaming effect of the suspension and/or to a fast drying. Two different speeds were tried, as highlighted in Table 3-6. A higher speed was resulting in the diminution of the grammage. For each speed the "craters" effect was observable. The use of a defoaming agent could probably reduce this effect.

Resulting wetting properties with water were measured. As shown in Figure 3-21, the static water contact angle was 142 ± 3 which is a very good result, close to the one observed with one coating at laboratory scale. For both grammage values, WCA was similar. No roll-off was measurable but a water shedding angle of around 81° was recorded. It is high but promising for further investigations.

**Table 3-6. Coating speed conditions tried and resulting average grammage.**

| Machine speed | Average grammage deposited |
|---|---|
| 13,5 m/min | 14.7 g/m² ± 0.9 |
| 18,5 m/min | 12.0 g/m² ± 1.5 |

PCC dusting effect was still observable due to the high amount of PCC compared to CNF. If compared to results from Chapter 3.2, the chosen ratio here, i.e. 10 could be enhanced to 15 or 20 to perhaps reach a stronger superhydrophobic behavior.

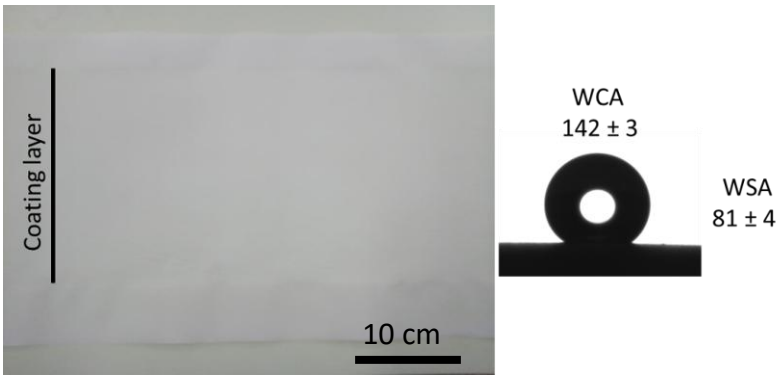


**Figure 3-21. Picture of the coated paper and resulting static water contact angle.**

## Conclusion and perspectives

The coating of CNF-silsesquioxane onto paper did not permit to obtain antimicrobial activity or interesting anti-adherence properties. However, interesting hydrophobic character of the coated layer was shown. Thus, the use of CNF-silsesquioxane in the preparation of a specific coating formulation with rough particles for superhydrophobic layer coating on a paper was evaluated. At the laboratory scale good results were obtained with a one pot coating of the suspension. Better results than those reached with the use of CNF-AKD or CNF-APMS were obtained. Moreover, there were obtained with fully upscalable products and coating method. It was also demonstrated that a five successive coating method permits achieving better results, probably because of layer destructuration during the process leading to higher roughness and consequently higher superhydrophobic character. An upscaling of the coating in one-pot was done. The viscosity was shown to be still processable. Very interesting results were obtained and 81° WSA was measured. Such results at pilot scale are very encouraging for further development of the formulations. Perhaps, the dusting effect could be overcome by a higher amount of CNF compared to PCC. But this question is for now stranded by the dry matter content of the initial CNF suspension.

## References


Arbatan, T., Zhang, L., Fang, X.-Y., Shen, W., 2012. Cellulose nanofibers as binder for fabrication of superhydrophobic paper. Chem. Eng. J. 210, 74–79. doi:10.1016/j.cej.2012.08.074

Balu, B., Breedveld, V., Hess, D.W., 2008. Fabrication of "Roll-off" and "Sticky" Superhydrophobic Cellulose Surfaces via Plasma Processing. Langmuir 24, 4785–4790. doi:10.1021/la703766c

Chen, Y., Zhang, Y., Shi, L., Li, J., Xin, Y., Yang, T., Guo, Z., 2012. Transparent superhydrophobic/superhydrophilic coatings for self-cleaning and anti-fogging. Appl. Phys. Lett. 101, 033701. doi:10.1063/1.4737167

Lozhechnikova, A., Bellanger, H., Michen, B., Burgert, I., Österberg, M., 2017. Surfactant-free carnauba wax dispersion and its use for layer-by-layer assembled protective surface coatings on wood. Appl. Surf. Sci. 396, 1273–1281. doi:10.1016/j.apsusc.2016.11.132

Marmur, A., 2004. The Lotus Effect: Superhydrophobicity and Metastability. Langmuir 20, 3517–3519. doi:10.1021/la036369u

Maury, C., 2014. Elaboration et caractérisation de matériaux hybrides à base de nanocelluloses et de nanoparticules inorganiques., Mémoire de Maîtrise, Université QUébec Montréal.

Swerin, A., Sundin, M., Wåhlander, M., 2016. One-pot waterborne superhydrophobic pigment coatings at high solids with improved scratch and water resistance. Colloids Surf. Physicochem. Eng. Asp. 495, 79–86. doi:10.1016/j.colsurfa.2016.01.058

Wang, H., Fang, J., Cheng, T., Ding, J., Qu, L., Dai, L., Wang, X., Lin, T., 2008. One-step coating of fluoro -containing silica nanoparticles for universal generation of surface superhydrophobicity. Chem. Commun. 0, 877–879. doi:10.1039/B714352D

# Conclusion

This **Chapter 3** is providing an overview of potential applications of modified CNF in paper functionalization and their limitations.

It was demonstrated in **Chapter 3.1** that 3-aminopropylsilane was reacting in a particular way to provide interesting greaseproff barrier properties. However, the inclussion of CNF seems to affect negatively this property. Very good hydrophobic properties are however obtained a slight decrease in adhesive property is observed. Unfortunately, the design coating is not fulfilling the industrial technical requirements.

In **Chapter 3.2**, the use of hydrophobic CNF in the replacement of synthetic latex binder in superhydrophobic surface coating was successfully demonstrated. CNF were shown to provide anti-crackling effect of the coating as well as the potential to coat with lower dry mater content due to their rheological behavior.

Lastly in **Chapter 3.3**, the use of CNF-silsesquioxane in coating application was shown to be unsufficient to reach low practical adhesion or antibacterial properties. Higher coating amount could be interesting perspectives. However, the very good hydrophobic properties were successfully used in coating formulation for superhydrophobic functionalization of paper. It was demonstrated to be upscalable at pilot scale as well.

# General conclusions and perspectives

# General conclusions and perspectives

This PhD project was focusing on how to use industrially nanocellulose to prepare functionalized specialty paper. More precisely, the main objectives were to assess the use of modified CNF in non-wetting, greaseproof, non-adherent or antibacterial paper. In this context, the modification of nanocellulose with organotrialkoxysilanes appeared to be a quick, aqueous and versatile way to achieve these goals. Indeed, this project being in an industrial context, it was necessary to adapt CNF surface modification toward more sustainable and easy to process pathway. As highlighted in **Chapter 1**, cellulose nanofibrils are promising vector of these silanes in coating process because of their high hydroxyl group content but also because of their controlled viscosity with a rheothinning behavior. Futhermore it permits controlled nucleation and growth of polyorganoalkoxysilane or silsesquioxane particles as well. As shown in Figure 1, the first step (Chapter 2) was to evaluate possible CNF-organotrialkoxysilanes interactions and then to applied this knowledge for potential coating applications in papermaking (Chapter3).

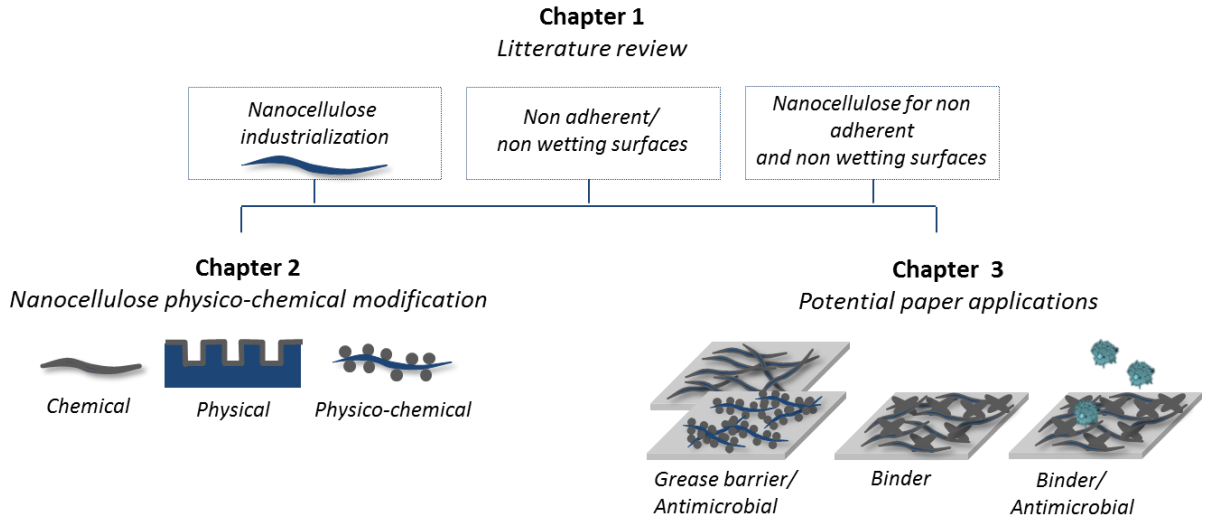


**Figure 1. Illustration of the manuscript organization and research themes.**

Before this project, cellulose nanofibrils industrial grade was not really available in spite of some announcement. Few pilot scale production and several companies claiming their own use in their production, but no marketed product was available at large scale. In three years, this problematic has evolved greatly, with commercial grade proposition from European and American companies (Table 1). But industrial manufacturing evolution has not

been the only field to evolve. At the same time great effort has been made in fundamental or applied research. In papermaking, the use of CNF was already studied by few research groups. Moreover, the number of researches still increased during the time of the project. Eventhough different scientific themes were already addressed with nanocellulose i.e. antibacterial, or greaseproof materials, results of this PhD are still giving additional new results toward these developments in specialty papers.

**Table 1. Overview of scientific publication on the subject before and during the project.**

| Scientific issue | Before October 2014 | During the project (2014-2017) |
|---|---|---|
| **Cellulose nano/microfibrils industrialization** | • Pilot scale production<br>• 3 start-up<br>• 14 companies in the market | • Industrial scale production and commercialization<br>• 1 start-up creation<br>• 9 additionnal companies in the market |
| **Cellulose nano/microfibrils applied to papermaking (coating and additive)** | • 1 book chapter<br>• 58 patents<br>• 35 articles | • 26 patents<br>• 25 articles |
| **Chapter 2 Cellulose nanofibrils chemical, physical and physico-chemical modification with poly-organoalkoxysilane or silsequioxane** | *Cellulose nano/micro fibrils and silane coupling agent*<br>• 1 PhD<br>• 6 patents<br>• 11 publications<br>*Cellulose nano/micro fibrils and silsesquioxane*<br>• 1 master thesis<br>• 5 articles | *Cellulose nano/micro fibrils and silane coupling agent*<br>• 1 patent<br>• 11 publications<br>*Cellulose nano/micro fibrils and silsesquioxane*<br>• No evolution |
| **Chapter 3 Modified CNF potential applications in paper functionnalization** | Cellulose micro/nanofibrils in superhydrophobic materials<br>• No patent<br>• 5 articles<br>Cellulose micro/nanofibrils in barrier, antimicrobial and antiadherent coating<br>• 20 patents<br>• 15 articles | Cellulose micro/nanofibrils in superhydrophobic materials<br>• No patent<br>• 6 articles<br>Cellulose micro/nanofibrils in barrier, antimicrobial and antiadherent coating<br>• 7 patents<br>• 19 articles |

This PhD contribution (5 posters, four publications) provides new insight on the use of CNF in papermaking coating applications with chemical modifications, which is a strategy much less studied. One key innovative approach of this PhD (almost never studied for CNF in paper) consists in the biomimetism of anti-adherent natural surfaces (like the famous lotus leaf) by designing a natural coating able to bring adapted roughness and chemistry at paper surface.

**Table 2. Key results of the overall PhD project.**

| Scientific issue | Key results |
|---|---|
| **Chapter 2**<br>**Cellulose nanofibrils chemical, physical and physico-chemical modification with poly-organoalkoxysilane or silsequioxane** | *CNF modification with poly-organotrialkoxysilane*<br>• Three different organotrialkoxysilanes studied<br>• Use of CNF as reactive biosourced material<br>➢ Particular reaction of APMS with CNF, hydrophobic and barrier CNF nanopaper<br>*CNF film structuration*<br>• Silicon molding failure<br>*CNF modification with silsesquioxane particles*<br>• Silsesquioxane formation investigation in water<br>• Silsesquioxane synthesis in CNF with different concentration parameters<br>➢ Highly hydrophobic CNF nanopaper with low amount of organotrialkoxysilane, antibacterial effect |
| **Chapter 3**<br>**Modified CNF potential applications in paper functionalization** | *Paper modification with CNF and poly-organotrialkoxysilane*<br>• APMS and APMS/CNF coating<br>• CNF/silsesquioxane coating<br>➢ APMS is filmogeneous and barrier to grease, hydrophobic coating<br>*Modified CNF as binder in superhydrophobic coating formulation*<br>• CNF-AKD and CNF silsequioxane Vs latex<br>➢ Superhydrophobic properties, lower solid content<br>*Superhydrophobic paperboard for bacterial anti-adhesion*<br>• *Three formulations compared*<br>➢ Commercial (without CNF) gives promising proof of concept, lower superhydrophobic property combined with antimicrobial CNF is promising too |

In the **first part** CNF possible interaction with organotrialkoxysilanes was studied in details with the idea of functionalization toward applications in the above mentioned products. The behavior of three organotrialkoxysilanes with different hydrophilic character was studied in order to use them as efficient as possible within the CNF modification procedure. Their interaction with CNF was also followed and APMS was determined as the most suitable silane to modify CNF surface in the context of an industrial product potentiality *(Chapter 1.1)*. Its molecular organization at the CNF surface was analyzed with high performance tool (Tof-SIMS) and hydrogen bonds seem playing a key role to explain differences between APMS *vs* TMPS. In this context CNF nanopapers with interesting properties have been obtained but also possibility of silsequioxane design were discovered. Indeed reaction between APMS and TMPS to create silsesquioxane particles was investigated. The influences of silane concentration in water as well as catalyst (or co-crosslinked silane) proportion were determined as key parameters in tuning particles size

*(Chapter 1.3.1)*. It appears that the synthesis of these particles was also possible inside the CNF network. It is probably the CNF interaction with organotrialkoxysilanes and their steric hindrance that permit the synthesis of ten times smaller particles. This modification brings a hydrophobic character to the formed nanopaper. It was also demonstrated that the amine content at the surface was sufficient to bring an antibacterial activity when 12 wt% APMS was included in the material *(Chapter 1.3.1)*. These results were highly novel and very promising to obtain rough and hydrophobic CNF network which could be used in coating. Table 2 and Table 3 are providing key results and perspectives of the *Chapter 2* respectively.

In the **second part**, knowledge and properties obtained in *Chapter 2* were applied to papermaking coating in order to reach non-wetting, greaseproof, anti-adherent or antibacterial paper.

The specific film forming behavior of APMS was demonstrated in this part showing very thin layer and very good grease barrier. Unfortunately, the addition of CNF in the suspension in order to improve its viscosity and barrier properties but also to lower the coating grammage of silane was proved to affect negatively their property. Also, antibacterial properties of such CNF-Silane coated paper were not sufficient probably because of too low amine quantity on the surface. For these reasons, evaluation of higher grammage coating would be interesting data to investigate. The antiadherence of the paper was better with the coating but did not reach sufficient value for industrial application. Same conclusions were observed with CNF-silsesquioxane coating. However both coating showed very interesting hydrophobic properties *(Chapter 2.1)*.

CNF were thus evaluated as a binder in the coating formulation of superhydrophobic paperboard biomimicking the nature. Different hydrophobic CNF, commercially available, CNF-polyorganotrialkoxysilane and CNF-silsesquioxane were tested with hydrophobic calcium carbonate particles. The innovative idea was to provide a solution for obtaining with a one-step coating a superhydrophobic surface. Commercial and CNF-silsesquioxane were found to provide interesting results. CNF permits to keep superhydrophobic properties or to stay close to it and to avoid coating layer crackling effect. As particles retention was lower than the conventional latex binder, further investigations on this point is proposed (Table 2 and Table 3). Lastly, such superhydrophobic coatings were assessed as potential anti-adhesion surface for bacteria. Promising results as a proof of concept were shown and

further implementation of antibacterial activity could lead to an interesting new paper functionalization.

As a conclusion, this work provides new results on the understandings of cellulose nanofibrils modifications with organotrialkoxysilanes. Very few studies were carried out on the use of modified nanocellulose in papermaking industry. This approach is giving innovative pathway from biomimetism toward paper functionalization. Table 3 summarizes possible perspectives in each chapter. It is hoped to provide starting research for further industrial development with the industrial partner future product development.

**Table 3. Perspectives of the overall PhD project.**

| Scientific issue | Perspectives |
|---|---|
| **Chapter 2**<br><br>**Cellulose nanofibrils chemical, physical and physico-chemical modification with poly-organoalkoxysilane or silsequioxane** | *CNF modification with poly-organotrialkoxysilane*<br>• Continue ToF-SIMS investigations to confirm molecule organisation<br>*CNF film structuration*<br>• Investigate other micro-molding fabrications<br>*CNF modification with silsesquioxane particles*<br>• Investigation of particles interaction with petri dish to overcome side effect<br>• Suspension imaging<br>• Particles formation on CNF film surface |
| **Chapter 3**<br><br>**Modified CNF potential applications in paper functionnalization** | *Paper modification with CNF and poly-organotrialkoxysilane*<br>• *Evaluate higher grammage coating*<br>• *Evaluate different coating technics*<br>*Modified CNF as binder in superhydrophobic coating formulation*<br>• Optimize particles attachment<br>• Do other pilot scale trials<br>• Try to replace oleate by other hydrophobizing material<br>*Superhydrophobic paperboard for bacterial anti-adhesion*<br>• Carry out quantitative testing<br>• Carry out measurement with CNF-silsesquioxane binder |

# French Abstract

# Résumé français

L'industrie papetière produit mondialement chaque année 400 millions de tonnes de matériaux. Le papier est omniprésent dans notre quotidien. Il est un support de communication, emballe nos aliments ou encore décore notre intérieur. Au niveau mondial, l'Europe se voit de moins en moins compétitive face aux marchés asiatiques grandissants qui mettent en place des machines à hauts rendements, sans compter l'arrivée du tout numérique qui a nettement impacté l'utilisation du papier. En conséquence, ces dix dernières années, les entreprises fabriquant des papiers dits « de commodités » à faible valeur ajoutée, comme le papier impression écriture, rencontrent des difficultés économiques, se focalisent sur la baisse des coûts ou se sont diversifiées. L'Europe conserve cependant une forte position dans le secteur des papiers dits « spéciaux », qui ont une haute valeur ajoutée mais aussi dans l'emballage ou les papiers d'hygiène.

Les papiers spéciaux se caractérisent par des propriétés plus complexes, dues à leurs caractéristiques physiques ou chimiques ou de surface. Ce sont, par example, les billets de banques, les papiers cigarettes, les papiers décor pour stratifiés, les papiers thermique, les papiers de filtration, les papiers dorsale d'étiquette anti-adherents, les papiers d'emballage ingraissables. Souvent utilisés dans des secteurs contraignants comme l'alimentaire ou le fiduciaire, ils sont soumis à des normes gouvernementales. Une de leur définition intrinsèque étant de répondre à un besoin spécifique, ils sont soumis aux évolutions sociétales. Ainsi, il est possible d'identifier aujourd'hui cinq facteurs majeurs impactants la recherche et le développement dans ce secteur : une augmentation des contrefaçons et un besoin de sécurité, la digitalisation, une forte demande de respect environnemental et de solutions biosourcés durables, de respect de la santé et enfin à l'évolution de la société vers un mode de vie « rapide » et individuel.

Dans ce cadre-là, les papiers ou cartons dit « ingraissables », souvent utilisés dans l'emballage de fast-food ou dans l'emballage d'aliments pour animaux se sont vus visés par une directive européenne. En effet, l'un des composants essentiels de la composition de la sauce de couchage, les perfluoropolymères ont été bannis du marché pour problèmes

environnementaux en 2008. La recherche de solutions est toujours d'actualité aujourd'hui, avec notamment la demande de l'utilisation de produits plus naturels.

Dans un autre cadre, plus médical, il n'est pas sans savoir que l'agence européenne de santé alerte depuis plusieurs années sur l'augmentation de la résistance antimicrobienne. Cette résistance implique que les traitements actuels de certains virus ou microbes deviennent inefficaces sur des souches qui ont mutées. Ce phénomène est apparu en partie à cause de l'utilisation excessive d'agents biocides par relargage. Outre le fait de polluer l'environnement, ces agents biocides sont diffusés dans le milieu ce qui permet aux souches de muter en souches résistantes. Pour limiter ceci, deux approches peuvent être envisagées afin de réduire le potentiel de pollution microbienne : le bactéricide par contact ou l'anti-bioadhésion des surfaces. Cette dernière ne permettant pas de « tuer » les bactéries mais d'empêcher leur prolifération sur une surface spécifique.

Ainsi, ce projet vise à l'élaboration de nouveaux revêtements pour des papiers spéciaux à très faibles grammages (< 60 g/m²). Ces revêtements devront avoir plus spécifiquement l'une des propriétés suivantes : être anti-adhérents, ingraissables, superhydrophobes ou antibactériens. Dans le cadre d'une démarche environnementale, il est proposé dans ce projet d'utiliser principalement des nanocelluloses (Figure 1), matériaux bio-sourcé issu du bois, en tant que vecteur de ces propriétés.

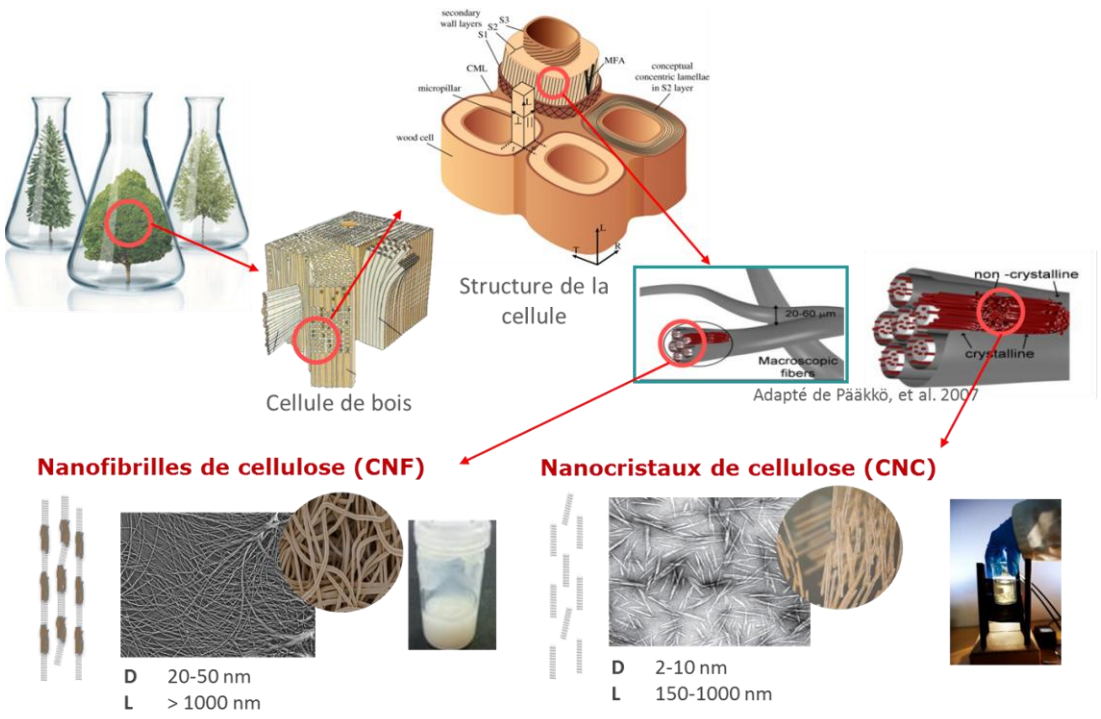


**Figure 1. Schéma récapitulatif de l'extraction des nanocelluloses du bois.**

**Les nanocelluloses** sont des nanoparticules extraites de la cellulose venant de la biomasse végétale. Elles sont biodégradables, très hydrophiles à cause de leur groupement hydroxyles et possèdent un facteur de forme très important. Elles se distinguent généralement en deux catégories, les nanocristaux de cellulose (CNC) et les nanofibrilles de cellulose (CNF). Les CNC sont des bâtonnets rigides et très cristallins assimilables à des « grains de riz » alors que les CNF sont des filaments souples plus long et capables de s'enchevêtrer assimilables à des « spaghettis ».

Dans ce projet, uniquement les nanofibrilles de cellulose (CNF) ont été utilisées. A l'état de suspension aqueuse, leurs grande surface spécifique ainsi que les nombreux groupements hydroxyles présents naturellement dans la cellulose leur confèrent une grande réactivité chimique mais aussi en font une suspension visqueuse à faible teneur en matières sèches et aux propriétés rhéo-fluidifiantes. A l'état solide, les « nano-papiers » de CNF sont denses, translucides, barrières à l'oxygène et aux graisses. Ces propriétés ajoutées à leur caractère biosourcé et biodégradable intéressent fortement les papetiers. L'innovation consisterait à les fonctionnaliser pour apporter de nouvelles propriétés. Elles pourront donc être utilisées, après modification, comme agent de couchage pour surface anti-adhérentes ou hydrophobes, voire superhydrophobes ou antibactériens. La figure 2 reprend l'organisation du manuscrit et souligne le passage de la modification physico-chimique des nanocelluloses (Chapitre 2) à l'application dans le domaine des papiers spéciaux.

Pour créer des papiers avec des surfaces anti-adhérentes, c'est l'énergie de surface qui doit être abaissée, et une macro-structuration peut éventuellement favoriser l'anti-adhérence. Afin d'obtenir des propriétés superhydrophobes, deux paramètres sont nécessaires : la

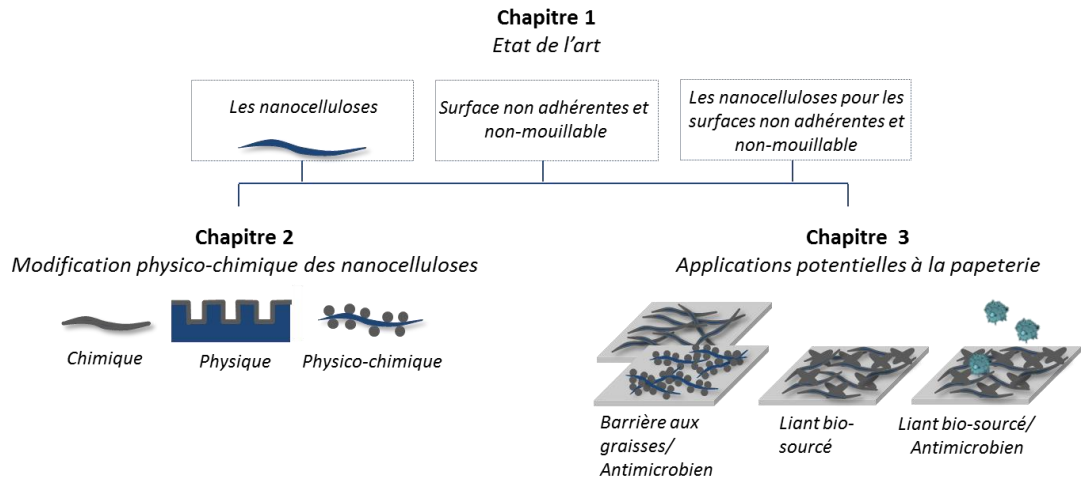


**Figure 2. Schéma récapitulatif de l'organisation du manuscrit.**

structuration de la surface ainsi que la modification du caractère hydrophile. Enfin, obtenir des propriétés antibactériennes ou d'anti-bioadhésion peut se faire par le greffage d'agent biocide dans le premier cas et par un revêtement ayant pour effet de ne pas rendre possible la formation d'un biofilm.

**La première partie du projet** (chapitre 2) s'est donc orientée sur l'étude de la modification chimique et de la structuration des films de CNF. L'utilisation d'organotrialkoxysilane a été choisie pour leur versatilité chimique mais aussi pour leur possible industrialisation en utilisant uniquement des milieux aqueux. Leur structure, proche du silicone, peut créer des surfaces hydrophobes et anti-adhérentes tout en apportant une autre fonctionnalité comme un agent bactéricide. Les interactions entre les CNF et trois organotrialkoxysilanes: Aminotrimethoxypropylsilane (APMS) ; trimethoxypropylsilane (TMPS) et trifluoro trimethoxypropylsilane (TFPS) ont été étudiées. Il a notamment été montré par une étude cinétique en RMN du Silicium à l'état solide ainsi que l'utilisation de technique de surface type TOF-SIMS que l'APMS interagissait de manière très différente par rapport aux deux autres. Il permet d'obtenir un caractère hydrophobe beaucoup plus prononcé mais aussi des propriétés filmogènes et barrières à l'oxygène très intéressantes. La présence de l'amine est aussi envisageable comme biocide.

Dans un second temps, c'est la structuration des films de CNF afin de leur conférer un caractère superhydrophobe qui a été étudiée. Pour cela, l'utilisation innovante de particules micro- nano-structurées formées en solution aqueuse avec les organotrialkoxysilanes et appelées silsesquioxanes a été proposée. La formation de particules et les paramètres influençant sur celle-ci ont été déterminés. Ensuite, c'est la fabrication de ces particules au sein des suspension des CNF et leur effet sur les propriétés hydrophobes qui a été faite. Il a été montré pour la première fois que le réseau des CNF et leur viscosité entraine la réduction des tailles de particules de silsesquioxanes et que les nano-papiers fabriqués possèdent de très bonnes propriétés hydrophobes ainsi qu'antibactériennes. Une reflexion sur une surface structurée modèle et différents paramètres de formes a même été lancée pour identifier les paramètres de rugosité et de distribution qui seraient clefs pour la suite sur les papiers spéciaux.

Ainsi ce chapitre a permis d'évaluer dans le contexte d'élaboration d'une surface anti-adhérente, superhydrophobe et antibactérienne des axes de recherches sur la chimie, la

physique et la physico-chimie appliqués à la cellulose nanofibrillée associée à des alkoxysilanes en milieu aqueux.

**La deuxième partie** (chapitre 3) a permis l'évaluation de ces résultats fondamentaux dans un contexte appliqué.

Tout d'abord, les nanocelluloses fonctionnalisées ont été évaluées en tant que liant dans une formulation utilisant des carbonates de calcium pour apporter la rugosité. L'objectif était de rendre superhydrophobes un carton en remplacement d'un produit pétro-sourcé. Les nanocelluloses ont eu un effet positif sur la couche en permettant de diminuer les craquelures tout en conservant le caractère superhydrophobe, le tout obtenu en une seule étape de couchage.

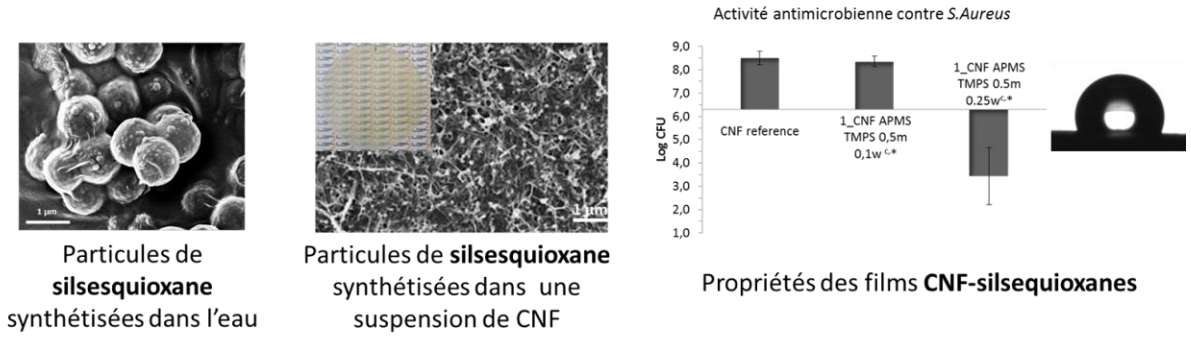


**Figure 3. Illustration des principaux résultats de l'étude sur la synthétisation de particules de silsesquioxane dans le réseau de CNF.**

Cette preuve de concept réussie, nous avons continué en modifiant la surface d'un papier par couchage de nanofibrilles modifiées par l'APMS ou par les silsesquioxanes. L'objectif était d'obtenir un papier spécial en terme d'anti-adhérence, hydrophobie et antibactérien. Seul un caractère hydrophobe prononcé a pu être obtenu avec une baisse légère de l'adhérence du papier. Il a été montré que la quantité nécessaire de couche afin d'obtenir un papier antimicrobien était toutefois trop faible dans ce cas-ci. Nous avons malgré tout continué notre démarche en passant à l'échelle pilote par un couchage bobine – bobine de notre meilleure formulation (Figure 4). Des résultats prometteurs concernant le caractère superhydrophobe ont été obtenus et une analyse plus complète, voir un essai à l'échelle industrielle, mériteraient d'être poursuivi.

Finalement, des essais d'adhésion microbienne ont été réalisés sur ces cartons fonctionnalisés afin d'ouvrir des perspectives pour l'emballage. Des premiers résultats qualitatifs se sont montrés prometteur pour une approche novatrice du concept d'antibactérien dans le cadre des papiers.

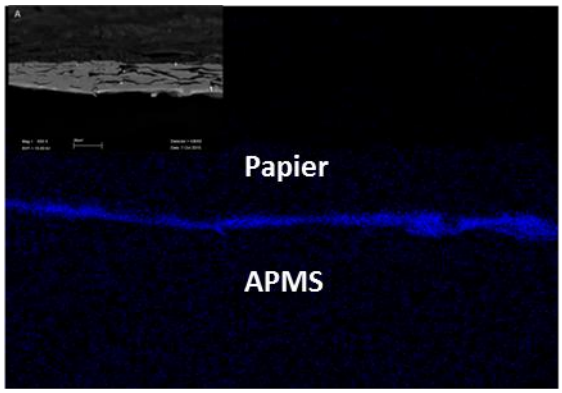


**Effet filmogène de l'APMS** sur le papier

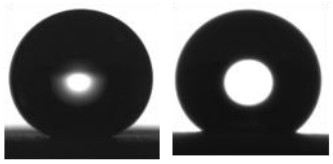


**CNF comme liant** pour formulation superhydrophobes

**Figure 4. Illustration des principaux résultats sur l'étude de l'application des CNF et des organotrialkoxysilanes dans la papeterie.**

En conclusion, ce projet s'est intéressé à l'interaction nanocellulose-organotrialkoxysilane et à la modification chimique et physico-chimique des CNF. Ainsi ces études ont permis l'évaluation du potentiel d'applications dans l'industrie des papiers spéciaux dans la recherche d'un papier anti-adhérent, superhydrophobe et antibactérien. Les interactions CNF et aminopropyl silane sont très intéressantes et complexes à interpréter. Cette thèse apporte quelques explications. En parallèle, les nanocelluloses ont un fort potentiel dans le couchage de papier et pour la première fois une solution a été proposée pour obtenir en une seule étape de couchage une surface superhydrophobe. Leur modification rendue très facile grâce aux organotrialkoxysilane en milieu aqueux semble pouvoir leur conférer d'autres propriétés. Ces dernières devront être encore optimisée mais le passage à l'échelle pilote a été validé et des perspectives pourraient s'envisager à l'échelle industrielle pour remplacer des solutions toxiques ou pétro-sourcées. Cette thèse ouvre donc la voie de l'obtention de papiers spéciaux de nouvelle génération une fois certains verrous levés tout en répondant aux questionnements liés aux interactions nanocellulose et aminosilane.

# Appendix n°1

# Appendix n°1.

## Bacterial adhesion measurement on superhydrophobic one side-coated paperboard

### Introduction

Interest has grown for antibacterial surfaces during last decades because of the need to avoid bacterial growth for example in food packaging or in hospitals to avoid nosocomial infection. Solutions are mostly based on leaching of active component from the material and EU raised the problem of antibacterial resistance which might be one of the first health challenges by 2040 (Kaur and Liu, 2016). New non leaching antibacterial surfaces are thus needed to avoid this antibacterial resistance development in developed countries.

In order to overcome such a problem, mainly two solutions have been investigated. The first one is straight and consists in immobilizing antibacterial molecule on the substrate surface. Several publications are proposing contact active antibacterial properties by grafting molecule on vector or directly on the material. Such strategy can be applied on cellulose, metal or glass for example and use in medical environment to kill directly bacteria on their surface when they start to colonize it (Fuchs and Tiller, 2006), (Saini et al., 2016a). The second is relying on anti-biofouling strategy. Biofouling is part of the cyclic microbial development in water and is defined by the adhesion of bacteria on the surface, which consequently form a biofilm, a special arrangement of the bacteria protecting it (O'Toole et al., 2000). Before and after biofilm, bacteria are in a "planktonic" state, meaning they are suspended in water and can colonize surfaces in surroundings. Antibiofouling property is reached by adaptation of the surface topography, mechanical properties and chemistry. It is reported that both combine approaches is the most efficient way to obtain an antibacterial material. In anti-biofouling approach, the surface functionalization with poly(ethylene glycol) (PEG) is often envisaged as a non-adherent surface toward proteins whose attachment is favorable for biofilm (Banerjee et al., 2011), (Bearinger et al., 2003). Water repulsive surfaces also called superhydrophobic and based on a nature mimicking system were also evaluated. As reviewed by Zhang et al. (2013) such an approach could reduce the force

between the substrate and the bacteria, thus permitting their easier removal before biofilm formation. The efficiency of superhydrophobic surfaces upon bacterial adhesion is still giving very contradictive results from study to study. This is explained by differences in measurement methods but also in bacteria choices whose size and morphology possibly affect results (Fadeeva et al., 2011). However, it was demonstrated several times that superhydrophobic surfaces are also limiting proteins absorption (Stallard et al., 2012), (Pernites et al., 2012).

Cellulose nanofibrils are a biobased material (Abitbol et al., 2016) with high hydroxyl group density which can be used as a versatile grafting site for different molecules (Habibi, 2014). Especially, CNFs could be used as a template for non-leaching antibacterial agent carrier (Saini et al., 2016b). Bacterial adhesion of CNF film modified by titania and 1H,1H,2H,2H-perfluorooctyl trimethoxysilane (PFOTMS) monolayer has been also investigated. The amphiphobic resulting material showed no bacterial adhesion of *E.Coli* strain after 1 min contact with the inoculum (Jin et al., 2012).

Recently it has been shown that CNFs can also be used as coating binder for one step paperboard superhydrophobic functionalization (Arbatan et al., 2012), (Reverdy et al., 2016). Surface can be structured by precipitated calcium carbonate (PCC) previously hydrophobized by sodium oleate giving rise to low water adhesion and high contact angle (150°).

In this study will be compared antibacterial activity, bacterial growth and adhesion on superhydrophobic and non superhydrophobic paperboard surface made with CNFs or with traditional latex styrene butadiene binder. Assessments are done with gram positive, i.e. *Staphylococcus Aureus* bacteria and *Bacillus Subtilis*. Materials are first compared in terms of water contact angle and water absorption.

## Material and methods

### Material

Coating suspensions were processed in water. Acicular aragonite precipitated calcium carbonate (PCC) (Sturcal H, Mineral Technologies Inc.) were the main material, used in order to provide micro and nano roughness to the coated layer. Sodium oleate (88-92%, Riedel-de Haen) was integrated in the suspension to provide calcium carbonate hydrophobic property. Styrene butadiene latex (DL-930, Dow Chemical), used as reference coating binder, has a 5°C glass transition and a dry matter content of 50%. Cellulose nanofibrils (CNF) were manufactured from bleached birch kraft pulp, mechanically and enzymatically pretreated and passed five times through a homogenizer (Ariete, GEA) and were delivered by CTP (France). The resulting suspension has dry matter content around 2wt%. A similar AKD nano emulsion hydrophobized grade was purchased to InoFib, France to obtain reference hydrophobized binder. CNF were also silane modified by simple adsorption of amino propyl trimethoxy silane (APMS) at a range of 20 wt%. CNF-APMS were used as hydrophobized binder carrying antibacterial molecule (amine).

Commercial Neverwet ® coating was also applied as a comparison and standard superhydrophobic layer.

The substrate was chosen to be a coated paperboard of 232 g/m² (Cupforma natura, Stora Enso).

### Methods

#### *Coating suspension preparation*

Following steps were done for obtaining the coating suspension formulations. First, sodium oleate was dissolve at 45°C for 10 min. Then, aragonite is added and mix for at least 20 min at around 30 wt% with respect to water. In the case of CNF-APMS r10 formulation part of CNF suspension was added previously to aragonite in order to reach this value. Finally, the binder: CNF AKD (5 wt%), CNF-APMS (9 wt%) or latex (20wt%) is added. Initial water is added to provide dry matter content of 18, 15 and 33% respectively for each binder.

#### *Coating procedure*

Coating was done with a laboratory scale bar coater (RK coater) depositing a 40µm wet film thickness. Coated cardboard were dried in air circulation oven for 2-3 minutes at 90°C for

latex and CNF-APMS formulations and 120°C for CNF-AKD one, in order to activate AKD hydrophobization layer.

*Surface properties measurement*

Measuring surface properties in term of water repellency and absorption permit the comparison and explanation in final bactericidal or adhesiveness toward bacteria. Static water contact angle was measured by optical device (OCA, Dataphysics) coupled with an analytical software to measure the angle made by the 5 µL water drop at the triple line. Same optical device was used for measuring water shedding angle by tilting the samples before depositing a 9µL water drop from a constant distance.

Water absorption was evaluated through the deposition of a red colored 5µL water drop on the sample surface. The drop was let on the sample for 2h and pictures permitted to quickly observed differences between coatings.

## Microbiology measurements

Three different methods were employed for quantifying or observing antibacterial effect of coating as well as bacterial adhesion:

*Antibacterial activity measurement*

AATCC test method 100-1998 was used for quantifying antibacterial activity of surfaces depending on the composition of the coating (oleate, latex,…). Briefly, bacteria in an inoculum approaching $10^5$ CFU/mL is deposited on the surface and let in incubator for 24h. Innoculum is extracted from the sample and colonies are then plated and counted. The difference between initial CFU/mL and final concentration permits to check the efficiency of antibacterial activity, of the sample. If a 2 log reduction is observed, the sample is considered as antibacterial, if a raised in concentration is measured, the samples has no antibacterial effect and if a constant concentration is measured, there is a bacteriostatic effect.

*Bacterial adhesion measurement*

Bacterial adhesion was measured by two different ways. The first one is a modification of AATCC test method 100-1998. Indeed, before extracting inoculum of the sample after the 24h incubation, the sample was washed with saline solution for 30 s. This way, it was expected to extract and count only bacteria coming from the adhesion onto the sample. A second protocol was established to permit the evaluation of all surfaces. Indeed, the deposition of inoculum on surface coated with commercial solution was not possible. As only

one side was coated and there was a risk of inoculum absorption from borders, a silicon sealant was used to fix the sample on a glass plate and provide a thick waterproof barrier to avoid its leaking. The functionalized surface was then immersed with 0.5 mL of a $10^5$ CFU/mL and let in contact for a desired time. The inoculum was washed out of the surface and subsequently washed six times with a 9 g/l saline solution and cut. Piece of sample were then directly poured plate in nutrient agar and let for 24h in incubation. Bacteria colonies

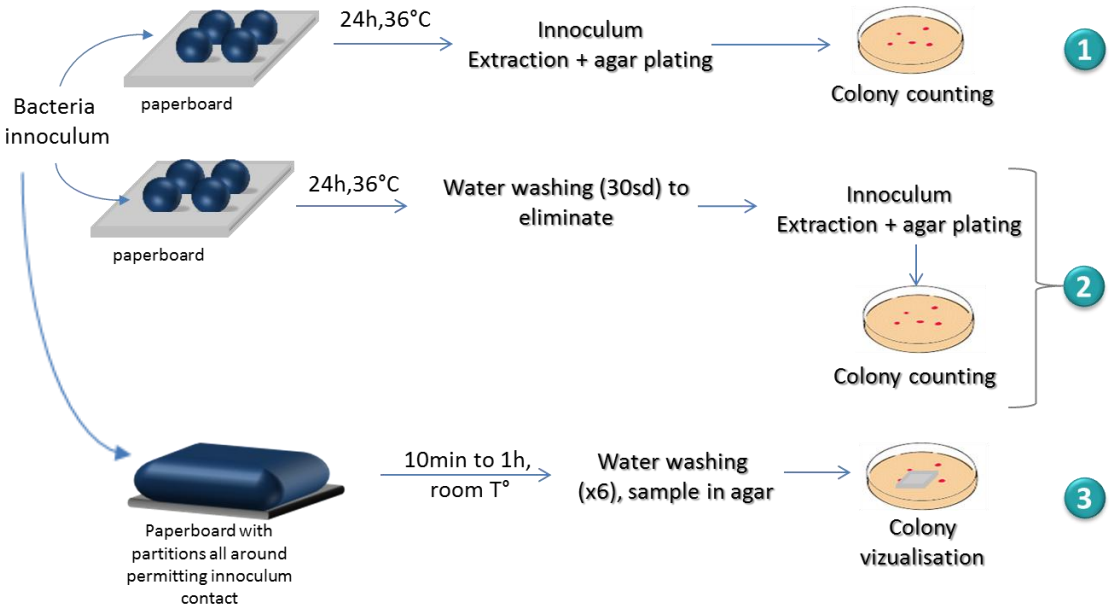


**Figure 1. Antibacterial activity and bacterial adhesion measurement methods scheme. 1: ATCC 100-1998 2: Modified ATCC 100-1998 and 3: developed protocol for assessing one surface only.**

were checked after incubation.

## Results and discussion

### *Surface properties*

As seen in Chapter 3.2 section, the functionalization with PCC, latex and sodium oleate is showing evidence of superhydrophobic state, as well as the formulation with CNF-AKD as shown in Figure 2. High loading PCC formulation with CNF-AKD achieved superhydrophobic 150° water contact angle. With CNF-APMS, contact angle of 125° was obtained. Lower amount of PCC has for consequence the drop of contact angle. The commercial Neverwet® coating was not measurable because the water drop is not staying on the surface and thus the image couldn't recorded. Such a behavior is typical of an extremely high superhydrophobic state, also called self-cleaning effect. Water shedding angle of this sample was thus 0° while SH-Latex r4 depicted a WSA of 2.5° and SH-CNF AKD of 17°. All the other surfaces were measured above 90°.


**Figure 2. Water drop image on surfaces after 5 s and subsequent measurement of contact angle at the triple line.**

Observation on absorbancy of a water drop showed that all coatings are depicting absorption at different scale. The coating SH-CNF AKD r20 does not permit long term water repellency as shown by Figure 3 after two hours. The water droplet started to get absorbed through the CNF layer after several minutes and rapidly spread into this CNF network layer.

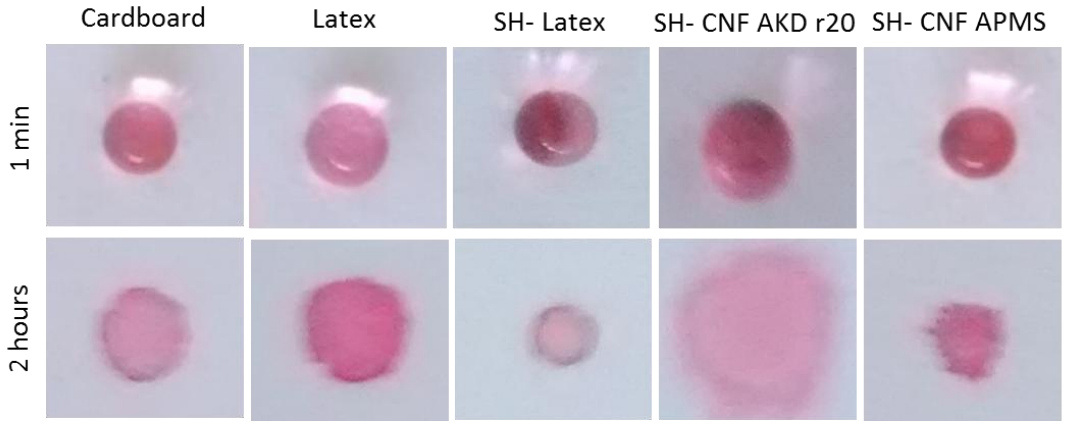


**Figure 3. Colored water drop images on sample surface after 1 min and after 2 hours (complete evaporation).**

The failure of CNF grafting with AKD, is probably the consequence. SH-CNF-APMS depicted

less absorption even though irregularities around frontiers are typical of a spreading through the material. In this case, the water is evaporated without penetrating the substrate. Almost no absorption was observed for SH-latex and bigger surface are observed with cardboard and latex due to the only hydrophobic state (and not superhydrophobic) leading to a higher spreading of the droplet. The next experiments will focus on this SH latex reference as it is supposed that no bacteria penetration is possible.

*Antibacterial assessment of the one step SH-latex coated paperboard*

Samples were first assessed for antibacterial activity in order to detect if one of the suspension ingredient was carrying bactericidal molecule. As shown in Figure 4, cardboard and latex alone possess bacteriostatic effect. However, when cardboard is coated with PCC, latex and oleate, leading to SH-latex sample, it could be considered as well as bacteriostatic but with a higher tendency to grow bacteria. As the cardboard is manufactured for beverage application, it would not be surprising to have a bactericidal molecule inside even though the information is not confirmed. In the latex as well, same is happening to obtain long-lasting emulsion without molds proliferation. The higher proportion to grow bacteria for SH-Latex could be the non-contact with these two parts due to high coating of PCC on the surface. For superhydrophobic Latex/PCC/Oleate formulation, the slight water adhesion defining the material is probably a center of bacteria anchoring and growth. Indeed, the disruption of air pockets over time at the interface leads to bacteria-surface contact (Truong et al., 2012). Oleate is proved to have no effect in killing.

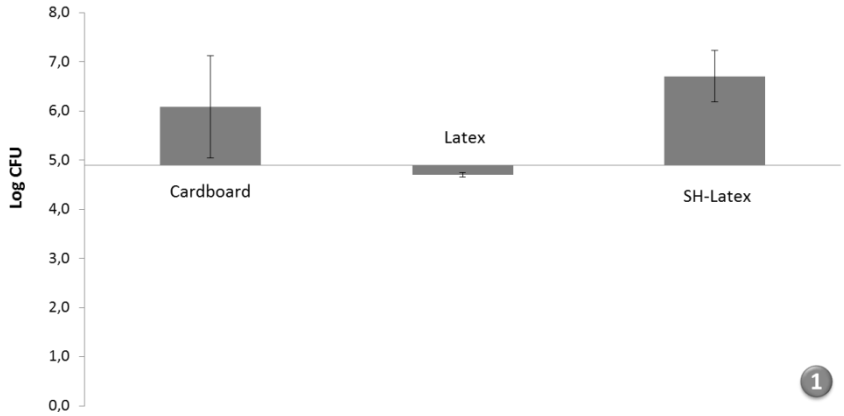


**Figure 4. Antibacterial activity measurement of cardboard surface, latex coating and SH-latex coating (PCC, latec, oleate).**

Modified test method consisting in measuring bacteria on the sample after washing for 30 s with saline solution was done for cardboard, latex coating and SH-Latex coating as well. Over 24 hours, and as confirmed by water adhesion test, the inoculum was totally adhering

to the material and no roll-off was possible anymore. Surprisingly, cardboard and latex coating seems to retain fewer bacteria on the surface than SH-latex coating as shown in Figure 5. SH-coating roughness is probably limiting bacteria washing while a growth inside the roughness is going on. This has been already observed by Scheuerman et al. (1998) on etched silicon substrates (but not superhydrophobic). On superhydrophobic lotus-like surface made with titanium, Truong et al. (2012) observed the concentration of bacteria in grooves and proposed a mechanism where trapped air between edges act as a barrier for bacteria adhesion and concentrate at this locations. While air bubbles disappear after long immersion (above 1h), and consequently the superhydrophobic state, the surface grooves

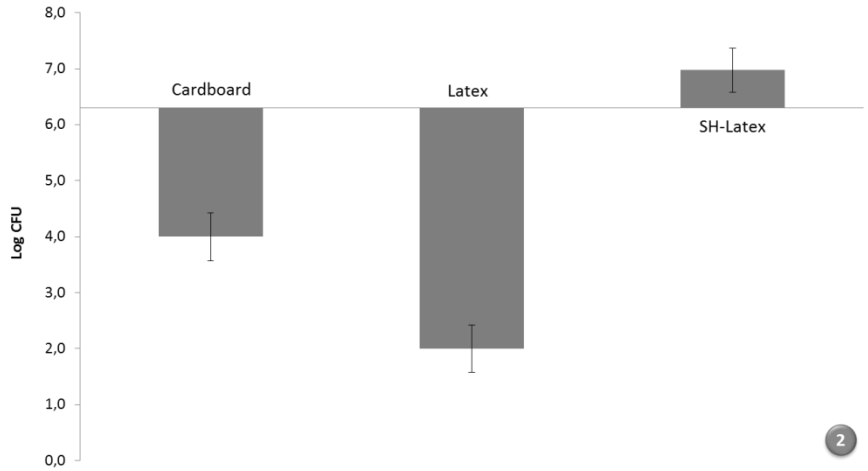


**Figure 5. Colony forming unit measured with the modified ATTCC 100-1998 expressed in log.**

get contaminated faster. This result could be linked to the time of contact between surface and inoculum (i.e. 24h), which is long comparing to water surface adsorption. This possibly favored the creation of a large anchored biofilm protecting bacteria against water washing along time. At the opposite, the surface wetting on paperboard and latex coated paperboard being smaller and smoother, and the adhesion is perhaps more limited in the range of 24h.

*Influence of contact time with bacteria*

Unfortunaltely, with this method, it was not possible to test commercial Neverwet® coating due to its high repellency of water and consequently of inoculum.

The last method permitted to assess all coated surfaces, even the commercial one, because of the forced contact with the surface during the considered time. It was used also to evaluate if there is a bacterial adhesion within shorter time (10 min and 1 hour). Bacterial adhesion was evaluated through a non-quantitative (observation) method. As demonstrated

by Figure 6, all surfaces displayed bacterial adhesion, even the commercial coating. It was noticed that a lower amount of colony were present for SH-commercial and SH-Latex formulations. This could be explained by the robustness of the superhydrophobic state which is higher for these samples than to that achieved with SH-CNF-AKD or CNF-APMS. As further work, the antibacterial activity of Neverwet® coating should be assessed by an adapted method from ATCC 100-1998. It would permit a clear cut confirmation that the low bacteria colony amount is due to superhydrophobic state rather than bactericidal effect. A quantitative measurement would give comparable results with literature on superhydrophobic paper, where only 1 to 7% of *E. Coli* bacteria deposited on the samples were found to be able to stay on the surface depending on washing method (water immersion or roll-off respectively) (Yang and Deng, 2008). However, the contact time used in their study was sensibly lower: less than 5 s. Test with gram negative bacteria seems also to be interesting to perform.

Lower amount of colony was also observed for (SH)-CNF APMS which could be due to synergistic effect of higher hydrophobic character and antibacterial amine releasing but this result should be compared with CNF-APMS coating, as further work discussion.

| Samples/Time of adhesion | 10 min | 1h |
|---|---|---|
| Cardboard | +++ | +++ |
| SH-Commercial | + | + |
| SH-Latex | ++ | ++ |
| SH-CNF-AKD | +++ | +++ |
| (SH)-CNF-APMS | ++ | ++ |


**Figure 6. Comparative table for adhesion during 10 min and 1 hour for all samples. It is a qualitative view of observation of bacteria colonies in petri dishes as shown at the bottom of the table.**

## Conclusion and perspectives

Bacterial adhesion on one side coated paperboard was assessed through two different methods after testing coating materials as potential biocidal agent. A first method, involving a washing step with saline solution, showed that over 24h contact with bacteria, the SH-Latex sample retained higher quantity of bacteria than the paperboard itself or than that coated with latex. This is explained by the bacteriostatic effect of the two last samples but also possibly by the surface topography differences. A novel method was also carried out by forced contact between sample and inoculum during a period of time shorter than 24h. This method enables the comparison with commercial superhydrophobic coating suspension, as well. Through qualitative analyses of the results, it was noticed that the more durable superhydrophobic coatings, which showed no absorption of water over time but probably slight adhesion, were depicting the less bacterial colonization. Although SH-CNF AKD did not show such result because of rapid inoculum penetration inside the material, it is encouraging for the further new development of antibacterial packaging strategy because of the proof of concept obtained with commercial superhydrophobic coating.

As work development, the evaluation by a dead/alive assay in combination with confocal microscopy counting would precise quantitatively the bacterial adhesion as well as the effect of antibacterial agent inside the coating. The use of the CNF-silsesquioxane developed in Chapter 2.2 could also be interesting.

## References


Banerjee, I., Pangule, R.C., and Kane, R.S. (2011). Antifouling Coatings: Recent Developments in the Design of Surfaces That Prevent Fouling by Proteins, Bacteria, and Marine Organisms. Adv. Mater. *23*, 690–718.

Bearinger, J.P., Terrettaz, S., Michel, R., Tirelli, N., Vogel, H., Textor, M., and Hubbell, J.A. (2003). Chemisorbed poly(propylene sulphide)-based copolymers resist biomolecular interactions. Nat. Mater. *2*, 259–264.

Fadeeva, E., Truong, V.K., Stiesch, M., Chichkov, B.N., Crawford, R.J., Wang, J., and Ivanova, E.P. (2011). Bacterial Retention on Superhydrophobic Titanium Surfaces Fabricated by Femtosecond Laser Ablation. Langmuir *27*, 3012–3019.

Fuchs, A.D., and Tiller, J.C. (2006). Contact-Active Antimicrobial Coatings Derived from Aqueous Suspensions. Angew. Chem. Int. Ed. *45*, 6759–6762.

Jin, C., Jiang, Y., Niu, T., and Huang, J. (2012). Cellulose-based material with amphiphobicity to inhibit bacterial adhesion by surface modification. J. Mater. Chem. *22*, 12562–12567.

Kaur, R., and Liu, S. (2016). Antibacterial surface design – Contact kill. Prog. Surf. Sci. *91*, 136–153.

O'Toole, G., Kaplan, H.B., and Kolter, R. (2000). Biofilm Formation as Microbial Development. Annu. Rev. Microbiol. *54*, 49–79.

Pernites, R.B., Santos, C.M., Maldonado, M., Ponnapati, R.R., Rodrigues, D.F., and Advincula, R.C. (2012). Tunable Protein and Bacterial Cell Adsorption on Colloidally Templated Superhydrophobic Polythiophene Films. Chem. Mater. *24*, 870–880.

Saini, S., Yücel Falco, Ç., Belgacem, M.N., and Bras, J. (2016a). Surface cationized cellulose nanofibrils for the production of contact active antimicrobial surfaces. Carbohydr. Polym. *135*, 239–247.

Saini, S., Belgacem, M.N., Salon, M.-C.B., and Bras, J. (2016b). Non leaching biomimetic antimicrobial surfaces via surface functionalisation of cellulose nanofibers with aminosilane. Cellulose *23*, 795–810.

Scheuerman, T.R., Camper, A.K., and Hamilton, M.A. (1998). Effects of Substratum Topography on Bacterial Adhesion. J. Colloid Interface Sci. *208*, 23–33.

Stallard, C.P., McDonnell, K.A., Onayemi, O.D., O'Gara, J.P., and Dowling, D.P. (2012). Evaluation of Protein Adsorption on Atmospheric Plasma Deposited Coatings Exhibiting Superhydrophilic to Superhydrophobic Properties. Biointerphases *7*, 1–12.

Truong, V. k., Webb, H. k., Fadeeva, E., Chichkov, B. n., Wu, A. h. f., Lamb, R., Wang, J. y., Crawford, R. j., and Ivanova, E. p. (2012). Air-directed attachment of coccoid bacteria to the surface of superhydrophobic lotus-like titanium. Biofouling *28*, 539–550.

Yang, H., and Deng, Y. (2008). Preparation and physical properties of superhydrophobic papers. J. Colloid Interface Sci. *325*, 588–593.

Zhang, X., Wang, L., and Levänen, E. (2013). Superhydrophobic surfaces for the reduction of bacterial adhesion. RSC Adv. *3*, 12003–12020.

# Appendix n°2
# Posters

# TEMPO modified cellulose nanocrystals as a biobased cross-linker for Poly vinyl alcohol films to enhance oxygen barrier properties at high humidity

Reverdy Charlène [1], Raynaud Sébastien [1,2], Guérin David [2], Dufresne Alain [1], Belgacem Naceur [1], Bras Julien [1]

[1] Laboratory of Pulp and Paper Science and Graphic Arts – LGP2 UMR 5518 / CNRS – Grenoble INP – Agefpi
[2] Centre Technique du Papier, Grenoble

## Context and objectives

**Cellulose nanocrystals** (CNCs) are often studied as fillers in composites because of their high aspect ratio and strength, enhancing polymer overall mechanical properties. CNCs films exhibit very good **oxygen barrier** properties due to their high crystallinity, but thin films are usually brittle. **Polyvinyl alcohol** (PVA) is also interesting in terms of oxygen barrier properties and flexibility for packaging,. Both of these materials have the advantage and disadvantage of being able to create a high amount of hydrogen bonds giving them their strength but also making their barrier properties drop tremendously in **humid conditions**.

This study aims at improving the oxygen barrier properties of PVA films in humid conditions by reducing their water sensitivity through the incorporation of **bio based TEMPO modified CNCs** in the range of 5 to 20 wt%. Our route is to functionalise CNCs by TEMPO-mediated oxidation and use their carboxyl groups to crosslink PVA by **esterification**, thus reducing the available -OH and chain mobility in contact with water.

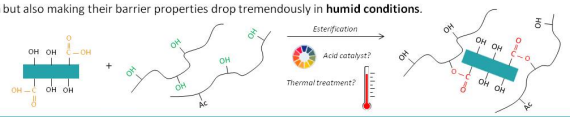


## Composite production and analysis

### Materials & Methods

**CNC**

Commercial source: The University of Maine

3,3 µm

**PVA**

Poval 6-98
n = 1 000

**Citric acid**

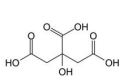

**PTSA**

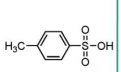

**TEMPO-mediated oxidation of CNC**

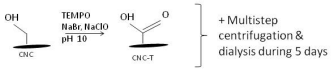


+ Multistep centrifugation & dialysis during 5 days

**Films casting and thermal treatment**

1. Solent casting (water)

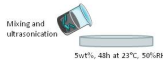


2. Thermal treatment

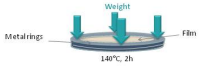


**Humidity absorption** / **Water absorption**

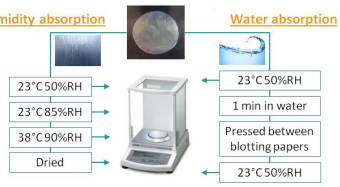


**Material characterization**

- **AFM** images were done at 3*3 µm using Nanoscope III, Veeco, Canada.
- **Conductometric titration** was done by dosage of a CNC-T suspension (pH<3 using HCl) with NaOH.

**Barrier characterization**

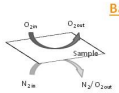


Oxygen permeability (OP)
23°C 50%RH and 23°C 85%RH
ASTM F 1927–98

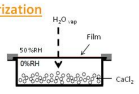


Water vapour permeability (WVP)
23°C 50%RH
TAPPI T 448 om-09

### Results & discussion

**Composite films**

| Formulations | Products ratios | | | |
|---|---|---|---|---|
| | PVA | CNC-T | PTSA | CA |
| 100:0 | 100 | | | |
| 95:5 | 95 | 5 | | |
| 80:20 | 80 | 20 | | |
| 95:5 PTSA | 95 | 5 | 0,5 | |
| 95:5 CA | 95 | 5 | | 0,5 |
| 100:0 CA | 95 | | | 0,5 |

✓ For each formulation we have **thermally treated** composites and **non thermally treated** composites

**TEMPO-oxidised CNCs (CNC-T)**

| | -[COOH] (µmol/g) | |
|---|---|---|
| CNC | 159 | ± 26 |
| CNC-T | 1550 | ± 83 |
| | **DO** | |
| CNC-T | 0,25 | ± 0,02 |

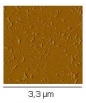

3,3 µm

✓ Carboxylic acids groups were **multiplied by 10** after TEMPO mediated oxidation as showed by conductimetric titration.
✓ AFM images confirmed a **low degradation** of CNC morphology. CNC oxidation was thus successful.

**Humidity absorption**

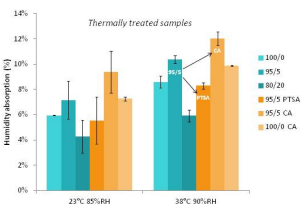


Reducing the humidity absorption
✓ **PTSA** as acid catalyst
✓ A **higher CNC-T ratio** of 20%

**Water absorption**

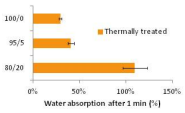


Non thermally treated samples
× Partial **solubilisation**
× **Stick** to the blotting paper

Thermally treated samples
× **High water absorption** with CNC-T
× No significant change using acids

**Water Vapour permeability**

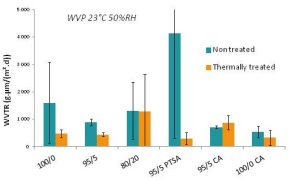


× No significant change in WVP is observed with the different samples.
✓ Barrier property is increase by **thermal treatment**.

**Oxygen permeability**

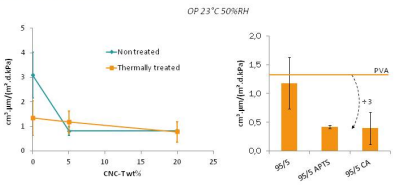


At 23°C and 50% RH, reducing the OP of PVA is possible by:
✓ Addition of **5% of CNC-T**
✓ Addition of **CA or PTSA** as acid catalyst followed by a **thermal treatment**
- Thus, thermal treatment of PVA can be avoided by addition of 5 % CNC-T. CNC-T might act as nucleating agent for PVA crystallization.

At 23°C and 85%RH:
× CNC-T addition and/or acids lowers the barrier
✓ At same CNC-T ratio, **acids improve the barrier**
- The increase in permeability at 23°C 85%RH might be due to the **hydrophilicity** of the CNC-T, especially as they bear **carboxylic groups**.
- Not enough **covalent bonds**?

## Conclusions & Perspectives

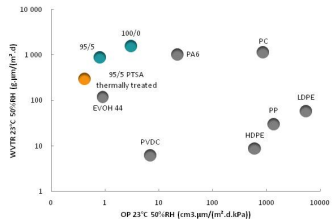


○ CNCs were **successfully TEMPO oxidised** but the esterification between PVA and CNC-T was not proved by FTIR. More precise data could be expected with NMR analysis.
○ The **water vapour barrier** was not significantly improved by addition of CNC-T and/or acids, only the **thermal treatment** had a positive effect.
○ The **oxygen barrier** of PVA films at 23°C 50%RH were improved by addition of 5wt% CNC-T. The nanocrystals might act as nucleating agent for PVA crystallization. It seems that **acids are beneficial** to the oxygen barrier as well, however at 85%RH this trend is not observed.
○ **Humidity absorption** from 50%RH to 85%RH showed a positive effect of the addition of **PTSA** and **20% of CNC-T**, proving changes of the material properties.
○ Compared to polymers used in industry for packaging, our films have very good **oxygen** barrier properties but the **water vapour** barrier should still be improved.

**Perspectives**

- NMR analysis
- Mechanical properties
- Higher CNC-T ratio with acids
- PVA + acid references

References
- Parallikar and al. , Journal of Membrane Science, 2008
- Lin and al. ACS Applied Materials & Interfaces, 2012
- Sirviö et al. ACS Applied Materials & Interfaces, 2015
- Nomer calculator, Independent Industrial polymer institute

Acknowledgment
- BRUZZESE SILLARD Cécile for AFM images

sebastien.raynaud@webCTP.com

# Xyloglucan and cellulose nanofibrils assembly for barrier material

Reverdy Charlène [*], Terrage Damien [*], Beury Nadège [¤], Moreau Céline [¤], Villares Ana [¤], Cathala Bernard [¤], Bras Julien [*]

[*] Laboratory of Pulp and Paper Science and Graphic Arts – LGP2 UMR 5518 / CNRS – Grenoble INP – Agefpi

[¤] UR 1268 Biopolymer, Interaction and Assemblies, INRA, F-44316 Nantes, France

## Abstract

Wood structure is complex and can be decomposed by chemical and mechanical treatment into several products. Cellulose at macro and nanoscale in form of fibers or crystals, hemicellulose and lignin are the major extractible components . Cellulose insure cell wall integrity. Extracted at nanoscale **cellulose nanocrystals** (CNCs) and **cellulose nanofibrils** (CNFs) demonstrate high mechanical properties as such but also good barrier properties regarding oxygen when rebuilt as a film[1]. Hemicellulose like **xyloglucans** (XG) plays important role in cell wall structure and wall flexibility insuring cellulose fibrils cohesion by interacting with it through hydrogen bonds. It can be extracted as a powder. **XG** doesn't interact in the same way with CNC depending on the XG/CNC ratio chosen [2]. The project focused on the influence of the presence of XG-coated CNCs on oxygen permeability, and water vapour permeability of composite CNF films but also on grease barrier property of a coated paper with the blend. Effect of thermal treatment was also investigated to check if hornification increases barrier performance.

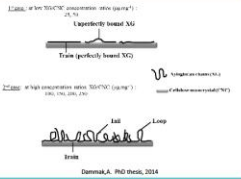


## Current collaboration work

### Introduction

This collaboration project named XYLOBAR was built by bringing together INRA Nantes research on **xyloglucans (XG)** and LGP2 knowledge on barrier properties measurement of CNF and CNC materials. INRA Nantes team proved that depending on xyloglucans ratio versus **celllulose nanocrystals (CNCs)** the arrangement of XG on nanocellulose surface was different. Thinking of wood construction in nature, this property could possibly be used for barrier property tuning as xyloglucan could act as a kind of double-side tape and could help in CNC/CNF interaction, limit pores and consequently increase barriers. Indeed it has been recently proved [3] that addition of CNC and thermal treatment favor barriers.

### Materials & Methods

**Materials**

XG of Tamarin were purchased from Megazyme as a powder. CNC and CNF were also commercial sources of The University of Maine and Centre Technique du Papier respectively.

**Films and coatings manufacturing**

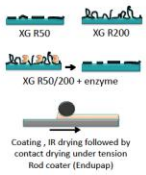


XG adsorption on CNCs was done by simply mixing both constituent for 18h at the desired ratio. When required, xyloglucanase was added to the blend and mix for 16h in order to remove all unbounded XG. Complexes were then centrifuged and dialyzed extensively.
Films were obtained by casting CNC/XG/MFC blend.

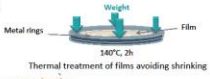


Thermal treatment of films avoiding shrinking

**Barrier characterization**

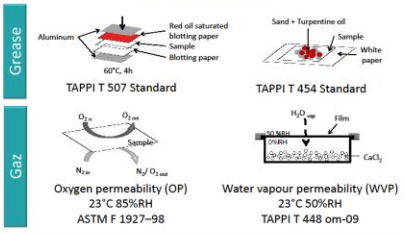


### Results & discussion

**Raw materials**

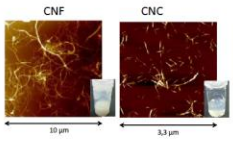


CNF and CNC were observed with AFM to measure dimensions of fibrils and crystals respectively of our raw materials.

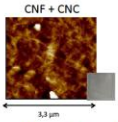


In films, CNF to CNC-XG ratio was 80/20 by weight. Film's surface were observed at the AFM and confirms nanostructure.

**Films**

**Water vapour permeability (50%RH)**

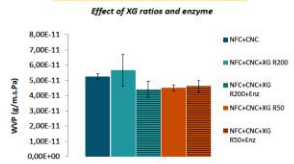


Addition of XG at different ratio in the matrix **doesn't affect significantly** water vapor permeability. Results are higher than literature probably because of high amount of xylose contained in CNC (20%). At 85% RH, same trend was observed.

**Oxygen permeability (85%RH)**

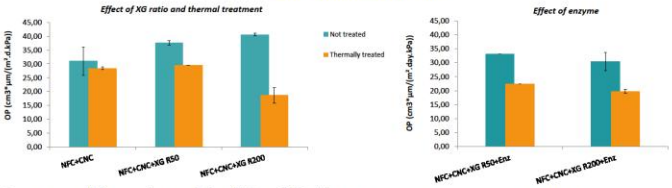


Oxygen permeability was decreased by addition of XG. This could be explained by the higher hydrophilicity of XG than cellulose so a higher sensitivity to the high humidity. But after **thermal treatment**, it shows that ratio 200 was beneficial to OP decreasing it by 50% when low decrease was observed without XG. Presence of XG favor hornification so improves barriers.

The enzyme removes any unbounded XG. Oxygen permeability dropped in each case confirming first hypothesis of destruction of barrier properties due to water sensitivity of XG. Both ratios react the same way with enzyme regarding OP and thermally treated samples shows close results from ratio 200 without enzyme action confirming the double side tape strategy.

**Coatings**

**Grease permeability**

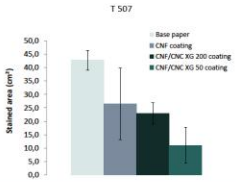


Coatings on thin paper (40 g/m²) was successfully achieved with rod coater. For each sample around **7g/m² ± 1** was applied on the surface by successive coatings and drying.
Homogeneous coating of CNF was difficult to achieve, explaining high standard deviation for T507 standard results. Both grease permeability measurement shows that there is a **greater impact of XG ratio of 50** than 200. XG seems to favor grease barrier by pores blocking.

T 454

| Sample | First stain time period | Stained area (*slow ****sample surface) |
|---|---|---|
| Base paper | 0<x<15 s | * |
| Paper + CNF | 0<x<15 s | * |
| Paper + CNF/CNC XG 200 | 0<x<30 s | * |
| Paper + CNF/CNC XG 50 | 60<x<180 s | * |

### Conclusions & Perspectives

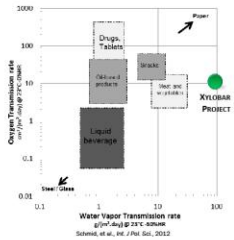


Films and coatings with CNF/CNC-XG blends were successfully produced. The presence of XG on CNCs was supposed to enhance cohesion between CNC and CNF to give better barrier properties of the material. About **oxygen barrier**, at 85%RH, the more XG added the less barrier is the material giving reason to believe that XG sensitivity toward water is impacting negatively the cohesion of the network. Enzyme treated films confirmed this hypothesis as OP values were decreased to almost reference values. Regarding **water vapor permeability**, no significant change was observed either at 50%RH nor at 85%RH. Probably, dissociate permeability of water vapor from water adsorption on films may show up a difference. When thermally treated, oxygen permeability decrease drastically with XG presence (enzymatically treated or not). Finally, coated paper with blends were proved to be more efficient against **grease permeability** when XG was added and specially at R50 ratio . R 50 ratio probably favors CNC-CNF cohesion, giving less permeability to the material to grease when tested at low relative humidity.

**PERSPECTIVES**

- OP at low RH
- Check films homogeneity with XG markers and AFM images on both sides of films
- Enhance water sensitivity by CNF chemical modification
- WVP of thermally treated films
- Water adsorption on films

**References**
[1] Lavoine and al, Carbohydrate Polymers, 2012
[2] Dammak and al., Biomacromolecules, 2015
[3] Bardet and al., Cellulose, 2015

**Acknowledgments**
- BRUZZESE SILLARD Cécile for AFM images

Julien.Bras@pagora.grenoble-inp.fr

# Superhydrophobic surfaces manufacturing with nanocellulose

Reverdy Charlène [*], Mazian Sedighi Moghaddam [¤], Mikael Sundin [¤], Agne Swerin [¤], Bras Julien [*]

[*] Laboratory of Pulp and Paper Science and Graphic Arts – LGP2 UMR 5518 / CNRS – Grenoble INP – Agefpi
[¤] SP Technical Research Institute of Sweden – Chemistry, Materials and Surfaces, Stockholm, Sweden

## Abstract

Researchers in natural fibers see opportunities in superhydrophobicity for fabrics or paper. The first challenge with natural fiber is their high hydrophilicity when the second is the perpetual search for water born coating in papermaking. These challenges were overcome by a one pot formulation comprising a latex binder, precipitated calcium carbonate and fatty acids to give their hydrophobicity to pigments [1]. In this study, we want to go further by replacing the petro-sourced latex with a new kind of fibers that are cellulose nanofibers (CNF).

Inspired by the Lotus leaf, superhydrophobic surfaces have been a center of interest in the last decade because of their high potential in industry for a variety of applications. It is seen as the next generation of surface for anti-fouling and corrosive retardant in navy industry but also in general anti corrosive materials industry. Now widely studied , mechanisms for manufacturing superhydrophobicity are well understood. Born from the alliance of low surface energy chemistry and physical structuration of surface, superhydrophobic materials give a water contact angle above 150° and a slidding angle below 10°.

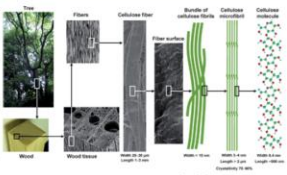


Isogai and al., Nanoscale, 2011

## Current collaboration work

### Introduction

Cellulose nanofibrils (CNFs) is a biobased and biodegradable nanoscale and fibrillar shape material extracted from trees. CNF tend to naturally form an entangled network that could possibly homogeneously disperse particles in coating applications for example.
In this study, cellulose nanofiber (CNF) is expected to act as a binder and dispersive agent for roughening particles that are essential for superhydrophobic surfaces.
This collaboration project between SP and LGP2 groups was done under COST Action ActinPack FP1405. Hereafter is presented the results of dynamic and static contact angle as well as SEM on coated surface.


### Materials & Methods

**Materials**

Acicular Aragonite (PCC) Sturcal H was provided by Specialty Minerals.
Sodium oleate (88-92%) was purchased from Riedel-de Haen.
Styrene Butadiene latex DL-930 was purchased from Dow Chemical. It has a Tg of 5°C and a dry matter content of 50%.
Neat nanocellulose manufactured from bleached birch pulp was purchased from CTP, France. AKD (Alkyl Ketene Dimer) hydrophobized reference CNF was purchased to InnoFib, France.
Amino propyl trimethoxy silane (APMS) 98% was purchased from Sigma Aldrich and used for modification of nanocellulose.
Substrate was chosen to be a paperboard of 230 g/m² from Stora Enso used for cups.

**Coatings preparation**

Coatings preparation include the following steps:
- Dissolve Sodium oleate at 45°C for 10min
- Add Aragonite and mix for at least 20min
- Add the binder and mix


**Measurements methods**

**Wetting measurements**

Wilhelmy method for measuring wetting properties as well as advancing and receding angle of porous and hygroscopic material is ruled by the following equation:

$$F(h,t)=P\gamma\cos\theta+Fw(t)-\rho Ahg$$

Samples were glued at the edge to avoid water penetration.

**Contact and roll-off angle**

Static contact angle measurements were done with a 5 µL water droplet.
Water shedding angle (WSA)[2] was measured by tilting the plate before dropping a 10 µL water drop to be able to compared with CNF based coating (water adhesion).

### Results & discussion

**Raw materials coating formulation**

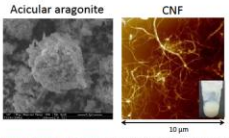


| | Composition of dry matter (wt%) | | | Dry Matter content (%) |
|---|---|---|---|---|
| | Pigments | Fatty acid | Binder | |
| Latex | 78,4 | 2,0 | 19,6 | 33,0 |
| CNF-APMS r10 | 88,9 | 2,2 | 8,9 | 15,0 |
| CNF-APMS r4 | 78,4 | 2,0 | 20,4 | 9,0 |
| CNF-AKD r10 | 91,0 | 0,3 | 8,7 | 15,0 |
| CNF-AKD r20 | 95,2 | 0,3 | 4,6 | 18,0 |

Different formulations had to be developed for replacing latex as the fatty acid was chemically altering the modified CNF. The high hydrophilicity of CNF as well as the higher water content was not favoring superhydrophobic state. Proportion of PCC had thus to be increased. Unfortunately, PCC seemed to leech off the surface with CNF when it is not the case in the presence of latex.

**Water shedding angle**

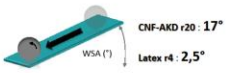


Water shedding angle was achieved with high loading PCC and CNF-AKD formulation. Roll-off angle was not measurable because of water adhesion on CNF-AKD r20 surface.

**Wetting measurements**

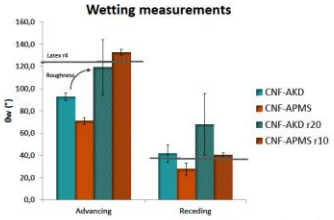


Wetting measurements were made only with one cycle as the sample became wet after withdrawal probably because of inhomogeneity in the coating and also absorption of water of CNF. Roll-off angle with an already tilted plate was achieved with high loading PCC and CNF-AKD formulation.

**SEM analysis**

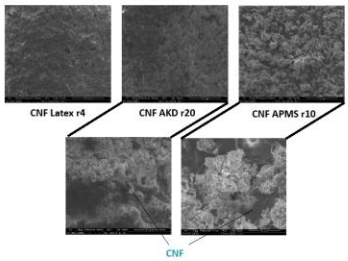


SEM images revealed surface topography of coated paperboard. When related to static water contact angle, closer packing of aragonites gives better hydrophobicity. CNF and high loading of PCC coating (CNF AKD r20) shows few CNF at the surface while low loading show more. This could explain water adhesion on the surface due to enlargement of pitch[3] and/or to strong attraction between water and cellulose eventhough CNF are previously hydrophobized.

**Static water contact angle**

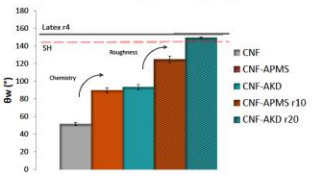


Latex coating is showing evidence of superhydrophobic state as expected. High loading PCC formulation with CNF-AKD achieved superhydrophobic 150° water contact angle. With CNF-APMS, contact angle above 125° wasn't obtained. Lower amount of PCC has for consequence the drop of contact angle.

## Conclusions & Perspectives

- A water repellent surface was successfully achieved with a combination of commercial AKD modified CNF and acicular aragonite.
- A water contact angle higher than 150° was obtained and a water shedding angle also.
- Wetting measurement were difficult because of water interaction with nanocellulose and paperboard and also because of porosity.
- Obtaining a superhydrophobic coating is related to close packing of aragonites regarding SEM images obtained. This close packing can be achieved with modified CNF but leeching of PCC is observed.
- Also, CNF appears at the surface, what is assumed to create the water adhesion. This water adhesion creates more a rose petal effect[3] surface than a Lotus effect meaning high static water contact angle with high adhesion of water.

**PERSPECTIVES**

- Achieve lower coating weight
- Different hydrophobization of CNF
- Hydrophobized PCC with a more stable fatty acid
- Use of different PCC and effects
- Have a look on antibacterial activity

References
[1] Swerin and al., Colloids and Surfaces A: Physicochem. Eng. Aspects, 2016
[2] Zimmermann and al., Textile research journal, 2009
[3] Bushan and al., Phi.trans. R. Soc. A , 2010

Acknowledgement
- COST Action ActinPak FP1405

Julien.Bras@pagora.grenoble-inp.fr
Charlene.reverdy@lgp2.grenoble-inp.fr

# Antibacterial materials development with contact active and micro-nano structured surfaces

Charlène REVERDY [1], Seema SAINI [1], Naceur BELGACEM [1], Julien BRAS [1,2]

[1] Univ. Grenoble Alpes, CNRS, Grenoble-INP, LGP2, 38000 Grenoble, France
[2] Institut Universitaire de France (IUF), 75000 Paris, France

## Abstract

Interest has grown for **antibacterial surfaces** during last decades because of the need to avoid bacterial growth in food packaging or presenting nosocomial infection in hospitals. But, solutions are mostly based on leaching of active component from the material and EU raised the problem of antibacterial resistance which might be one of the first health challenges by 2040. New **non leaching** antibacterial surfaces are thus needed to avoid bacterial resistance.

**Cellulose nanofibrils** is a biobased material with high hydroxyl group density which can be used as a versatile grafting site for different molecules. And especially, CNFs could be used as a template for non leaching antibacterial agent carrier[1]. Structuring the surface by increasing roughness and use low surface energy component can lead to low water adhesive surface such has **superhydrophobic (SH)** materials. Such SH structure can reduce or delay growth of bacteria on the surface[2].
In this study will be compared antibacterial activity, bacterial growth and adhesion on superhydrophobic and non superhydrophobic coating on paperboard made with CNFs or not. Assessments are done with gram+ Staphylococcus Aureus bacteria and Bacillus Subtilis. Materials will also be compared in terms of surface properties.

## Introduction

In this study, **superhydrophobic coatings and strucutred surfaces** are expected to delay or **reduce bacterial growth** on a cardboard. **Cellulose nanofiber** (CNF) as a replacement of usual latex binder could provide in addition to its renewability, a site for antibacterial grafting in addition to superhydrophobicity of the SH coating. A collaboration project between SP and LGP2 groups was done under COST Action ActinPack FP1405 to formulate the coatings. Hereafter is presented the results of surface properties and the antibacterial activity of the coated paperboard.

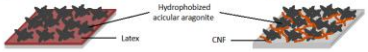


## Current work

### Materials & Methods

**Materials**

**Acicular Aragonite (PCC)** Sturcal H was provided by Specialty Minerals.
**Sodium oleate** (88-92%) was purchased from Riedel-de Haen.
**Styrene Butadiene latex** DL-930 was purchased from Dow Chemical with a Tg of 5°C and a dry matter content of 50%.
**Cellulose nanofibrils** (CNF) manufactured from bleached birch pulp was purchased from CTP, France. AKD (Alkyl Ketene Dimer) hydrophobized reference CNF was purchased to InnoFib, France. Amino propyl trimethoxy silane (APMS) 98% was purchased from Sigma Aldrich and used for modification of nanocellulose.(CNF-APMS) possess antimicrobial activity.
Commercial NeverWet® coating was also applied as a comparison.
Substrate was chosen to be a **paperboard** of 232 g/m² Cupforma natura from Stora Enso.

**Coatings preparation**

Coatings preparation include the following steps:
- Dissolve Sodium oleate at 45°C for 10min
- Add Aragonite and mix for at least 20min
- Add the binder: CNF AKD (5wt%), CNF APMS(9%) or latex (20%)


- Coat at 5m/min and dry 2-3 min at 90°C for latex and CNF-APMS formulations and 120°C for CNF-AKD

**Microbiology measurements methods**

- **AATCC Test Method 100-1998** was used for quantifying antibacterial activity of surfaces due to composition of the coating (oleate, latex,...). Shortly, bacteria in solution is deposited on the surface and let in incubator for 24h. Colony are then plate and count. The growth value between inoculum concentration and final bacteria amount on the sample is reported.

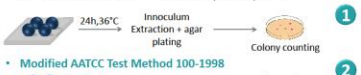


- **Modified AATCC Test Method 100-1998**

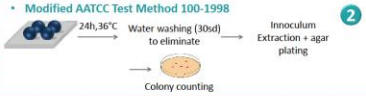


A protocol for **bacterial adhesion** was adapted for checking the presence of bacteria on the surface of one-side coated paperboard:
A silicone sealant was used to fix the sample on a glass plate and provide a thick waterproof barrier for bacteria inoculum.
Sample surface was immersed in 1mL of a $10^5$ CFU/mL and let in contact for a desired time. Sample were then washed 6 times with 9g/L saline solution and cut. Piece of sample were then poured plate in nutrient agar and let 24h in incubation. Bacteria colony presence was checked after incubation.

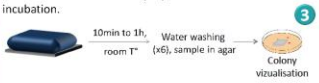


All samples were previously sterilized at 70°C overnight before handling.

### Results & discussion

**Surface properties**

**Static water contact angle**


Latex coating is showing evidence of superhydrophobic state as expected. High loading PCC formulation with **CNF-AKD achieved superhydrophobic** 150° water contact angle. With CNF-APMS, contact angle above 125° wasn't obtained. Lower amount of PCC has for consequence the drop of contact angle.

**Water shedding angle** [3]

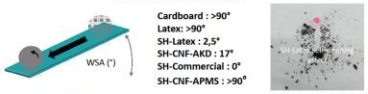


**Water shedding angle** was achieved with high loading PCC and CNF-AKD formulation. Roll-off angle was not measurable because of water adhesion on SH-CNF-AKD surface.

**Water absorption**

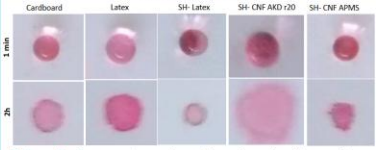


**Water adhesion** was observed on all samples after 2 hours. It was noticed that SH coating with CNF-AKD tends to spread the water immediately and start to be absorbed. This is also observed with CNF-APMS binder but not with latex.

**Antibacterial activity**


**Bacterial growth with S.Aureus** was assessed on superhydrophobic reference surface and was shown on all samples. Commercial SH was not tested as it wasn't possible to let innoculum drops on the surface.
Latex seems to have a bacteriostatic effect but when PCC are added to the mixture to obtain a particular roughness, it seems that **bacterias get attached to the particles.** For superhydrophobic Latex/PCC/Oleate formulation, the slight water adhesion defining the material is probably a center of bacteria anchoring and growth. Oleate is proved to have no effect in killing.

**Bacterial adhesion (S.Aureus)**

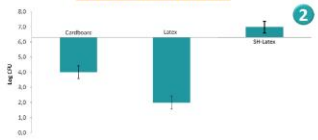


This test was first chosen without water washing as superhydrophobic surfaces were expected to repeal water. Unfortunately, over 24h, **water adhesion was total** or extremely high and roll-off of innoculum drops was not possible.
Interestingly, less S.Aureus were still on samples when not treated with PCC. This could be explained by either the bacteriostatic effect or the **durable hydrophobic properties** of cardboard and latex over time or both combined effects.
Formulation with PCC get absorption of water that possibly favoured the creation of an anchored biofilm protecting bacterias against water washing.

**Bacterial adhesion (B. Subtilis)** 3

The test here, was to assessed bacterial adhesion within shorter time and be able to compare results to commercial robust superhydrophobic coating.
**Bacterial adhesion** was evaluated through a non-quantitative method after 10 min and 1 hour contact with bacteria. All surfaces displayed bacterial adhesion. It was noticed that a lower amount of colony were present for SH-commercial SH and SH-Latex formulations.
The presence of bacteria could also be assigned for innoculum penetration through the material after time.

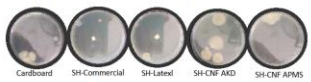


| Samples/Time of adhesion | 10 min | 1h |
|---|---|---|
| Cardboard | ● ● ● | ● ● ● |
| SH-Commercial | ● | ● |
| SH-Latex | ● ● | ● ● |
| SH-CNF-AKD | ● ● ● | ● ● ● |
| (SH)-CNF-APMS | ● ● | ● ● |

● Few colonies ● ● Some colonies ● ● ● Lots of colonies
(based on visual observation on 2 petri dishes)

## Conclusions & Perspectives

- **Antibacterial activity** against S.Aureus was assessed on superhydrophobic cardboard and micro-nano structured surfaces. PCC or oleate don't seem to have an antibacterial activity. Roughened surface gave higher bacterial growth at 24h.
- **Bacterial adhesion** was assessed with S.Aureus with a modified method. After 24h, the high water absorption of the coatings resulted in higher development of bacteria.
- A shorter test with commercial **SH coating** was done with B.Subtilis. All surfaces at 10 or 60 min display bacterial attachement.
- Less adhesion was observed for SH sufaces.

**PERSPECTIVES**

- Enhanced SH with CNF robustness
- Bacterial adhesion on CNF-APMS/PCC/Oleate with confocal microscopy and dead/alive assay and comparison with CNF-APMS alone
- S.Aureus bacterial adhesion quantitative assessment with confocal microscopy on third method
- Comparison of Bacteria number = F(roughness)

References
[1] Saini and al., ACS Applied materials & interfaces, 2015
[2] Zhang and al., RCS Advances, 2015.
[3] Zimmermann and al., Textile research journal, 2009

Acknowledgement
- COST Action ActinPak FP1405
- Agne Swerin, Mazlar Sedighi Moghaddam,Mikael Sundin. SP Stockholm

Julien.Bras@pagora.grenoble-inp.fr
Charlene.reverdy@lgp2.grenoble-inp.fr
Seema.saini@lgp2.grenoble-inp.fr

# Multitechnique Study of Aminopropyltrimethoxysilane Polysiloxane Network Orientation on Cellulose Nanofibrils Surface

C. Reverdy[1], C. Gablin[2], D. Leonard[2], J. Bras[1], N. Belgacem[1]

[1] Univ. Grenoble Alpes, CNRS, Grenoble INP, LGP2, F-38000 Grenoble, France.

[2] Univ Lyon, CNRS, Université Claude Bernard Lyon 1, ENS de Lyon, Institut des Sciences Analytiques, UMR 5280, 5 rue de la Doua, F-69100 Villeurbanne, France.

## Context

In materials science, organosilanes are key molecules in the applications of adhesion promoters, coupling agent or even as surface primers. In particular, aminopropyltriethoxysilane or (3-Aminopropyl)trimethoxysilane (APMS) are depicting a singular reactivity due to their high affinity towards water and high natural pH thanks to the presence of an amine group within their structure. These features are responsible for a high solubility in water, a fast hydrolysis process of the ethoxy or methoxy groups but also for their capacity to undergo self-condensation giving rise to Si-O-Si polysiloxane network [1]. Some studies attempted to characterize the linear, cyclic or branched character of the formed network depending on the reaction conditions, as the amine group is able to form hydrogen bonds interacting with the condensation processes [2-3].

As the most abundant polymer in the world, cellulose is extracted from biomass and is given a large interest due to its renewability and biodegradability. Nature assembles this polymer in fibers which are commonly used in paper and textile industries. In these macro-fibers, cellulose nanofibrils (CNFs) are arranged to give the strength of the above mentioned and they are nowadays easily isolated. The applications of these original nano-scale materials are expected to range from composites reinforcing material to rheological modifiers or emulsion stabilizers and barrier films. With a high aspect ratio and high hydroxyl group content, CNFs are seen as a perfect tunable bio-template as well. However, its inherent hydrophilic character is a recurrent problem in different material applications.

In this work, APMS was studied as a potential modifier for tuning the hydrophilicity of CNF. A multitechnique approach was developed in order to determine in which way the APMS oligomers are interacting with cellulose nanofibrils.

## Current work

### Goal of this specific study

The hydrolyzation/condensation process of APMS in 100% aqueous solution was studied by $^{29}$Si NMR. APMS affinity toward CNF was also monitored by QCM-D and compared with other organotrimethoxy silane. The resulting material surface and the barrier properties of CNF films were assessed. Interestingly, the prepared materials showed rather good hydrophobic features although the presence of the hydrophilic amine group. This is raising questions about the APMS organization on the nanocellulose network as the amine could interact through hydrogen bonds with the hydroxyl group of cellulose and consequently affect the silylation process. In this multi-technique approach, ToF-SIMS analyses were thus employed to try to ascertain the polysiloxane layer orientation onto the nanocellulose surface.

### Materials & Methods

**Materials**

(3-Aminopropyl)trimethoxysilane (APMS) and propyltrimethoxysilane (TMPS) were bought to Sigma Aldrich as well as N-hydroxysuccinimide (NHS) and 1-éthyl-3-(3-diméthylaminopropyl)carbodiimide.

Cellulose nanofibrils (CNF) manufactured from bleached birch pulp was purchased to CTP, France. It has been submitted to an enzymatic pretreatment followed by five passes through high pressure homogenizer in order to defibrillate macroscopic fibers.

**Methods**

*Film formation*


*29 Si NMR*

Silanes were hydrolyzed in their deuterated solvent at a 10wt% at natural pH for APMS and pH 2.3 for TMPS (acetic acid).

Spectra were recorded on a Bruker AVANCE400 spectrometer with a BB/1H/D Z-GRD 10mm probe with a resonance at 79.4914 MHz for $^{29}$Si et 400.1316 MHz for $^{1}$H.

*QCM-D*

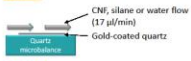


1. CNF 0.2 wt%
2. Water
3. APMS 10 wt% or TMPS 10 wt% pH 2.3
4. Water

*ToF-SIMS*

Time-of-Flight Secondary Ion Mass Spectrometry (ToF-SIMS) measurements were carried out on a TRIFT III ToF-SIMS instrument from Physical Electronics operated with a pulsed 22 keV $Au^+$ ion gun (ion current of 2 nA) rastered over a 300 µm × 300 µm area. An electron gun was operated in pulsed mode at low electron energy for charge compensation. The ion dose was kept below the static conditions limit. Data were analyzed using the WinCadence software. Mass calibration was performed on hydrocarbon secondary ions.

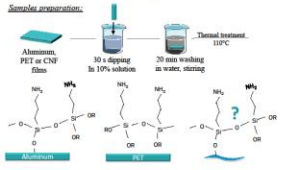


Three samples were analyzed in order to help interpreting results: a forced orientation (Al case), a non-differenciated orientation (PET case) and the CNF-APMS sample.

### Results & discussion

**Nanocellulose**

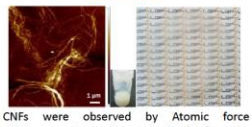

CNFs were observed by Atomic force microscopy in order to check for the nanoscopic scale and the good fibrillation quality. Translucent films were obtained from the drying of the suspension by casting.

**Film surface properties**

| Type | $\Theta_w$ | Std Dev |
|---|---|---|
| CNF | 38 | 8 |
| CNF_APMS | 81 | 4 |
| CNF_TMPS | 68 | 2 |

The addition of 10 wt% APMS with respect to CNF gives higher hydrophobicity than TMPS. Regarding the hydrophilic character of the amine group, this raises questions about the surface orientation of the modification.

QCM-D results show that both TMPS and APMS adsorb on CNF. TMPS interaction with CNF (OH-OH interaction) is slower compared to APMS as highlighted by the time needed to stabilize the signal after introduction of the chemical. It can be also noticed that TMPS desorption curve end above beginning level of the curve, and this could be explained by swelling of CNF due to acetic acid.

**$^{29}$Si NMR**

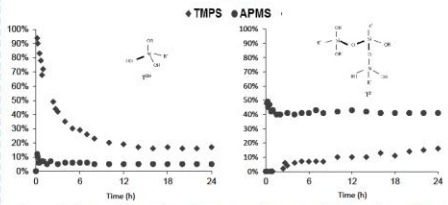


The model propyl chain silane, TMPS, is evolving quite slowly in the medium. All alkyls groups are fully hydrolyzed during first second but decrease at the same rate T1 (not shown) are formed in the medium. T2 are in a small amount after 2h30 and never gets higher than 20% while T3 is not formed. With its highly hydrophilic amine function, APMS at pH of 9,5 reacts rapidly and stabilize during the two first hours. 100% of the initial structure decomposed in T3OH, T1, T2 and T3 during the first 10 minutes. This is confirming previous results on reactivity of alkoxysilanes [1].

**QCM-D**

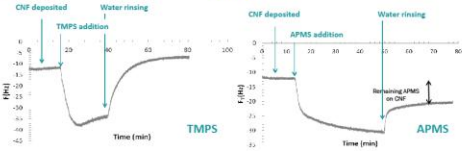


**ToF-SIMS**

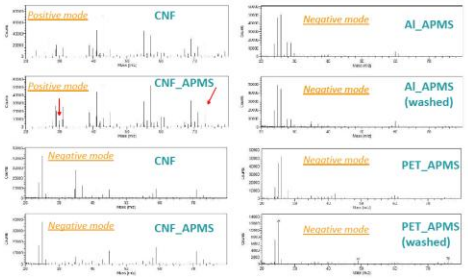


*Positive mode ToF-SIMS spectra of CNF and CNF-APMS & negative mode ToF-SIMS spectra of CNF and CNF-APMS in the 20 < m/z < 80 range*

*Negative mode ToF-SIMS spectra of Al-APMS, Al-APMS (washed), PET-APMS, PET-APMS (washed) in the 20 < m/z < 80 range*

ToF-SIMS results indicate :

(1) Limited extent in surface modification of CNF (low relative intensity for $CH_2NH_2^+$, $CN^-$ detected in negative mode instead of $C_2H_2^-$, siloxane signatures)

(2) Reference samples (Al, PET) indicate strong modification with grafting (Al case, limited decrease in intensity of characteristic signatures after washing) or no grafting (PET characteristic peaks such as m/z=76 are clearly detected after washing)

(3) 26 ($CN^-$) / 28 ($Si^-$) ratio values exhibit trends that can be interpreted in terms of difference in orientation. CNF-APMS being characterized by relatively lower amine content (low relative intensity m/z=26 for that sample may also be partly related to $C_2H_2^-$)

| samples | 26 ($CN^-$) / 28 ($Si^-$) ratio |
|---|---|
| CNF_APMS | 3.9 ± 0.8 |
| Al_APMS | 3.9 ± 0.7 |
| Al_APMS (washed) | 4.9 ± 1.1 |
| PET_APMS | 4.9 ± 1.0 |

## Conclusions & Perspectives

- APMS is reacting differently in water due to its high hydrophilicity and basic pH. It hydrolyzed and condensed faster than comparable propytrimethoxysilane as shown by 29 Si NMR.
- TMPS is adsorbing on CNF through hydroxyl-hydroxyl groups but desorbs immediately after rinsing as proved by QCM-D. However APMS do not desorb completely, pointing out either a stronger interaction, a covalent linkage or a steric hindrance.
- CNF film hydrophobicity is higher with APMS. ToF-SIMS results indicated a limited surface modification but with a more limited amine content.

### Perspectives

Further orientation studies should be carried out, e.g. by including preliminary chemical modification of CNFs to trigger a specific surface chemical reaction that should lead to differences in orientation at the top surface that ToF-SIMS may highlight thanks to its high surface sensitivity.

References
[1] M.-C. Brochier Salon, M.N. Belgacem, Colloids Surf. Physicochem. (2010)
[2] S. Naxing, J.L. Koenig, H. Ishida, J. Macromol. Sci. (1983)
[3] R. Peña-Alonso, F. Rubio, J. Rubio, J.L. Oteo, J. Mater. Sci. (2008).

julien.bras@pagora.grenoble-inp.fr
didier.leonard@univ-lyon1.fr

Acknowledgement
• Marie-Christine Brochier-Salon

# English Abstract

The aim of this work is to implement new properties to a paper based material via the use of functional nanocelluloses. Nanocelluloses are nanoparticles extracted from wood and distinguished in two categories: Cellulose Nanofibrils (CNFs) and Cellulose Nanocrystals (CNCs). This work has only been carried out with CNFs. The chemical reactivity of CNFs was used to functionalize them with organotrialkoxysilanes. The entangled network and highly viscous suspension of CNFs was also used to synthesize silsesquioxane particles with limited size to impart (super)hydrophobic and antimicrobial properties. Knowledge obtained through the study of model CNFs films was then applied to paper based material coating. The functional CNFs were evaluated for its use in an antimicrobial, anti-adherent, greaseproof or superhydrophobic paper surface.

***Keywords:*** *Nanocellulose, cellulose nanofibrils, organosilanes, silsesquioxane, specialty paper*

# Résumé Français

Ce projet s'est focalisé sur l'ajout de nouvelles propriétés à des papiers grâce à l'utilisation de nanocelluloses fonctionnelles. Ces nanocelluloses sont des nanoparticules extraites du bois qui peuvent être divisées en deux catégories : les nanofibrilles de cellulose (CNFs) et les nanocristaux de cellulose (CNCs). Ce travail s'est essentiellement penché sur l'utilisation des CNFs. Leur réactivité chimique a été utilisée afin de les fonctionnaliser avec des organotrialkoxysilanes. C'est aussi leur fort enchevêtrement ainsi que la grande viscosité de ces CNFs en suspension qui ont été utilisés afin de synthétiser des petites particules de silsesquioxane pour rendre le matériau final antimicrobien et (super)hydrophobe. Les connaissances obtenues à travers l'étude sur des films modèle de CNFs ont ensuite été appliquées au couchage du papier. Ces CNFs fonctionnelles ont donc été évaluées pour le développement d'un papier possédant une surface antimicrobienne, anti-adhérente, barrière aux graisses ou superhydrophobe.

***Mots-clés:*** *Nanocellulose, nanofibrilles de cellulose, organosilanes, silsesquioxane, papiers spéciaux*